Geographical Variation in Social Structure, Morphology, and Genetics of the New World Honey Ant *Myrmecocystus mendax*

by

Ti H. Eriksson

A Dissertation Presented in Partial Fulfillment
of the Requirements for the Degree
Doctor of Philosophy

Approved July 2018 by the
Graduate Supervisory Committee:

Jürgen Gadau, Co-Chair
Jay Taylor, Co-Chair
Jennifer Fewell
Bert Hölldobler
Robert Johnson
Stephen Pratt

ARIZONA STATE UNIVERSITY

August 2018

ABSTRACT

Persistent cooperation between unrelated conspecifics rarely occurs in mature eusocial insect societies. In this dissertation, I present evidence of non-kin cooperation in the Nearctic honey ant *Myrmecocystus mendax*. Using microsatellite markers, I show that mature colonies in the Sierra Ancha Mountain of central Arizona contain multiple unrelated matrilines, an observation that is consistent with primary polygyny. In contrast, similar analyses suggest that colonies in the Chiricahua Mountains of southeastern Arizona are primarily monogynous. These interpretations are consistent with field and laboratory observations. Whereas cooperative colony founding was observed frequently among groups of Sierra Ancha foundresses, founding in the Chiricahua population was restricted to individual foundresses. Furthermore, Sierra Ancha foundresses successfully established incipient laboratory colonies without undergoing queen culling following emergence of the first workers. Multi-queen laboratory Sierra Ancha colonies also produced more workers and repletes than haplometrotic colonies, and when brood raiding was induced between colonies, queens of those with more workers had a higher survival probability.

Microsatellite analyses of additional locations within the *M. mendax* range suggest that polygyny is also present in some other populations, especially in central-northern Arizona, albeit at lower frequencies than that in the Sierra Anchas. In addition, analyses of multiple types of genetic data, including microsatellites, the mitochondrial barcoding region, and over 2000 nuclear ultra-conserved elements indicate that *M. mendax* populations within the southwestern U.S. and northwestern Mexico are geographically structured, with strong support for the existence of two or more divergent

clades as well as isolation-by-distance within clades. This structure is further shown to correlate with variation in queen number and hair length, a diagnostic taxonomic feature used to distinguish honey ant species.

Together, these findings suggest that regional ecological pressures (e.g. colony density , climate) may have acted on colony founding and social strategy to select for increasing workforce size and, along with genetic drift, have driven geographically isolated *M. mendax* populations to differentiate genetically and morphologically. The presence of colony fusion in the laboratory and life history traits in honey ant that are influenced by colony size, including repletism, brood raiding, and tournament, support this evolutionary scenario.

DEDICATION

To my parents, Jimmy and Thuha Eriksson, for their unending support, encouragement, and love.

ACKNOWLEDGMENTS

I am very grateful to my co-chairs, Jürgen Gadau and Jay Taylor, for their intellectual and material support throughout this endeavor. Despite his busy schedule, Jürgen always find time to answer questions and help refining my work. Jay's mentoring has been indispensable, and without his love of birding and collecting zeal, half of the specimens in this dissertation would not have been available. I am also thankful to Stephen Pratt for his wisdom on navigating statistics and academia, to Bert Hölldobler for his knowledge of *Myrmecocystus*, to Jennifer Fewell for graciously allowing my colonies (and mess) to take up precious space in her laboratory for so long, and to Bob Johnson for contributing and identifying specimens of this taxonomically challenging group of ants. My appreciation also goes to Christian Rabeling and his laboratory, especially to Marek Boroweic and Jeff Sosa-Calvo for their valuable support and contribution to the UCE project.

I want to thank the entire amazing Social Insects Research Group at ASU for the intellectual stimulation, laughter, and support that have helped keep me afloat, especially Ioulia Bespalova, Abby Finkelstein, Johnathon Jackson, Christina Kwapich, and Ben Pyenson. I also want to acknowledge Elizabeth Cash, Josh Gibson, Martin Helmkampf, and Rick Overson for their guidance during my early days in the Gadau Lab at ASU. Thanks go to Kevin Haight for getting me into the Thursday-at-Boulder's routine, as well as Yohan Cho and Zach Shaffer for regularly letting me borrow their six-legged subjects for outreach. Field work would not have been possible without Kevin Demater, Christian D'Orgeix, Harry Grissom, Brandon Siqueiros, Asia (Joana) Sulich, and Rafael Testai. Last but not least, thanks to my cat, Martin, for allowing me to pet him daily.

TABLE OF CONTENTS

Page

LIST OF TABLES

LIST OF FIGURES

Figure Page

CHAPTER 1

INTRODUCTION

According to Hamilton's inclusive fitness theory, cooperation among kin evolved in the eusocial Hymenopterans because non-reproductive helpers increase their inclusive fitness by helping to rear reproductive relatives (i.e. kin selection, Hamilton 1964). This model predicts that inclusive fitness benefits for workers erode as the number of reproductives increases and within-group relatedness decreases. Indeed, a singly mated ant queen monopolizing reproduction maximizes not only her direct fitness, because all sexual offspring produced are hers, but also the inclusive fitness of her workers, as her daughters are more related to their sisters ($r = 0.75$) than to their own offspring ($r = 0.5$). However, the average relatedness between workers and sexuals in the nest drops as queen number and mating frequency increase. Thus the inclusive fitness gain from cooperating diminishes. These costs may have induced the evolution of queen culling when cooperative founding does occur (i.e. pleometrosis, Rissing and Pollock 1987), and explained why monogyny is more common in the ant world and likely the ancestral state (Schrempf and Heinze 2006; Schmid-Hempel and Crozier 1999).

Interestingly, cooperation in the absence of relatedness has evolved multiple times in ants. Primary polygyny, the social structure characterized by multiple, unrelated foundresses jointly establishing a new colony and co-reproducing throughout its lifespan (Haney 2017; Hölldobler and Wilson 1990) has been reported in four subfamilies and 14 genera. Primary polygyny is well documented in Myrmicinae, with new cases being discovered regularly (Gotoh et al. 2017; Rubin et al. 2013) and with the best studied systems including *Pogonomyrmex californicus* (Overson et al. 2016; Johnson 2004),

Veromesor pergandei (Helms Cahan and Helms 2012; Pollock and Rissing 1985), and *Solenopsis invicta* (Ross and Fletcher 1985; Tschinkel and Howard 1983). These model systems have contributed significantly to our understanding of the distribution, ecology, and evolution of cooperation in the absence of kinship. In contrast, despite being the second most speciose subfamily (Bolton et al. 2007), Formicinae does not proportionally have as many well substantiated examples of primary polygyny (~0.11% vs. ~0.18% in Myrmicinae; Haney 2017; Bolton et al. 2007). There is some evidence of non-kin cooperation in *Cataglyphis aenescens* (Cronin et al. 2016), *Formica podzolica* (DeHeer and Herbers 2004), *Myrmecocystus mimicus* (Hölldobler et al. 2011; Bartz and Hölldobler 1982), and *Oceophylla smaragdina* (Schlüns et al. 2009). Unfortunately, the data are often insufficient to demonstrate primary polygyny with high confidence. For instance, the *C. aenescens* and *F. podzolica* studies reported queen number and intracolonial relatedness estimates suggestive of multiple unrelated queens, but did not mention colony founding mechanism or any observation on queen cooperation (Cronin et al. 2016; DeHeer and Herbers 2004). This is understandable given the difficulty of intercepting mating flights and excavating colonies in the field.

To account for the evolution of cooperation among unrelated individuals, Hamilton's inclusive fitness theory has to invoke mutualism. When unrelated queens associate, cooperative interactions are expected to increase individuals' chance of survival and reproduction directly or indirectly through colony attributes such as colony workforce size and genetic variability (Keller and Reeve 1994; Rissing and Pollock 1988). In fact, there is evidence in multiple taxa that the number of workers a colony can produce and field is positively correlated with the number of reproducing queens (Bartz

and Hölldobler 1982; Tschinkel and Howard 1983; Mintzer 1987). Worker number per colony and survival outcome in the context of intraspecific competition is also correlated (Bernasconi and Strassmann 1999). Likewise, enhanced resistance against pathogens and increased task performance lend support to the genetic variability hypothesis (Slaa et al. 2014; Hughes and Boomsma 2004). In term of ultimate causation, ecological conditions have been suggested to be a significant driver of queen number evolution (Gadau and Fewell 2009). For instance, ant communities at higher latitudes tend to have a greater proportion of polygynous species, which suggests a selective role of low temperature (Heinze and Hölldobler 1994). Species exhibiting secondary monogyny and/or primary polygyny also experience intense intraspecific competition in early colony development (Tschinkel and Howard 1983), or live in arid environments (Cronin et al. 2016; Rissing et al. 2000; Rissing and Pollock 1988). Some taxa face both abiotic and biotic pressures (Rissing and Pollock 1987; Bartz and Hölldobler 1982).

Although beneficial, non-kin cooperation usually exists as a polymorphism, occurring at high frequency in only certain parts of a species range without completely replacing monogyny (Overson et al. 2016; Helms and Cahan 2012). Alternatively, it has been proposed that social variation can be a feature of populations undergoing speciation or having already diverged (Ross and Fletcher 1985). Localized selection on queen number may generate a cascade of changes in heritable behavioral and physiological traits, differentiating the genomes of populations. If gene flow is reduced, selection and genetic drift become even more effective at creating structure, and conspecific populations diverge and become distinct species over time. As this process takes place, morphological differences may accumulate through genetic hitchhiking (Via and West

2008). However in taxa with very recent ancestry or that are experiencing balancing selection, discrete morphological variation may be absent or highly inconspicuous, and therefore can be missed by traditional taxonomy (Bickford et al. 2006; Santos et al. 2006). Such cryptic diversity may only be revealed by an integrative approach, employing multiple sources of evidence along with molecular markers (Steiner et al 2010; Seifert and Csösz 2015; Nettel-Hernanz et al. 2015).

Honey ants of the genus *Myrmecocystus* are promising candidates to study the evolution of social structure variation and how it influences speciation. There are three main reasons to support this assertion. First, honey ants possess adaptive life history traits related to desert survival that likely synergize with increasing queen number, including repletism, brood raiding, and tournament behavior (Bartz and Hölldobler 1982; Snelling 1976). Thus it is conceivable that social structure variation is more widespread than the currently available data suggest. Second, *Myrmecocystus* populations inhabit or are surrounded by xeric environments characterized by high temperature (Kay 1978; max soil surface temperature: 70°C, per. obs.). It is therefore predicted that speciation rate is higher in honey ants relative to more temperate adapted taxa, according to the energy-speciation hypothesis (Kaspari et al. 2004). Third, spatial distribution is quite variable among congeners with some taxa broadly disperse in regions covering almost a million square kilometers (e.g. *M. mexicanus*), while others are found restricted to significantly smaller areas (e.g. only 25,000 square kilometers for *M. ewarti*, estimated from Snelling 1976). In widely distributed taxa, mating and dispersal activities of distant populations are likely asynchronous, due to their dependency on localized and erratic monsoon rains. This disparity in timing of reproductive activities, coupled with natural and manmade

habitat fragmentation, is expected to reduce gene flow between sites, increasing the efficiency of drift and local adaptation in differentiating populations.

Anecdotally, there are at least ten potentially new, undescribed *Myrmecocystus* species discovered since the 1990's (RA Johnson, P Ward, M Boroweic, per. com.). There is also already evidence of founding strategy and social structure variation, albeit in a single species. In some populations, *M. mimicus* (Snelling 1976) is capable of pleometrosis with queen reduction (Bartz and Hölldobler 1982), and some field colonies may have multiple gynes (Hölldobler et al. 2011). In contrast, *M. depilis*, the sister species of *M. mimicus*, is obligatorily monogynous (Hölldobler et al. 2011). This observation is consistent with the idea that change in queen number can be a driver of speciation (Gadau and Fewell 2009, Chapter 26).

Despite the influential study of *M. mimicus*, our understanding of the social structure in the Nearctic honey ants is still taxonomically limited. Recently, the discovery of multiple populations of *Myrmecocystus mendax* presents an opportunity to expand the investigation of social variation in this charismatic group. *M. mendax* is one of the largest honey ant species, with range extends from northern Sonora (Mexico) to northern Colorado, and from southern Nevada and California to central Texas (USA; Snelling 1976). Populations in Arizona and northern Sonora are found in mid elevation, mountainous regions (Snelling 1976). Workers forage during daytime, travelling far from the nest to gather carbohydrate exudates from plants and plant-feeding insects and scavenge for dead arthropods, often crossing into neighbors' territory (Snelling 1976, per. obs.). Colonies can reach two to five thousands individuals, hundreds of which can be repletes (Conway 2003; unpublished data; R Mendez per. com.). Tournament activities

have been observed in two different localities (per. obs.), with a few hundred major workers congregating and displaying (e.g. raising gaster, standing on stilt legs). Based on observations from two years at the population on the Sierra Ancha mountain ranges, mating flights occurred in late afternoon to early evening (2:30-6:30 PM) following heavy rainfall on previous day(s). Sexuals took flight and quickly mated. Upon landing, foundresses immediately searched for nest sites and commenced digging; many were interrupted and eliminated by conspecific and heterospecific workers and other predators (per. obs.). Before the next morning, the majority of surviving foundresses have finished settling into incipient nest cavities. These observations suggest that *M. mendax* colonies are territorial, foundresses and incipient colonies face great odds from abiotic and biotic sources to survive and become established, and that cooperation with unrelated individuals may be sufficiently beneficial to overcome the downstream costs such as the loss of reproductive fitness due to resource sharing.

In this dissertation, I explore the social structure variability and evolutionary relationships among populations of *M. mendax*. I describe in Chapter Two the founding strategy and queen number variation in two allopatric populations, using a combination of molecular and observational data. In addition, I show how increasing queen number may provide benefits to colonies and queens. Chapter Three expands the social structure survey to additional populations distributed throughout Arizona and northern Sonora, and includes analyses of genetic subdivision. Here I also relate social and genetic variation with temperature and precipitation patterns to suggest that climate may have played a role in the evolution of polygyny in the focal populations. Chapter Four presents a biogeographical analysis of *M. mendax*, and uses the phylogeographical inferences to

interpret variation in queen number as well as hair length, a character suggested by Snelling to have evolutionary significance in the *melliger* morphospecies group. I also show significant genetic evidence of cryptic diversity within *M. mendax*. Lastly in Chapter Five, I combine all findings to speculate on the mechanism of social evolution in this taxon, and to make predictions about its future evolutionary trajectory.

CHAPTER 2

A CASE STUDY OF VARIATION IN COLONY FOUNDING BEHAVIOR AND SOCIAL ORGANIZATION OF *MYRMECOCYSTUS MENDAX*

Introduction

The number of reproducing queens (-gyny) plays a major role in shaping the genetic structure and social environment of ant colonies. For species in which workers do not participate in colony founding (i.e. independently colony founding), gyny can be fixed or vary over time (Hölldobler and Wilson 1990). The simplest social structure consists of foundresses starting new colonies alone (i.e. haplometrosis) and monopolizing reproduction thereafter (i.e. monogyny). In a number of taxa, monogynous colonies can adopt related queens thereby triggering secondary polygyny. Less commonly, colonies are cooperatively established by multiple, usually unrelated foundresses (i.e. pleometrosis). Polygyny that arises from these associations is often short-lived. Supernumerary queens are subsequently culled following emergence of the first workers, or minims, resulting in secondary monogyny (Hölldobler and Wilson 1990). However, queen culling does not always occur, as pleometrotic colonies may retain the original co-foundresses which continue to co-reproduce over their lifetime (Hölldobler and Wilson 1990; Overson et al. 2011). This social structure, termed primary polygyny, is rare in ants, having been documented in between 20-30 species of ~15,000 described taxa (Brian Haney per. com.; Bolton et al. 2007). When present, primary polygyny often co-occurs with other social structures at frequencies varying with geography (Ross and Fletcher 1985; Overson 2011; Helms and Helms Cahan 2012). Primary polygyny is best documented in Myrmicinae (e.g. Mintzer and Vinson 1985; Ross and Fletcher 1985;

Rissing et al. 1986; Hagen et al. 1988; Johnson 2004; Overson 2011; Gotoh et al. 2017). In contrast, convincing evidence of stable polygyny following pleometrosis is much less common in the other ant subfamilies, including Formicinae (e.g. Gadau et al. 1998; Schlüns et al. 2009; Hölldobler et al. 2011).

Pleometrosis has been repeatedly shown to lead to incipient polygyny which can increase the rate of brood production (Walloff 1957; Tschinkel and Howard 1983; Johnson 2004; Offenberg et al. 2012) and the total number of workers a colony produces (Bartz and Hölldobler 1982; Tschinkel and Howard 1983; Mintzer 1987; Trunzer et al. 1998; Johnson 2004; Offenberg et al. 2012). These extra workers can boost colony survivorship which is often dependent on having a large workforce defending the nest and amassing resources necessary for survival (Bernasconi and Strassmann 1999). For incipient colonies of pleometrotic species, the selective pressure from territoriality can be intense. Neighboring nests often engage in brood raiding, during which the competitors attack each other to steal brood and kill queens, resulting in the decimation of the defeated colonies (Bartz and Hölldobler 1982; Rissing and Pollock 1988; Tschinkel 1992; Adams and Tschinkel 1995). If such significant territorial pressures persist in the population, natural selection may favor colonies that maintain polygyny for its advantage in boosting worker production. In the honey ant *Myrmecosystus mimicus*, for example, incipient and adult colonies with more workers were more successful in non-aggressive, ritualized territorial confrontations (tournaments) and brood raids (Hölldobler 1976; Bartz and Hölldobler 1982; Hölldobler et al. 2011; Kronauer et al. 2003). Tournament is a less costly strategy to defend spatiotemporal territory boundaries, and can draw and occupy large number of workers from the dueling colonies (Hölldobler 1981). Therefore,

a large workforce may increase a colony's odds of successfully conducting raids and defending the territory and nesting site. Indeed, there is genetic evidence of unrelated matrilines in mature *M. mimicus* colonies (Hölldobler et al. 2011); however, the absence of queen culling is yet to be confirmed.

Here I combine genetic data and behavioral observations to demonstrate primary polygyny in *Myrmecocystus mendax,* another diurnal species of honey ants. *M. mendax* inhabits semiarid, mountainous habitats throughout the southwestern United States and northern Mexico, and has fully claustral queens (Snelling 1976). Based on two focal populations, *M. mendax* appears to be socially polymorphic with primary polygyny prevailing at one site while monogyny predominates at the other one. Queens from both populations have a high frequency of polyandry. I hypothesized that polygyny would have positive effects on colony growth and survival, and predicted that latency to minim emergence, workforce size, and queen survival during brood raids scales with foundress number in laboratory colonies. Furthermore, I present evidence that incipient polygyny hastens the development of repletes in pleometrotic *Myrmecocystus* colonies (Bartz and Hölldobler 1982). Repletes are typically large workers that store liquid nutrients in their internal crops for long periods of time to supply nest-mates. Those with the most liquid are colloquially called honeypots, from which the genus has derived its common name honey ants. With more workers available in pleometrotic colonies to forage, the rate of food acquisition will increase and subsequently will increase, which in turn will accelerate the development of repletes. Together, these benefits to growth and survival may explain the presence of primary polygyny in *M. mendax*.

Materials and methods

Sampling

M. mendax colonies were sampled from the Sierra Ancha (abbreviated SIE-A, 33.78475°, -110.97103°, Gila County - AZ) and Chiricahua mountain ranges (abbreviated CHI, 31.90046°, -109.22757°, Cochise County - AZ) along roadsides and trails in 2010 - 2011. These populations were chosen to increase the chance of finding behavioral variation, based on their locations and proximity. The Sierra Anchas are part of an extensive mountain range in central Arizona, while the Chiricahua Mountains are one of the Madrean sky islands in southeast Arizona. The sites are separated by 270 km of arid environments unsuitable for *M. mendax*. GPS coordinates were obtained from 100 SIE-A and 51 CHI colonies. Field identification used heuristic characters including worker coloration and odor, as well as habitat characteristics (Snelling 1976; Jürgen Gadau, Bert Hölldobler, Ray Mendez, and Robert Johnson per. com.). I selected 11 adult colonies from each population for genotyping. Several workers from each colony were identified to species by R.A. Johnson. Vouchers were deposited in the Hasbrouck Insect Collection at Arizona State University. Workers were collected as they exited the nest or were within 5 cm of the entrance and exhibited no territorial behaviors (Figure 2.1A), and were preserved immediately in 70-95% ethanol. I also genotyped 21 female alates, retrieved 10 cm below the nest entrance from colony SIE14 of the SIE-A population. If the colony is polygynous, multiple matrilines are expected to be represented in both workers and alates. To study founding behavior, queen survival, and colony development, I collected foundresses from the CHI population in 2014 (n = 145) and the SIE-A population in 2013 and 2015 (n = 138 and 125, respectively) and used these to

establish laboratory colonies. Foundresses were captured while searching for nest site on the ground, excavating, or from inside freshly dug incipient nests, and were classified as haplometrotic foundresses if they were alone or pleometrotic if associated with at least one other queen.

Genotyping

A total of 660 workers (n = 30 per colony) were genotyped to estimate gyny and mating frequency. Genomic DNA was isolated using a Chelex® (Bio-Rad, Inc., Hercules, CA) -based method (Gadau 2009). Four microsatellite markers were amplified by PCR: Mm3, Mm4, Mm5 (Kronauer and Gadau 2002), and FE17 (Gyllenstrand et al. 2002). Table 2.1 lists marker statistics estimated from workers. Each 20 µl reaction consisted of 13 µl of ultrapure water, 4 µl of 5X Colorless GoTaq Reaction Buffer (w/1.5 mM $MgCl_2$), 0.4 µl of 10 mM dNTP mix, 0.7 µl of 10 mM of each primer (one was fluorescently labelled), 0.2 µl of Taq DNA Polymerase (~5 u/µl), and 1 µl of DNA template (concentration varied). Two thermal profiles were used, one for the Mm loci (denaturation: 2 min at 94°C; elongation: 30 cycles each for 20 sec at 94°C, 30 sec at 56°C, and 1 min at 72°C; termination: 5 min at 72°C), and the other for FE17 (denaturation: 2 min at 94°C; elongation: 30 amplification cycles each for 20 sec at 94°C, 30 sec at 51°C, and 1 min at 72°C; termination: 5 min at 72°C). PCR products were analyzed by a 4300 DNA Analyzer (LI-COR, Inc., Lincoln, NE). The Saga Generation 2 software (LI-COR) was used to score alleles. Standardization was performed to identify shared and unique alleles in colonies and populations. For the alates, DNA extraction and PCR followed the protocols described above and only the Mm loci were amplified. PCR

products were analyzed by an ABI 3730 DNA Analyzer. Allele calls were made using the Genemapper® program (Thermo Fisher Scientific). All genotypes generated in this Chapter are provided in Appendix A.

Colony founding and raiding experiments

In 2013, SIE-A foundresses were placed into 8-ounce glass jars lined with a 5-cm layer of plaster of Paris and filled with autoclaved moistened soil. Natural co-foundresses were kept together, and haplometrotic and roaming foundresses were added to some natural associations to increase group size or induced pleometrosis. In 2014 and 2015, each foundress was first put into a glass tube with a moistened cotton ball. Within 24 hours after collection, foundresses were weighed to the nearest 0.1 mg using a microbalance (2014 - Mettler AT261 DeltaRange, error 0.1-0.2 mg; 2015 - Sartorius CP323S, error 1 mg), then randomly assigned to be haplometrotic or pleometrotic and marked on the dorsal pronotum and mesonotum with nontoxic paint. Pleometrotic foundresses were given unique colors (red, yellow, green) or bicolor combinations (e.g. red-yellow), and placed inside cylindrical plastic containers (diameter: 8.41 cm x depth: 3.33 cm) lined with Plaster of Paris or Hydrostone (donut-shape, thickness: 0.5-1 cm x depth: 2 cm) and filled with autoclaved moistened soil. Co-foundress interactions were briefly scanned at the beginning of founding in 2013 and 2015. In 2014, nine pairs of marked CHI foundresses were observed for four minutes each in empty cylindrical containers (see dimensions above). A random queen from each pair was placed in the container first, followed by the other queen one minute later. Four behaviors were recorded: standing on top (a queen climbs and stands on top of the other), displaying

(raise postured, Figure 1A), fighting (grappling or chasing), and neutral antennating (queens antennate and then move away from each other).

After minims emerged, colonies were moved to observation nests, which were plastic containers (length: 10.95 cm x width: 10.95 cm x depth: 3.50 cm) lined with plaster of Paris or Hydrostone. Colonies were watered and fed once a week on a diet consisting of 4 ml of water, 4 ml of honey-sucrose solution, and *ad libitum* mealworms. Queen and minim numbers were counted from photographs regularly for the next three months. I examined the relationship between founding strategy and replete production in 2015. Repletes have been found in field *M. mendax* colonies (Conway 2003; Topoff and Mendez per. com.) and started to appear in SIE-A 2015 laboratory colonies around 50 days after colony initiation. Both callow and mature workers can become repletes (per. obs.). I compared the proportion of repletes in haplo- and pleometrotic laboratory colonies from the SIE-A 2015 cohort at days 48 and 81 after colony initiation. Because no quantitative definition of a replete has been published, I developed a quantifiable measure to distinguish repletes from non-repletes. Repletes were defined as workers with the membrane connecting the first and second gastral tergites visibly stretched based on photographs (Figure 2.1B). To verify that this identification character is robust, I used it to identify repletes and non-repletes from laboratory colonies, and compared their ratios of the gastral width to head width (GH) measured from photographs using the program Fiji (Schindelin et al. 2012). I selected 13 SIE-A laboratory colonies with 10 or more repletes at day 48 and measured six ants, including three workers with stretched intersegmental membrane between the first and second gastral tergites and three workers without visible stretching (N = 78). On average, the GH ratio of workers with stretched

membrane was significantly greater than those without (stretched: 1.50 ± 0.02, no stretching: 1.22 ± 0.02, paired t-test, $t = 8.74$, $df = 12$, $P < 0.001$), justifying our use of the intersegmental membrane to distinguish repletes and non-replete workers.

In 2014 and 2015, I studied the effect of workforce size on queen survival during brood raiding by pairing incipient laboratory colonies of different worker numbers that were placed in an arena (length: 10.95 cm x width: 10.95 cm x depth: 3.50 cm); only water was provided initially. The distance between nest entrances was fixed at 11 cm, which is within the range seen between SIE-A incipient field colonies (per. obs.). In each pair, the colony with more workers was designated as the larger colony, and its rival the smaller colony. In pairs where queen number differs between rivals, larger colonies usually had more queens and pupae. Pairing combinations based on queen number are listed in Table 2.2. All pairs were scanned once every hour for the first seven hours and subsequently every 24 hours for up to 30 days. Observation stopped when a colony in the pair experienced queen death or when 30 days had elapsed. Honey-sucrose solution was provided seven days after the experiment started. In 2015, some paired SIE-A colonies fused, i.e. all surviving queens, workers, and brood of both colonies moved into the same nest. I genotyped second-and-third-instar larvae and all surviving queens in two fused colonies (Appendix A) to examine if relocated queens of fused colonies reproduce, using the three Mm loci. The developmental stage of the larvae and the latency between fusion and sampling ensured that the genotyped larvae were produced after fusion. For the purpose of this analysis, original queens were defined as queens that remained in their original nest, and relocated queens were individuals that moved from their original nest. Table 2 lists the sample sizes of the behavioral experiments and analyses.

Statistics

For the genetic analyses, specimens missing data at two or more loci were excluded and all genotypes from the same population were analyzed simultaneously. Colony allele frequencies were estimated with R (R Core Team 2013), and used to estimate population frequencies by averaging over all colonies in each population. Population allele frequencies were then used in MATESOFT, COLONY, and relatedness analyses. Expected and observed heterozygosity were obtained using the R package *diveRsity* (Keenan et al. 2013). To analyze SIE14 alates, allele frequencies were estimated by pooling the alate and 2010 field SIE-A worker genotypes (n = 21 and 314, respectively). MATESOFT v1.0 (Moilanen et al. 2004) was used to estimate the pedigree effective mate number ($m_{e,p}$) in colonies compatible with monogyny; rejected colonies were inferred to be polygynous. COLONY v2.0.6.1 (Wang 2004) was employed to infer matrilines and patrilines in all colonies. The minimum number of male mates per queen was estimated from parental genotypes reconstructed by COLONY. Rare matrilines, represented by a single worker in each colony, were excluded from calculations involving inferred matrilines to avoid bias. Pairwise intracolonial relatedness of workers (r_{ww}), female alates (r_{FF}), and inferred matrilines (r_{QQ}) were estimated using Queller and Goodnight's method (1989) as modified by Lynch and Ritland (1999) using the package *related* (Pew et al. 2015). To examine the power of the SIE-A relatedness analyses, I simulated genotypes for each colony using the corresponding inferred matriline number and the population allele frequencies and compared their average relatedness with observed estimates using a custom R script (available upon request). I tested r_{ww} in scenarios where doubly mated nest-mate gynes are all unrelated, or descendants of one to

eight unrelated mothers. I also tested the probability of the observed r_{QQ} being consistent with unrelated or related nest-mate gynes. Each scenario was simulated 1,000 times.

Foundress survival probability was estimated with a Kaplan-Meier survival curve using data spanning at least 60 days following colony founding with the *survival* package (Therneau and Grambsch 2000; Therneau 2015). The power of these analyses was calculated using the *powerSurvEpi* package (Qiu et al. 2012). Nearest-neighbor distances (NND) between field colonies were estimated using PASSaGE 2 (Rosenberg and Anderson 2011). I found that the NND between SIE-A colonies (54.84 ± 27.40 m) was significantly less than that between CHI colonies (209.31 ± 4.36 m; two-tailed Mann-Whitney U test, $W = 3828$, $P < 0.001$). To examine how workforce size influences queen survival during raids, an index was calculated for each colony pair by taking the difference between the queen number ratio in the larger colony after and before raiding and the ratio of the smaller colony. Where the larger colony has proportionally fewer or more queen deaths than its rival, the index takes positive or negative values, respectively. I tested the relationship between this index and the natural log of the worker number ratio between the larger and smaller pair-mates with a linear regression model. Non-parametric post-hoc tests were implemented using the package *PMCMR* (Pohlert 2014). All averages are reported with (±) standard errors. Detailed MATESOFT and COLONY analysis conditions, technical caveats, and raw data are provided in the Appendix B.

Results

Social structure of mature field colonies

COLONY and MATESOFT detected polygyny in both populations, but significantly more frequently in SIE-A (Table 2.3, Fisher's exact tests, $P < 0.01$). COLONY inferred at least one rare matriline (i.e. represented by a single worker) in one CHI and ten SIE-A colonies. When these matrilines are excluded, SIE-A colonies still have significantly more matrilines per colony than CHI colonies (Table 2.3, SIE-A: 6.27 ± 0.83 matrilines, CHI: 1.18 ± 0.12 matrilines; one-tailed Mann-Whitney U test, $W = 119$, $P < 0.001$). Note, seven matrilines were inferred from the SIE14 female alates ($n = 21$); this is evidence that at least for this polygynous colony multiple queens produce workers and alates. Relatedness simulations support the presence of primary polygyny in the SIE-A population, showing that the observed r_{ww} and r_{QQ} in six SIE-A colonies are generally consistent with all nest-mate gynes being unrelated or descendants of at least two mothers (i.e. some but not all gynes are related, Table 2.3). The average SIE-A r_{ww} was significantly lower than that of CHI (SIE-A: 0.18 ± 0.05, CHI: 0.57 ± 0.04; one-tailed Mann-Whitney U test, $W = 24$, $P < 0.001$). There was a significant negative relationship between COLONY-inferred matriline number and r_{ww} (adjusted $R^2 = 0.741$, $F_{1,9} = 29.61$, $\beta = -0.057$, $P < 0.001$) but not with r_{QQ}. For colony SIE14, the r_{QQ} estimated from workers and female alates was less than and not significantly different from zero, respectively (worker: -0.05 ± 0.02, one-sample t-test, $t_{20} = 1.54$, $P = 0.139$; alate: 0.04 ± 0.02, one-sample t-test, $t_{14} = -2.39$, $P = 0.020$). CHI colonies' r_{ww} was significantly greater than 0.25 (Table 2.3), the value expected among offspring of a single polyandrous queen (one-tailed t-tests, *P values* < 0.05), therefore consistent with monogyny.

COLONY results suggest that polyandry occurs in both populations (Table 2.3). There were fewer polyandrous SIE-A matrilines (with at least two patrilines) than CHI matrilines (SIE-A: 45.44 ± 4.9%, CHI: 95.45 ± 4.55%, one-tailed Mann-Whitney U test, $W = 4.5$, $P < 0.001$). SIE-A matrilines associated with fewer patrilines than CHI matrilines (SIE-A: 2 ± 0.15 patrilines, CHI: 3 ± 0.28, one-tailed Mann-Whitney U test, $W = 23$, $P < 0.01$). MATESOFT estimated a $m_{e,p}$ of 1.44 ± 0.05 (jackknife standard deviation) for CHI colonies ($n = 8$). To obtain an estimate for the SIE-A population, I selected two COLONY-inferred matrilines each with at least ten workers and analyzed them with MATESOFT (Table 2.3). The estimated $m_{e,p}$ for SIE-A matrilines was 1.13 ± 0.03.

Effects of foundress number on queen survival and colony development

In 2014, all 125 CHI foundresses collected were haplometrotic. CHI foundresses exhibited antagonism when forced to associate in the laboratory. Territorial behaviors were seen in eight of the nine queen pairs observed (standing on top = 5 pairs, displaying = 8, fighting = 3). In contrast, 47.4% and 5.4% of SIE-A natural founding events were pleometrotic in 2013 and 2015 ($n = 19$ and 56), respectively. Up to four SIE-A foundresses were seen excavating together. SIE-A co-foundresses did not exhibit antagonistic behaviors towards each other in the field or in the laboratory. The average live weight of SIE-A foundresses in 2015 was significantly higher than CHI foundresses in 2014 (SIE-A: 74.4 ± 0.62 mg, CHI: 63.6 ± 0.41; two-tailed Mann-Whitney U Test, $W = 1553.5$, $P < 0.001$).

The survivorship of SIE-A foundresses in the first 60 days following colony initiation was independent of the initial foundress number in 2013 (Figure 2.2A, Wald test, $P = 0.057$) and 2015 (Figure 2.2B, Wald test, $P = 0.90$), but live weight did have a small but significant effect on survival (Cox hazard ratio < 0.001, $P < 001$; Wald test, $P = 0.001$). The proportional hazard assumption was satisfied in both 2013 and 2015. On the other hand, CHI foundress survivorship was negatively affected by foundress number (Cox hazard ratio = 3.5, 95% CI: 1.77-6.97, $P < 0.001$; Wald test, $P = 0.002$), but not by live weight ($P = 0.65$). Correlating scaled Schoenfeld residuals and time revealed that different foundress numbers have non-proportional hazards ($\rho = -0.33$, $\chi^2 = 3.91$, $P = 0.048$). Specifically, survivorship of pleometrotic CHI foundresses declined sharply after day 40 relative to haplometrotic foundresses (Figure 2.2C) in part due to queen culling by minim (per. obs.). The interaction between foundress number and time was significant as expected (Cox hazard ratio = 0.68, 95% CI: 0.60-0.77, $P < 0.001$). The power of each analysis was at least 90%.

Minim emergence latency differed between populations ($SIE\text{-}A_{2015}$: 33.05 ± 0.19 days, CHI_{2014}: 36.38 ± 0.29 days; exact two-tailed Mann-Whitney U test, $W = 1911$, $P < 0.001$) but not between founding strategies (asymptotic two-tailed Mann-Whitney U test, $W = 1129.5$, $P = 0.120$). Linear regression analysis showed that foundress number and colony age have positive effects on worker production in laboratory colonies. In the 2013 SIE-A laboratory population, worker number positively correlated with foundress number (Figure 2.3A, adjusted $R^2 = 0.144$, $F_{2,154} = 14.06$, $P < 0.001$, $\beta = 7.34$, $P < 0.001$), but not colony age. In 2015, worker production was significantly influenced by both foundress number (Figure 2.3B, adjusted $R^2 = 0.347$, $F_{2,290} = 78.51$, $P < 0.001$, $\beta = 10.16$, $P <$

0.001) and colony age (β = 0.15, P < 0.01). Foundress number and colony age also contributed to increased worker production in 2014 CHI colonies (Figure 2.3C, adjusted R^2 = 0.421, $F_{2,199}$ = 74.17, P < 0.001, β = 11.21 and 0.33, respectively, P values < 0.001). Similarly, foundress number and colony age influenced the average number of workers produced by each queen (adjusted R^2 = 0.140, $F_{2,640}$ = 53.31, P < 0.001), estimated by dividing the total number of workers by the foundress number. Per-queen production rose over time (β = 0.116, P < 0.001) but decreased with foundress number (β = -2.23, P < 0.001). In 2015 SIE-A colonies, 14.65 ± 5.80 % of the workforce in haplometrotic colonies (n = 12) and 23.83 ± 3.28% in pleometrotic colonies (n = 32) were made up of repletes at day 48 following colony initiation. These proportions differed significantly (exact one-tailed Mann-Whitney U test, W = 122.5, P = 0.033). However, the replete populations decreased in the following 35 days, to 8.36 ± 2.78% for haplometrotic colonies (n = 15) and 13.64 ± 1.96% for pleometrotic colonies (n = 34). Although these latter proportions did not differ significantly (P = 0.071), the difference between haplo- and pleometrotic colonies remained in the same direction.

Effects of worker number on queen survivorship during brood raids

In 2014, CHI laboratory colonies between 150 and 160 days-old were paired to examine the effect of worker number on brood raiding. These colonies had on average 34.5 ± 6.15 workers, with larger colonies having 2.9 ± 0.26 times (range 1.9 - 4.3) more workers than smaller rivals. In one 1-vs-2 pair (i.e. consists of a one-queen colony and a two-queen colony), the larger colony had a single queen, and in three 1-vs-1 pairs one colony had no brood when the experiment started. Queen mortality occurred in all CHI

pairs 2.45 ± 0.46 days after nests were connected. At the end of the experiment, 13 of 24 queens survived (54.2%), 10 of which were from the larger colonies (76.9%). Queens of larger colonies died in only 27% of the 11 pairs. However, linear regression did not reveal a significant relationship between workforce size and queen survivorship in the CHI samples. Surviving brood and workers from smaller colonies were eventually relocated to larger colonies in 82% and 91% of the pairs (n = 11), respectively.

In 2015, 92-day-old SIE-A colonies with an average of 35.54 ± 2.42 workers were paired. Larger colonies had 1.59 ± 0.09 times (range 1.05-2.84) more workers than smaller rivals. The larger colonies had one queen in two 1-vs-2 pairs, and one colony had no pupa at the beginning of the experiment in four pairs. In contrast to the CHI experiment, queen mortality occurred in only 10 of the 26 SIE-A pairs (38.5%) 11.1 ± 1.81 days after first contact. Eighty four of 96 queens survived the encounter, 54 of which belonged to the larger colonies. Mortality occurred earlier for queens from smaller colonies (9.33 ± 1.61 days, n = 6 queens) than for queens of larger colonies (13.2 ± 3.47 days, n = 5 queens) but this difference was not significant (two-tailed Mann-Whitney U test, W = 9, P = 0.16). In 70% of 26 pairs, the larger colony suffered fewer queen deaths. Linear regression showed the log ratio of worker number was positively correlated with the queen survival index (Figure 2.4; adjusted R^2 = 0.15, $F_{1,24}$ = 5.28, β = 0.689, P = 0.031). In other words, the survival probability of queens from larger colonies increased as the difference in workforce size increases in the larger colony's favor. Surviving brood and workers of rival colonies were eventually found together in the larger colony's nest in 58% and 62% of the pairs, respectively.

Unexpectedly in the 2015 SIE-A experiment, 29 of the 84 surviving queens (34.5%) relocated with their brood and workers to the rival's nest. These fusion events prevented unambiguous determination of the winning colony in 20 pairs, and occurred in all pairing combinations (1-vs-1: 20%, 1-vs-2: 25%, 2-vs-2: 10%, 1-vs-3: 25%, 2-vs-3: 20%, $N = 20$). Relocated queens often originated from smaller colonies (12 cases or 60%), but logistic regression failed to detect a significant relationship between workforce size difference and the relative size of the relocated queens' original colony. After the competition experiment was finished, marked relocated queens were found alive without detectable injuries, being groomed and fed by workers, and in most cases survived in their new home for several months. Two fused colonies were genotyped on day 279 and 304 after fusion, respectively, to determine the reproductive status of queens. Overall, the genotype profiles showed that original and relocated queens co-reproduced in fused colonies (Table 2.4), with 4-30% of the larval genotypes assigned to relocated queens. All Mm loci amplified for all queens while 14.3-17% of the sampled larvae failed to amplify one in three loci. In both colonies, the original queens shared no alleles at any loci examined, and one of the original queens shared an allele at one of the loci with a relocated nest-mate queen. Hence errors from misassigning larvae to queens are unlikely to account for these results.

Discussion

Taken together, these data demonstrate the existence of a social polymorphism in *M. mendax*. Unlike the Chiricahua (CHI) population, the Sierra Ancha (SIE-A)

population is overall characterized by more frequent pleometrosis, a higher frequency of polygyny, and greater number of reproductives in adult colonies. Moreover, relatedness estimates of field colonies and observations of colony founding in the laboratory suggest that primary polygyny occurs in the SIE-A population. Simulations showed that the observed intracolonial relatedness of multiple SIE-A colonies is consistent unrelated queens co-reproducing (Table 2.3). Low but non-zero relatedness coefficients (r) can come from primary-polygynous colonies (Helms Cahan and Helms 2012) since the estimate is influenced by queen number and the sampling distribution of sibships (e.g. sampling more family members tend to increase the estimate). Although low levels of within-colony relatedness can also be explained by the adoption of related, outbreeding queens over many generations (Keller 1995), pleometrosis arose repeatedly among random, likely unrelated SIE-A foundresses in the laboratory in 2013 and 2015, and led to stable polygynous colonies (Figure 2.2A, B). The absence of relatedness among female sexuals of colony SIE14 is further evidence that there were multiple unrelated queens reproducing in this colony. In contrast, the CHI data are consistent with predominantly haplometrosis and monogyny in adult colonies. Pleometrosis was not observed during the field collection following the mating flight in 2014, and when CHI foundresses were induced to jointly found new colonies in the laboratory, most immediately exhibited territorial behaviors. Queen aggression typically resulted in early mortality and the majority of two-foundress colonies rapidly reduced to monogyny (Figure 2.2C). I predict that pleometrosis and polygyny are rare in the CHI population and that if occur pleometrosis will usually lead to secondary monogyny and polygyny is a result of adopting closely related queens.

The large variation in the frequency of pleometrosis between 2013 and 2015 at the SIE-A field site is puzzling, and there is no satisfactory explanation for this observation. The 2015 mating flight started much later (6 PM vs. 2:30PM in 2013) which may leave foundresses with little time to mate and form groups before nightfall. Alternatively, perhaps the frequency of pleometrosis depends on foundress density and the number of foundresses was lower in 2015. This observation raises the possibility that the CHI population may experience similar fluctuations, and that pleometrosis may occur more frequently than observed by us. Indeed there is (rare) evidence in laboratory colonies of CHI foundresses cooperating. Similarly, it is not possible to entirely rule out primary polygyny because there were a small number of laboratory pleometrotic CHI colonies which retained all foundresses after workers emerged. In addition, 18% of adult CHI colonies genotyped had signature of multiple matrilines, and multiple related gynes can produce workers with relatedness coefficient similar to a single polyandrous gyne (Table 2 in Keller 1995). Despite these caveats, data from multiple sources still support a consistent and significant difference in social structure between the two focal populations.

Polyandry was detected in both populations, with CHI queens more likely to mate multiply and having more mates on average than SIE-A queens (Results). The power to detect patrilines associated with SIE-A matrilines was lower than CHI counterparts due to the presence of multiple matrilines in SIE-A colonies, and hence fewer workers per matriline for analysis. Multiple mating by queens increases intracolonial genetic diversity and has been suggested as an adaptation in advanced eusocial insects (Palmer & Oldroyd 2000). In particular, mating frequency has been shown to be positively correlated with

pathogen resistance (Hughes and Boomsma 2004), task specialization (Oldroyd and Fewell 2007), and colony productivity and fitness (Matilla and Seeley 2007). Our results are also consistent with the genetic variability hypothesis, which predicts that polyandry should be more common in monogynous populations than in polygynous populations because there are costs associated with multiple mating and polygyny already increases intracolonial genetic diversity (Keller and Reeve 1994). This pattern has been found in some studies (Keller and Reeve 1994; Schmid-Hempel and Crozier 1999; Hughes et al. 2008) but is absent in others (Pedersen and Boomsma 1999; Overson 2011).

Intraspecific variation in social structure has been observed in only one other congener, *M. mimicus*, which exhibits primary and secondary monogyny as well as some evidence of primary polygyny (Wheeler 1917; Bartz and Hölldobler 1982; Hölldobler et al. 2011). *M. mimicus* and *M. mendax* are congeners but not sister species (Snelling 1976; Kronauer et al. 2004). *M. mimicus* inhabits drier habitats at lower elevations than *M. mendax* (Snelling 1976) but the two species share similar life history features including repletism, territorial display, and brood raiding. On the other hand, very little is known about the social structure of the remaining *Myrmecocystus* taxa. *M. depilis*, the sister species of *M. mimicus*, is inferred to be obligatorily monogynous from genetic data (Hölldobler et al. 2011). Similarly, *M. mexicanus*, which belongs to the subgenus of nocturnal honey ants, was consistently found to have a single queen in excavated colonies (Conway 1980; Conway 1983; Conway 1990). These observations suggest that primary polygyny is probably a rare derived trait in this genus.

I hypothesize that primary polygyny is adaptive in *M. mendax*, due to its influence on the size of the workforce. Laboratory experiments consistently showed a positive

relationship between the numbers of foundresses and workers produced in incipient colonies across multiple years and populations (Figure 2.3). Having a large workforce confers several important benefits for *M. mendax* colonies during the ergonomic growth phase. I found that young laboratory colonies with multiple foundresses generally had more repletes than haplometrotic colonies. This trend can be explained by multi-queen colonies having more workers that can either serve as repletes or forage for extra food to feed the repletes. Additionally, territorial tournaments and raiding have been observed in *M. mendax* at the SIE-A field population (per. obs.) and our colony competition experiments showed that there is an advantage in terms of queen survival. Having more workers than the competitor during brood raids (Figure 2.4) increases the survival likelihood of queens. However, an absolute difference in worker number does not always prevent mortality for queens from the larger colony.

Certain ecological conditions may favor primary polygyny despite its downstream costs to individual queens in terms of sharing reproduction, because retention of multiple reproductives allows for advantages associated with workforce size to be maintained (Gadau and Fewell 2009). Despite the benefits to growth and survival during the ergonomic phase, queen cooperation can eventually become costly when the colony reaches sexual maturity. Per-capita production of sexual offspring is constrained by resource partitioning among nest-mate gynes. Cooperative gynes are also perpetually at risk of being taken advantage of by their nest-mates. If there are cheating queens that reduce their worker output to produce disproportionally more sexuals, the colony may destabilize unless the other gynes reduce their personal output of sexuals to maintain the workforce. These costs to reproductive fitness are maximized when gynes are not related

and consequently share no inclusive fitness, but ameliorated in secondary-monogynous colonies (Fournier and Keller 2001; Heinze et al. 2001; Fournier et al. 2004). This raises the question: why is polygyny still maintained in some pleometrotic *M. mendax* colonies? I propose that the evolution of primary polygyny in this species may be driven in part by colony density and territorial competition selecting for colonies with large workforce. Higher concentration of mature colonies at the SIE-A population (NND_{SIE-A} = 54.84 ± 27.40 m) likely reduces the availability of nesting sites and increases predation risks for incipient colonies, which in turn selects for pleometrosis. High colony density also results in greater overlap between territories and reduces resource availability, which can increase the frequency and severity of territorial conflicts. As adjacent colonies grow, those able to maintain a larger workforce are better at outcompeting neighbors. These dynamics might also explain why all of SIE-A adult field colonies sampled were polygynous (Table 2.3) even though haplometrosis was observed in the field (52.6 and 94.6% in 2013 and 2015, respectively) and in the laboratory. Naturally occurring haplometrotic colonies in the SIE-A population may have low survivorship and be less likely to reach reproductive maturity than pleometrotic counterparts. The rarity of polygyny in the CHI population (Table 2.3) can be explained by the lower density of mature colonies (NND_{CHI} = 209.31 ± 4.36), which suggests that intercolonial competition is less severe here and that the benefit of having a large workforce is small. Hence, haplometrosis leading to monogyny may be the the fittest strategy for queens where selection for cooperation is weak or absent, because it incurs no cost to sexual output.

I speculate that if there is strong selection for a large workforce in the SIE-A population, then mechanisms enabling colonies to increase queen number are also

favored here. Indeed, relatedness estimates of some SIE-A field colonies are consistent with secondary polygyny (Table 2.3), and laboratory colonies fused frequently during brood raids. There is also circumstantial evidence of queen adoption and colony fusion in the SIE-A field population (video recordings). Fusion has been reported in other polygynous species (Vásquez and Silverman 2008; Guénard et al. 2016) and proposed as one of several mechanisms generating polygyny secondarily (Crozier and Pamilo 1996). However, colony fusion is thought to be restricted to unicolonial species lacking territoriality (Passera 1994). *M. mendax* workers from the SIE-A population readily assumed the lateral display posture (Figure 1A), a stereotypical territorial behavior in honey ants (Hölldobler 1976), when interacting with non-nest-mate workers. Furthermore, brood raiding between laboratory colonies caused queen death, and adult field colonies were seen engaging in tournaments as well as raiding and killing queens of incipient colonies (per. obs.) These observations suggest that the SIE-A population is not unicolonial. Fusion can evolve even if there are costs associated with polygyny such as reduction in per-queen productivity and the emergence of reproductive skew, provided that the net fitness gain is positive for queens. Like primary polygyny, the fitness benefit of fusion is probably associated with the increase in workforce size. However, it is not clear why colonies would accept queens unrelated to resident gynes. One possibility is that adding queens can serve as insurance or contribute to future capacity of the colony to produce workers, and these benefits could compensate for low relatedness. High colony density can increase the frequency of encounter between neighbors and select for fusion due to the higher probability of queen survival in colonies with larger workforce when raiding occurs (Figure 2.4; Giraud et al. 2002). Mechanisms such as fusion and adoption

may maintain haplometrosis as a viable founding strategy in populations where there is strong selection for polygyny, given that haplometrotic colonies survive long enough to gain additional reproductive. Perhaps primary polygyny, queen adoption, and colony fusion are all present in the SIE-A population and can explain the fact that all mature field colonies analyzed in this work were polygynous despite the large proportion of haplometrotic founding events in 2015 (94.6%). Alternatively, if primary polygyny is the only viable strategy for SIE-A queens, haplometrosis would be an evolutionary dead end and should eventually disappear from this population.

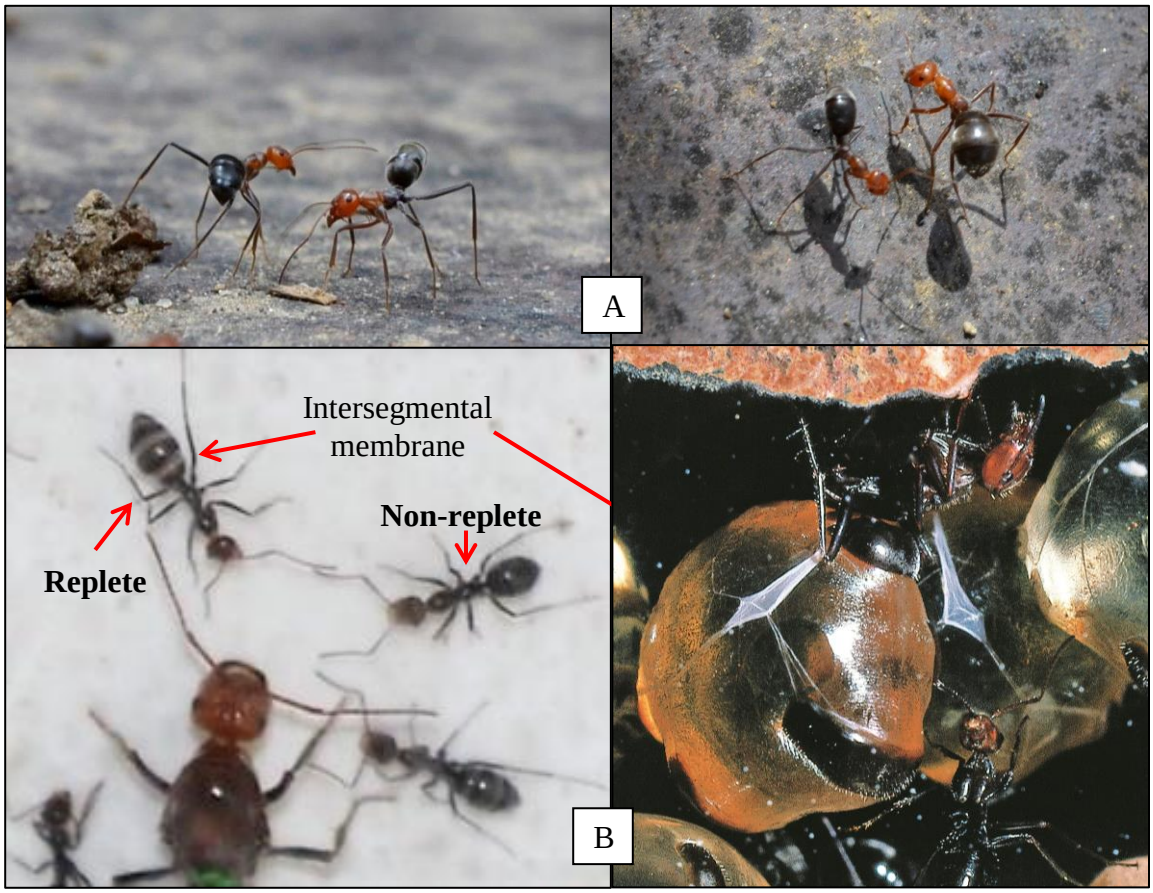

Figure 2.1. Panel A- *M. mendax* workers engaging in lateral display with stilted legs and raised gasters, a typical territorial behavior of honey ants, in the field (photographed by T. Eriksson). Panel B- A developing replete and a non-replete worker in a laboratory colony from the SIE-A 2015 cohort (right); note the difference in the stretching of the intersegmental membrane between the developing replete and a fully developed honeypot (left, photographed by B. Hölldobler).

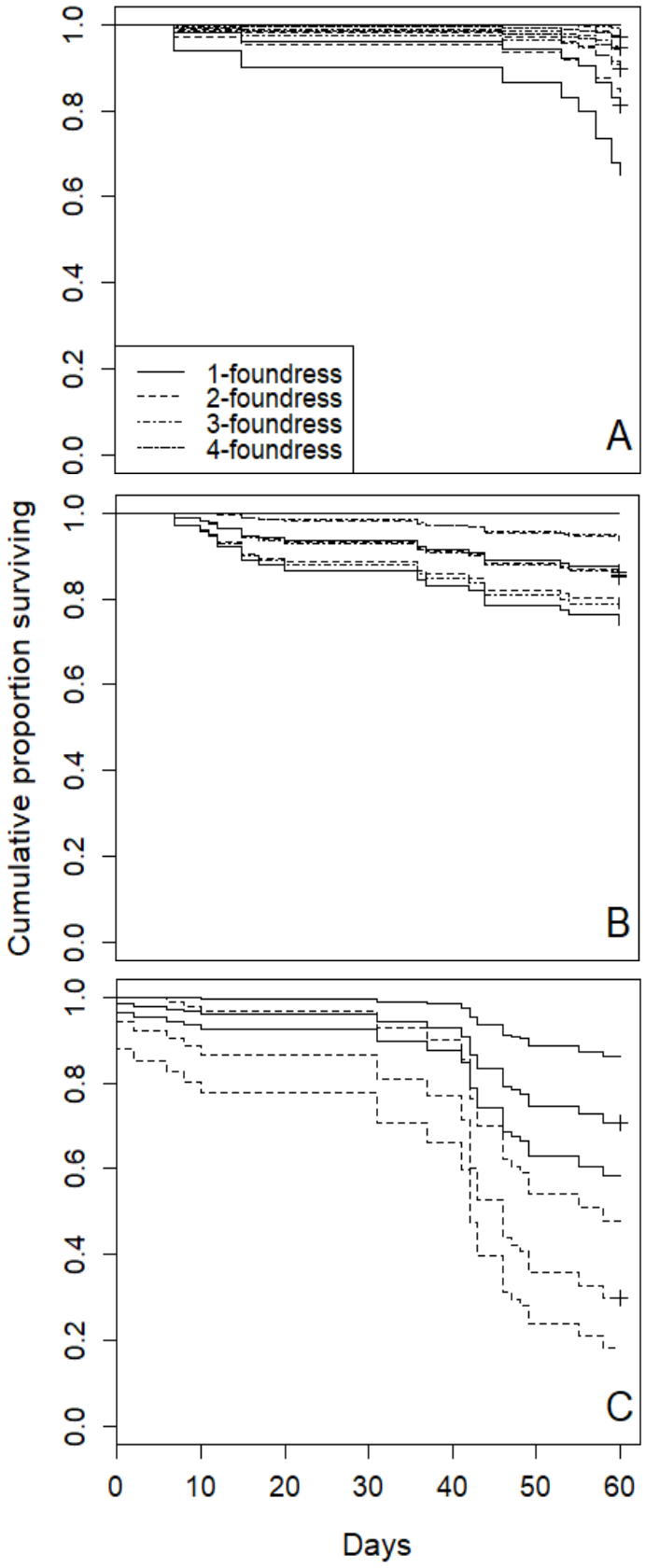

Figure 2.2. Kaplan–Meier foundress survival curves of the first 60 days after colony founding. Foundress number did not have any significant effect in SIE-A laboratory colonies (2013: A, 2015: B) but did in CHI colonies (2014: C). Each estimated curve (ends with + sign) comes with a 95% confidence envelope.

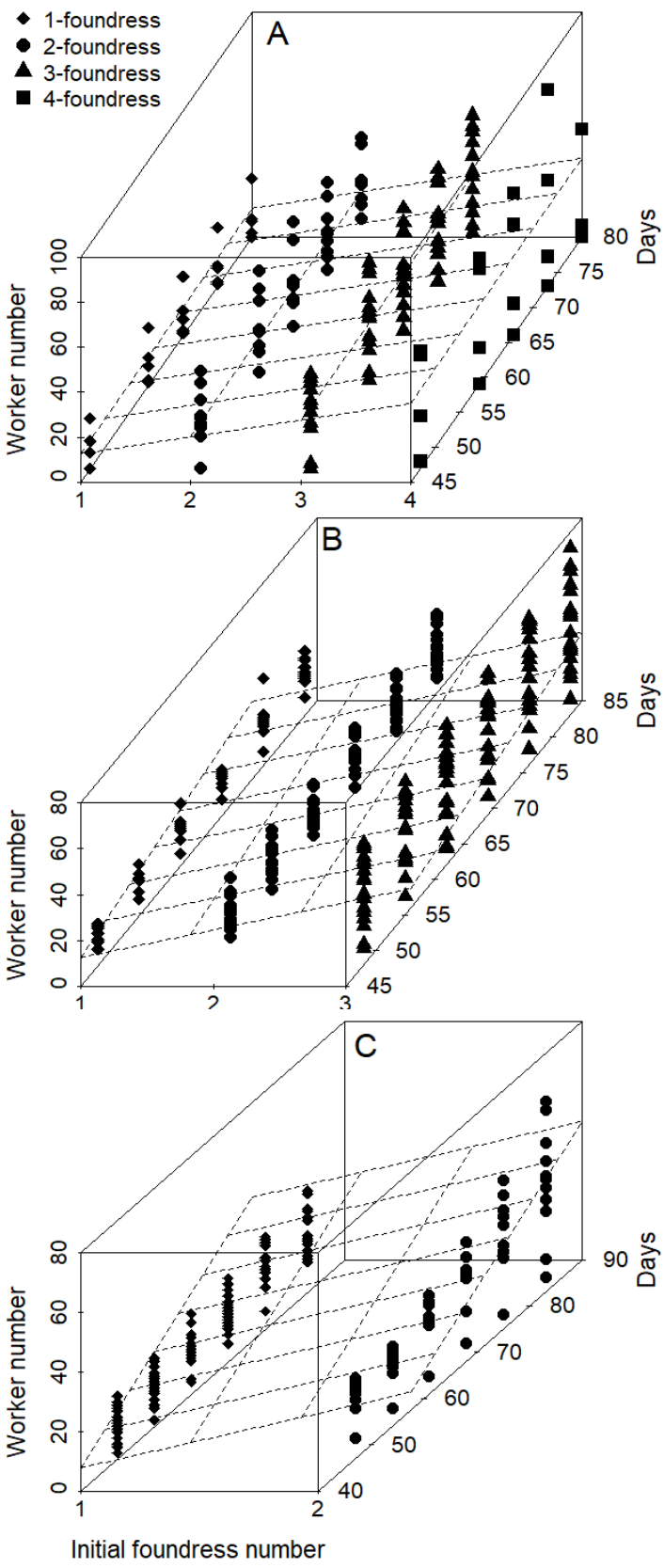

Figure 2.3. Worker production in laboratory colonies started by different number of foundresses between days 45-85 after founding. Foundress number has a significant, positive effect on worker number in SIE-A colonies of 2013 (A) and 2015 (B), and CHI colonies of 2014 (C). Dashed planes show the relationships of the data predicted by linear regression models.

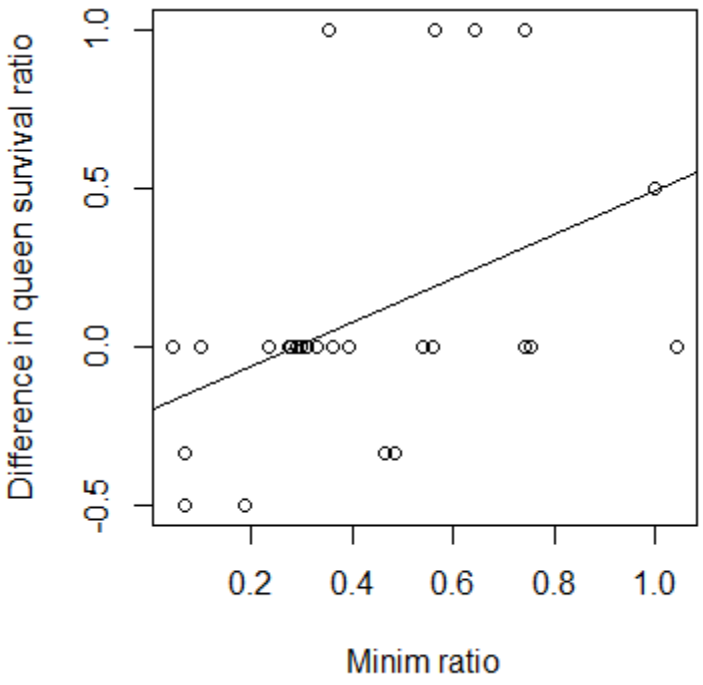

Figure 2.4. The relationship between minim ratio (log scale) and queen survival difference in paired SIE-A 2015 laboratory colonies. Each circle represents a pair. Positive and negative y-values correspond with the larger and smaller colonies suffered fewer queen deaths, respectively, while zeros indicate no difference. A linear regression model ($F_{1, 24}$ = 5.28, P = 0.031) suggested the likelihood of queen survival correlates with the asymmetry in workforce size between interacting colonies.

Table 2.1. Descriptions of microsatellite loci used in this study. The number of genotypes (n), the number of alleles (A), and the observed (H_o) and expected (H_e) heterozygosity for each population (CHI/ SIE-A) are listed.

Locus	**Size range (bp)**	**n**	**A**	**H_{obs}**	**H_e**
Mm3*	133-203/137-209	302/306	21/34	0.96/0.89	0.92/0.95
Mm4*	276-370/258-349	280/308	22/32	0.74/0.91	0.93/0.94
Mm5*	189-253/175-251	302/307	17/36	0.78/0.95	0.88/0.95
FE17**	129-193/131-225	294/302	5/36	0.41/0.78	0.46/0.92

*Kronauer and Gadau 2002, **Gyllenstrand et al. 2002

Table 2.2. Behavioral experiments and analyses (1st column) conducted in each population and year (2nd column). Sample sizes for each experimental group (3rd column) are separated by colons as follow: *laboratory colony founding*, *worker production* and *foundress survival*: one-, two-, three-, and four-foundress colonies; *minim emergence*: haplometrotic and pleometrotic colonies; *raiding*: 1-vs-1, 1-vs-2, 1-vs-3, 2-vs-2, and 2-vs-3 pairs (number refers to queen number of paired colonies, e.g. a 1-vs-1 pair consists of two colonies each has a single queen).

Experiment/analysis	**Population**	**n**
Laboratory colony founding	SIE-A 2013	17, 18, 24, 8 colonies
	SIE-A 2015	16, 19, 22 colonies
	CHI 2014	20, 20 colonies
Worker production	SIE-A 2013	6, 9, 13, 4 colonies
	SIE-A 2015	12, 17, 18 colonies
	CHI 2014	25, 12 colonies
Foundress survival	SIE-A 2013	11, 34, 63, 32 queens
	SIE-A 2015	16, 38, 66 queens
	CHI 2014	20, 40 queens
Minim emergence	SIE-A 2015	21, 23 colonies
	CHI 2014	32, 13 colonies
Raiding	SIE-A 2015	4, 6, 7, 3, 6 pairs
	CHI 2014	9, 2 pairs

Table 2.3. Queen number, mating frequency, and relatedness coefficient (worker: r_{ww}, inferred matrilines: r_{QQ}) estimated from (n) worker genotypes. Gyny was inferred from MATESOFT analyses. Matriline and patriline numbers were estimated from COLONY results (excluding rare matrilines). Superscripts designated simulation results: estimated relatedness coefficients are consistent with all matrilines being unrelated (a), a mixture of unrelated and related individuals (b), or related (c).

Colony	**n**	**Gyny**	**Matriline number**	**Patriline number**	r_{ww}	r_{QQ}
CHI2	30	mono	1	3	0.441	-
CHI3	27	mono	1	4	0.750	-
CHI4	26	mono	1	2	0.589	-
CHI6	30	poly	1	3	0.511	-
CHI8	29	poly	1	3	0.327	-
CHI9	28	poly	2	2.5	0.575	0.196
CHI10	29	mono	2	1.5	0.580	0.06
CHI11	28	mono	1	4	0.766	-
CHI12	28	mono	1	4	0.425	-
CHI17	28	mono	1	4	0.533	-
CHI20	25	mono	1	2	0.750	-
SIE6	24	poly	5	2.4	0.169^{b}	0.114^{c}
SIE7	25	mono	2	1.3	0.518^{c}	-0.127^{b}
SIE8	30	poly	7	2.4	0.134^{b}	0.130^{c}
SIE9	30	poly	8	2.6	0.101^{b}	0.078^{a}
SIE10	30	poly	8	2.1	0.035^{b}	0.019^{a}
SIE12	29	poly	6	1.7	0.046^{b}	0.037^{a}
SIE14	30	poly	7	2.3	0.053^{a}	0.016^{a}
SIE16	29	poly	2	2.0	0.510^{c}	0.329^{c}
SIE17	25	poly	2	1.5	0.285^{c}	-0.104^{c}
SIE18	26	poly	6	1.3	0.091^{b}	0.065^{a}
SIE20	30	poly	8	2.5	0.039^{b}	0.026^{a}

Table 2.4. The number of larvae and queens genotyped for two fused colonies, and the queens' identity (original or relocated) and their respective representation in the larva sample.

Colony	**Larva**	**Number of surviving queens**		**Queen representation**	
		Original	Relocated	Original	Relocated
SIE_L25-43	46	2	2	69.57%	30.43%
SIE_L24-49	28	2	1	96.43%	3.57%

CHAPTER 3

A MULTI-POPULATION ANALYSIS OF SOCIAL VARIATION, GENETIC STRUCTURE, AND ECOLOGY IN *MYRMECOCYSTUS MENDAX*

Introduction

Intraspecific variation in gyny and queen number has been observed in many ant species (Heinze and Keller 2000; Keller and Reeve 1994; Rissing and Pollock 1988). A population may engage in both monogyny and polygyny with frequencies that vary geographically (Ross and Fletcher 1985; Overson 2011; Helms and Helms Cahan 2012). A positive relationship between latitude and the frequency of polygynous species has been documented in a number of alpine and arboreal taxa (Heinze 1993; Heinze and Hölldobler 1994). In the ant fauna of the American Southwest, this trend is observable in *Veromessor pergandei* (Helms and Cahan 2012), but is inverted in *Pogonomyrmex californicus* (Overson et al. 2011).

The relationship between latitude and polygyny may be mediated by climate. Predominantly polygynous populations have been found in habitats with extreme temperatures and low humidity, and there is some evidence that these abiotic factors play a selective role in the evolution of social variation (Gadau and Fewell 2009). For instance in colder climates, polygyny is thought to be involved in reducing freezing and starvation mortality by enabling metabolic heat and food exchange (Leirikh 1989; Heinze et al. 1996). Similarly, queen cooperation may provide mechanisms to cope with desiccation and heat shock, two major causes of mortality in workers and queens in hot, xeric environments (Kay and Whitford 1975; Whitford et al. 1975; Rissing et al. 1986; Johnson

2004). For instance, pleometrosis may enable the excavation of deeper, better insulated incipient nests and reduce cuticle abrasion in co-foundresses, a type of damage associated with increased water loss (Johnson 2004). Alternatively, mature colonies can adopt related (daughter) queens, eliminating the costs of independent colony founding. Having multiple reproducing queens can also increase the efficiency of worker turnover, a predictor of colony fitness (Kwapich et al. 2017) that may be particularly important in habitats where food availability and accessibility is seasonal and the foraging window is short, thus heightening intraspecific competition.

Here I demonstrate that *M. mendax* is socially polymorphic in populations outside of the Sierra Anchas (cf. Chapter One) across Arizona and northern Sonora, and exhibits substantial population substructuring. I describe the relationships between the genetic structure and social variation, and between social variation and two abiotic variables, temperature and precipitation. Lastly, I speculate about the roles of geographical isolation and climate-mediated selection on social structure in shaping the observed genetic structure.

Materials and methods

Sampling

The study area was defined by a 140,000-km^2 rectangle centered at 32.870820°, -110.437851°. In addition to the Sierra Ancha and Chiricahua populations (Chapter Two), thirteen new locations were sampled in 2013-2017, bringing the total number of populations examined to 15 (Figure 3.1). Six sites are located in mountain ranges in

central and northern Arizona (Sierra Ancha, Mt. Ord, Show Low, Pinal Peak, Sedona, and Superstitions). The remaining nine sites are situated in sky islands in southeastern Arizona (Chiricahuas, Dragoons, Huachucas, Mt. Graham, Mt. Lemmon, Patagonia, Santa Ritas, and Whetstones) and northern Sonora (Sierra Buenos Aires). These two groups will be referred to collectively as the northern and southern sites, respectively. The coordinates and abbreviations of the sites, which will be used from this point forward, are in Table 3.1.

Coordinates of all colonies discovered at each site were used to estimate nearest-neighbor distance (NND, Table 3.1). At each new site, workers from 7 - 10 colonies were genotyped (n = 10 workers/colony). Genotypes of SIE-A and CHI colonies from 2011 (presented in Chapter Two) were randomly sampled to form subsets containing 10 genotypes per colony. Following sample-size standardization, these colonies were included in the analyses of this chapter. In total, 139 colonies across 15 geographical populations were analyzed.

Genotyping

DNA extraction and PCR amplification of the four microsatellite loci (Mm3, 4, 5, and FE17) for workers of new sites followed the protocols established in the Chapter Two. The size of amplified fragments was analyzed using an ABI 3730 DNA Analyzer, and alleles were scored using Genemapper® program (ThermoFisher Scientific). I identified unique and shared alleles at the colony, site, and total population levels. Only standardized genotypes were used in downstream statistical analyses. To perform the SIE-A and CHI rarefaction, representative workers from 2010 field colonies were re-

genotyped using the ABI sequencer, and used as standards to size-normalize the remaining genotypes. Marker statistics for each population are in Table 3.2. All genotypes generated in this Chapter are provided in Appendix C.

Statistics

Social variation

Queen number and mating frequency inferences followed the protocol described in the previous chapter. MATESOFT was used to estimate the pedigree effective mate number ($m_{e,p}$) and proportion of multiply mated queens (D_{est}) in colonies compatible with monogyny; rejected colonies were inferred to be polygynous. COLONY was use to infer matrilines and patrilines in all colonies. The minimum number of male mates per queen was estimated from parental genotypes reconstructed by COLONY. Matrilines inferred by COLONY were categorized as either rare (associated with a single worker in a colony) or common (represented by two or more workers in a colony). Intracolonial relatedness was estimated for workers (r_{ww}) using the package *related*. Excluding rare matrilines, the Shannon-Weaver diversity index (H') was calculated for each colony to take into account both the matriline number and the reproductive skew among nest-mate matrilines, by the package *vegan* (Oksanen et al. 2016). H' increases with matriline number and the evenness of reproductive contribution. Due to the lack of colony founding observations for the new populations, this chapter describes variation in gyny but not in the mode through which it arose (e.g. primary vs. secondary). Sampled colonies were assumed to have reached maturity, or at the very least have developed beyond the founding stage due to the presence of major workers at the nest entrance,

many of which were collected and genotyped (per. obs.) and at least one was pinned for most colony (see voucher collection).

Genetic structure and gene flow

Allele counts and richness, observed (H_{obs}) and expected heterozygosity (H_{exp}), F_{is} (Weir and Cockerham 1984), pairwise θ (a commonly used estimator of F_{st}, Weir and Cockerham 1984), and pairwise G''_{st} (an unbiased estimator of F_{st}, Meirmans and Hedrick 2011) were estimated using the package *diveRsity*. I tested for Hardy-Weinberg equilibrium and population differentiation using the program GENEPOP v1.2 (Raymond and Rousset 1995; Rousset 2008). I also estimated the number of migrants per generation (Nm) using the private allele method (Barton and Slatkin 1986, implemented in GENEPOP) and from θ (by applying the absolute values of θ to the formula$Nm = \frac{1-\theta}{4*\theta}$).

To test for isolation by distance among sites (IBD), I examined the correlation between the matrices of genetic (θ and G''_{st}) and geographical distance using GENEPOP, which called the program ISOLDE to perform Mantel tests (4999 permutations each). The geodesic distances between sites were calculated by the package *geosphere* (Hijmans 2015) using the coordinates of a randomly chosen field colony; the coordinates of the Southwestern Research Station were used for CHI instead. I used the program STRUCTURE (Pritchard et al. 2000) to characterize the genetic composition of the sampled sites. STRUCTURE analyzed three separate datasets using the admixture model without any priors, each comprised of a different worker genotype from each colony; runs were conducted using the admixture model, but ignore site membership. For the

STRUCTURE analysis and F_{st} estimation, the dataset comprised of all 15 populations, each with all of its colonies represented by a single, randomly chosen worker genotype (*n* = 7 - 10 colonies). I also used partial Mantel tests, implemented in the package *vegan*, to examine whether or not genetic and geographical distance influenced the distribution of social variation. Each partial Mantel test contains 999 permutations and estimated the Pearson r statistic.

Climate variation

To assess climate variability in Arizona, I obtained longitudinal data from the online archive of the Western Regional Climate Center (https://wrcc.dri.edu). The dataset included 272 monitoring stations across the state and spanned 1892 – 2010 (119 years). Coordinates and elevation of the stations were also retrieved. The number of years with record for each station ranging from eight to 119 years, with an average of 53.7 years. Using linear regression analysis, I examined how latitude, longitude, and elevation influenced the following climate variables: monthly average ambient temperature, monthly maximum and minimum ambient temperatures, annual number of days below 0°C and above 32°C, seasonality (the standard deviation of the monthly average temperature of all months) and annual precipitation. I then predicted the conditions at *M. mendax* sites using the fitted linear equations and spatial data of all 139 colonies genotyped, and examined the relationships between climate and social structure.

Results

Queen number

The microsatellite data generated in this study provide evidence that polygyny occurs in other locations beside SIE-A (cf. Chapter Two). MATESOFT and COLONY inferred multiple matrilines in 10-50% of HUA, LEM, ORD, PIN, and SED colonies (Table 3.3). CHI, DRA, SIE-B, SHO, and WHE also have signature of polygyny in 10-25% of colonies according to COLONY but not MATESOFT. The remaining four populations were consistently inferred to be monogynous using both methods. HUAC and LEM have one and two colonies, respectively with r_{ww} significantly lower than 0.25 (Figure 3.2, one-tailed exact Wilcoxon test, $P < 0.05$). Eight of ten SIE-A rarefied colonies have r_{ww} significantly lower than 0.25. For the other sites, colonies inferred to be polygynous by COLONY and MATESFOT have r_{ww} equal to or greater than 0.25. Polygynous colonies in new sites have between 1.1 ± 0.1 and 1.6 ± 0.221 common matrilines, on average (i.e. matrilines represented by more than one worker). There was a consistent positive relationship between matriline number and the frequency of polygynous colonies (Figure 3.3, linear regressions, $F_{1,13} = 146.6$, adjusted $R^2 = 0.91$, *P values* < 0.001). This correlation still remained when all monogynous populations were excluded (linear regressions, $F_{1,5} = 46.02$, adjusted $R^2 = 0.88$, *P values* < 0.005). The results of rarefied SIE-A and CHI data showed that the queen number inferences of Chapter Two were robust even when samples where reduced from 30 to ten workers per colony.

Mating frequency

Polyandry was detected in all populations. Excluding SIE-A with an insufficient number of maternal sibships, on average the global D_{est} was 0.93 ± 0.06 (range = 0.7 - 1). COLONY inferred polyandrous matrilines in 67.17 ± 5.2% of colonies (range = 30 - 100%), with polyandrous colonies being significantly more common (n = 139 colonies, χ^2 = 15.89, df = 1, P < 0.001). The number of patrilines associate with each matriline per colony was 1.77 ± 0.07 (Table 3.3), with double-mating being more common than higher mating frequencies (Figure 3.4, n = 93 colonies, χ^2 = 40.01, df = 1, P < 0.001). The $m_{e,p}$ averaged across sites was 1.72 ± 0.063. Patriline number and frequency of polyandrous colonies estimated by COLONY were positively correlated (linear regression, β = 1.2, $F_{1,13}$ = 49.81, adjusted R^2 = 0.77, P < 0.001), but neither variables had a significant relationship with matriline number nor frequency of polygynous colonies. Colonies with $r_{ww} \leq 0.5$ were present in all sites (Figure 3.2, one-tailed exact Wilcoxon test, P < 0.05). COLONY patriline and common matriline numbers together accounted for most of the r_{ww} variation (multiple linear regression, β_{patr} = -0.2, β_{matr} = -0.3, $F_{2,12}$ = 63.97, adjusted R^2 = 0.9, P *values* < 0.001).

Genetic structure

Several signatures of population subdivision were detected in the genotype data. Across all sites and loci, there were fewer heterozygotes than expected under Hardy-Weinberg equilibrium (global tests, H_1 = heterozygote deficiency, P < 0.001). Likewise, allele and genotype distributions differed significantly between sites (Fisher's exact test, df = 8, P < 0.001). STRUCTURE identified three well-supported genetic clusters that

explain the variation in 139 colonies (Figure 3.5). Some proportion of each cluster was present in each analyzed colony representative (frequency range = 0.012 - 0.97), suggesting some degree of admixture. Cluster 1 was most evident in the northern sites (average across colonies >50%), while Cluster 2 and 3 dominated southern sites (Figure 1). However, there were two exceptions to this association. SHO, one of the northernmost sites, has a higher proportion of Cluster 3, while LEM, situated in the Santa Catalina Mountains of southern Arizona, has a greater representation of Cluster 1 (Figures 3.1 and 3.5). The structure is supported by θ and G''_{ST} estimates of genetic distance between populations (Tables 3.4 and 3.5). Specifically, within-cluster distances are significantly smaller than between-cluster distances for both estimators (θ: Kruskal-Wallis test, χ^2 = 63.24, df = 3, $P < 0.001$; Nemenyi test, $P_{between\ vs.\ within} < 0.001$; G''_{ST}: Kruskal-Wallis test, χ^2 = 67.27, df = 3, $P < 0.001$; Nemenyi test, $P_{between\ vs.\ within} < 0.001$)

Gene flow

The global *Nm* estimated from private alleles was 1.12 migrants/generation, lower than estimates from among southern and northern sites (1.34 and 1.53, respectively). *Nm* estimated from θ (Table 3.6) suggested sites assigned to the same genetic cluster exchanged relatively higher numbers of migrants than sites belong to different clusters (within cluster = 76.16 ± 57.38 migrants/generation, between clusters = 3.02 ± 0.21 migrants/generation; Wilcox test, W = 81, $P < 0.001$). Although on average there were fewer migrants among northern sites than among southern sites (θ, northern = 8.19 ± 1.62, southern = 71.06 ± 55.98), the difference was not significant (Wilcox test, W = 263.5, P = 0.73). A non-significant difference was also observed between clusters.

Significant IBD was detected in the complete sample (Mantel test, Spearman Rank correlation one-tailed $P_\theta = 0.0016$ and $P_{G"ST} = 0.002$). IBD was also detected among northern sites ($P_\theta = 0.044$ and $P_{G"ST} = 0.011$) and Cluster 1 members ($P_{G"ST} = 0.023$), but not among either southern sites ($P_\theta = 0.322$ and $P_{G"ST} = 0.23$) or among members of Clusters 2 and 3 ($P_{G"ST} = 0.16$). Figure 6 shows that genetic and physical distances are not positively correlate when SHO and LEM are compared with the other sampled populations. In particular, pairwise $G"_{ST}$ values suggests that SHO is more closely related to distant sky island sites (0.354 ± 0.081), than it is to other nearby northern sites (0.822 ± 0.031; Wilcox rank sum test, $W = 2$, $P < 0.005$; Table 3.5). The opposite pattern can be seen for LEM, but the statistical measure is not significant (northern = 0.438 ± 0.106, southern = 0.738 ± 0.052; Wilcox rank sum test, $W = 9$, $P = 0.059$; Table 5).

Relationships between social and genetic structures

A relationship between social structure variation and genetic structure was supported by some analyses. There was a significant positive correlation between the MATESOFT polygyny frequency and $G"_{ST}$ by site (Partial Mantel test, $r = 0.21$, $P = 0.002$), but not with geographical distance between sites and not with θ. This relationship with genetic distance was not observed with COLONY estimates. MATESOFT polygyny frequency differed significantly between the genetic clusters (Kruskal-Wallis test, $\chi^2 = 7.186$, $df = 2$, $P = 0.028$); specifically, polygyny occurred more frequently in Cluster 1 (28.75%) than Cluster 3 (2.86%; Dunn's test, $P = 0.046$). The same pattern could be seen with the COLONY estimates of polygyny frequency and matriline number, but the differences between clusters were not significant. The interaction terms of the proportion

of the clusters represented in colonies predicted gyny (MATESOFT estimates, multiple logistic regression, $P_{Clusters1,3} = 0.0348$, $P_{all\ three} = 0.0171$) and matriline number (COLONY all and common matrilines, multiple linear regressions, $P < 0.05$). Furthermore, MATESOFT polygyny frequency positively correlated with H_{obs} (linear regression, $\beta_{gyny} = 0.0018$, $F_{1,13} = 5.7$, adjusted $R^2 = 0.25$, $P = 0.033$), and with average allele richness (linear regression, $\beta = 0.024$, $F_{1,13} = 7.467$, adjusted $R^2 = 0.32$, $P = 0.017$)

Climate trends

According to historical data, the climate of Arizona varied geographically. Monthly average temperature was negatively correlated with latitude and elevation (multiple linear regression, $\beta_{lat} = -0.40$, $\beta_{elv} = -0.0061$, $F_{2,269} = 519.3$, adjusted $R^2 = 0.79$, *P values* < 0.001). Monthly minimum temperature have negative relationships with all spatial attributes (multiple linear regression, $\beta_{lat} = -0.98$, $\beta_{long} = -1.17$, $\beta_{elv} = -0.0063$, $F_{3,267} = 106.1$, adjusted $R^2 = 0.54$, *P values* < 0.001), while maximum temperature correlated negatively with latitude and elevation but positively with longitude (multiple linear regression, $\beta_{lat} = -0.45$, $\beta_{long} = 0.25$, $\beta_{elv} = -0.0071$, $F_{3,268} = 106.1$, adjusted $R^2 = 0.98$, *P values* < 0.001). The annual number of days with subzero temperature was positively correlated with latitude and elevation (multiple linear regression, $\beta_{lat} = 7.78$, $\beta_{elv} = 0.084$, $F_{2,269} = 599.3$, adjusted $R^2 = 0.8$, *P values* < 0.001), while days over 32°C correlated positively with latitude and longitude but negatively with elevation (multiple linear regression, $\beta_{lat} = 1.37$, $\beta_{long} = 4.9$, $\beta_{elv} = -0.097$, $F_{3,268} = 2014$, adjusted $R^2 = 0.97$, *P values* < 0.05). Seasonality increased with latitude and decreased with elevation (multiple linear regression, $\beta_{lat} = 0.12$, $\beta_{elv} = -0.00041$, $F_{2,269} = 6.88$, adjusted $R^2 = 0.042$, *P values* <

0.05). Total yearly precipitation decreased with latitude and longitude but increased with elevation (multiple linear regression, β_{lat} = -5.01, β_{long} = -2.91, β_{elv} = 0.024, $F_{3,268}$ = 147.6, adjusted R^2 = 0.62, *P values* < 0.001).

Climate variation and social polymorphism

The monthly average temperature was a positive predictor of MATESOFT frequency of polygynous colonies (multiple logistic regression, β_{ave} = 229, P = 0.002); there were also significant interaction effects among monthly average, maximum, and minimum temperatures (P < 0.05). Temperature also correlated with COLONY all matriline number (multiple linear regression, β_{ave} = 38.31, β_{min} = -28.18, β_{max} = -19.4, $F_{7,120}$ = 91.63, adjusted R^2 = 0.13, *P values* < 0.05) with significant interactions present. The numbers of days below 0°C and above 32°C both increased the likelihood of polygyny (multiple logistic regression, β_{below0} = 0.077, $\beta_{above32}$ = 0.085, *P values* < 0.05), and their interactions influenced matriline number (both all and common matriline number, multiple linear regressions, β = 0.0003 - 0.0008, *P values* < 0.05). Colony gyny and matriline number were also positively correlated with seasonality (logistic regression, β_{gyny} = 4.88, P < 0.01; linear regression, $\beta_{all.mat}$ = 2.25, $F_{1,126}$ = 91.63, adjusted R^2 = 0.067, P < 0.005). Precipitation was negatively correlated with polygyny (logistic regression, β = -0.11, P = 0.007), and matriline number (both all and common matriline, linear regressions, β < -0.01, adjusted R^2 = 0.05, *P values* < 0.01). Northern sites and members of Cluster 1 were predicted to have experienced more days during which foraging condition is suboptimal (below 0°C and above 32°C), less precipitation annually, and

greater magnitude of seasonality than southern sites and members of Clusters 2 and 3 (Figure 3.7; Wilcox tests, *P values* < 0.05).

Discussion

The comprehensive sociogenetic analysis described in this chapter provides additional evidence of social variation and polygyny in *M. mendax*. Queen number estimates suggest that multi-matriline colonies are present in HUAC, LEM, ORD, and SED (Figure 3.1). However, the intracolonial relatedness estimates of most of these colonies were more consistent with monogyny (Figure 3.2). It is possible that reproduction is skewed or sampling was biased if there are in fact multiple gynes in these colonies; alternatively, nest-mate gynes may be related (Keller 1995) or supernumerary matrilines are artefacts of brood raiding. Further analysis of LEM and HUAC colonies with r_{ww} less than 0.25 showed that r_{ww} is effectively zero, suggesting primary polygyny (Figure 3.2). However without colony founding observation, this result is insufficient to suggest that cooperation among non-kin is present outside of SIE-A. In addition, the developmental stage of colonies and the extent of brood raiding are unknown, further limiting the power of the inferences. Conservatively, polygyny is probably infrequent but not rare in *M. mendax*, occurring in about one in three populations in the area encompassing Arizona and northern Sonora with 10 – 100% of colonies containing multiple matrilines. SIE-A is the upper extreme, with the highest frequency of polygynous colony and matriline number per colony observed so far.

On the other hand, polyandry is widespread across populations. Queens often mate with multiple males (Table 3.3), with double-mating being most frequent (Figure

3.4). An average effective paternity frequency of 1.72 suggests that most males contribute genetically to producing offspring. The negative relationship between polygyny and polyandry observed in the previous chapter was not significant in this larger set of samples. This result is therefore inconsistent with the genetic variability hypothesis as an explanation for the evolution of polyandry or polygyny, which predicts the presence of a negative correlation where there are costs to multiple-mating and increasing intracolonial genetic diversity is beneficial (Keller and Reeve 1994). However, it is possible that the observed paternity is a minimum estimate of mating frequency (Strassman 2001), and perhaps genotyping the spermatheca of mated queens is necessary to obtain more accurate estimates of mating frequencies to address this hypothesis.

COLONY and MATESOFT inferred different gyny in 8.6% of colonies examined (n = 139). In five and seven instances, MATESOFT detected signatures of multiple queens but not COLONY and vice versa, respectively. Discrepancies occurred in both northern (n = 8) and southern populations (n = 7). One possible explanation may pertain to how the programs handle errors such as sequencing artefacts and mistyping mistakes. Both programs reconstruct queen genotypes from worker multilocus genotypes and population allele frequencies. MATESOFT reconstructs one locus at a time while assuming the lowest possible number of male mates that can explain the worker genotypes (Moilanen et al. 2004). When encountering a locus at which a putative queen has to be heterozygous for and multiple mating is likely, MATESOFT would raise the polygyny exception if it detects more than one putative queen genotype present in all workers of a given colony. Therefore MATESOFT inferences are likely more sensitive to genotyping errors, which are not accounted for in its algorithm, leading to an

overestimation of queen number in some datasets. On the other hand, COLONY employs a maximum likelihood approach to search for putative matrilines in a genotype space defined in part by user-given parameters such as mating behaviors of males and females (i.e. single or multiple mating) while simultaneously accounting for mistyping error and allele dropout. The best configuration returned to user depends on the likelihood calculations, which can sometimes overestimate queen number even in datasets apparently compatible with monogyny.

Genetic structure in *M. mendax* in the region examined is evident from a global deficiency of heterozygotes, signatures of genetic differentiation and reduced levels of gene flow between sites compare to within sites. Specifically, most populations are mixtures containing genetic material derived from up to three distinct genetic clusters (Figures 3.1 and 3.7). The observed subdivision can be explained partially by geographic isolation. A global signature of IBD was detected, with an overall *Nm* estimated from private alleles of 1.12. Significant IBD is also present among northern populations, but not among southern populations on Madrean sky islands. This result is somewhat unexpected because the average geographical distance between northern populations (n = 6) is not significantly different from that of the sky islands (n = 9; Wilcox test, W = 288, P = 0.721), and both regions have similarly low rates of recent migration (*Nm* estimated from private alleles, south = 1.34 migrants/generation, north = 1.53 migrants/generation; Yamamichi and Innan 2012), and moderate to high on longer time scales (south = 71.06 migrants/generation, north = 8.19 migrants/generation). There was no evidence of population bottlenecks, as the level of genetic diversity was comparable between regions (Table 3.1). Perhaps high mutation rates in our microsatellite markers and large

population size are limiting the rate at which variation is lost to drift, even when regional admixture is weak or absence.

In addition, selection on social structure mediated by climate may also contribute to the observed population structure. The effects of climate on shaping biodiversity have been characterized for oceanic islands (Abbot 1947; Gillespie and Roderick 2002). In ants, polygyny is often associated with higher latitude and extremely hot, cold, or dry climate (Table 2.1 in Gadau and Fewell 2009). The data suggest that *M. mendax* colonies in warmer and drier areas are likely to have more queens, and sites experiencing more dramatic change in monthly temperature or longer periods during which foraging is suboptimal also tend to have a higher frequency of polygynous colonies. The climate gradients extending from southern to northern Arizona can create selective pressures that vary spatially, to which local populations must adapt. Like other ectotherms, ants rely on the external environment to maintain physiological homeostasis and are therefore probably more vulnerable to the extreme conditions. High temperature and low humidity, characteristics of xeric environments, can directly cause mortality in workers and queens through desiccation and heat shock (Kay and Whitford 1977; Lach et al. 2009). Low levels of annual precipitation and unpredictable rainfall pattern can also reduce the abundance and accessibility of food sources. Furthermore, temperature at both extremes can create behavioral barriers that narrow the daily and yearly foraging period (Kay and Whitford 1977; per. obs.). It is clear that abiotic conditions can negatively impact colony fitness.

There is circumstantial evidence that abiotic conditions affect foraging activity in *M. mendax*. In the field, I have observed foragers succumb to high surface temperatures

(60 - 70°C), and heat avoidance behaviors from workers (e.g. running on stilt legs, resting on vegetation, retreating from sun exposure). Desiccation was shown to be more lethal for liquid-feeding genera (Whitford et al. 1975). I have also recorded footages of tournaments, and termite foraging following monsoon rains in *M. mendax*. The tournament behavior is thought to have evolved in *M. mimicus* as a mean to more economically defend food sources with unpredictable availability, such as termites (Hölldobler and Lumsden 1980; Hölldobler 1981). *M. mendax* colonies are also likely to have to compete for temporally and spatially variable resources influenced by climate (e.g. termites, dead arthropods, nectars), necessitating territoriality. Climate data suggest that in certain part of the range colonies are under more environmental pressures (Figure 3.7), which may promote the evolution of queen cooperation. Using a critical thermal minimum of 12°C and critical thermal maximum of 45°C (Kay and Whitford 1977) and ambient temperature recorded at colony SIE5 (n = 93,519 time points, June 2015 - January 2017), I estimated that *M. mendax* colonies at the SIE-A site experience about 170 days during which foraging would slow or cease altogether due to unfavorable temperature, leaving about half a year of optimal foraging conditions. The reduced window of activity likely increases competition among neighboring colonies, especially when colonies at the same site share a generally similar activity pattern.

Polygyny may provide means for *M. mendax* colonies to cope with unfavorable abiotic conditions. Multiple reproductives increase the rate of worker production, which may increase the efficiency of replacing workers lost to abiotic stressors, among other factors. Polygynous colonies may also be able to outperform monogynous counterparts when it comes to defending territory and the nest as well as when stockpiling resources,

due to the production of a larger workforce (elaborated in Chapter Two). The positive correlation between matriline number and the frequency of polygynous colonies (Figure 3) is consistent with what has been observed in other species (Keller 1995), and supports the role of competition as a driving force of polygyny in *M. mendax*. As polygyny becomes more frequent locally, colonies are selected to maintain high queen number to effectively compete with neighbors. However, the observed distance between neighboring colonies (NND), a rough proxy of competition pressure, does not correlate with polygyny frequency and matriline number. This is likely due to the low power of NND estimates, which for most sites were obtained from a relatively small number of colonies (n = 7 - 14). Additionally, the average observed heterozygosity and allele richness have positive relationships with the frequency of polygynous colonies and matriline number, suggesting a link between genetic diversity and the evolution of polygyny in *M. mendax*. Intracolonial genetic variability is known to influence a number of important properties in social insect colonies including division of labor (Julian and Fewell 2004), task specialization and performance (Oldroyd and Fewell 2007; Slaa et al. 2014), and disease resistance (Hughes and Boomsma 2004), and of colony fitness in general (Matilla and Seeley 2007).

It has been speculated that queen number variation can facilitate divergence and ultimately speciation (Gadau and Fewell 2009). This may be occurring in *M. mendax*. There is some indirect evidence of reproductive isolation not entirely explainable by geographical proximity. Consider the SHO and LEM sites, both of which appear to exchange more migrants and share more genetic similarity with non-adjacent sites (Figures 3.1 and 3.5; Tables 3.4, 3.5, and 3.6). LEM and SHO colonies are mostly

defined by Clusters 1 and 3, respectively (Figure 3.5). A Partial Mantel test controlling for geographical distance showed that sites more similar genetically also have similar frequency of polygynous colonies. Polygyny appears to spread very slowly, evident from the low frequency of polygyny in sites adjacent to the highly polygynous SIE-A, and low migration rates observed. This is consistent with loss of long-range dispersal (Gadau and Fewell 2009). In addition, although the phenotype can reach new habitats, local conditions may not be suitable to maintain it.

In conclusion, social polymorphism is present in *M. mendax*, with the evolution of polygyny possibly mediated directly or indirectly by climate. Together with geographic isolation, selection on social structure may also have contributed to genetic differentiation (MATESOFT polygyny frequency and G''_{ST}; Partial Mantel test, $r = 0.21$, $P = 0.002$). The observed patterns of differentiation raise the possibility of ongoing divergence, which may eventually result in speciation. Examples of closely related species with different social structure distribution are known (*M. mimicus* vs. *M. depilis*: Hölldobler et al. 2011; *Neivamyrmex*: Rettenmeyer and Watkins II 1978). This topic will be explored in greater details in the next chapter.

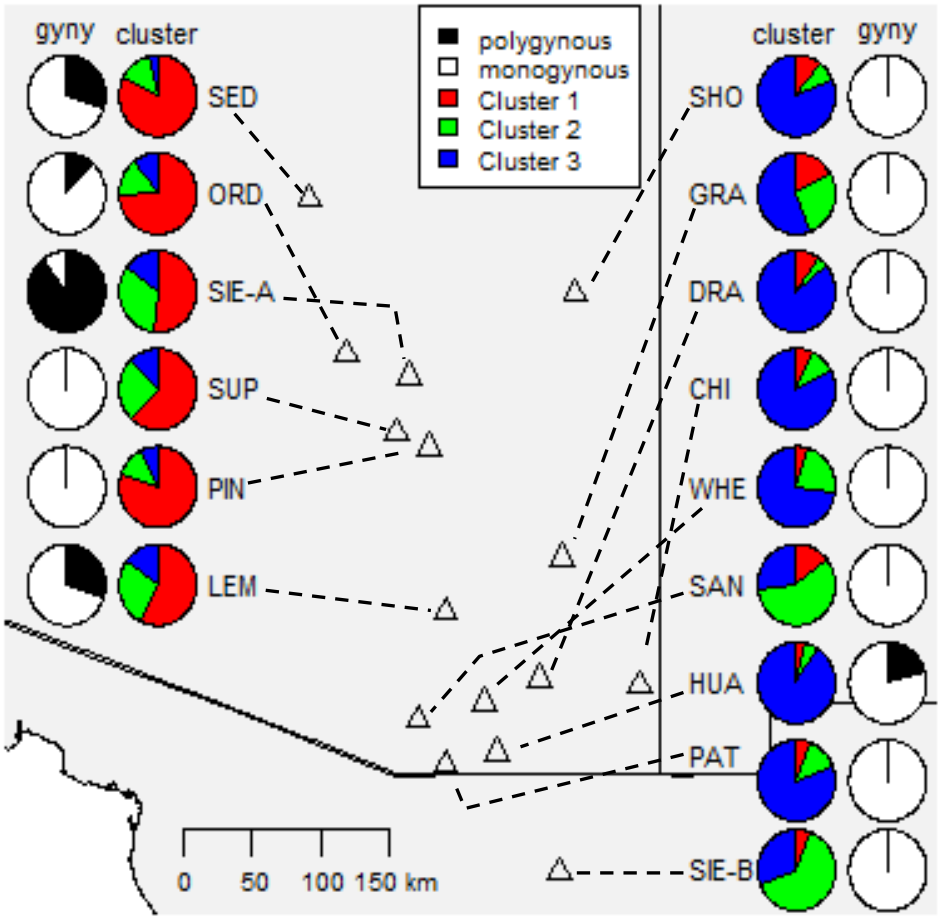

Figure 3.1. A map of the study area. Colored pie charts illustrate the genetic composition. Black-and-white charts illustrate social variation.

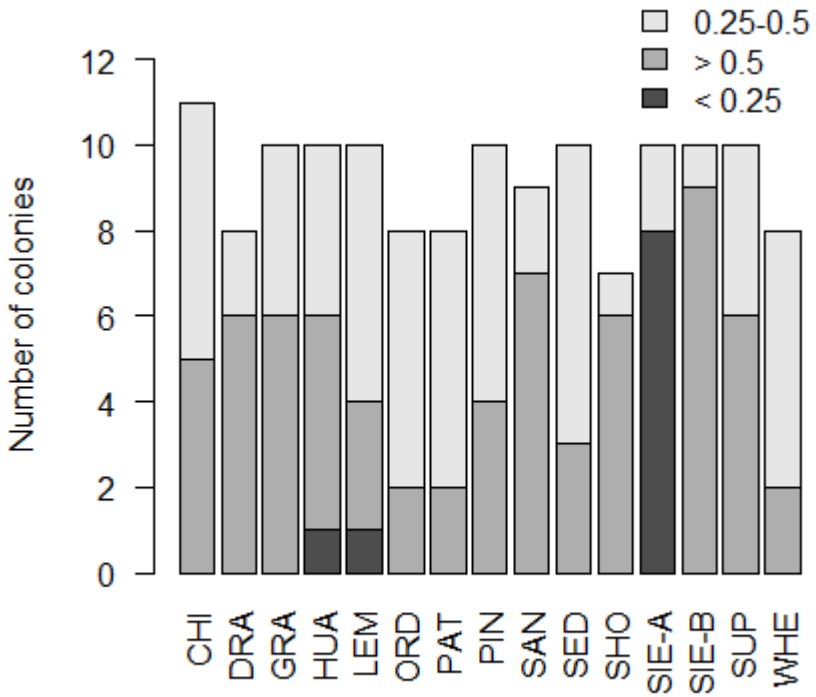

Figure 3.2. Distribution of worker relatedness in *M. mendax* populations. Only HUAC, LEM, and SIE-A have colonies with r_{ww} significantly less than 0.25 (darkest shade).

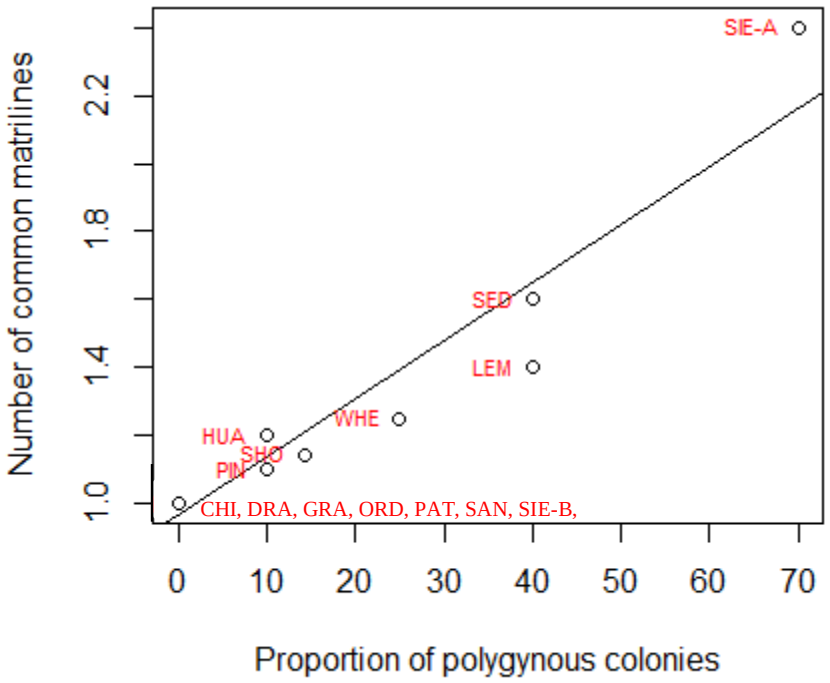

Figure 3.3. The number of common matrilines was positively correlated with the proportion of COLONY-inferred polygynous colonies (linear regression, $F_{1,13}$ = 146.6, adjusted R^2 = 0.91, $P < 0.001$)

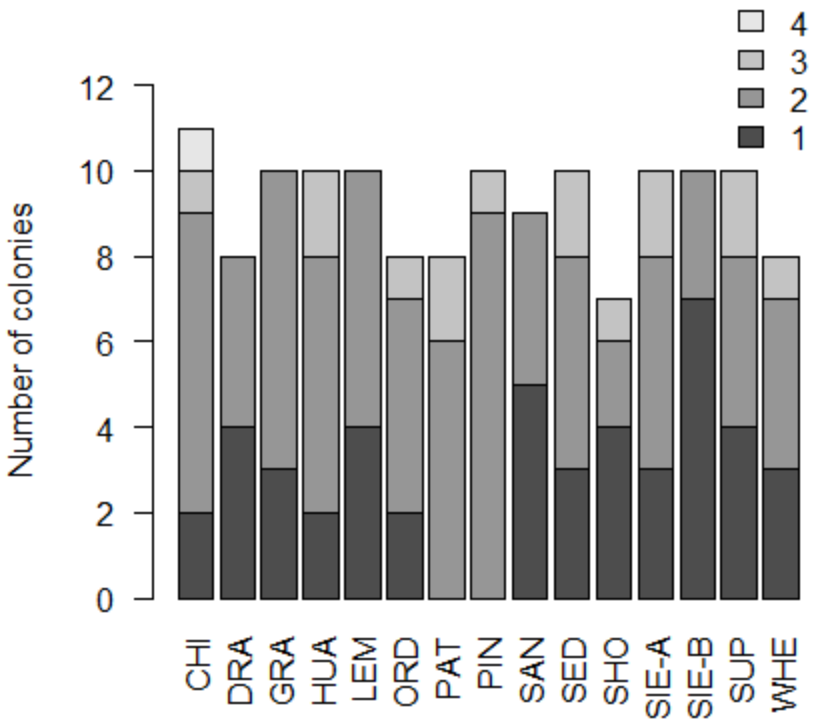

Figure 3.4. The number of patrilines associates with each matriline estimated by COLONY. Polyandry is present in all populations, and holds the majority in most.

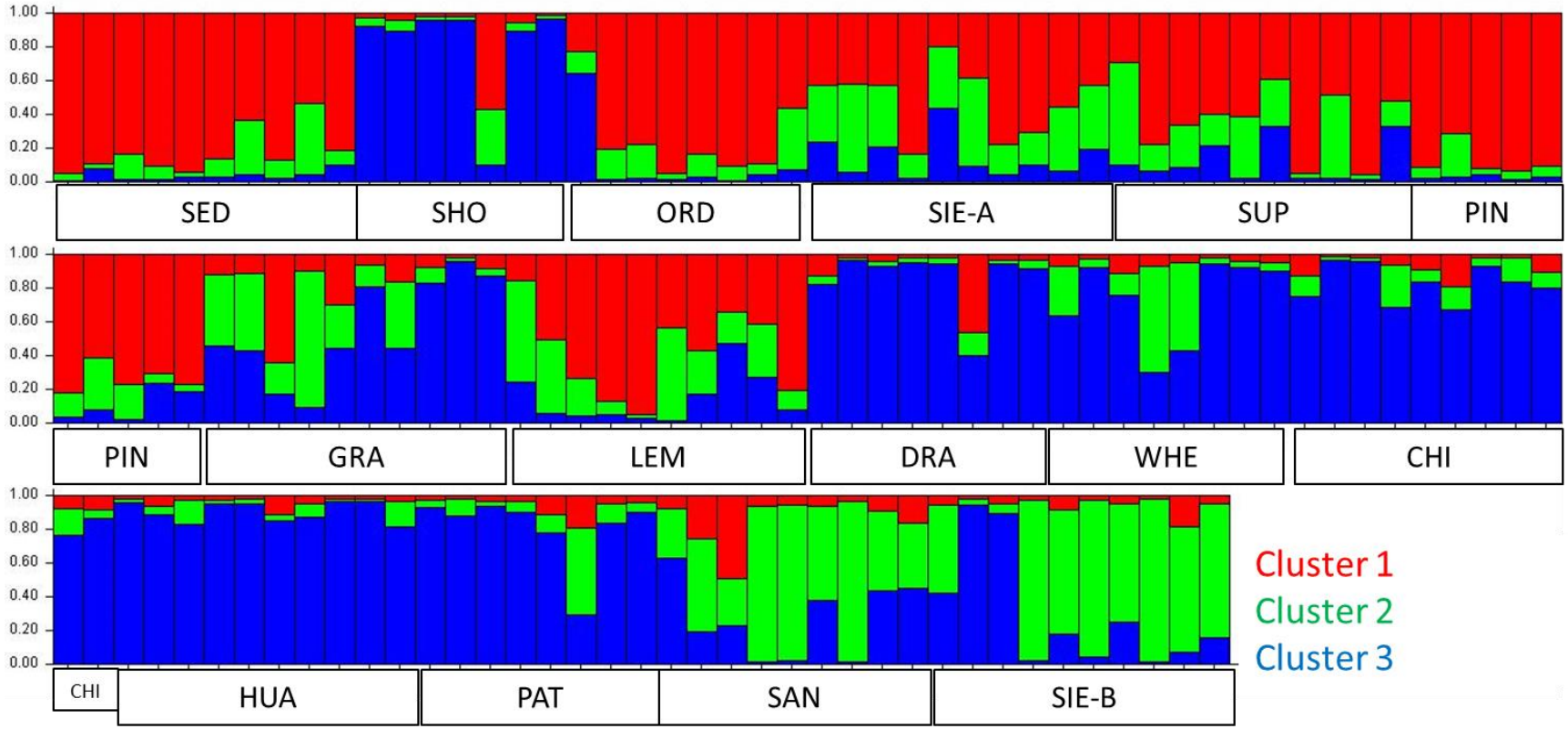

Figure 3.5. The genetic composition of 15 populations as inferred by STRUCTURE. With some exceptions, most colonies are defined by one of three clusters, with Cluster 1 dominating most norther sites and Cluster 2 and 3 are prominent in the southern sites.

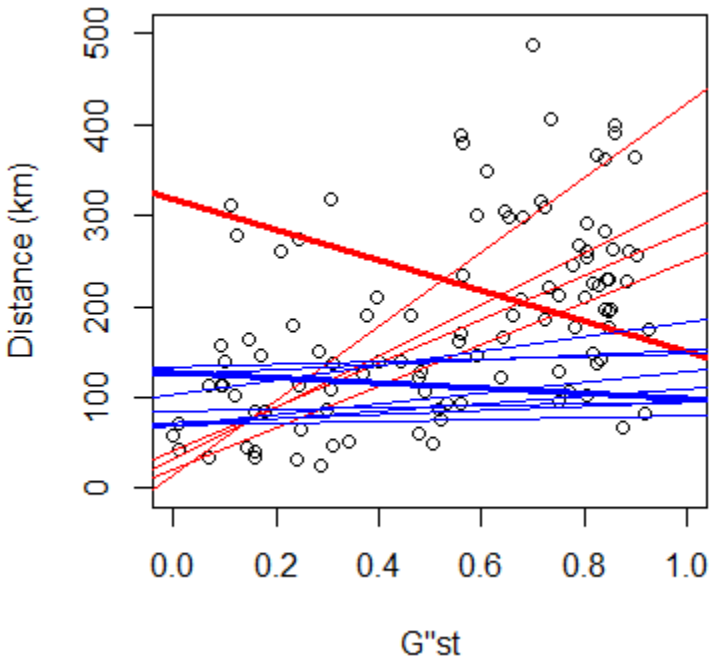

Figure 3.6. Plot of pairwise geographical distance and *G"st*. Northern populations (red regression lines) have a significant positive relationship between genetic and geographical distances, except SHO (bolded red line). There is a positive trend in Southern populations except for LEM (bolded blue line), but none is significant.

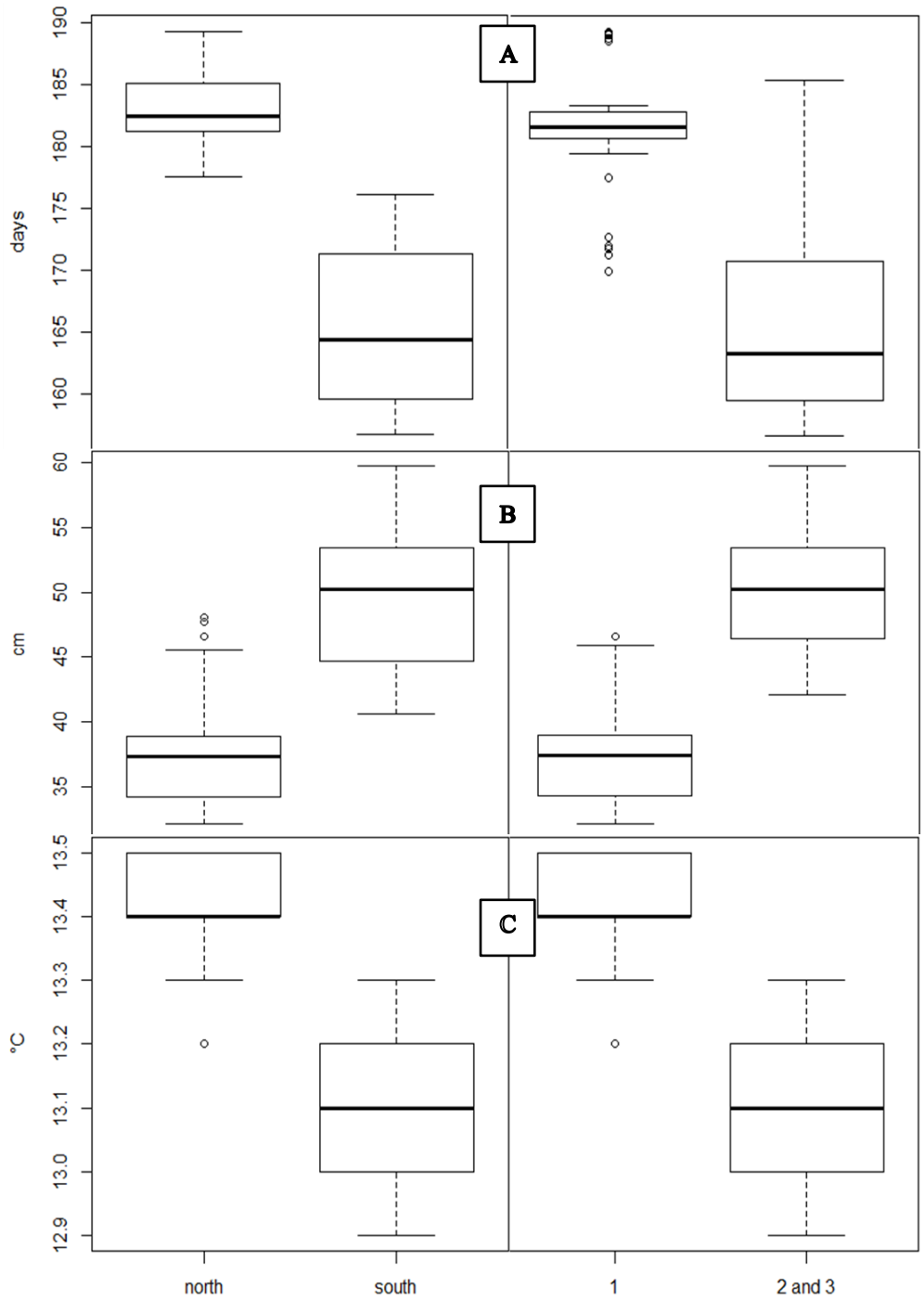

Figure 3.7. Abiotic difference between geographical regions (left panels) and genetic clusters (right panels). Northern sites, most of which associate primarily with Cluster 1, are predicted to have more suboptimal foraging days (A), receive less precipitation annually (A), and experience greater temperature fluctuation throughout a year than southern sites, which associate with Clusters 2 and 3.

Table 3.1. Sites analyzed in this chapter, with approximate GPS coordinates. The number of colonies currently known at each site (n) and the average nearest-neighbor distance estimate (NND) are also given.

Sites (abbreviation)	**Latitude, longitude**	**n**	**NND (m)**
Chiricahua (CHI)	31.90046°, -109.22757°	51	196.73
Dragoons (DRA)	31.922778°, -109.966944°	8	54.43
Huachucas (HUAC)	31.469761°, -110.304269°	12	37.91
Mt. Graham (GRA)	32.662326°, -109.794601°	13	385.97
Mt. Lemmon (LEM)	32.334655°, -110.697279°	14	222.21
Mt. Ord (ORD)	33.918889°, -111.437500°	9	125.68
Patagonia (PAT)	31.456581°, -110.667989°	13	84.43
Pinal Peak (PIN)	33.332980°, -110.833293°	50	32.12
Santa Ritas (SAN)	31.670556°, -110.898333°	12	126.29
Sedona (SED)	34.868482°, -111.733514°	32	78.25
Show Low (SHO)	34.266852°, -109.972765°	8	246.43
Sierra Ancha (SIE-A)	33.78475°, -110.97103°	100	52.37
Sierra Buenos Aires (SIE-B)	30.738750°, -109.818400°	10	391.31
Superstitions (SUP)	33.432186°, -111.058690°	14	79.80
Whetstones (WHE)	31.808611°, -110.388056°	8	326.44

Table 3.2. Microsatellite statistics, including the number of alleles (in the order of Mm3, 4, 5, and FE17), allele richness, inbreeding coefficient (F_{is}), and the observed (H_{obs}) and expected (H_{exp}) heterozygosity. CHI and SIE-A values were estimated from rarefied data of ten workers per colony.

Site	**Allele count**	**Allele richness**	F_{is}	H_{obs}/H_{exp}			
				Mm3	Mm4	Mm5	FE17
CHI	20, 22, 15, 5	8.57	0.08	0.96/0.91	0.86/0.93	0.84/0.88	0.44/0.43
DRA	13, 21, 12, 4	8.64	-0.052	0.96/0.88	0.94/0.94	1/0.89	0.38/0.33
HUAC	18, 25, 16, 8	8.80	0.127	0.91/0.91	0.98/0.94	0.91/0.9	0.21/0.26
GRA	18, 18, 14, 10	8.49	0.11	0.99/0.92	0.81/0.92	0.87/0.89	0.67/0.6
LEM	16, 21, 15, 15	8.59	0.096	0.96/0.91	0.96/0.89	0.73/0.81	0.78/0.85
ORD	19, 24, 13, 9	8.70	0.09	0.85/0.89	0.99/0.94	0.76/0.86	0.52/0.72
PAT	20, 17, 15, 3	7.96	0.123	0.94/0.93	0.81/0.84	0.78/0.87	0.53/0.49
PIN	21, 15, 23, 11	8.68	0.099	0.86/0.92	0.62/0.85	1/0.93	0.77/0.8
SAN	18, 20, 13, 9	8.79	0.061	0.98/0.92	0.97/0.92	0.79/0.77	0.64/0.8
SED	20, 17, 13, 18	8.56	0.09	0.77/0.89	0.91/0.88	0.97/0.9	0.79/0.84
SHOW	9, 11, 11, 3	6.75	0.023	0.86/0.81	0.87/0.87	0.8/0.81	0.46/0.38
SIE-A	29, 27, 30, 26	11.21	-0.01	0.91/0.94	0.94/0.93	0.97/0.94	0.89/0.89
SIE-B	19, 21, 14, 17	9.74	0.007	0.98/0.92	0.96/0.91	0.72/0.84	0.93/0.88
SUP	21, 19, 21, 11	9.59	0.025	0.99/0.93	0.87/0.91	1/0.93	0.61/0.59
WHE	19, 22, 16, 3	9.08	0.216	0.8/0.93	0.65/0.94	0.96/0.92	0.16/0.17

*with at least one colony significantly less than 0.25

Table 3.3. Descriptive statistics and the number of colonies analyzed at each site (n). The percentage of polygynous colonies was inferred by MATESOFT (M) and COLONY (C, based on all/common matrilines). Frequency of polyandrous colonies and patriline number were estimated COLONY. The proportion of multiply-mated queens (D_{est}) was estimated by MATESOFT. Worker relatedness (r_{ww}) was estimated using R. The Shannon-Weaver index (H') was estimated from common matrilines.

Site	**n**	**% polygyny**		**matriline number (C)**		**% polyandry (C)**	D_{est} **(M)**	**Patriline number (C)**	r_{ww}	H' **(common)**
		M	C	all	common					
CHI	11	0	18.2/0	1.18 ± 0.12	1	72.7	1	2.09 ± 0.251	0.57 ± 0.035	0
DRA	8	0	12.5/0	1.13 ± 0.13	1	50	1	1.5 ± 0.189	0.64 ± 0.043	0
HUAC	10	20	20/10	1.3 ± 0.21	1.2 ± 0.2	80	0.8	1.97 ± 0.21	0.54 ± 0.055*	0.1
GRA	10	0	0/0	1	1	70	1	1.7 ± 0.15	0.59 ± 0.039	0
LEM	10	30	50/40	2 ± 0.36	1.4 ±.16	60	0.7	1.5 ± 0.15	0.45 ± 0.072*	0.39
ORD	8	12.5	25/0	1.25 ± 0.16	1	75	0.88	1.88 ± 0.2	0.54 ± 0.040	0
PAT	8	0	0/0	1	1	100	1	2.25 ± 0.16	0.48 ± 0.052	0
PIN	10	10	10/10	1.1 ± 0.1	1.1 ± 0.1	100	0.9	2.1 ± 0.1	0.52 ± 0.037	0.061
SAN	9	0	0/0	1	1	44.4	1	1.44 ± 0.18	0.71 ± 0.040	0
SED	10	30	50/40	1.8 ± 0.29	1.6 ± 0.22	80	0.7	1.83 ± 0.23	0.48 ± 0.045	0.4
SHOW	7	0	28.6/14.3	1.29 ± 0.18	1.14 ± 0.14	42.9	1	1.57 ± 0.3	0.66 ± 0.032	0.07
SIE-A	10	90	100/70	5.9 ± 0.74	2.4 ± 0.37	80	0.1	1.88 ± 0.23	0.18 ± 0.058*	1.84
SIE-B	10	0	10/0	1.1 ± 0.1	1	30	1	1.3 ± 0.15	0.70 ± 0.031	0
SUP	10	0	0/0	1	1	60	1	1.8 ± 0.25	0.57 ± 0.046	0
WHE	8	0	25/25	1.25 ± 0.16	1.25 ± 0.16	62.5	1	1.75 ± 0.25	0.51 ± 0.053	0.17

*with at least one colony significantly less than 0.2

Table 3.4. Pairwise θ estimated from genotype data. Sites are colored according to cluster membership (red: Cluster 1, green: Cluster 2, blue: Cluster 3).

θ	CHI	DRA	HUAC	GRA	LEM	ORD	PAT	PIN	SAN	SED	SHO	SIE-A	SIE-B	SUP
DRA	-0.0001													
HUAC	0.0084	-0.0026												
GRA	0.0120	0.0232	0.0104											
LEM	0.1007	0.1421	0.1205	0.0533										
ORD	0.0961	0.1483	0.1293	0.0720	0.0329									
PAT	0.0244	0.0345	0.0257	0.0064	0.0979	0.1199								
PIN	0.0987	0.1415	0.1215	0.0695	0.0204	0.0286	0.1155							
SAN	0.0744	0.0894	0.0758	0.0281	0.0498	0.0880	0.0306	0.0800						
SED	0.0924	0.1292	0.1312	0.0642	0.0597	0.0270	0.1159	0.0449	0.0856					
SHO	0.0436	0.0486	0.0199	0.0342	0.1263	0.1394	0.0587	0.1252	0.0990	0.1465				
SIE-A	0.0768	0.1133	0.1059	0.0462	0.0071	0.0205	0.0854	0.0236	0.0410	0.0243	0.0993			
SIE-B	0.0342	0.0704	0.0713	0.0335	0.0505	0.0483	0.0585	0.0579	0.0390	0.0558	0.0808	0.0314		
SUP	0.1021	0.1389	0.1334	0.0619	0.0329	0.0237	0.1164	0.0287	0.0902	0.0536	0.1351	0.0106	0.0608	
WHE	0.0099	-0.0030	0.0056	0.0053	0.1252	0.1392	0.0173	0.1208	0.0752	0.1316	0.0185	0.0991	0.0613	0.1280

Table 3.5. Pairwise G''_{ST} estimated from genotype data. Sites are colored according to cluster membership (red: Cluster 1, green: Cluster 2, blue: Cluster 3).

G''_{ST}	CHI	DRA	HUAC	GRA	LEM	ORD	PAT	PIN	SAN	SED	SHO	SIE-A	SIE-B	SUP
DRA	0.0093													
HUAC	0.0686	-0.0011												
GRA	0.1204	0.1571	0.0986											
LEM	0.8169	0.9198	0.8063	0.5585										
ORD	0.7224	0.8868	0.804	0.6757	0.3754									
PAT	0.171	0.1792	0.1585	0.0922	0.7492	0.8407								
PIN	0.7311	0.8473	0.7526	0.6367	0.243	0.2968	0.8015							
SAN	0.5544	0.5318	0.4769	0.2841	0.5201	0.8069	0.2385	0.7217						
SED	0.7363	0.8229	0.8597	0.6443	0.679	0.308	0.8601	0.4627	0.84					
SHO	0.2429	0.207	0.1095	0.2331	0.8183	0.8341	0.305	0.7513	0.5915	0.9265				
SIE-A	0.7883	0.8819	0.8543	0.6417	0.1471	0.3106	0.8065	0.34	0.5655	0.3987	0.7705			
SIE-B	0.3109	0.4835	0.5157	0.3943	0.6608	0.5649	0.4889	0.6518	0.4434	0.7018	0.5583	0.6107		
SUP	0.7793	0.8526	0.846	0.5903	0.3669	0.2481	0.83	0.2883	0.8395	0.5606	0.8261	0.1589	0.7142	
WHE	0.0947	0.0117	0.0687	0.0928	0.8761	0.9033	0.141	0.7822	0.5035	0.9007	0.1231	0.8475	0.4782	0.8468

Table 3.6. Pairwise *Nm* estimated from θ. Sites are colored according to cluster membership (red: Cluster 1, green: Cluster 2, blue: Cluster 3).

Nm	CHI	DRA	HUAC	GRA	LEM	ORD	PAT	PIN	SAN	SED	SHO	SIE-A	SIE-B	SUP
DRA	2138.83													
HUAC	29.67	96.51												
GRA	20.64	10.53	23.72											
LEM	2.23	1.51	1.82	4.44										
ORD	2.35	1.44	1.68	3.22	7.35									
PAT	10.00	6.99	9.49	39.02	2.30	1.84								
PIN	2.28	1.52	1.81	3.35	12.00	8.49	1.91							
SAN	3.11	2.55	3.05	8.63	4.77	2.59	7.93	2.88						
SED	2.45	1.68	1.66	3.65	3.94	9.01	1.91	5.32	2.67					
SHO	5.48	4.90	12.34	7.07	1.73	1.54	4.01	1.75	2.28	1.46				
SIE-A	3.00	1.96	2.11	5.16	34.85	11.97	2.68	10.36	5.84	10.06	2.27			
SIE-B	7.07	3.30	3.26	7.21	4.70	4.92	4.03	4.07	6.16	4.23	2.85	7.71		
SUP	2.20	1.55	1.62	3.79	7.35	10.30	1.90	8.45	2.52	4.42	1.60	23.29	3.86	
WHE	24.95	82.70	44.31	47.29	1.75	1.55	14.19	1.82	3.07	1.65	13.29	2.27	3.83	1.70

CHAPTER 4

THE RELATIONSHIP BETWEEN PHYLOGEOGRAPHY AND POLYMORPHISM IN *MYRMECOCYSTUS MENDAX*

Introduction

Observed phenotypic variation between individuals may correspond to fixed differences between reproductively isolated species, or polymorphism arose among conspecifics due to genetic drift and local adaptation (Suarez et al. 1999; Overson 2011; Helms & Cahan 2012). Distinguishing these scenarios can be difficult. For instance, when two sibling species have recently diverged, they may exhibit little phenotypic difference or genetic differentiation (e.g. due to introgression or incomplete lineage sorting). Such species complexes pose a challenge to interpreting variation in natural populations.

As the use of molecular data becomes routine in species discovery and delimitation in Formicidae, it is apparent that many described species actually comprise multiple genetically distinct, potentially non-interbreeding taxa with a high degree of morphological similarity (i.e. cryptic species, Bickford et al. 2006; e.g. *Messor* - Schlick-Steiner et al. 2006; *Formica* - Bernasconi et al. 2010; *Tetramorium* - Steiner et al. 2010; *Ectatomma* - Nettel-Hernanz et al. 2015). Cryptic species are in fact common in arthropods (e.g. Wilcox et al. 1997; Hebert et al. 2004; Bickford et al. 2006). These observations further emphasize the importance of identifying diagnostic traits with

greater delimitation resolution, particularly for species exhibiting significant degree of phenotypic variation.

In a comprehensive systematic review of the genus *Myrmecocystus*, R.R. Snelling noted extensive hair length variation in *M. mendax*. He described the presence of a short-haired form in the northern part of the species range with longest pronotal hairs 0.58 to 0.6 times the length of the minimum ocular diameter (MOD), and a long-haired type co-occurring with the short-haired form in the southern localities with the longest pronotal hairs 0.70-0.75 x MOD and sometimes up to 1.30 x MOD (1976, pg. 27). The difference was pronounced, prompting Snelling to hypothesize that *M. mendax* may contain cryptic taxa: "There is no question, in my mind, of two species being represented, nor that the southern form can be set up as a subspecies: the cline is too fully developed." (1976, pg. 41)

Besides being an indicator of possible cryptic diversity, this variation in hair length complicates the identification of *M. mendax* with respect to its closely related congeners, *M. melliger* and *M. placodops*. The diagnostics that separate these three taxa rely on hair length and head shape of major workers (head width > 1.5 mm). *M. melliger* is a rectangular-headed, long-haired species, with pronotal hair length greater than the major axis of the eye. On the other hand, *M. placodops* majors have more spherical, "orbiculate" heads and shorter hairs, with longest pronotal hair at most 0.5 x MOD (minimum ocular diameter, the minor axis of the eye). Intermediate on the hair length spectrum is *M. mendax*, with longest pronotal hair 0.6 x MOD at minimum and 0.75 x MOD on average, and head shape similar to *M. melliger*. *M. mendax* reproductive

females are indistinguishable from *M. melliger*, and males cannot be morphologically differentiated from *M. melliger* and *M. placodops* (Snelling 1976). Snelling openly acknowledged the difficulty in differentiating *M. mendax* using workers, stating that "erect body hairs are subject to much variation through the entire range of the species and have been a source for confusion in the past and for frustration to the present writer." Identification is challenging without majors, and even more so where species ranges overlap such as in southeastern Arizona and northern Sonora (Figure 4.1).

Here I describe a biogeographical analysis of *M. mendax*, motivated by the findings of social structure variation in the previous chapters and of a hair length cline by Snelling (1976). First, I inferred the phylogenetic history of natural populations by reconstructing mitochondrial and nuclear gene trees. I then examined the geographical distribution of the inferred phylogenetic structure. Lastly I tested Snelling's cryptic diversity hypothesis by estimating the divergence between *M. mendax* subclades and analyzing how hair length and queen number patterns correlated with the phylogeny. I also discuss Snelling's hypotheses concerning the evolution of the *melliger* group, which proposed that either *M. melliger* or *M. placodops* split first from the common ancestor of the group.

Materials and methods

Sampling

M. mendax was sampled extensively in Arizona between 2010 and 2017 (Figure 4.1B, Table 4.1). Other parts of the range included were California, Colorado, New

Mexico, Texas, and Mexico. The phylogenetic analyses also included seven other taxa of the subgenus *Endiodioctes* representing four morphological groups (in parentheses) and serving as putative outgroups: *M. melliger* (*melliger*), *M. placodops* (*melliger*), *M. semirufus* (*melliger*), *M. mimicus* (*mimicus*), *M. flaviceps* (*flaviceps*), *M. kennedyi* (*kennedyi*), and *M. wheeleri* (*kennedyi*). *M. melliger*, *M. placodops*, and *M. semirufus* along with *M. mendax* are placed in the *melliger* group (Snelling 1976). Specimens were contributed in part by J. E. Taylor, R. A. Johnson, P. Ward, and S. Cover, and A. Wild, as well as by institutions including the University of Texas Insect Collection at Austin, the University of Texas at El Paso, and the Museum of Comparative Zoology at Harvard. Species identity of loaned specimens was verified by M. Boroweic and R. A. Johnson. Identification of new materials relied initially on heuristics (e.g. body coloration, odor, and habitat) and was later confirmed using the key also by M. Boroweic and R. A. Johnson. Vouchers will be deposited at the Arizona State University's Hasbrouck Insect Collection. Sequences generated by this work will be archived in the Dryad Digital Repository.

mtDNA sequencing and analyses

Genomic DNA was isolated from ethanol-preserved workers using the Chelex protocol described in Chapter Two. A region of the mitochondrial cytochrome oxidase subunit 1 (COI) was amplified using the LCO/HCO primer pair (Folmer et al. 1994). Each 23-µl reaction consisted of 15.9 µl of ultrapure water, 5 µl of 5X Colorless GoTaq Reaction Buffer (w/1.5 mM $MgCl_2$), 0.5 µl of $MgCl_2$ (50 mM), 0.5 µl of 10 mM dNTP

mix, 0.5 µl of each of the primers (10 mM), 0.1 µl of Taq DNA Polymerase (~5 u/µl), and 2 µl of DNA template (actual concentration varied). The thermal profile consisted of the following cycle: denaturation: 3 min at 94°C; elongation: 38 cycles each for 1 min at 94°C, 1 min at 45°C, and 1:30 min at 72°C; termination: 5 min at 72°C. Each double-stranded DNA product was sequenced for both directions from two samples each contained 1 µl of the PCR product, 1 µl of one of the primers (2.5 mM), and 5 µl of ultrapure water. Samples were sent to the ASU DNA Laboratory for Sanger sequencing using an ABI 3730 DNA Analyzer. The number of specimens sequenced is listed in Table 4.1. The program Sequencer® (Gene Codes Corporation) was used to trim primer sequences, to call ambiguous bases, and to form consensus sequences for each specimen. To verify that the mitochondrial gene COI was amplified instead of pseudogenized nuclear mtDNA (NUMT), nucleotide sequences were translated to identify the reading frame using MEGA 7.0.26 (Kumar et al. 2016). In addition to de novo sequences, COI sequences of *M. mendax*, *M. placodops*, *M. melliger*, *M. mimicus*, *M. flaviceps*, *M. kennedyi*, and *M. wheeleri* from a previous study were obtained from Genbank to supplement the mtDNA analysis (Kronauer et al. 2004).

An alignment was made from 133 sequences (Table 4.1), and used to infer a Maximum Likelihood (ML) tree implementing the General Time Reversible model with invariant sites and a gamma distribution of mutation rates across sites (GTR + G + I). The shape parameter was set to 0.4 based on the median of the posterior distribution of a BEAST biogeographical analysis (see below). The initial tree used to initiate tree search was constructed by applying Neighbor-Join and BioNJ algorithms to a matrix of pairwise

distances estimated using the Maximum Composite Likelihood (MCL) approach. All positions containing gaps and missing data were eliminated. Codon positions included were 1st+2nd+3rd+Noncoding. Nodal support was estimated from 1000 bootstrap replicates.

BEAST (Bouckaert et al. 2014) was used to perform a biogeographical analysis on 118 *M. mendax* mtDNA sequences from 22 locations. The program implemented the discrete phylogeographical model developed by Lemey et al. (2009). In this model, sampling location is treated as a discrete, neutrally evolving character and migration is assumed to follow a reversible Markov chain with a uniform stationary distribution on regions. To control the number of pairwise migration rates that need to be estimated, the rate matrix is parametrized using a Bayesian variable selection strategy termed the stochastic search variable method (SSVM). This method assigns a prior distribution to the number of non-zero migration rates which favors sparse rate matrices with relatively few positive rates. In addition, SSVM not only estimates the magnitude of the migration rate between each pair of populations but also the posterior probability that the rate is nonzero. Larger Bayes factors indicate stronger evidence of migration and rates with factors >2 are considered as providing significant evidence of migration. The analysis was conducted using the Bayesian skyline model with piecewise linear population growth over six time intervals, and the GTR + G + I substitution model (five gamma categories) with a strict molecular clock. A Markov chain lasting 100 million generations were run, with sampling taking place every 50,000 generations, following a burn-in period lasting

20 million generations. The results were used to estimate the migration rates, their inclusion probabilities, and Bayes factors.

UCE sequencing and analyses

All UCE sequences in this study were generated de novo from samples varying in age and condition. Most specimens were collected in 2010-2017 and preserved in ethanol, while the remainder consisted of a mixture of point-mounted and ethanol-preserved specimens dated 1978-2016 (Table 4.1). The outgroups included *M. melliger*, *M. placodops, M. semirufus, M. flaviceps*, *M. kennedyi*, *M. mimicus*, and *M. wheeleri*. Detailed descriptions of the sequencing preparation pipeline are included in Appendix B. To obtain genomic DNA with suitable quality, extraction was performed non-destructively using the Qiagen DNeasy Blood and Tissue Kit (Qiagen, Valencia, CA, USA) with a modified protocol. Each specimen was pierced thrice with a size 00 pin on the ventral surface of the head, the thorax, and between two gastral sternites. DNA isolates were sheared to normalize fragment size to about 600 base pairs (bp) using a Qsonica machine (Newton, CT, USA), followed by library preparation and enrichment. The final quality control step was done with a qPCR. An ant-specific probe set was used (Branstetter et al. 2017). Concentration of samples was quantified throughout the preparation pipeline using a Qubit fluorometer (ThermoFisher Scientific, USA). Intermediate samples were stored at -20°C. All pools were combined and sent for Illumina sequencing at the University of Utah (Salt Lake city, UT).

Raw reads were cleaned, assembled to contigs, and aligned to UCE probes using the PHYLUCE pipeline (Faircloth 2015). The FASTQ data were trimmed using Illumiprocessor, a wrapper around Trimmomatic (Bolger et al. 2014), with default settings (LEADING:5, TRAILING:15, SLIDINGWINDOW:4:15, MINLEN:40). Assemblies were done using Trinity v20140717 (Grabherr et al. 2011) with the phyluce_assembly_assemblo_trinity wrapper. Orthology was assessed by matching the assembled contigs to enrichment probe sequences with phyluce_assembly_match_contigs_to_probes (min_coverage=50, min_identity=80). This step generated a SQLite database which was then used to build FASTA files for the 2,524 orthologous loci with phyluce_assembly_get_match_counts, phyluce_assembly_get_fastas_from_match_counts, and phyluce_assembly_explode_get_fastas_file.

MAFFT v7.310 (Katoh and Standley 2013) with default settings was used to align all UCE sequences, supplemented by AMAS (Borowiec 2016) for alignment wrangling and obtaining summary statistics and Aliview (Larsson 2014) for visualization. Although alignment trimming has been recently criticized (Tan et al. 2015), alignments were trimmed because of substantial computational burden associated with analysis of untreated data with high proportion of gaps, using trimAl (Capella-Gutierrez et al. 2009) with the "gappyout" algorithm, a relatively relaxed algorithm for removal of gaps. Visual inspection of alignments revealed that occasionally sequences were misaligned towards flanks. A custom R script (R Core Team) that utilized packages *ape* (Paradis et al. 2004, 2012), *seqinr* (Charif and Lobry 2007), *doParallel*, and *plyr* was used to automatically

identify and discard the misaligned sequences. The script first generates a matrix of uncorrected p-distances from a UCE locus alignment and for each taxon it computes average p-distance to all other taxa. Then it creates a distribution of average per-locus p-distances for each taxon and detects outliers defined as sequences above three standard deviations from the mean of that distribution, resulting in ~1 % of all individual sequences classified as outliers. Once identified, the script removes outliers using AMAS.

In the first phylogenetic analysis, alignments of individual genes from 92 specimens (Table 4.1) were concatenated to form a super-alignment, which was given to IQ-TREE (Nguyen et al. 2015) to infer a Maximum Likelihood (ML) phylogeny. ModelFinder (Kalyaanamoorthy et al. 2017) as implemented in IQ-TREE (Nguyen et al. 2015) was used for model selection under the Akaike information criterion corrected for small sample sizes (AICc) and analyzed the concatenated data matrix partitioned by locus (Chernomor et al. 2016). To assess node support, 2000 iterations of Ultrafast Bootstrap Approximation was performed (Minh et al. 2013). To test the robustness of the partitioned concatenated analysis, an unpartitioned analysis under HKY+4G model was also performed, which was the most common model identified as best under AICc for single loci. For the second analysis, the weighted statistical binning pipeline (Mirarab et al. 2014) was applied to the UCE loci with a more balanced taxon/individual sampling (*n* = 34 specimens) and used ASTRAL-III (Zhang et al. 2018) to infer individual and species trees by summarizing gene trees (i.e. individuals mapped to species assumed to be monophyletic). This method takes into account variation in the evolutionary history of different genes when reconstructing species or population trees, by grouping gene trees

with similar bootstrap support. A tree was estimated for each locus using IQ-TREE. Single-locus trees were grouped into "supergene" bins using the statistical binning pipeline (Bayzid et al. 2015; Mirarab et al. 2014). These bins were used to infer supergene trees using IQ-TREE with unlinked branch lengths among partitions. The ASTRAL-III input was "weighted" by multiplying each supergene tree by the number of UCE loci from which the tree was inferred from. Branch length and support were measured in coalescent units and local posterior probability, respectively (Sayyari and Mirarab 2016).

Root placement on gene trees

While an unpublished topology suggested that a clade containing *M. kennedyi* and *M. flaviceps* is more ancestral in the subgenus *Endiodioctes* (O'Meara 2008), a recent publication supported *M. wheeleri* as the basal taxon (Kronauer et al. 2004). Hence in the following analyses, all trees were rooted by *M. wheeleri*. Note that placing the root on *M. kennedyi* and *M. flaviceps* had no effect on the topology of the *melliger* group.

Sequence divergence

Kimura-2-parameter (K2P) distance and nucleotide diversity were estimated from mtDNA and UCE sequences using MEGA 7.0.26. K2P distance measures the number of nucleotide substitutions, while nucleotide diversity metrics are more appropriate for polymorphism data. These metrics assumed homogeneity in the rate of variation among lineages and a gamma distribution of substitution rate among sites with a shape parameter

α of 0.4. Variance was estimated with 1000 bootstrap replicates. In two separate analyses, *M. mendax* sequences were treated as a single monophyletic group, then partitioned into subclades as inferred by the phylogenetic analyses.

Phenotypic variation

To estimate hair length variation in *M. mendax*, I used photography to measure in micrometer the length of the longest pronotal hair from lateral view, the minimum ocular diameter (MOD, i.e. minor axis of the eye), and head width (HW, head margins at the posterior of the eyes) from frontal view of 496 workers in 170 colonies (Table 4.1). Photographs were taken and processed using the Leica Application Suite v4.5.0 (Leica Microsystems, Switzerland) and the Helicon Focus v6.7.1Pro software (Ukraine). Measurement of were performed with Fiji (Schindelin et al. 2012). Queen number estimates were taken directly from Chapter Three.

Statistics and data visualization

Phylogenetic trees were formatted using FigTree (Rambaut 2009), TreeGraph 2.14.0-771 beta (Stöver and Müller 2010), and MEGA 7.0.26. Statistics and other graphics were produced with RStudio v1.1.442 using the following packages: *ape* v5.1 (Paradis et al. 2004), *maps* v3.3.0 (Becker et al. 2018), *mapdata* v2.3.0 (Becker et al. 2018), *maptools* v0.9.2 (Bivand and Lewin-Koh 2017), *mapplots* v1.5 (Gerritsen 2014), *ggplot2* (Wickham 2009), *ggfortify* (Horikoshi and Tang 2016; Tang et al. 2016); *cluster* (Maechler et al. 2018), and *ggtree* v1.10.5 (Yu et al. 2017).

Results

mtDNA trees

The total COI alignment contained 660 nucleotides. The Maximum Likelihood tree was reconstructed from 526 positions, 102 of which were parsimony-informative. There was a substantial AT% bias (A+T = 71.8%, Table 4.2), comparable to other ant taxa (Smith et al. 2005). Node support varied substantially across clades (Figure 4.2, range: 4 - 99%). The overall topology showed *M. mendax* haplotypes forming three well supported monophyletic group (bootstrap = 99%). The "red clade" included nine localities (Figure 4.2, red circle), including HUAL, LEM, MIN, ORD, PIN, PINE, SED, and SIE-A. A second large "blue clade" were populated by 11 sites (Figure 4.2, blue circle), including CHI, DRA, HUAC, GRA, KIT, PAT, SAN, SHO, WHE, NM, and SIE-B. Notably these two clades were not found together in any of the locations that were visited. There was also a third, smaller "green clade" that was only sampled in locations where the other two monophyletic groups were found (Figure 4.2, green circle), including HUAC, PAT, SAN, SED, SIE-A, SIE-B, SUP, and WHE. The sole Colorado sample grouped with the blue clade. Most terminal branches were very short and joined by weakly to moderately supported nodes (7 - 72%), resulting in numerous polytomies. The group that contains the blue clade and the Colorado sample formed an assemblage with *M. melliger* and *M. placodops*, rendering *M. mendax* paraphyletic within this phylogeny. However, the nodal support of this grouping was low (Figure 4.3, bootstrap = 34%). Collapsing nodes with less than 50% bootstrap support resulted in a polytomy, failing to resolve the evolutionary relationships between the three inferred *M. mendax* clades.

Specimens heuristically identified as *M. mendax* collected from California and Nevada in 2017 clustered with *M. placodops* and *M. flaviceps* instead, suggesting that these were misidentified.

The Bayesian phylogeographical analysis of the *M. mendax* COI data yielded a maximum-clade-credibility (MCC) tree containing three clades essentially identical to those recovered by the ML analysis (Figure 4.3). In contrast to the ML tree, the MCC topology suggested that the green clade is more closely related to the red clade.

UCE trees

Out of the 99 taxa sent for sequencing, one failed to sequence, five failed to recover 25-60% of loci, and one had fragmented reads. Between 1,015 and 2,358 UCE loci were recovered from the remaining 92 taxa, covering 2,506 out of the 2,524 loci targeted. For downstream analyses, only loci with 70 or more taxa (n = 2,231 loci) and taxa with at least 78% of UCE loci sequenced with high quality reads (n = 92 taxa) were retained. The single-locus alignments were on average 681-bp long. The complete, concatenated alignment included 92 taxa, spanned 2,231 loci and had 1,520,549 bps. There were 50,813 parsimony-informative sites and 17.6 % of missing data and gaps in the matrix.

The partitioned analysis recovered a highly supported, well resolved ML tree (Figure 4.4, bootstrap = 56-100%). Monophyly of the *melliger* group was 100% supported. *M. placodops* was the first taxon to branch off from the common ancestor of this group. The next divergence separated *M. semirufus* from *M. melliger* and *M. mendax*.

M. mendax was monophyletic and consisted of five well supported clades (bootstrap = 100). One major clade was represented by samples from eight of the nine sites found in the red COI clade (the missing locality, SUP, lacked UCE data), and was sister to a smaller clade represented by samples from two of the eight locations containing the green COI clade. A second major clade was found in eight of the 11 locations with samples from the blue COI clade (one of the four missing locations, KIT, was excluded by quality control). Two SIE-B sequences clustered with two other specimens also from Mexico to make up another small clade (orange). The last clade (light blue) consisted of two New Mexico and two Colorado specimens. The unpartitioned analysis yielded a tree clustering sequences from the green, orange, blue, and light blue clades of the partitioned analysis into a single clade, while retaining the red clade as inferred in the partitioned analysis.

Sequences from the same locality were usually most closely related to each other. Exceptions were present in ORD, HUAC, DRA, WHE, CHI, and most notably SAN and SIE-B (Figure 4.4). SAN sequence Hop3 clustered with PAT sequences in the green clade, but Hop11 was grouped with specimens identified morphologically as *M. melliger*. SIE-B sequence Bue1 was also more closely related with *M. melliger* while Bue2 and Bue4 were members of the *M. mendax* orange clade. Consistent with the mtDNA analysis, sequences from California and Nevada specimens clustered with *M. semirufus* and *M. placodops*, providing further that these specimens were misidentified. Furthermore, the positions of seven external specimens were inconsistent with their original identification (asterisks, Figure 4.4). Three specimens identified as *M. placodops* were grouped within *M. mendax*. Two specimens identified as *M. mendax* clustered with

M. melliger and *M. placodops*, respectively. Lastly, two specimens identified as *M. mendax* and *M. placodops* grouped more closely with *M. semirufus*.

The species tree analysis utilized 2,225 of the 2,231 UCE loci, excluding six loci with too few variable sites to estimate trees from. The species tree was inferred from 369 supergene trees, with each of the eight described species represented by a single sequenced specimen (Figure 4.5). The *melliger* group was monophyletic, with the branching order as follow: *M. placodops* splits first from the last common ancestor, then *M. semirufus*, and with *M. melliger* and *M. mendax* being sister clades. As for non-*melliger* taxa, *M. kennedyi* and *M. flaviceps* were more closely related than either to *M. mimicus*. However, this relationship had a relatively low level of support (posterior probability = 0.62) and short branch length (< 0.1 coalescent unit).

Comparing mtDNA and UCE trees

There were 50 *M. mendax* specimens, all from different colonies, that were represented on both the mtDNA and UCE ML trees (Table 4.3). Comparing the ML mtDNA and UCE trees side by side showed that both marker types converged on a similar topology, with most specimens clustered on the COI tree also grouped together on the UCE tree. Out of the 50 *M. mendax* specimens represented on both trees, 42 consistently formed monophyletic groups (Figure 4.6, solid lines; Table 4.3). There were eight exceptions, one each in HUAC, PAT, SAN, SIE-A and WHE populations, and three SIE-B colonies (Figure 4.6, dashed lines; Table 4.3). Two SIE-B colonies in the green mtDNA clade formed a separate UCE clade with two external specimens (Figures 4.4 and

4.6, orange). One SAN colony and one SIE-B colony grouped with specimens identified as *M. melliger* on the UCE tree, but clustered with the green *M. mendax* clade on the COI tree (Figure 4.6, black dashed line; Table 4.3). There was no colony assigned to both red and blue clades. Subsequent analyses and discussions will focus primarily on the 41 colonies in which mtDNA and UCE data reached a consensus on clade assignment, in particular those in the red and blue clades.

Sequence divergence

COI divergence was estimated from 47 sequences, including 41 *M. mendax* colonies from the three main consensus clades (n = 18 red, 3 green, 20 blue), two *M. placodops*, two *M. semirufus*, and two *M. mimicus* taxa. When treated as a single clade, the average K2P distance within *M. mendax* was 0.0467 ± 0.0074, two times larger than the mean distance within *M. placodops* (0.0222 ± 0.0064) and *M. mimicus* (0.0199 ± 0.0062, Table 4.4). *M. semirufus* haplotypes were essentially identical. When treated separately, K2P estimates within individual *M. mendax* clades were below 0.02 (average = 0.0055 ± 0.0017, Table 4.4). The average distance between the red and blue clades was 0.0805 ± 0.0158, comparable to values of congeners (*M. semirufus* – *M. placodops*: 0.0856 ± 0.016, *M. mimicus* – *M. placodops*: 0.0882 ± 0.0144; Table 4.5) and greater than the distances between *M. placodops* and the blue and green clades (*M. placodops* - green: 0.0619 ± 0.0173, *M. placodops* - blue: 0.0619 ± 0.0162; Table 4.5). Nucleotide diversity estimated from *M. mendax* mtDNA were in agreement with K2P distances, with the average nucleotide diversity within clades (π_S) of 0.0055 ± 0.0011 and the total

nucleotide diversity across all *M. mendax* clades (π_T) of 0.0467 ± 0.0075 (Table 6). The coefficient of nucleotide differentiation (N_{ST}) was 0.8821 ± 0.0232.

The UCE K2P estimates were derived from 55 sequences, which included the same 41 *M. mendax* colonies as mentioned in the previous paragraph, as well as two *M. melliger*, two *M. flaviceps*, two *M. mimicus*, two *M. placodops*, and five *M. semirufus* specimens. When *M. mendax* sequences were treated as a single clade, the average within-clade K2P distance was 0.0023 ± 0.0001, comparable to some congeners (*M. melliger* = 0.0024 ± 0.001, *M. semirufus* = 0.0023 ± 0.001; Table 4.4). Individual *M. mendax* clades have an average within-group distance of 0.002 (Table 4), lower than the average between-clade distance of 0.0025 (Table 4.7). The between-clade average was lower than distances between congeners (Table 4.7). UCE sequences of *M. mendax* clades were more similar to those of *M. melliger* (average = 0.0032) than *M. placodops* (average = 0.006; Table 4.7) and *M. placodops* (average = 0.006). The average interspecific divergence was 0.0064. Average nucleotide diversity within *M. mendax* clades was slightly lower than the total diversity (Table 4.6), and N_{ST} estimated from nuclear UCE was 0.1244, seven times lower than the mtDNA estimate (Table 4.6).

Phylogeography

Based on the UCE tree, clades tend to be spatially segregated (Figure 4.7A); however there was some evidence of gene flow and admixture between genetic units when taking mtDNA and microsatellite data into account (Chapter Three; Figures 4.7B and 4.7C). Considering only members of the consensus clades, colonies of the red clade

are primarily found at more western longitudes (Kruskal-Wallis test, $\chi^2 = 35.168$, $df = 3$, $P < 0.001$; Nemenyi test, $P_{red\text{-}blue} < 0.001$) and lower elevations (Kruskal-Wallis test, $\chi^2 = 14.919$, $df = 3$, $P < 0.01$; Nemenyi test, $P_{red\text{-}blue} < 0.001$) than the blue clade. The red clade also appears to associate with higher latitude than the blue clade, but no statistical significance was found in the post-hoc test (Kruskal-Wallis test, $\chi^2 = 18.722$, $df = 3$, $P < 0.001$; Nemenyi test, $P_{red\text{-}blue} = 0.66$). A principle component analysis (PCA) of 44 colonies with genetic and GPS data illustrated these differences, with the first two components explaining 88.4% of the variation in the data (Figure 4.8). PC1 correlated with longitude, elevation, and consensus clade, while PC2 suggested an effect of latitude. The probability eclipse of the red clade did not overlap with any other group.

The Bayesian analysis of the *M. mendax* mtDNA sequences suggests that there is gene flow between members of the same clade but not between those of different clades (Figure 4.9). This observation explained the composition of most populations. There was evidence of admixture between LEM and SUP (probability = 0.972, Table 4.8), which was also supported by the MCC tree topology. SHO was connected with three sky island populations, and also with NM (probability = 0.893, Table 4.8).

Mapping populations onto ecological regions showed that the red clade was mostly found in Arizona/New Mexico Mountain forests, while the green and blue clades and colonies with conflicting mito-nuclear clade assignment were mostly associated with Sierra Madre Occidental pine-oak forests (Figure 4.10). These ecoregions are spatially non-overlapping but share some common faunal features (Griffith et al. 2014).

Hair length variation

In the workers examined, head width (HW) ranged from 0.866 to 2.023 mm (average = 1.437 ± 0.0119 mm), similar to the distribution described by Snelling (0.9 – 1.9 mm, 1976). HW explained most of the variation of the minimum ocular diameter (MOD, Figure 4.11A, adjusted R^2= 0.857, $F_{1,494}$ = 2957, β = 0.115, P < 0.001) but less of pronotal hair length (Figure 4.11B, adjusted R^2= 0.422, $F_{1,494}$ = 361.6, β = 0.220, P < 0.001). The distribution of the hair-length-MOD ratio is unimodal and right-skewed (Figure 4.11C, average = 0.806 ± 0.0124).

The model fitted on hair length was improved substantially when the genetic structure inferred from all molecular data was added as a categorical variable, in addition to HW (coding: red = 1, green = 2, blue = 3; adjusted R^2= 0.622, $F_{2,482}$ = 401.4, β_{HW} = 0.216, $\beta_{genetic}$ = -0.0356, P < 0.001). Regressing hair length within each individually genetic group showed HW and hair length correlated well for ants of the red clade (Figure 4.12, adjusted R^2= 0.811, $F_{1,211}$ = 908, β = 0.278, P < 0.001) and blue clade (adjusted R^2= 0.772, $F_{1,173}$ = 589.5, β = 0.159, P < 0.001), but less well for the green clade (adjusted R^2= 0.267, $F_{1,51}$ = 14.93, β = 0.234, P < 0.001) and for ants from colonies in which mtDNA and UCE data disagreed on clade membership (adjusted R^2= 0.417, $F_{1,52}$ = 38.88, β = 0.224, P < 0.001). The three *M. mendax* clades have different hair length distributions (Kruskal-Wallis test, χ^2 = 216.88, df = 3, P < 0.001) which were most obvious when examining major workers (HW ≥ 1.5 mm, Figure 4.13). Specifically, majors of the red clade have longer hair than those of the blue clade (average: red = 1.137, blue = 0.701; Kruskal-Wallis test, χ^2 = 92.099, df = 3, P < 0.001). This pattern can

be illustrated on the phylogenetic trees (Figure 4.14). In a PCA examining the relationships between phylogenetic structure and phenotypic variation, PC1 correlated clade membership and hair length, explaining 57.2% of the variation in the complete data (Figure 4.15). The probability eclipse of the red clade overlapped with that of specimens with conflicting mtDNA and UCE clade assignment.

In addition to genetic grouping, variation in hair length is correlated with inferred average minimum and maximum monthly temperatures (adjusted R^2= 0.541, $F_{3,125}$ = 51.25, $\beta genetic$ = -0.169, $\beta min.temp$ = 0.0525, $\beta max.temp$ = -0.0628, P values < 0.01), suggesting an effect of climate on hair length distribution. However, the direction of effect is not apparent when examining the regression coefficients, suggesting a more complex relationship.

Social structure variation

With respect to the mtDNA ML tree, there were significantly more polygynous colonies (estimated in Chapter Three) in the red clade than in the blue clade (Kruskal-Wallis test, χ^2 = 25.08, df = 2, P < 0.001; Nemenyi test, $P_{red\text{-}blue}$ = 0.0029); green was not significantly different from red and blue (Figure 4.14A). The same results were obtained with queen number estimated by COLONY taken from Chapter Three. A difference in polygyny frequency was also detected among UCE clades, but the post-hoc test did not reveal any pairwise significance, probably due to lower sample size (Figure 4.14B). There was no correlation between clade membership and variation in mating strategy and patriline number.

Discussion

Although there is a spatial component, geography alone does not fully explain the genetic structure of *M. mendax*. Consider the red and blue clades. Molecular data suggest that there is gene flow within these clades (Figure 4.6, Table 4.8). However, there is no evidence for gene flow and admixture between these clades, even where geographical distance is unlikely a barrier to dispersal. For instance, all LEM and SHO sequences were assigned entirely to the red and blue clades on the mtDNA and UCE trees, respectively (Figures 4.2 – 4.4), despite the proximity of these populations to those of the other clades (Figure 4.7). Additional sampling may reveal connectivity between these two clades, but so far the separation has been consistent across all localities. Evidence for admixture and migration has primarily been found between the red and green clades, and the green and blue clades. Indeed, five specimens clustered within the green mtDNA clade are distributed across several UCE clades including red and blue, and three specimens clustered within the blue mtDNA clade clustered with other UCE clades except with red (Figure 4.6).

In his revision, Snelling noted that a significant difference in hair length separated *M. mendax* samples from Colorado, northern New Mexico and Arizona, Nevada and California from those of Texas and southern New Mexico and Arizona (Figure 4.1A). "In large workers of the northern, short-haired form, the longest hairs of the pronotum are 0.58-0.6 x the MOD…", and "From the Edwards Plateau of central Texas to the mountains of southern Arizona a distinctive, long-haired form predominates, but does not wholly replace 'normal' mendax" (pg. 40, Snelling 1976). The geographical distribution

of hair length variation in contemporary populations contradicted some of Snelling's remarks. For example, major workers in all of the northern Arizona and New Mexico populations, including PIN, SUP, SIE-A, ORD, PINE, SHO, MIN, HUAL, SED, and NM, have the maximum hair-length-to-MOD ratio exceeding Snelling's short-haired threshold of 0.6 (Figure 4.16). In fact, these populations should be characterized as long-haired. On the other hand, my data corroborated Snelling's observations regarding the southern populations. Measurements showed both hair forms co-occurring at six locations in southeastern Arizona (HUAC, WHE, DRA, CHI, PAT, and GRA) and one location (SIE-B) in northern Sonora. Specimens with the longest hair of all samples (>1.4x MOD) were from SAN and SIE-B, localities with colonies that share genetic similarity with *M. melliger*, a closely related species with long hair that is probably parapatric or sympatric with *M. mendax* at these sites (Figures 4.1A, 4.6, and 4.16). Based on the collection records and distribution map presented in the genus revision (Figure 4.1A), it is likely that Snelling only had hair data from PINE, SED, and NM, and thus may have missed finding the long-haired form at other northern sites including PIN, SUP, SIE-A, ORD, and HUAL (Figures 4.1A and 4.16). There was no contemporary sample with short hair found at PINE, SED, and NM, but admittedly sample size and coverage was limited at NM and especially PINE. It is possible that the short-haired form only occurs within specific microhabitats in these localities, and its absence from the data was attributable to sampling bias. Alternatively, the distribution of may have shifted since Snelling's investigation due to climate change.

Thermoregulation in a desert ant, *Cataghlyphis bombicina*, has been recently found to be influenced by surface pilosity (Shi et al. 2015), and a global phenotypic database showed a correlation between hairiness and open, warm habitats (Parr et al. 2017). In *M. mendax*, the pattern inferred from the best-fitting linear regression model was ambiguous, although it did not exclude a relationship between temperature and hair length variation. The regression coefficients showed that hair length significantly increases with decreasing maximum monthly temperature and with increasing minimum temperature; the same relationships were observed when analyzing only major workers and the entire worker size distribution, with and without accounting for genetic structure. Since the temperature data were inferred from historical climate and geolocation data, it is possible they do not accurately reflect the actual conditions experienced by colonies. Furthermore, hair length may correlate with hair density or other pilosity properties, which may fit the temperature profile better. Alternatively, the observed hair length pattern may have been shaped purely by drift.

Based on the variation in social structure observed between SIE-A and CHI described in Chapter Two, it was predicted that populations more closely related to SIE-A would exhibit a higher degree of polygyny. According to the sequence data, however, social structure was only weakly correlated with the UCE phylogeny (Figures 4.13 and 4.14), although colonies belonging to the red clade were more likely to have more queens. The small number of sites exhibiting polygyny suggests that it may have evolved independently in different populations. The occurrence of queen cooperation is dependent on favorable tradeoffs and a suite of phenotypic changes, thus likely making its evolution

difficult and highly site-specific. A second possibility is that polygyny is a shared derived character of the red clade, and simply was not detected in some populations due to natural temporal fluctuation (see Chapter Two). Alternatively, polygyny could be an ancestral character present in the common ancestor of all *M. mendax* that became lost repeatedly, perhaps due to a relaxation of selective pressures. However, it is more likely that monogyny is the ancestral state, because it is more widespread in *Myrmecocystus* (Snelling 1976).

The COI K2P distance estimated from all *M. mendax* specimens was nearly 5% (Table 4.4), above the 2-3% threshold to be considered a single Molecular Operational Taxonomic Unit (MOTU, Smith et al. 2005). Average intraspecific divergence was estimated to be 1.9% in North American ant fauna, and MOTUs designated using the 2-3% threshold correlated well with morphological identification (Smith et al. 2005). Within-clade COI K2P estimates ranged 0.1 - 1%, well below the MOTU threshold and closer to intraspecific estimates of *M. placodops* and *M. mimicus* (~2%), and the distance between the red and blue clades (8%) was similar to those between congeners (Table 4.6). Diversity estimates provide support for similar conclusions (Table 4.6). In contrast, nuclear loci are not as divergent. K2P estimates of all *M. mendax* UCE sequences are similar to intraspecific distances in congeners (Table 4.4), and the distances between individual *M. mendax* clades are smaller than those between congeners (Table 4.7). The observed difference in divergence may be explained by the difference in rate of evolution and effective population size between the mitochondrial and nuclear genes (Hurst and Jiggins 2005; Moritz et al. 1987).

Despite weak support for many of the interior nodes of the COI ML tree, the topological congruence between the COI and UCE trees lends confidence to the relationships recovered. Since mtDNA is maternally inherited and the female is the primary dispersing sex in ants, the inferred topology likely reflects historical processes related to female dispersal. The subdivision in *M. mendax* was sufficiently ancient to enable coalescence of nuclear genes. Because of the smaller effective population size, mitochondrial loci are expected to coalesce more rapidly following vicariant events (Zink and Barrowclough 2008) while nuclear loci may lag behind. According to UCE data, *Myrmecocystus* split from a *Lasius*-like ancestor about 20-25 million years ago (MYA, Blaimer et al. 2015). Assuming an arthropod COI clock with divergence rate of 1.2-1.5% per million years (Caccone and Sbordoni 2001), it is estimated from the K2P distance between the *M. mendax* red and blue clades that these groups split from a common ancestor around 6.7 ± 1.3 MYA or 5.4 ± 1.1 MYA (Table 5). Another, more rapid substitution rate of 2.3 % (Brower 1994) shifted the estimate to around 3.5 ± 0.7 MYA. Overall, these values suggest that *M. mendax* populations probably diverged during the Pliocene (2.6-5.3 MYA) or late Miocene (5.3-23 MYA, Gibbard et al. 2009), a time during which the uplifting of the Rocky Mountains and other geological processes may have changed the climate and landscape in significant ways that enabled population expansion and isolation. During the Pleistocene, the Arizona climate was probably much cooler and wetter (Fellows 2005). Contemporary *M. mendax* populations in Arizona are found on mountainous regions where temperature is not as extreme and precipitation is higher relative to lower desert habitats. This leads me to think that the red and blue clades

became isolated from each other after the last series of glacial movements. As northern ice sheet receded and regional climate warmed and became drier, local populations adapted to glacial conditions have to move up the elevation gradient to find suitable habitats, reducing gene flow between lineages inhabiting different part of the range.

Cumulatively, the genetic, morphological, and behavioral data supported Snelling's hypothesis of cryptic diversity in *M. mendax*. Populations of this morphospecies can be separated into at least two genetic units that inhabit relatively discrete geographical and ecological regions (Figure 4.10). The UCE data, which spanned a larger spatial scale, suggested additional diversity is present (Figure 4.7A). Despite finding significant molecular divergence, more analyses and data are needed to assess whether these genetic units constitute discrete, reproductively isolated taxa (see Chapter Five). Additional work is also needed to draw the evolutionary boundary between *M. mendax* and its two sister species, *M. placodops* and *M. melliger*, and to find more reliable identification characters. It was suggested that *M. mendax* and *M. melliger* are sister species based on morphological similarities in workers, queens, and males (Snelling 1976, pg. 35). Snelling advanced another hypothesis based on the geographical distribution of hair length variation, proposing that *M. mendax* and *M. placodops* evolved from a *M. melliger*-like ancestor (Snelling 1976, pg. 41). The UCE analyses supported the sister relationship of *M. mendax* and *M. melliger* with high confidence (Figures 4 and 5), and *M. placodops* to be the most ancient lineage of the trio. In contrast, the mtDNA showed *M. melliger* and *M. placodops* nesting with *M. mendax* (Figure 4.2). However,

the nodal support for this relationship is low, indicating insufficient resolution due to a lack of informative characters.

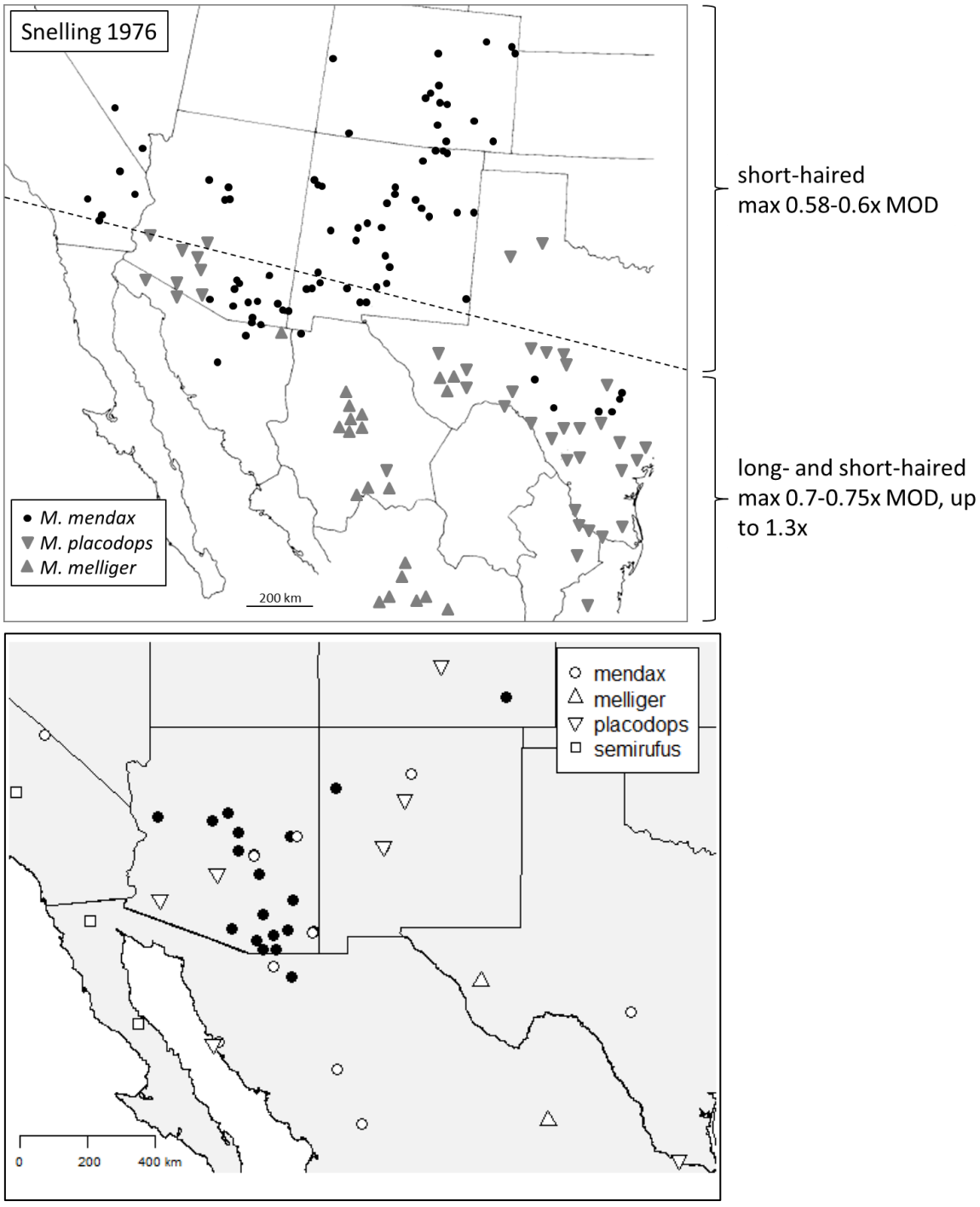

Figure 4.1. Top panel – Historical distribution of *M. mendax* (and its hair forms), *M. melliger*, and *M. placodops* (modified from Snelling 1976). Bottom panel – Distribution of *melliger* group specimens gathered for the present study; all localities have at least one UCE sequence; for *M. mendax* localities, dark circle indicate hair length data are available.

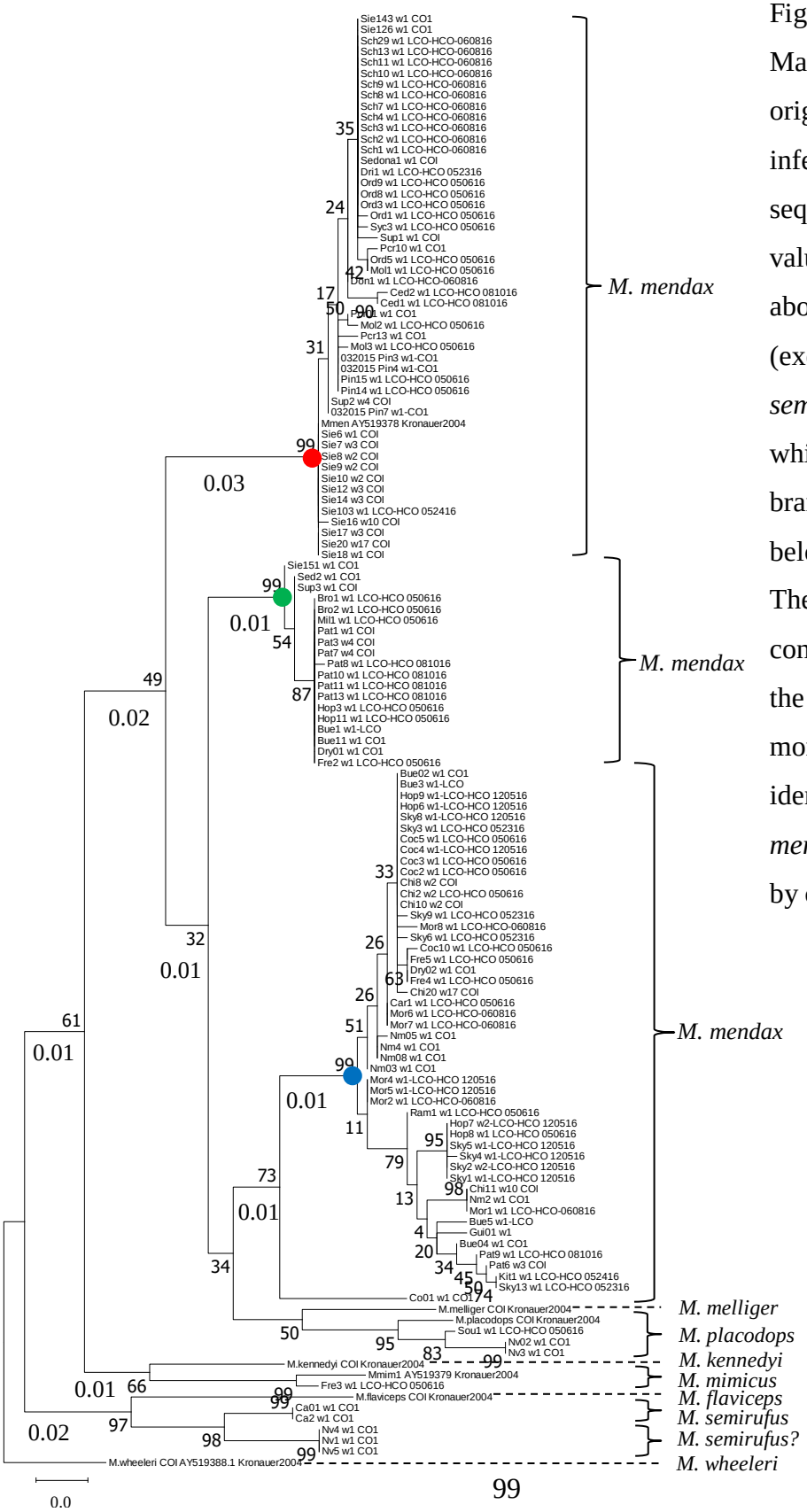

Figure 4.2. Maximum Likehood original phylogram inferred from COI sequences. Bootstrap values are printed above the branches (except for *M. semirufus* clade), while selected branch lengths are below the branches. The three clades containing most of the specimens morphologically identified as *M. mendax* are marked by colored circles.

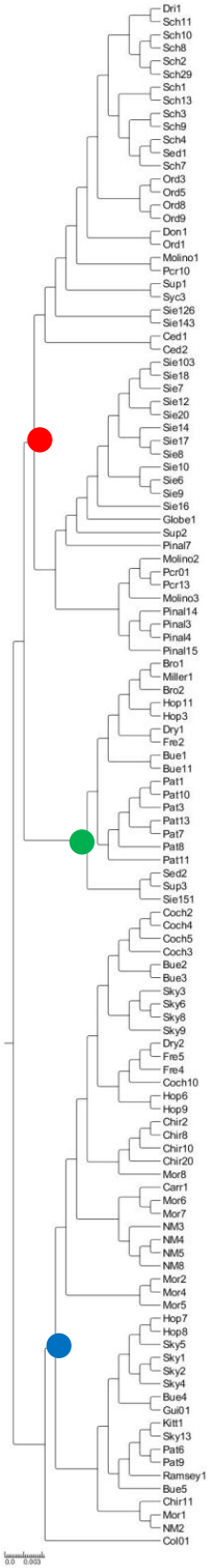

Figure 4.3. Maximum Clade Credibility cladogram inferred from COI sequences by a Bayesian phylogeographical analysis. Note the similarity in topology with the Maximum Likelihood tree (Figure 4.2).

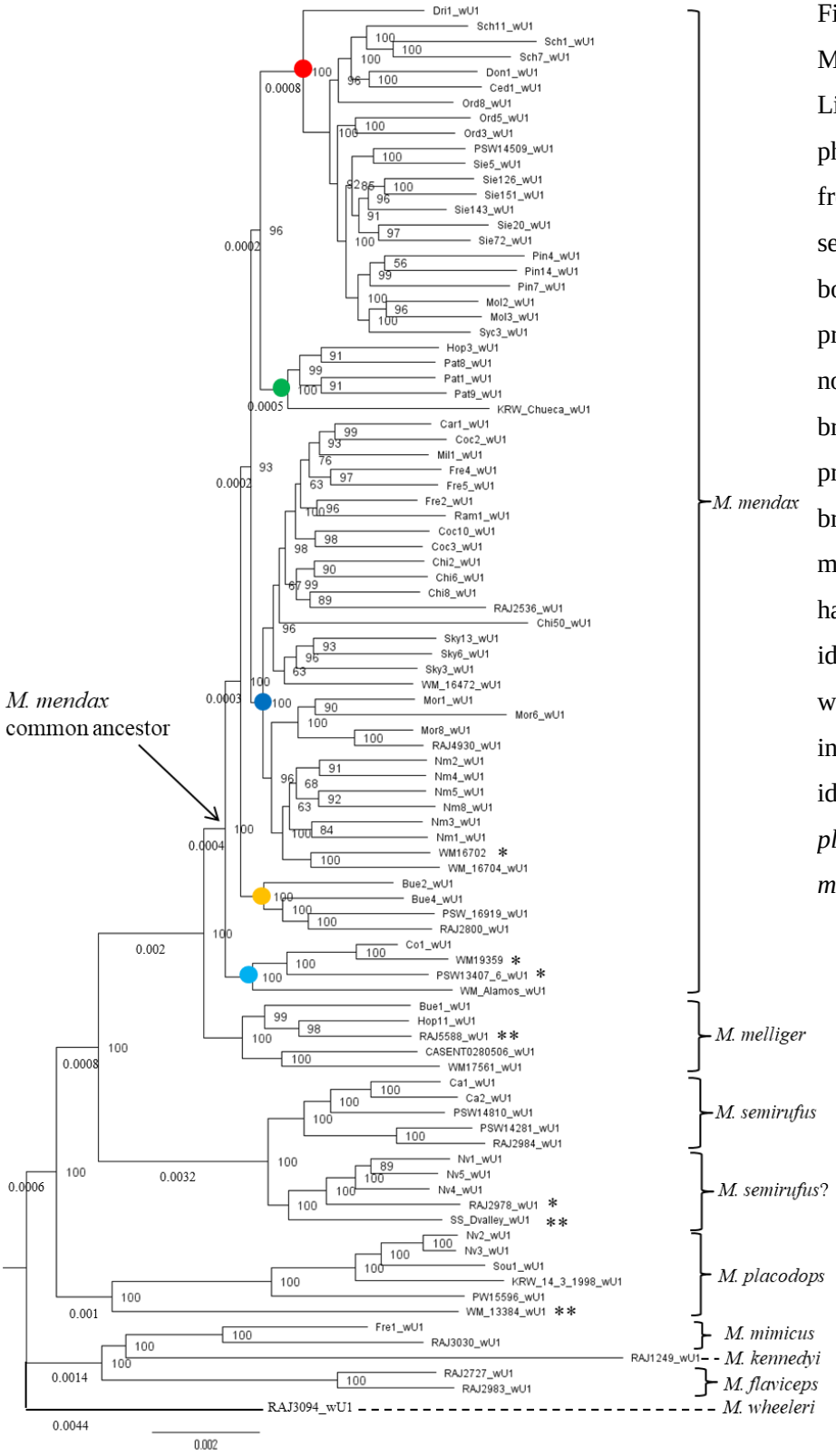

Figure 4.4. Maximum Likelihood original phylogram inferred from UCE sequences. Ultrafast bootstrap values are printed next to each node. Selected branch lengths are printed below the branches. Taxa marked by asterisks had morphological identity in conflict with molecular inference (originally identified as **M. placodops*, or ***M. mendax*).

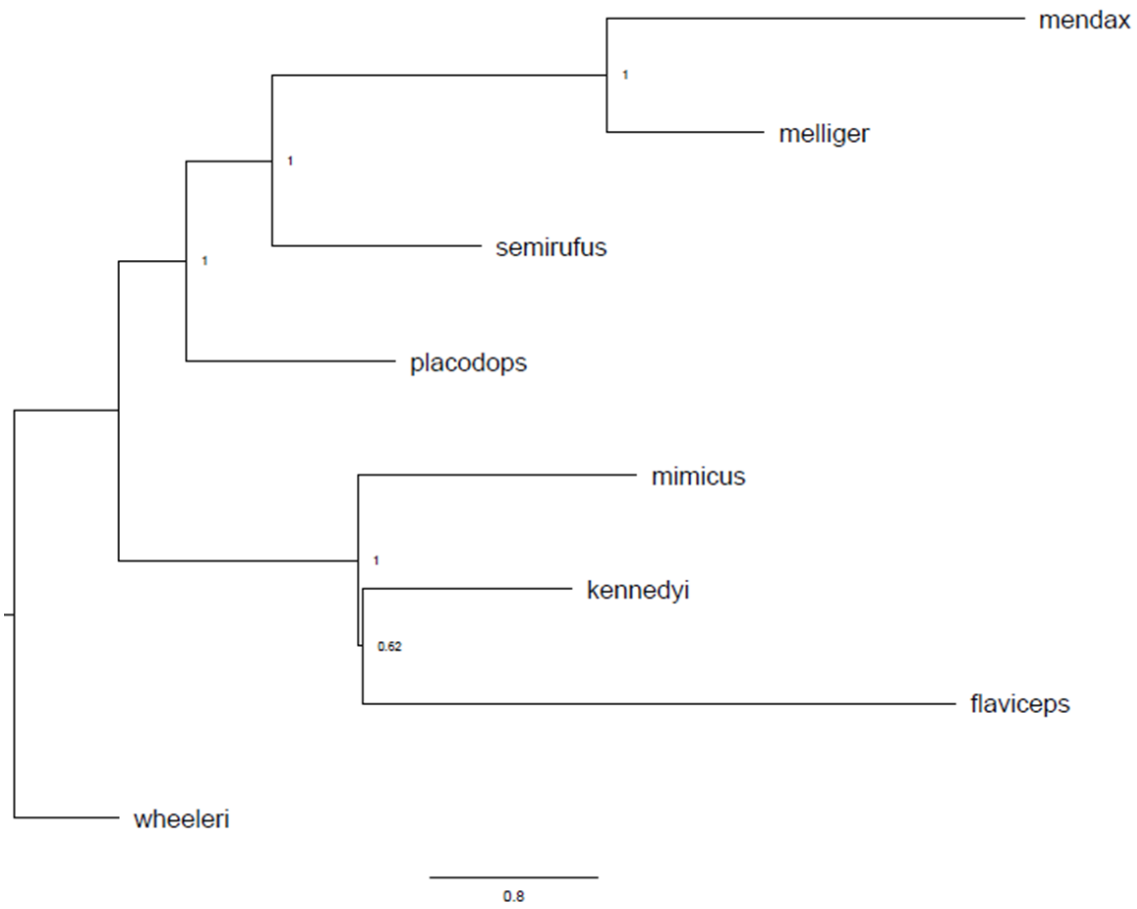

Figure 4.5. Species phylogram inferred from UCE data. *M. mendax* and *M. melliger* are sister taxa on this tree, with *M. placodops* being more basal. Posterior probabilities are printed next to each node. Branch lengths are measured in coalescent units.

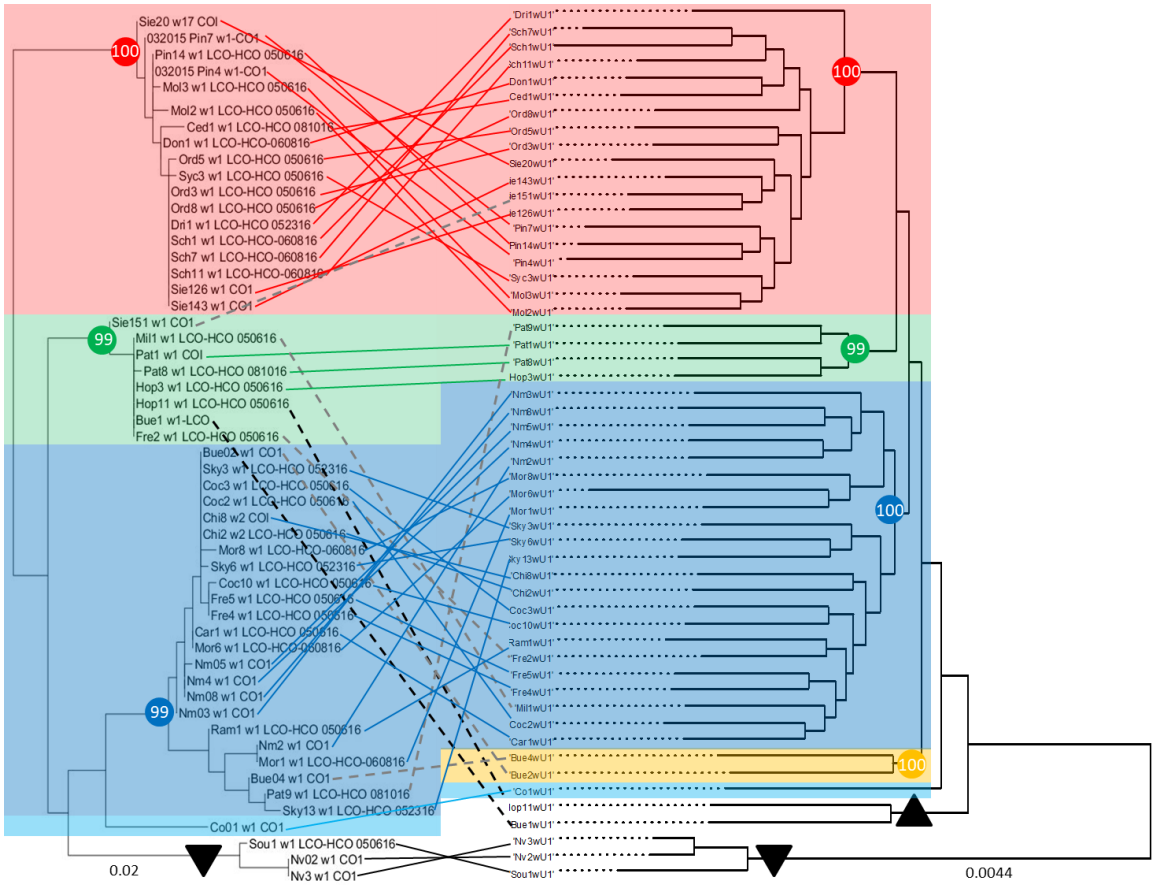

Figure 4.6. Mirror image display of the partial Maximum Likelihood mtDNA tree (left) and UCE tree (right). Inferred clades are color-coded. Sequences on both trees from the same colony are linked by lines. Solid lines signify consistent clade membership on both trees, while dashed lines denote incongruency. Relevant node support values are printed in colored circles. The clade marked with upward triangle groups with *M. melliger* specimens on the full tree. The clade marked with the downward triangle grouped with *M. placodops* specimens.

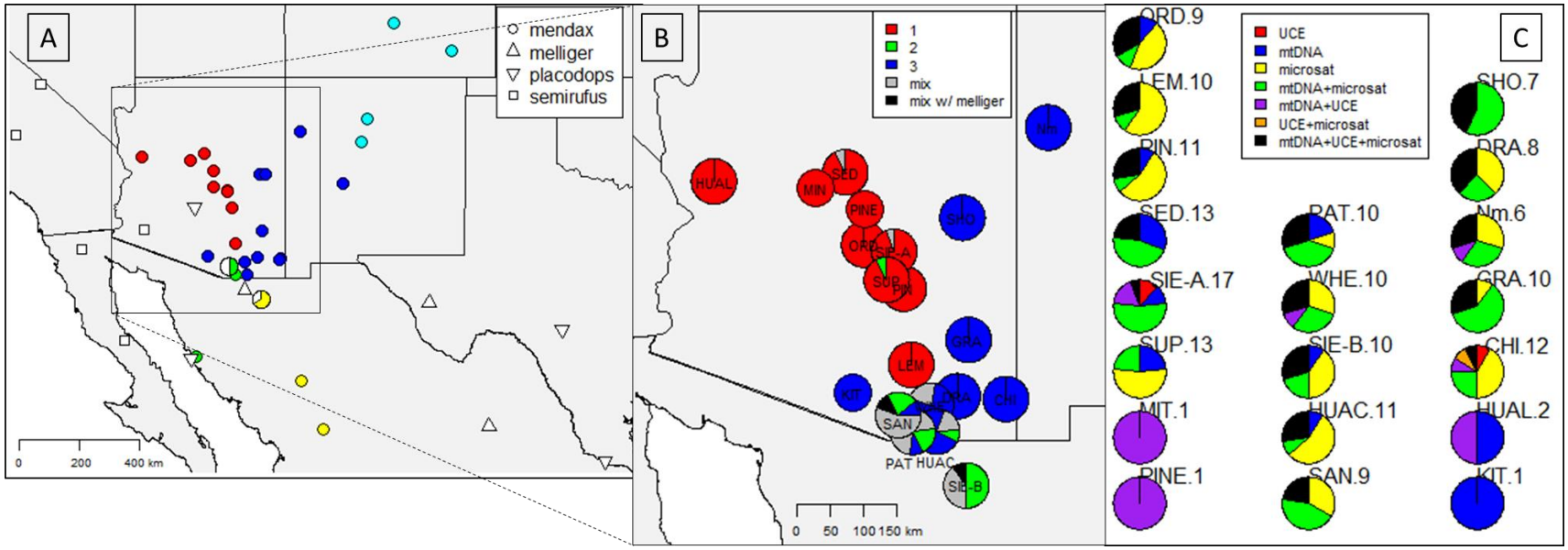

Figure 4.7. (A) Distribution of UCE-inferred *M. mendax* clades represented by colored circles. (B) Focal *M. mendax* populations color-coded base on clade composition. (C) The number of colonies and types of data used to infer the genetic structure at each population.

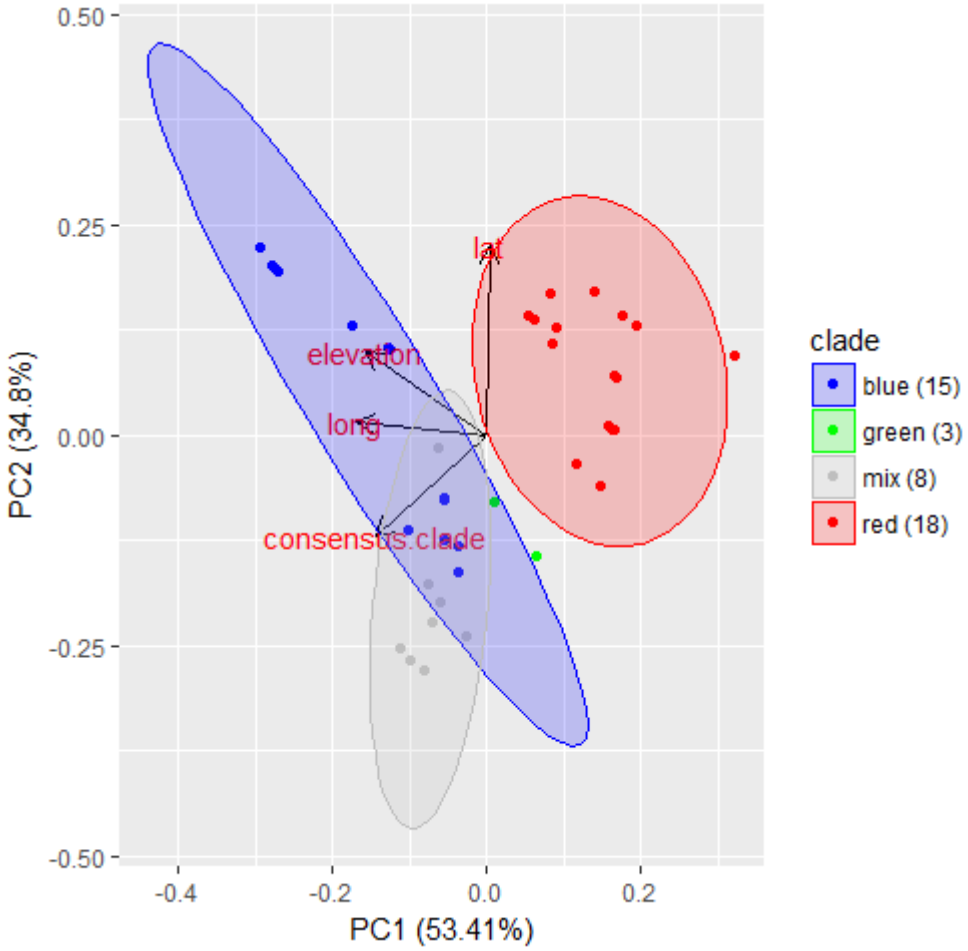

Figure 4.8. Principle components 1 and 2 show correlations between consensus clades (inferred from UCE and mtDNA trees) and latitude, longitude, and elevation. Sample sizes are given in the legend.

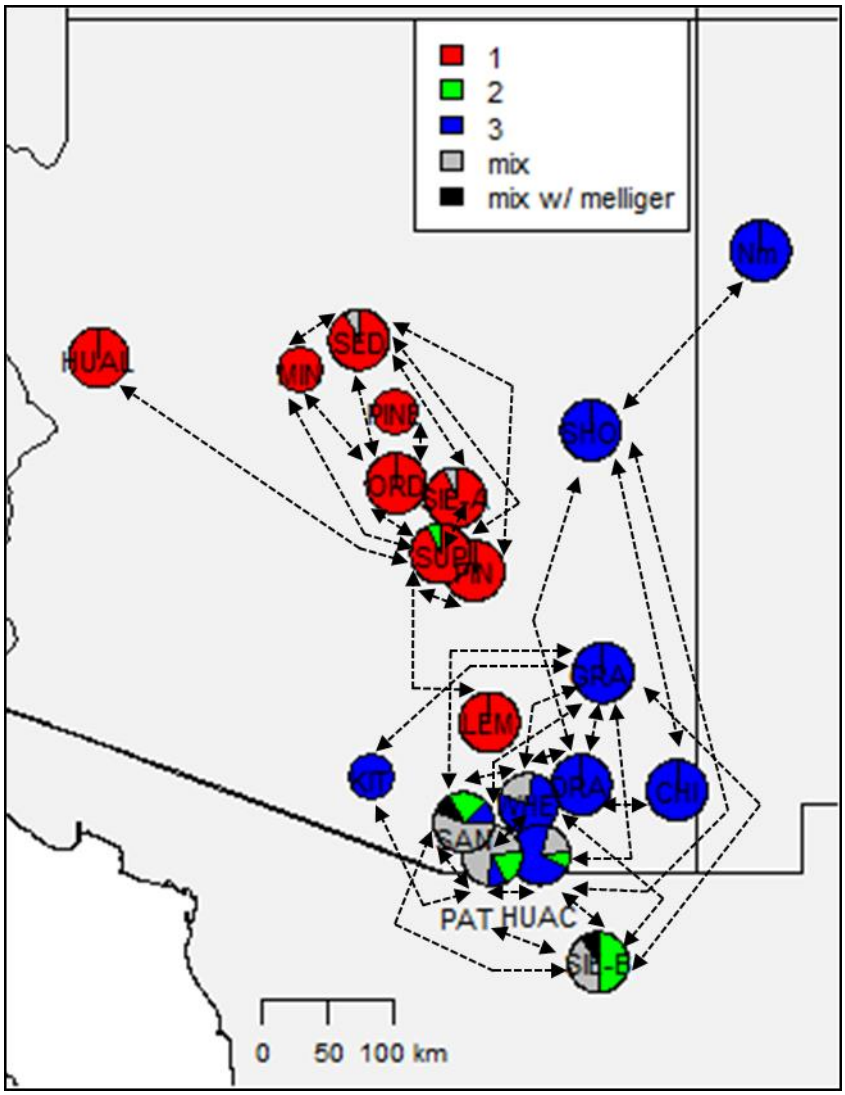

Figure 4.9. Gene flow map of focal *M. mendax* populations, inferred from the Bayesian phylogeographical analysis.

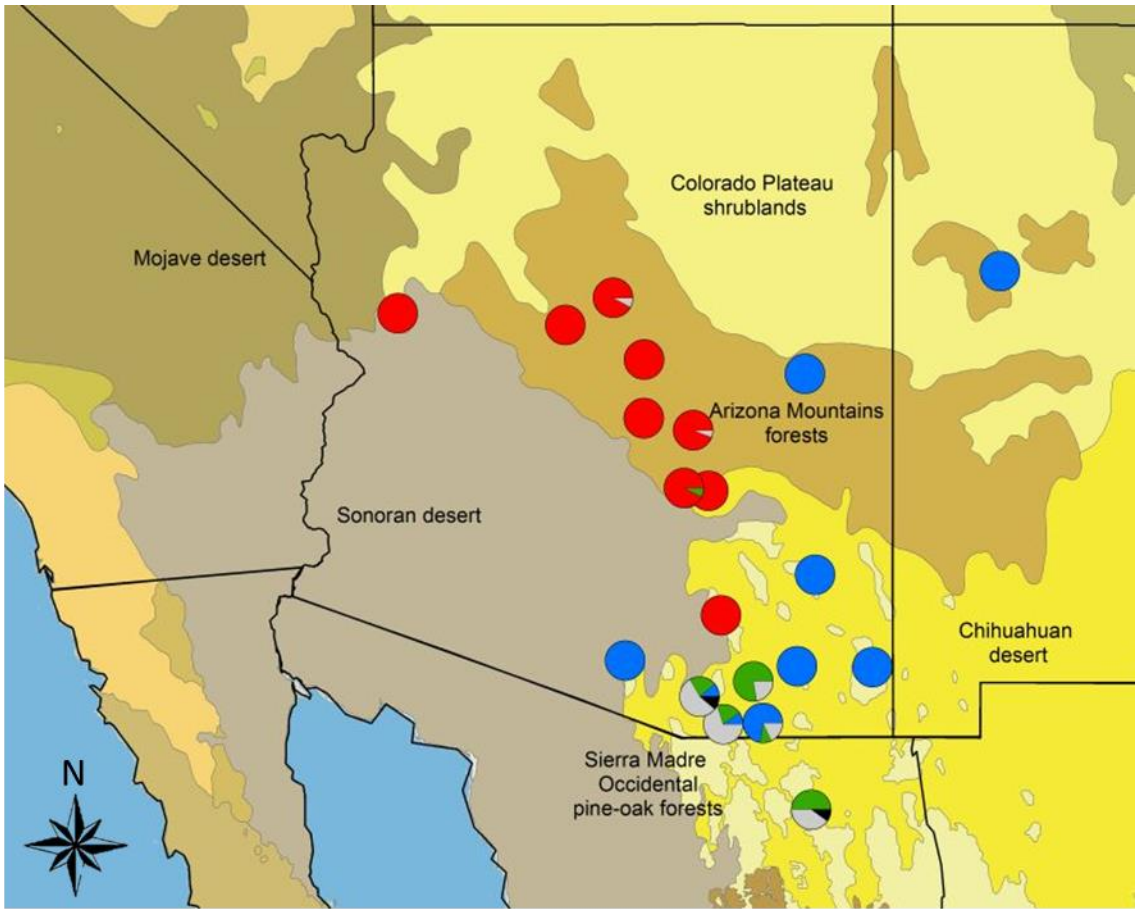

Figure 4.10. Ecological region map of focal *M. mendax* populations. Colors in pie charts represent the genetic structure inferred from mtDNA and UCE sequences (Figure 4.9).

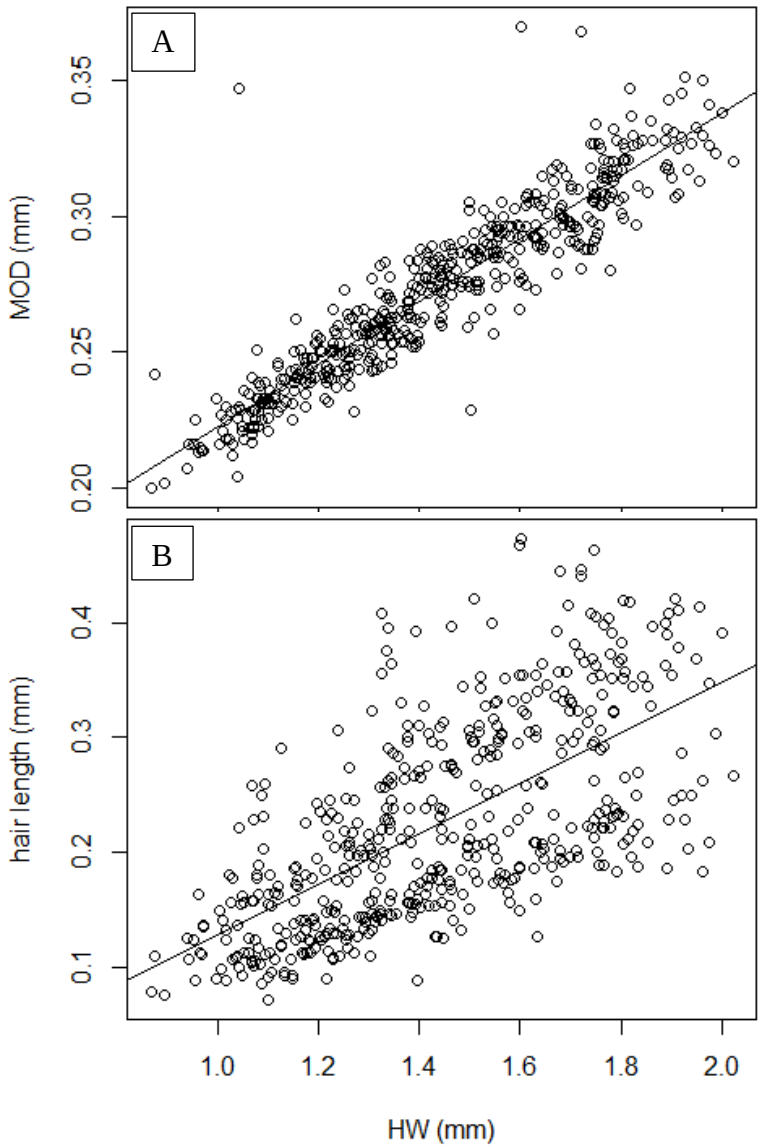

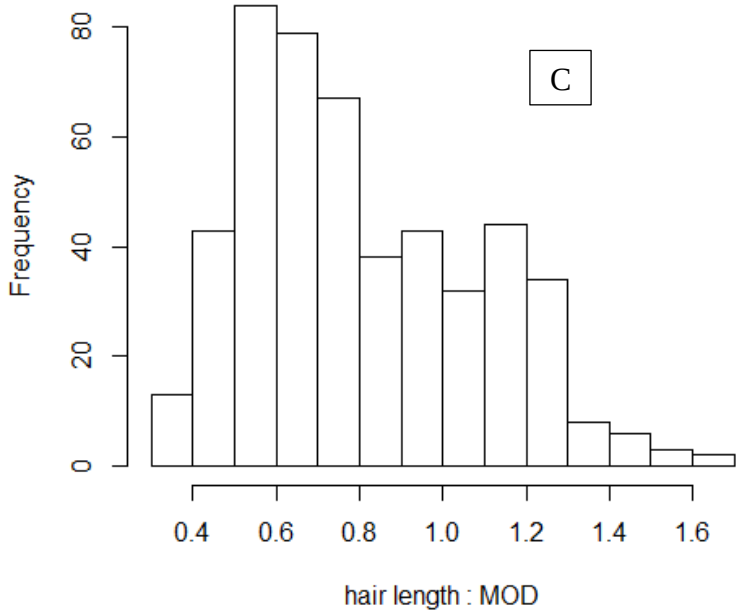

Figure 4.11. Minimum ocular diameter (MOD - panel A) and hair length (panel B) correlated with head width (HW) of all measured *M. mendax* workers. Panel C – The distribution of the ratio

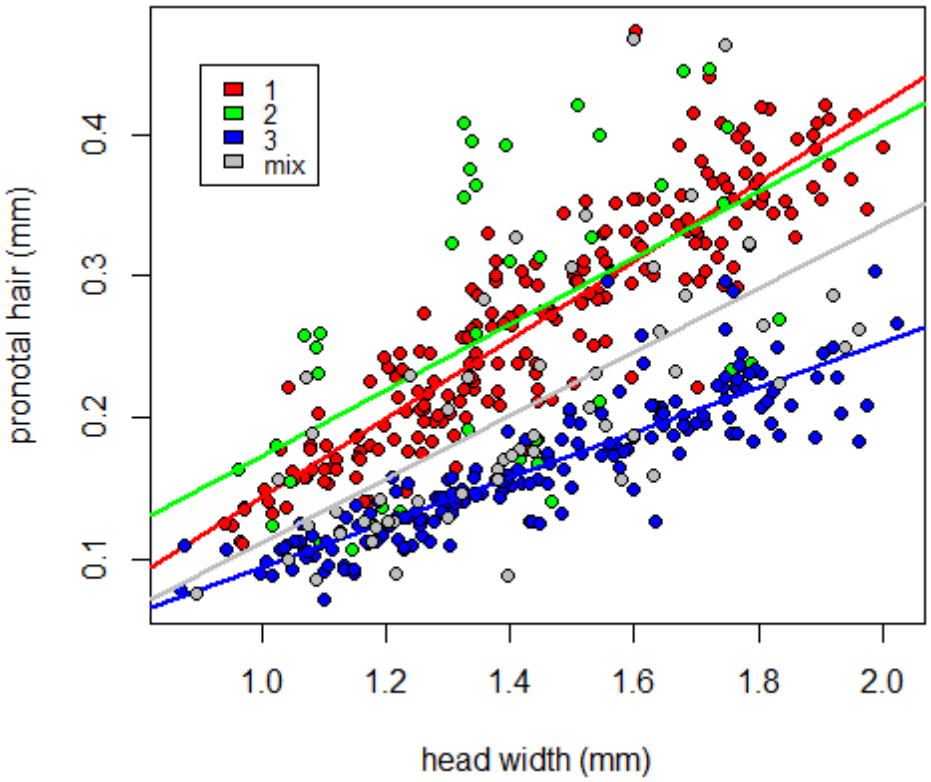

Figure 4.12. Hair length correlated with head width in *M. mendax* colonies of each inferred consensus clade and colonies with incongruent clade assignment.

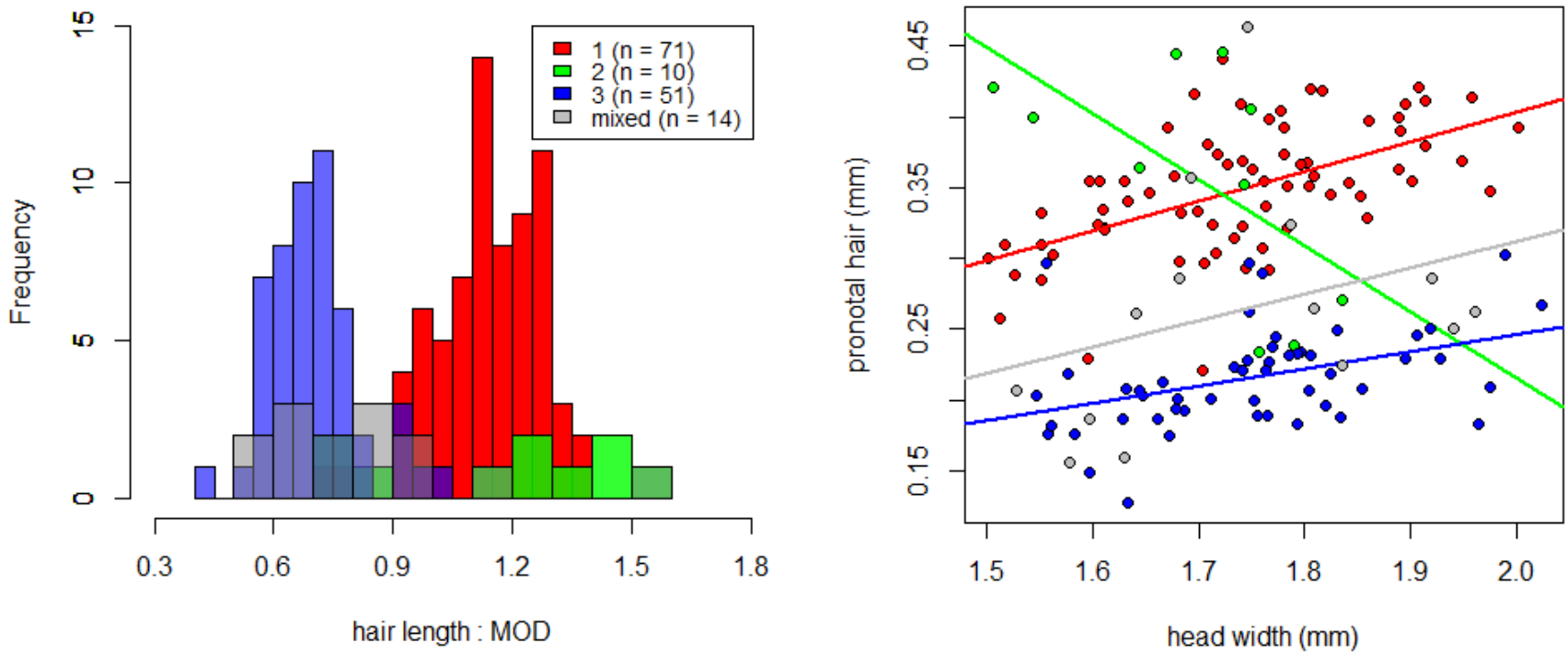

Figure 4.13. Major workers of red and blue clades have different hair-length-to-MOD distributions (left). Those in the red clades have longer hair; this is also apparent when plotting hair length against head width (right).

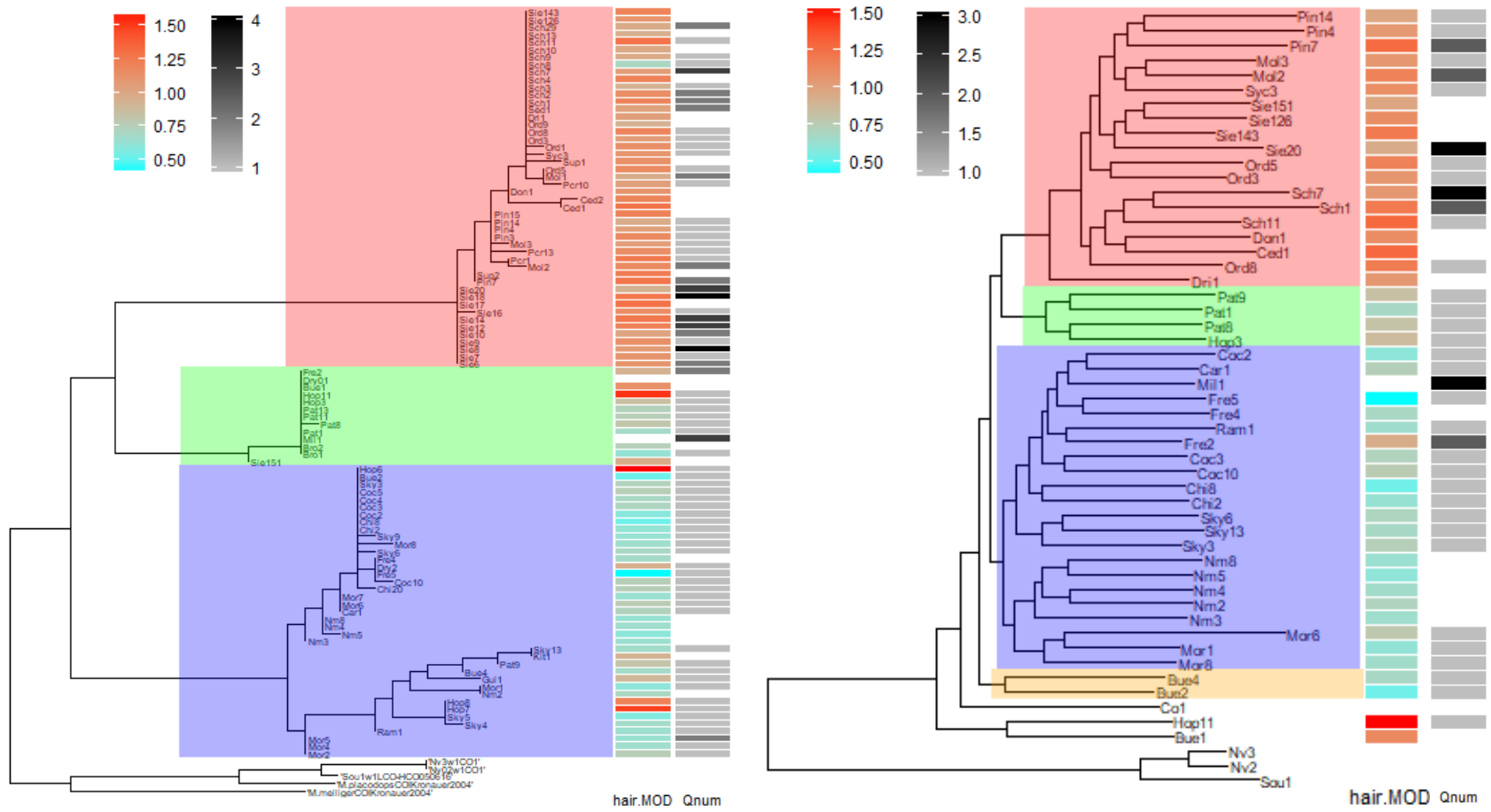

Figure 4.14. Hair length (red-blue scale) and queen number (black-white scale) vary across the partial mtDNA (left) and UCE tree (right). Colonies with long-haired workers and multiple queens tend to be in the red clade.

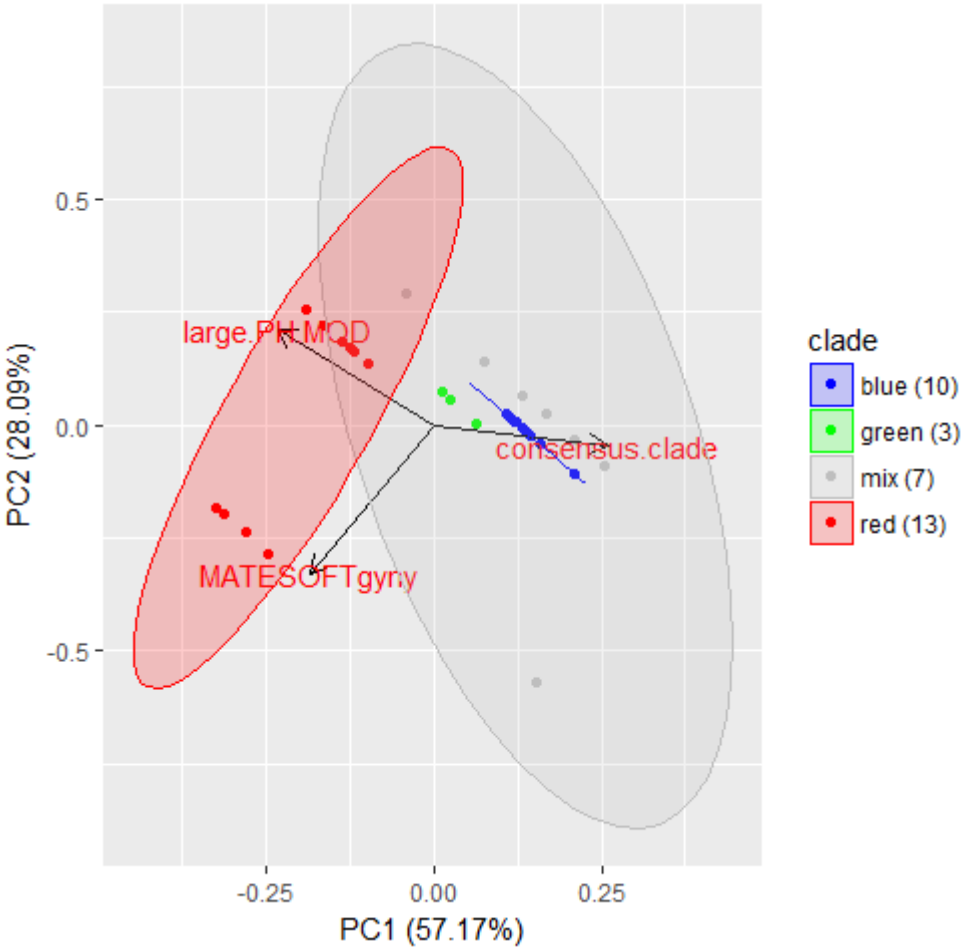

Figure 4.15. Principle components 1 and 2 show correlations between consensus clades (inferred from mtDNA and UCE population trees) and colony gyny and the hair-length-to-MOD ratio of major *M. mendax* workers. Sample sizes are given the in the legend.

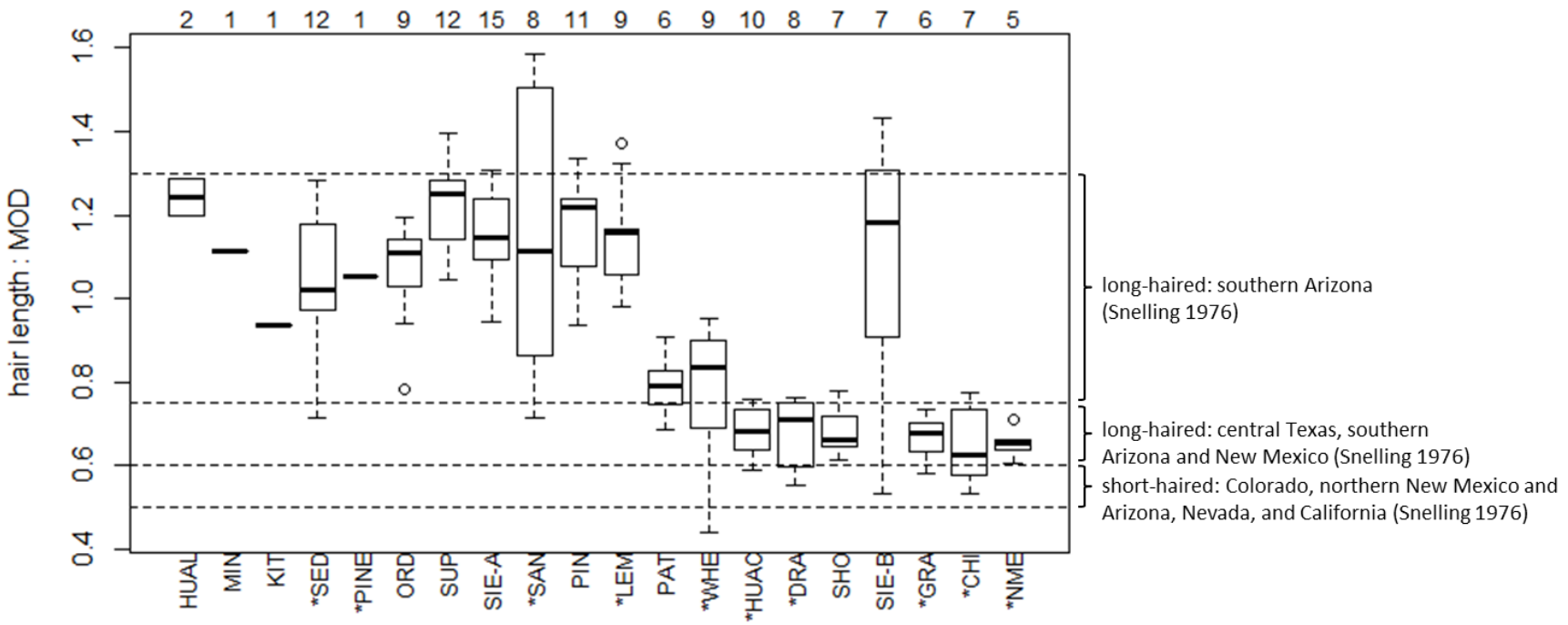

Figure 4.16. Hair length distribution of major workers by locality as measured from specimens collected in 2010-2017 (left to right: west to east). Areas mentioned by Snelling in his 1976 work are marked with asterisks. Sample sizes are above the top margin of the graph. Modern northern populations (PIN, SUP, SIE-A, ORD, PINE, SHO, HUAL, SED, and NM) do not fit into the short-haired category as previously observed by Snelling. On the other hand, some southern populations (SIE-B, HUAC, WHE, DRA, CHI, and GRA) contain

Table 4.1. A summary of samples studied in this chapter. Specimens are grouped based on their original morphological identification. Sequenced colonies are listed as follow: number of colonies with both UCE and mtDNA data, with UCE data only, and with mtDNA data only. The number of colonies with workers measured for hair length variation is listed in the last column.

Identified as	**Location**	**Sites (abbreviation)**	**Latitude, longitude**	**Colony abbreviation**	**Sequenced colony**	**Morphometry**
M. mendax (2010-2017)	Arizona, USA	Chiricahua (CHI)	31.90046°, -109.22757°	Chi	2, 2, 3	13
		Dragoons (DRA)	31.922778°, -109.966944°	Coc	3, 0, 2	8
		Huachucas (HUAC)	31.469761°, -110.304269°	Car, Bro, Mil, Ram	3, 0, 2	11
		Hualapai (HUAL)	34.752106°, -113.804922°	Ced	1, 0, 1	2
		Mt. Graham (GRA)	32.662326°, -109.794601°	Sky	3, 0, 1	10
		Kitt Peak (KIT)	31.96538°, -111.621°	Kit	1, 0, 0	1
		Mt. Lemmon (LEM)	32.334655°, -110.697279°	Mol	3, 0, 1	10
		Mingus Mt. (MIN)	34.65761°, -112.196°	Don	1, 0, 0	1
		Mt. Ord (ORD)	33.918889°, -111.437500°	Ord	3, 0, 2	9
		Patagonia (PAT)	31.456581°, -110.667989°	Pat	3, 0, 6	9
		Pinal Peak (PIN)	33.332980°, -110.833293°	Pin	3, 0, 2	11
		Pine (PINE)	34.38594°, -111.4364°	Dri	1, 0, 0	1
		Santa Ritas (SAN)	31.670556°, -110.898333°	Hop	2, 0, 3	9
		Sedona (SED)	34.868482°, -111.733514°	Sed, Sch	3, 0, 10	13
		Show Low (SHO)	34.266852°, -109.972765°	Mor	3, 0, 4	7
		Sierra Ancha (SIE-A)	33.78475°, -110.97103°	Sie	4, 2, 11	15
		Superstitions (SUP)	33.432186°, -111.058690°	Pcr, Sup	0, 0, 6	13
		Whetstones (WHE)	31.808611°, -110.388056°	Dry, Fre, Gui	3, 0, 3	9
	California, USA	California (CA)	34.089867°, -116.426032°	Ca	2, 0, 0	0
	Colorado, USA	Colorado (CO)	37.74474°, 103.484481°	Co	1, 0, 0	1
	New Mexico, USA	New Mexico (NM)	35.462485°, -108.543841°	Nm	5, 1, 0	6
	Nevada, USA	Nevada (NV)	36.281282°, -115.434989°	Nv	5, 0, 0	0
	Mexico	Sierra Buenos Aires (SIE-B)	30.738750°, -109.818400°	Bue	3, 0, 3	11
M. mendax (from other collections)	Arizona, USA	-	-	-	0, 3, 1*	0
	California, USA	-	-	-	0, 1, 0	0
	New Mexico, USA	-	-	-	0, 2, 0	0
	Texas, USA	-	-	-	0, 2, 0	0

	Mexico	-	-	-	0, 4, 0	0
M. melliger	Texas, USA	-	-	-	0, 1, 0	0
	Mexico	-	-	-	0, 1, 1*	0
M. placodops	Arizona, USA	-	-	-	0, 3, 2*	0
	Colorado, USA	-	-	-	0, 1, 0	0
	New Mexico, USA	-	-	-	0, 1, 0	0
	Texas, USA	-	-	-	0, 1, 0	0
	Mexico	-	-	-	0, 1, 0	0
M. semirufus	California, USA	-	-	-	0, 1, 0	0
	Mexico	-	-	-	0, 2, 0	0
M. mimicus	Arizona, USA	-	-	-	0, 1, 1	0
	Mexico	-	-	-	0, 1, 1*	0
M. flaviceps	California, USA	-	-	-	0, 0, 1*	0
	Mexico	-	-	-	0, 2, 0	0
M. kennedyi	Arizona, USA	-	-	-	0, 0, 1*	0
	Mexico	-	-	-	0, 1, 0	0
M. wheeleri	California, USA	-	-	-	0, 0, 1*	0
	Mexico	-	-	-	0, 1, 0	0
Total					**57, 35, 67**	**170**

*at least one sequence from Kronauer et al. 2004

Table 4.2. Summary statistics of sequence data.

Marker	**Number of taxa**	**Alignment length (bp)**	**Coverage (bp)**	**Variable sites**	**Parsimony informative sites**	**A%**	**T%**	**G%**	**C%**
COI	133	660	526	163	102	30.2	41.6	11.5	16.7
Concatenated UCE	92	1520549	?	115427	50813	29.221	29.039	21.007	20.733

Table 4.3. A list of colonies represented on both the mtDNA and UCE Maximum Likelihood trees. The position of each colony on both mtDNA and UCE inform the consensus clade assignment. Colony code can be found in Table 1.

Pop	**Col ID**	**mtDNA ML**	**UCE ML**	**consensus**
CHI	Chi2	blue	blue	blue
CHI	Chi8	blue	blue	blue
DRA	Coc10	blue	blue	blue
DRA	Coc2	blue	blue	blue
DRA	Coc3	blue	blue	blue
GRA	Sky13	blue	blue	blue
GRA	Sky3	blue	blue	blue
GRA	Sky6	blue	blue	blue
HUAC	Car1	blue	blue	blue
HUAC	Mil1	green	blue	mix
HUAC	Ram1	blue	blue	blue
HUAL	Ced1	red	red	red
LEM	Mol2	red	red	red
LEM	Mol3	red	red	red
LEM	Syc3	red	red	red
MIN	Don1	red	red	red
NM	Nm2	blue	blue	blue
NM	Nm3	blue	blue	blue
NM	Nm4	blue	blue	blue
NM	Nm5	blue	blue	blue
NM	Nm8	blue	blue	blue
ORD	Ord3	red	red	red
ORD	Ord5	red	red	red
ORD	Ord8	red	red	red
PAT	Pat1	green	green	green
PAT	Pat8	green	green	green
PAT	Pat9	blue	green	mix
PIN	Pin14	red	red	red
PIN	Pin4	red	red	red
PIN	Pin7	red	red	red
PINE	Dri1	red	red	red
SAN	Hop11	green	*M. melliger*	mix
SAN	Hop3	green	green	green
SED	Sch1	red	red	red

SED	Sch11	red	red	red
SED	Sch7	red	red	red
SHO	Mor1	blue	blue	blue
SHO	Mor6	blue	blue	blue
SHO	Mor8	blue	blue	blue
SIE-A	Sie126	red	red	red
SIE-A	Sie143	red	red	red
SIE-A	Sie150	green	red	mix
SIE-A	Sie20	red	red	red
SIE-B	Bue1	green	*M. melliger*	mix
SIE-B	Bue2	blue	orange	mix
SIE-B	Bue4	blue	orange	mix
WHE	Fre2	green	blue	mix
WHE	Fre4	blue	blue	blue
WHE	Fre5	blue	blue	blue
COL	Co1	light blue	light blue	light blue

Table 4.4. K2P distance within clades and populations, estimated from COI and UCE sequences of only colonies with both types of data available. *M. mendax* sequences were treated as a single clade (all), and split into individual groups (red, green, and blue) as inferred by the phylogenetic analyses. Maximum distance estimated from clades with more than two sequences is provided in parentheses. Estimation variance from bootstrapping is given after the ± sign.

Clade	**mtDNA**	**UCE**
Red	0.0052 ± 0.0017 (0.0102)	0.0022 (0.0027)
Green	0.0012 ± 0.0011 (0.0015)	0.003 (0.003)
Blue	0.0102 ± 0.0024 (0.03)	0.0025 (0.0035)
M. mendax (all)	0.0467 ± 0.0074 (0.091)	0.0025 (0.0032)
M. melliger	na	0.0024 ± 0.0001
M. placodops	0.0222 ± 0.0064	0.0028 ± 0.0001 (0.0045)
M. semirufus	0	0.0023 ± 0.0001(0.0036)
M. mimicus	0.0199 ± 0.0062	0.003 ± 0.0001
M. flaviceps	na	0.0018 ± 0.0001

Table 4.5. K2P pairwise distance between clades, estimated from COI sequences. Only *M. mendax* sequences from the consensus clades were included.

	red	green	blue	*M. mimicus*	*M. placodops*
red					
green	0.0589 ± 0.0119				
blue	0.0805 ± 0.0158	0.0575 ± 0.0186			
M. mimicus	0.1044 ± 0.0119	0.1045 ± 0.0146	0.0974 ± 0.0141		
M. placodops	0.0813 ± 0.0177	0.0619 ± 0.0173	0.0619 ± 0.0162	0.0882 ± 0.0144	
M. semirufus	0.1096 ± 0.0115	0.0938 0.0144	0.1049 ± 0.0181	0.0966 ± 0.0113	0.0856 ± 0.016

Table 4.6. Measures of population differentiation estimated from *M. mendax* sequences in the consensus clades.

	$\boldsymbol{\pi_S}$	$\boldsymbol{\pi_T}$	$\mathbf{N_{ST}}$
mtDNA	0.0055 ± 0.0011	0.0467 ± 0.0075	0.8821 ± 0.0232
UCE	0.0022	0.0025	0.1244 ± 0.0057

Table 4.7. K2P pairwise distance between clades, estimated from UCE sequences. Only *M. mendax* sequences from the consensus clades were included.

	red	green	blue	*M. melliger*	*M. placodops*	*M. semirufus*
red						
green	0.0026 ± 0.0001					
blue	0.0025 ± 0.0001	0.0024 ± 0.0001				
M. melliger	0.0033 ± 0.0001	0.0033 ± 0.0001	0.0031 ± 0.0001			
M. placodops	0.006 ± 0.0001	0.0061 ± 0.0001	0.006 ± 0.0001	0.0061 ± 0.0001		
M. semirufus	0.0055 ± 0.0001	0.0056 ± 0.0001	0.0055 ± 0.0001	0.0056 ± 0.0001	0.0069	
M. flaviceps	0.0065 ± 0.0001	0.0065 ± 0.0001	0.0065 ± 0.0001	0.0065 ± 0.0001	0.0071 ± 0.0001	
M. mimicus	0.006 ± 0.0001	0.006 ± 0.0001	0.006 ± 0.0001	0.0052 ± 0.0001	0.0066 ± 0.0001	0.0072

Table 4.8. Gene flow results from the Bayesian phylogeographical analysis of *M. mendax* mtDNA. Color coding of sites reflects the phylogenetic composition of each site according to the mtDNA Maximum Likelihood tree. Pairs with posterior probability above 0.5 are bolded.

Site 1	Site 2	Bayes factor	probability
CHI	DRA	2.53	0.208
WHE	DRA	3.16	0.247
DRA	GRA	3.01	0.238
HUAC	GRA	4.26	0.306
KIT	GRA	**18.65**	**0.659**
PAT	GRA	**18.79**	**0.661**
SAN	GRA	**52.63**	**0.845**
SIE-B	GRA	**9.85**	**0.505**
WHE	GRA	5.13	0.347
SIE-B	HUAC	2.01	0.172
SUP	HUAL	7.94	0.451
PAT	KIT	3.41	0.261
ORD	MIN	2.32	0.194
SUP	MIN	4.16	0.301
SHO	NM	**81.33**	**0.893**
SUP	ORD	8.34	0.464
HUAC	PAT	8.76	0.476
SIE-B	PAT	5.91	0.38
ORD	PINE	4.2	0.303
PAT	SAN	3.56	0.269
SIE-B	SAN	3.16	0.247
MIN	SED	5	0.341
ORD	SED	5.81	0.376
PINE	SED	**10.82**	**0.529**
SIE-A	SED	2.05	0.175
SUP	SED	**60.7**	**0.863**
CHI	SHO	**33.9**	**0.778**
DRA	SHO	2.2	0.185
HUAC	SHO	5.5	0.363
Globe	SIE-A	**261.87**	**0.964**
SUP	SIE-A	**76.8**	**0.888**

LEM	SUP	**331.08**	**0.972**
PIN	SUP	**35.49**	**0.786**
PAT	WHE	3.95	0.29
SAN	WHE	2.04	0.174
SIE-B	WHE	5.27	0.353

CHAPTER 5

CONCLUSION

Below I discuss the findings of Chapters Two, Three, and Four to highlight the most important results and to speculate on the evolution and distribution of *M. mendax*. I also make some suggestions on future directions for investigators who are interested in working with this charismatic group of ants.

This dissertation has revealed several novel features of *M. mendax* biology. Most notable is the discovery of primary polygyny in the Sierra Ancha Mountains of Arizona in Chapter Two, adding another Formicine and the second *Myrmecocystus* to the short list of species with this social structure. Among the most compelling evidence for primary polygyny in this population is the absence of relatedness among female alates sampled in 2016 from the colony designated SIE14. The most parsimonious explanation for this observation is that they are offspring of multiple, unrelated nestmate gynes. This is corroborated by the relatedness estimates obtained from field workers and inferred queen genotypes (Table 2.3), as well as by behavioral observations in the field and from laboratory experiments (Figures 2.2 and 2.3). Those who wish to continue studying this aspect of *M. mendax* biology should excavate at least one mature colony in this population to count queens and to genotype them and their brood. The presence of more than one reproductively active queen in a field colony is an important piece of evidence that is still missing in this system.

In addition, some attention should be given to colony fusion in the Sierra Ancha population, as preliminary observations in the field and in the laboratory suggested that it occurs. Colony fusion has been reported in a few unicolonial (Vásquez and Silverman 2008) and non-unicolonial species (Gotoh et al. 2017). It was surprising to find this phenomenon in *M. mendax* because it is generally uncommon and theoretically unexpected. However, the presence of colony fusion would explain the high genetic diversity and queen number estimated from field colonies (Tables 2.2 and 2.3). Conservatively, up to eight matrilines were detected in about half of the colonies genotyped in this population (Table 2.3). However, I observed that natural foundress associations contained four queens at most, with two or three being more common. Furthermore, Bartz and Hölldobler (1982) showed that the optimal association size for *M. mimicus* is three to four queens. While it is possible that more than four *M. mendax* foundresses can establish a primary-polygynous colony, my observations suggest that colony fusion may contribute to increasing queen number after colony founding at the Sierra Ancha population. The asymmetry in the relative contribution of resident and adopted queens to the brood in fused laboratory colonies (Table 2.4) resembled an example in *Formica* (Holzer et al. 2009), which showed evidence of a reproductive hierarchy based on the order of membership, i.e. original foundresses reproduce more than adopted queens. Still, the occurrence of colony fusion in natural *M. mendax* populations remains to be verified and quantified. It may be useful to monitor the Sierra Ancha population in the months following the mating flight, as neighboring incipient colonies are likely to merge according to the results of the brood raiding experiment. To

better quantify the fusion process, an experiment could be conducted by first rearing laboratory colonies with known microsatellite genotypes and then introducing them into genotyped field colonies. If the laboratory queens are successfully adopted and integrated, their multilocus genotypes should appear in the field colony's workforce in the following months and sexuals in the subsequent years.

The correlation between the genetic structure and the eco-geographical regions (Figures 4.7 and 4.10) suggests that the environment may have played a role in shaping phenotypic differences among populations. Non-kin cooperation is thought to be rare due to the difficulty of the benefits of cooperation offsetting the costs, except in extreme ecological circumstances that favors cooperation (e.g. hot and dry, cold, or high colony density). Although regression models suggested that average monthly temperature and precipitation have significant explanatory powers on the frequency of polygyny and queen number per colony (Chapter Three), neither can satisfactorily explain the high frequencies observed in the Sierra Ancha population. According to historical climate data, Sierra Ancha colonies were inferred to have experienced significantly lower average monthly temperatures than Mt. Lemmon and Superstitions colonies (Kruskal-Wallis test, $\chi^2 = 99.677$, $df = 13$, $P < 0.001$; Nemenyi test, $P_{SIE\text{-}AvsLEM} = 0.02$, $P_{SIE\text{-}AvsSUP} < 0.001$), but did not differ from monogynous colonies at other localities. Similarly, Sierra Ancha colonies received significantly less precipitation than those at Huachucas, Patagonia, Santa Ritas, and Sierra Buenos Airies (Kruskal-Wallis test, $\chi^2 = 121.43$, $df = 13$, $P < 0.001$; Nemenyi test, *P values* < 0.05), but were not different from other sites. The results in Chapter Two suggest that there is a correlation between polygyny frequency and

colony density estimated from nearest-neighbor distances at the Sierra Ancha population. However, this relationship disappeared when all populations were analyzed (Table 3.1). One unaccounted factor that may have explanatory power is heterospecific competition. *M. mendax* at the Sierra Anchas experiences a high density of *Dorymyrmex sp.* and *Pogonomyrmex sp.* (per. obs.). The numerous *Dorymyrmex sp.*, while only active at dawn and dusk, are effective at displacing *M. mendax* from food sources. Likewise, *Pogonomyrmex sp.* workers regularly interfered with *M. mendax* foragers, going after dead arthropods. Therefore, interspecific competition may influence the evolution of primary polygyny in this *M. mendax* population.

Furthermore, the historical abiotic conditions experienced by *M. mendax* colonies were inferred from climatic data recorded at weather stations likely not located within the studied field populations. Similarly, the nearest-neighbor distances of many populations were estimated from a relatively small number of nests; only a few populations were visited in multiple years and thus have more complete colony records. Despite the absence of a direct link between social variation and ecological conditions, the relationships between queen number, worker production, replete development, and queen survival during brood raids still support the idea that selection acts on queen number to increase workforce size.

Rapidly evolving microsatellite loci provide insight into demographic processes, such as migration and admixing that have happened in the recent past. My dissertation shows that the population structure inferred from four microsatellite loci agreed with the mtDNA and UCE trees in suggesting that at least two to three genetically distinct taxa

exist within *M. mendax* populations. Colonies that belong to the red consensus clade (Figure 4.6) tend to have significantly higher representation of Cluster 1 (Kruskal-Wallis test, $\chi^2 = 20.75$, $df = 3$, $P < 0.001$; Nemenyi test, $P_{red\text{-}blue} < 0.05$) and lower proportion of Cluster 3 (Kruskal-Wallis test, $\chi^2 = 21.98$, $df = 3$, $P < 0.001$; Nemenyi test, $P_{red\text{-}blue} < 0.05$) than the blue clade, as inferred by STRUCTURE (Figure 1, also see Chapter Three). If these two clades are indeed distinct taxonomic units, their divergence may have been driven in part by selection on traits that relate to queen cooperation. Characters with underlying genetic basis such as queen pheromone (Van Demeer and Alonson 2002), cuticular hydrocarbon profile and chemosensory receptor sensitivity (Johnson and Sunström 2012), as well as aggressiveness (Rissing and Pollock 1987) for examples, can contribute to reproductive isolation between different populations. In invasive species, genetic bottlenecks have been linked to reduced nestmate recognition capacity and intraspecific aggression, traits associated with polygyny (Ross 1993; Keller and Passera 1989). The relationship between genetic diversity and aggression was not seen in *M. mendax*, since neutral loci are similarly variable in polygynous and monogynous populations (Table 3.2), and intraspecific aggression is still present in the highly polygynous Sierra Ancha population (per. obs.). However, interestingly, aggression is virtually absent among Sierra Ancha queens, but not between monogynous Chiricahua queens (Figure 2.2). It is possible that loci associated with recognition and aggressiveness, not microsatellites, are less variable in polygynous populations, and analyzing protein-coding regions in the available UCE data would reveal the expected correlation. Alternatively, there may be non-genetic components in cuticular hydrocarbon

profiles (Martin and Drifhout 2009), perhaps linked to diet or nest substrate, that mask or homogenize expressed genetic variation, facilitating pleometrosis and primary polygyny in some populations but not others.

Regarding the seven specimens with conflicting taxonomic and molecular identities (i.e. morphologically identified as one species but clustered with another based on DNA data; Figure 4.4), morphological convergence, especially pilosity, can explain some of the discrepancies. Specimens WM16702, WM19359, PSW13407_6 were originally keyed out as *M. placodops*, the short-haired relative of *M. mendax*; yet these specimens clustered with short-haired *M. mendax* instead. RAJ5588, a long-haired specimen, grouped with *M. melliger* samples on the UCE tree, despite the initial identification as *M. mendax*. The short-haired WM_13384, similarly identified as *M. mendax*, turned out to be more closely related to *M. placodops*. Some of these specimens are not major workers (per. obs.), making accurate identification extremely challenging. For instance, the head width of PSW13407_6 is only 1.4 mm, below the 1.7-mm threshold to be considered a major according to Snelling. Adding more complications, RAJ2978 and SS_DValley, identified as *M. placodops* and *M. mendax*, respectively, associated instead with *M. semirufus*, the smaller, short-haired species of the *melliger* group. Altogether these observations underscore the importance of collecting appropriate specimens and the necessity of finding alternative diagnostic characters for some members of this morphospecies group. Natural variation in body size and hair length makes it challenging even for taxonomic experts provide accurate identifications. For *M. mendax*, now that a better understanding of the population subdivision is in place, more

consistent and informative phenotypic traits can be identified. Anecdotally, *M. mendax* workers were thought to secrete a unique glandular odor resembling citrus when disturbed; however I found that this odor is also present in California *M. semirufus* and thus is not a good field indicator for *M. mendax*.

Overall, Snelling's hypothesis of cryptic complexity within *M. mendax* is supported by the findings of this thesis. More work is needed to determine how *M. mendax* should be split into sub-taxa. Although the phylogenetic and morphometric analyses consistently recovered at least two distinct subgroups, it remains unclear the degree to which the genetic and phenotypic variation in these groups overlap with *M. melliger* and *M. placodops*. In the mtDNA analysis, low sample size for both of these taxa and a lack of parsimony-informative SNPs resulted in a poorly supported relationship with *M. mendax* (Figure 4.2). The character-rich UCE analysis had substantially greater resolution, generating a tree with a highly supported sister relationship between *M. mendax* and *M. melliger*. *M. semirufus* clustered with other taxa of the *melliger* group on the UCE tree (Figure 4.4) but not on the COI tree (Figure 4.2). There also appear to be enough pilosity variation in *M. melliger* to generate uncertainty when separating samples from areas of northern Sonora where the distributions of *M. melliger* and *M. mendax* likely overlap (Snelling 1976; M. Boroweic and R.A. Johnson, per. com.). Lastly, there is some evidence that these two species may occasionally hybridize or have not yet finished sorting into distinct genetic lineages at Santa Ritas and Sierra Buenos Aires, with one colony in each population having a mtDNA haplotype more similar to *M. mendax* while a nuclear UCE sequence more closely related to *M.*

melliger (Figures 4.2 and 4.4). It was suggested that the UCE *M. melliger* clade is actually made up of long-haired *M. mendax* (R.A. Johnson, per. com.). If this is the case, the relationships among *M. mendax*, *M. melliger*, and *M. placodops* remain unresolved. This is not likely, however, because each of the *M. melliger* specimens was identified by one of three different ant taxonomists (R.A. Johnson, W. McKay, and P. Ward).

Because of these observations, future work should examine the degree and geographical extent of genetic and morphological variation in *M. melliger* and *M. placodops*. As Snelling had already suggested, it would be informative to identify areas where these taxa are sympatric or parapatric, which would enable a closer look at interspecific interactions and how they shape patterns of gene flow and phenotypic variability within and between these species. Concerning the cryptic variation within *M. mendax*, it may also be useful to investigate phenotypes associated with recognition and reproductive isolation such as cuticular hydrocarbon, sex pheromones, and male genitalia.

REFERENCES

Abbott, Ian. “Numbers of Plant, Insect and Land Bird Species on Nineteen Remote Islands in the Southern Hemisphere.” *Biological Journal of the Linnean Society*, vol. 6, no. 2, June 1974, pp. 143–52. *Crossref*, doi:10.1111/j.1095-8312.1974.tb00719.x.

Adams, Eldridge, and Walter Tschinkel. “Effects of Foundress Number on Brood Raids and Queen Survival in *Solenopsis invicta*”. Behav Ecol Sociobiol, vol 37, 1995, pp. 232-242.

Alonso, Leeanne, and Robert Vander Meer. “Queen Primer Pheromone Affects Conspecific Fire Ant (*Solenopsis invicta*) Aggression.” *Behavioral Ecology and Sociobiology*, vol. 51, no. 2, Jan. 2002, pp. 122–30. *Crossref*, doi:10.1007/s002650100417.

Barton, N. H., and M. Slatkin. “A Quasi-Equilibrium Theory of the Distribution of Rare Alleles in a Subdivided Population.” *Heredity*, vol. 56, no. 3, June 1986, pp. 409–15. *Crossref*, doi:10.1038/hdy.1986.63.

Bartz, Stephen H., and Bert Hölldobler. “Colony Founding in *Myrmecocystus mimicus* Wheeler (Hymenoptera: Formicidae) and the Evolution of Foundress Associations” *Behavioral Ecology and Sociobiology*, vol. 10, no. 2, 1982, pp. 137–47.

Bayzid, Md Shamsuzzoha, et al. “Weighted Statistical Binning: Enabling Statistically Consistent Genome-Scale Phylogenetic Analyses.” *PLOS ONE*, edited by Nico Cellinese, vol. 10, no. 6, June 2015, p. e0129183. *Crossref*, doi:10.1371/journal.pone.0129183.

Bernasconi, Christian, et al. “Molecular Markers Allow Sibling Species Identification in Red Wood Ants (*Formica rufa* Group).” *Systematic Entomology*, vol. 35, no. 2, Apr. 2010, pp. 243–49. *Crossref*, doi:10.1111/j.1365-3113.2009.00503.x.

Bernasconi, Giorgina, and Joan E. Strassmann. “Cooperation among Unrelated Individuals: The Ant Foundress Case.” *Trends in Ecology & Evolution*, vol. 14, no. 12, Dec. 1999, pp. 477–82. *Crossref*, doi:10.1016/S0169-5347(99)01722-X.

Bickford, David, et al. “Cryptic Species as a Window on Diversity and Conservation.” *Trends in Ecology & Evolution*, vol. 22, no. 3, Mar. 2007, pp. 148–55. *Crossref*, doi:10.1016/j.tree.2006.11.004.

Bivand, Roger, and Nicholas Lewin-Koh. “maptools: Tools for Reading and Handling Spatial Objects.” R package version 0.9-2., 2017, https://CRAN.R-project.org/package=maptools

Blaimer, Bonnie B., et al. “Phylogenomic Methods Outperform Traditional Multi-Locus Approaches in Resolving Deep Evolutionary History: A Case Study of Formicine Ants.” *BMC Evolutionary Biology*, vol. 15, no. 1, Dec. 2015. *Crossref*, doi:10.1186/s12862-015-0552-5.

Bolger, Anthony M., et al. “Trimmomatic: A Flexible Trimmer for Illumina Sequence Data.” *Bioinformatics*, vol. 30, no. 15, Aug. 2014, pp. 2114–20. *Crossref*, doi:10.1093/bioinformatics/btu170.

Bolton, B., Alpert, G., Ward, P. S., and P. Naskrecki. “Bolton's Catalogue of ants of the world: 1758-2005”. Cambridge, Mass.: *Harvard University Press*, CD-ROM, 2007.

Borowiec, Marek L. “AMAS: A Fast Tool for Alignment Manipulation and Computing of Summary Statistics.” *PeerJ*, vol. 4, Jan. 2016, p. e1660. *Crossref*, doi:10.7717/peerj.1660.

Bouckaert, Remco, et al. “BEAST 2: A Software Platform for Bayesian Evolutionary Analysis.” *PLoS Computational Biology*, edited by Andreas Prlic, vol. 10, no. 4, Apr. 2014, p. e1003537. *Crossref*, doi:10.1371/journal.pcbi.1003537.

Branstetter, Michael G., et al. “Enriching the Ant Tree of Life: Enhanced UCE Bait Set for Genome-Scale Phylogenetics of Ants and Other Hymenoptera.” *Methods in Ecology and Evolution*, edited by Samantha Price, vol. 8, no. 6, June 2017, pp. 768–76. *Crossref*, doi:10.1111/2041-210X.12742.

Brower, A. V. “Rapid Morphological Radiation and Convergence among Races of the Butterfly *Heliconius erato* Inferred from Patterns of Mitochondrial DNA Evolution.” *Proceedings of the National Academy of Sciences*, vol. 91, no. 14, July 1994, pp. 6491–95. *Crossref*, doi:10.1073/pnas.91.14.6491.

Caccone, Adalgisa, and Valerio Sbordon. “MOLECULAR BIOGEOGRAPHY OF CAVE LIFE: A STUDY USING MITOCHONDRIAL DNA FROM BATHYSCIINE BEETLES.” *Evolution*, vol. 55, no. 1, Jan. 2001, pp. 122–30. *Crossref*, doi:10.1111/j.0014-3820.2001.tb01278.x.

Capella-Gutierrez, S., et al. “TrimAl: A Tool for Automated Alignment Trimming in Large-Scale Phylogenetic Analyses.” *Bioinformatics*, vol. 25, no. 15, Aug. 2009, pp. 1972–73. *Crossref*, doi:10.1093/bioinformatics/btp348.

Chernomor, Olga, et al. “Terrace Aware Data Structure for Phylogenomic Inference from Supermatrices.” *Systematic Biology*, vol. 65, no. 6, Nov. 2016, pp. 997–1008. *Crossref*, doi:10.1093/sysbio/syw037.

Conway, John R. “The seasonal occurrence of sexual brood and the pre- and post-nuptial behavior of the honey ant, *Myrmecocystus mexicanus* Wesmael, in Colorado.” *New York Entomological Society*, vol. 88, 1980, pp. 7-14.

Conway, John R. “Nest Architecture and Population of the Honey Ant, *Myrmecocystus mexicanus* Wesmael (Formicidae), in Colorado.” *The Southwestern Naturalist*, vol. 28, no. 1, Feb. 1983, p. 21. *Crossref*, doi:10.2307/3670588.

Conway, John R. “Notes on repletes, myrmecophiles, and predators of honey ant nests (*Myrmecocystus mexicanus*) (Hymenoptera: Formicidae) in Arizona.” *Journal of the New York Entomological Society*, 1990, pp. 103–107.

Conway, John R. “ARCHITECTURE, POPULATION SIZE, MYRMECOPHILES, AND MITES IN AN EXCAVATED NEST OF THE HONEY POT ANT, *MYRMECOCYSTUS MENDAX* WHEELER, IN ARIZONA.” *The Southwestern Naturalist*, edited by Steven Goldsmith, vol. 48, no. 3, Sept. 2003, pp. 449–50. *Crossref*, doi:10.1894/0038-4909(2003)048<0449:APSMAM>2.0.CO;2.

Cronin, A. L., et al. “High Inter-Colonial Variation in Worker Nestmate Relatedness and Diverse Social Structure in a Desert Ant from Mongolia.” *Insectes Sociaux*, vol. 63, no. 1, Feb. 2016, pp. 87–98. *Crossref*, doi:10.1007/s00040-015-0439-x.

Crozier R.H., and P. Pamilo. “Evolution of Social Insect Colonies: Sex Allocation and Kin Selection.” *New York: Oxford University Press.* 1996.

DeHeer, C. J., and J. M. Herbers. “Population Genetics of the Socially Polymorphic Ant *Formica podzolica*.” *Insectes Sociaux*, vol. 51, no. 4, Nov. 2004, pp. 309–16. *Crossref*, doi:10.1007/s00040-004-0745-1.

Faircloth, Brant C., et al. “Target Enrichment of Ultraconserved Elements from Arthropods Provides a Genomic Perspective on Relationships among Hymenoptera.” *Molecular Ecology Resources*, vol. 15, no. 3, May 2015, pp. 489–501. *Crossref*, doi:10.1111/1755-0998.12328.

Fellows, Larry D. “THE ICE AGE AND IMPACTS ON ARIZONA.” Arizona Geological Survey, vol. 35, no. 1, 2005, pp. 1-3.

Fournier, D., et al. “Significant Reproductive Skew in the Facultatively Polygynous Ant *Pheidole pallidula*.” *Molecular Ecology*, vol. 13, no. 1, Jan. 2004, pp. 203–10. *Crossref*, doi:10.1046/j.1365-294X.2003.02036.x.

Fournier, Denis, and Laurent Keller. “Partitioning of Reproduction among Queens in the Argentine Ant, *Linepithema humile*.” *Animal Behaviour*, vol. 62, no. 6, Dec. 2001, pp. 1039–45. *Crossref*, doi:10.1006/anbe.2001.1848.

Gadau J and Fewell J. “Organization of Insect Societies: from Genome to Sociocomplexity.*” Harvard University Press*, Cambridge, 2009.

Gadau, J., et al. “Determinants of Intracolonial Relatedness in *Pogonomyrmex rugosus* (Hymenoptera; Formicidae): Mating Frequency and Brood Raids.” *Molecular Ecology*, vol. 12, no. 7, July 2003, pp. 1931–38. *Crossref*, doi:10.1046/j.1365-294X.2003.01853.x.

Gadau, Jürgen, et al. “Oligogyny by Unrelated Queens in the Carpenter Ant, *Camponotus ligniperdus*.” *Behavioral Ecology and Sociobiology*, vol. 44, no. 1, Oct. 1998, pp. 23–33. *Crossref*, doi:10.1007/s002650050511.

Gerritsen, Hans. “mapplots: Data Visualisation on Maps.” R package version 1.5.1., 2018, https://CRAN.R-project.org/package=mapplots.

Gibbard, Philip L., et al. “Formal Ratification of the Quaternary System/Period and the Pleistocene Series/Epoch with a Base at 2.58 Ma.” *Journal of Quaternary Science*, vol. 25, no. 2, Feb. 2010, pp. 96–102. *Crossref*, doi:10.1002/jqs.1338.

Gillespie, Rosemary G., and George K. Roderick. “A RTHROPODS ON ISLANDS : Colonization, Speciation, and Conservation.” *Annual Review of Entomology*, vol. 47, no. 1, Jan. 2002, pp. 595–632. *Crossref*, doi:10.1146/annurev.ento.47.091201.145244.

Giraud, T., et al. “Evolution of Supercolonies: The Argentine Ants of Southern Europe.” *Proceedings of the National Academy of Sciences*, vol. 99, no. 9, Apr. 2002, pp. 6075–79. *Crossref*, doi:10.1073/pnas.092694199.

Gotoh, A., et al. “Social Structure of the Polygynous Ant, *Crematogaster osakensis*.” *Insectes Sociaux*, vol. 64, no. 1, Feb. 2017, pp. 123–31. *Crossref*, doi:10.1007/s00040-016-0522-y.

Grabherr, Manfred G., et al. “Full-Length Transcriptome Assembly from RNA-Seq Data without a Reference Genome.” *Nature Biotechnology*, vol. 29, no. 7, July 2011, pp. 644–52. *Crossref*, doi:10.1038/nbt.1883.

Griffith, G.E., J.M. Omernik, C.B. Johnson, and D.S. Turner. “Ecoregions of Arizona (2 sided color poster with map, descriptive text, summary tables, and photographs).” U.S. Geological Survey Open-File Report 2014-1141, map scale 1:1,325,000, 2014, http://dx.doi.org/10.3133/ofr20141141.

Guénard, B., et al. “Extreme Polygyny in the Previously Unstudied Subtropical Ant *Temnothorax tuscaloosae* with Implications for the Biogeographic Study of the Evolution of Polygyny.” *Insectes Sociaux*, vol. 63, no. 4, Nov. 2016, pp. 543–51. *Crossref*, doi:10.1007/s00040-016-0498-7.

Gyllenstrand, Niclas, et al. “Polymorphic Microsatellite DNA Markers in the Ant *Formica exsecta*.” *Molecular Ecology Notes*, vol. 2, no. 1, Mar. 2002, pp. 67–69. *Crossref*, doi:10.1046/j.1471-8286.2002.00152.x.

Hagen, Robert H., Smith, Deborah R., and Steven W. Rissing. “Genetic Relatedness among Co-Foundresses of Two Desert Ants, *Veromessor pergandei* And *Acromyrmex versicolor* (Hymenoptera: Formicidae).” *Psyche*, vol. 95, 1998, pp. 191-201.

Hamilton, W.D. “The genetical evolution of social behavior.” *J. Theoret. Biol.*, vol. 7, 1964, pp. 17-52.

Haney, Brian R. “Ecological Drivers and Reproductive Consequences of Queen Cooperation in the California Harvester Ant *Pogonomyrmex californicus*.” Dissertation. Arizona State University, 2017.

Hebert, P. D. N., et al. “Ten Species in One: DNA Barcoding Reveals Cryptic Species in the Neotropical Skipper Butterfly *Astraptes fulgerator*.” *Proceedings of the National Academy of Sciences*, vol. 101, no. 41, Oct. 2004, pp. 14812–17. *Crossref*, doi:10.1073/pnas.0406166101.

Heinze, J. “Queen-queen interactions in polygynous ants.” *Queen number and sociality in insects*, 1993, pp. 334-361.

Heinze, J., et al. “Reproductive Skew and Queen Relatedness in an Ant with Primary Polygyny.” *Insectes Sociaux*, vol. 48, no. 2, June 2001, pp. 149–53. *Crossref*, doi:10.1007/PL00001758.

Heinze, J. and B. Hölldobler. “Ants in the cold.” Memorabilia Zoologica, vol. 48, 1994, pp. 99-108.

Heinze, Jürgen, and Laurent Keller. “Alternative Reproductive Strategies: A Queen Perspective in Ants.” *Trends in Ecology & Evolution*, vol. 15, no. 12, Dec. 2000, pp. 508–12. *Crossref*, doi:10.1016/S0169-5347(00)01995-9.

Heinze, J., M. Stahl, and B. Hölldobler. “Ecophysiology of hibernation in boreal Leptothorax ants (Hymenoptera: Formicidae).” *Écoscience*, vol. 3, 1996, pp. 429–435.

Helms Cahan, S., and K. R. Helms. “Relatedness Does Not Explain Geographic Variation in Queen Cooperation in the Seed-Harvester Ant *Messor pergandei*.” *Insectes Sociaux*, vol. 59, no. 4, Nov. 2012, pp. 579–85. *Crossref*, doi:10.1007/s00040-012-0255-5.

Helms, K. R., and S. Helms Cahan. “Large-Scale Regional Variation in Cooperation and Conflict among Queens of the Desert Ant *Messor pergandei*.” *Animal Behaviour*, vol. 84, no. 3, Sept. 2012, pp. 499–507. *Crossref*, doi:10.1016/j.anbehav.2012.05.019.

Hijmans J., Robert. “geosphere: Spherical Trigonometry.” R package version 1.5-7., 2017. https://CRAN.R-project.org/package=geosphere.

Hölldobler, B. “Tournament and Slavery in a Desert Ant.” *Science*, vol. 192, 1976, pp. 912-914.

Hölldobler, B., and C.J. Lumsden. “Territorial Strategies in Ants.” *Science*, vol. 210, 1980, pp. 732-39.

Hölldobler, B. “Foraging and spatiotemporal territories in the honey ant *Myrmecocystus mimicus* Wheeler (Hymenoptera: Formicidae).” *Behavioral ecology and sociobiology*, vol. 9, 1981, pp. 301–314.

Hölldobler B., and E.O. Wilson. “The ants.” *Harvard University Press*, 1990.

Hölldobler B., Grillenberger, B., and J. Gadau. “Queen Number and Raiding Behavior in the Ant Genus *Myrmecocystus* (Hymenoptera: Formicidae).” *Myrmecological News*, vol. 15, 2011, pp. 53-61.

Holzer, Barbara, et al. “Foreign Ant Queens Are Accepted but Produce Fewer Offspring.” *Oecologia*, vol. 157, no. 4, Oct. 2008, pp. 717–23. *Crossref*, doi:10.1007/s00442-008-1101-3.

Hughes, W.O., and J.J Boomsma. “Genetic diversity and disease resistance in leaf-cutting ant societies.” *Evolution*, vol. 58, 2004, pp. 1251–1260.

Hughes, W. O. H., et al. “Multiple Paternity or Multiple Queens: Two Routes to Greater Intracolonial Genetic Diversity in the Eusocial Hymenoptera.” *Journal of Evolutionary Biology*, vol. 21, no. 4, July 2008, pp. 1090–95. *Crossref*, doi:10.1111/j.1420-9101.2008.01532.x.

Hurst, G. D., and F. M. Jiggins. “Problems with Mitochondrial DNA as a Marker in Population, Phylogeographic and Phylogenetic Studies: The Effects of Inherited Symbionts.” *Proceedings of the Royal Society B: Biological Sciences*, vol. 272, no. 1572, Aug. 2005, pp. 1525–34. *Crossref*, doi:10.1098/rspb.2005.3056.

Johnson, Christine A., and Liselotte Sundström. “Cuticular Chemistry of Two Social Forms in a Facultatively Polygyne Ant (Hymenoptera: Formicidae: *Formica truncorum*).” *Annales Zoologici Fennici*, vol. 49, no. 1–2, Apr. 2012, pp. 1–17. *Crossref*, doi:10.5735/086.049.0101.

Johnson, Robert A. “Colony Founding by Pleometrosis in the Semiclaustral Seed-Harvester Ant *Pogonomyrmex californicus* (Hymenoptera: Formicidae).” *Animal Behaviour*, vol. 68, no. 5, Nov. 2004, pp. 1189–200. *Crossref*, doi:10.1016/j.anbehav.2003.11.021.

Julian, Glennis E., and Jennifer H. Fewell. “Genetic Variation and Task Specialization in the Desert Leaf-Cutter Ant, *Acromyrmex versicolor*.” *Animal Behaviour*, vol. 68, no. 1, July 2004, pp. 1–8. *Crossref*, doi:10.1016/j.anbehav.2003.06.023.

Kalyaanamoorthy, Subha, et al. “ModelFinder: Fast Model Selection for Accurate Phylogenetic Estimates.” *Nature Methods*, vol. 14, no. 6, May 2017, pp. 587–89. *Crossref*, doi:10.1038/nmeth.4285.

Kaspari, Michael, et al. “Energy Gradients and the Geographic Distribution of Local Ant Diversity.” *Oecologia*, vol. 140, no. 3, Aug. 2004, pp. 407–13. *Crossref*, doi:10.1007/s00442-004-1607-2.

Katoh, K., and D. M. Standley. “MAFFT Multiple Sequence Alignment Software Version 7: Improvements in Performance and Usability.” *Molecular Biology and Evolution*, vol. 30, no. 4, Apr. 2013, pp. 772–80. *Crossref*, doi:10.1093/molbev/mst010.

Kay, Carol Ann R. “Preferred temperatures of desert honey ants (Hymenoptera: Formicidae).” *Journal of Thermal Biology*, vol. 3, 1978, pp. 213-217.

Kay, Carol Ann Rolph, and Walter G. Whitford. “Critical Thermal Limits of Desert Honey Ants: Possible Ecological Implications.” *Physiological Zoology*, vol. 51, no. 2, 1978, pp. 206–13.

Keenan, Kevin, et al. “DiveRsity : An R Package for the Estimation and Exploration of Population Genetics Parameters and Their Associated Errors.” *Methods in Ecology and Evolution*, edited by Robert B. O’Hara, vol. 4, no. 8, Aug. 2013, pp. 782–88. *Crossref*, doi:10.1111/2041-210X.12067.

Keller, Laurent. “Social Life: The Paradox of Multiple-Queen Colonies.” *Trends in Ecology & Evolution*, vol. 10, no. 9, Sept. 1995, pp. 355–60. *Crossref*, doi:10.1016/S0169-5347(00)89133-8.

Keller, Laurent, and Hudson K. Reeve. “Genetic Variability, Queen Number, and Polyandry in Social Hymenoptera.” *Evolution*, vol. 48, no. 3, June 1994, p. 694. *Crossref*, doi:10.2307/2410479.

Kronauer, D. J. C., et al. “Genetic Evidence for Intra- and Interspecific Slavery in Honey Ants (Genus *Myrmecocystus*).” *Proceedings of the Royal Society B: Biological Sciences*, vol. 270, no. 1517, Apr. 2003, pp. 805–10. *Crossref*, doi:10.1098/rspb.2002.2288.

Kronauer, D.J.C., et al. “Phylogenetics of the New World Honey Ants (Genus *Myrmecocystus*) Estimated from Mitochondrial DNA Sequences.” *Molecular Phylogenetics and Evolution*, vol. 32, no. 1, July 2004, pp. 416–21. *Crossref*, doi:10.1016/j.ympev.2004.03.011.

Kronauer, Daniel J. C., and Jürgen Gadau. “Isolation of Polymorphic Microsatellite Markers in the New World Honey Ant *Myrmecocystus mimicus*.” *Molecular Ecology Notes*, vol. 2, no. 4, Dec. 2002, pp. 540–41. *Crossref*, doi:10.1046/j.1471-8286.2002.00311.x.

Kumar, Sudhir, et al. “MEGA7: Molecular Evolutionary Genetics Analysis Version 7.0 for Bigger Datasets.” *Molecular Biology and Evolution*, vol. 33, no. 7, July 2016, pp. 1870–74. *Crossref*, doi:10.1093/molbev/msw054.

Kwapich, Christina L., et al. “The Ecological and Genetic Basis of Annual Worker Production in the Desert Seed Harvesting Ant, *Veromessor pergandei*.” *Behavioral Ecology and Sociobiology*, vol. 71, no. 8, Aug. 2017. *Crossref*, doi:10.1007/s00265-017-2333-1.

Keller, L., and L. Passera. “Mating System, Optimal Number of Matings, and Sperm Transfer in the Argentine Ant *Iridomyrmex humilis*.” *Behavioral Ecology and Sociobiology*, vol. 31, no. 5, 1992, pp. 359–66.

Lach, Lori, et al., editors. “Ant Ecology.” *Oxford University Press*, 2010.

Larsson, Anders. “AliView: A Fast and Lightweight Alignment Viewer and Editor for Large Datasets.” *Bioinformatics*, vol. 30, no. 22, Nov. 2014, pp. 3276–78. *Crossref*, doi:10.1093/bioinformatics/btu531.

Leirikh, A. N. “Sezonnye izmeneniya kholodoustoichivosti murav’ev na verkhnei Kolyme.” *Izvestiya Akademii Nauk SSSR: Seriia Biologicheskaia*, vol. 5, 1989, pp. 752–59.

Lemey P., Rambaut A., Drummond A.J., and M.A. Suchard. “Bayesian phylogeography finds its roots.” *PLoS Comput Biol.* vol. 5, 2009, pp. 1-16, e1000520.

Lynch, Michael, and Kermit Ritland. “Estimation of pairwise relatedness with molecular markers.” *Genetics*, vol. 152.4, 1999, pp. 1753-1766.

Martin, Stephen, and Falko Drijfhout. “A Review of Ant Cuticular Hydrocarbons.” *Journal of Chemical Ecology*, vol. 35, no. 10, Oct. 2009, pp. 1151–61. *Crossref*, doi:10.1007/s10886-009-9695-4.

Mattila, H. R., and T. D. Seeley. “Genetic Diversity in Honey Bee Colonies Enhances Productivity and Fitness.” *Science*, vol. 317, no. 5836, July 2007, pp. 362–64. *Crossref*, doi:10.1126/science.1143046.

Meirmans, Patrick G., and Philip W. Hedrick. “Assessing Population Structure: FST and Related Measures: INVITED TECHNICAL REVIEW.” *Molecular Ecology Resources*, vol. 11, no. 1, Jan. 2011, pp. 5–18. *Crossref*, doi:10.1111/j.1755-0998.2010.02927.x.

Minh, B. Q., et al. “Ultrafast Approximation for Phylogenetic Bootstrap.” *Molecular Biology and Evolution*, vol. 30, no. 5, May 2013, pp. 1188–95. *Crossref*, doi:10.1093/molbev/mst024.

Mintzer, A.C. “Primary polygyny in the ant *Atta texana*: number and weight of females and colony foundation success in the laboratory.” *Insectes Sociaux*, vol. 34, 1987, pp. 108-117.

Mintzer, Alex and S. B. Vinson. “Cooperative Colony Foundation by Females of the Leaf cutting Ant *Atta texana* in the Laboratory.” *Journal of the New York Entomological Society*, vol. 93, no. 3, 1985, pp. 1047-1051.

Mirarab, S., et al. “Statistical Binning Enables an Accurate Coalescent-Based Estimation of the Avian Tree.” *Science*, vol. 346, no. 6215, Dec. 2014, pp. 1250463–1250463. *Crossref*, doi:10.1126/science.1250463.

Moilanen, Atte, et al. “Matesoft: A Program for Deducing Parental Genotypes and Estimating Mating System Statistics in Haplodiploid Species.” *Molecular Ecology Notes*, vol. 4, no. 4, Dec. 2004, pp. 795–97. *Crossref*, doi:10.1111/j.1471-8286.2004.00779.x.

Moritz, C., Dowling T. E., and W. M. Brown. “EVOLUTION OF ANIMAL MITOCHONDRIAL DNA: RELEVANCE FOR POPULATIONBIOLOGY AND SYSTEMATICS.” *Ann. Rev. Ecol. Syst.*, vol. 18, 1987, pp. 269-292.

Nettel-Hernanz, Alejandro, et al. “Biogeography, Cryptic Diversity, and Queen Dimorphism Evolution of the Neotropical Ant Genus *Ectatomma* Smith, 1958 (Formicidae, Ectatomminae).” *Organisms Diversity & Evolution*, vol. 15, no. 3, Sept. 2015, pp. 543–53. *Crossref*, doi:10.1007/s13127-015-0215-9.

Nguyen, Lam-Tung, et al. “IQ-TREE: A Fast and Effective Stochastic Algorithm for Estimating Maximum-Likelihood Phylogenies.” *Molecular Biology and Evolution*, vol. 32, no. 1, Jan. 2015, pp. 268–74. *Crossref*, doi:10.1093/molbev/msu300.

Offenberg, J., et al. “Development Rate and Brood Production in Haplo- and Pleometrotic Colonies of *Oecophylla smaragdina*.” *Insectes Sociaux*, vol. 59, no. 3, Aug. 2012, pp. 307–11. *Crossref*, doi:10.1007/s00040-012-0221-2.

Oldroyd, Benjamin P., and Jennifer H. Fewell. “Genetic Diversity Promotes Homeostasis in Insect Colonies.” *Trends in Ecology & Evolution*, vol. 22, no. 8, Aug. 2007, pp. 408–13. *Crossref*, doi:10.1016/j.tree.2007.06.001.

O'Meara, Brian C. “Using trees: *Myrmecocystus* phylogeny and character evolution and new methods for investigating trait evolution and species delimitation.” Dissertation. University of California, Davis, 2008.

Overson, R., et al. “Distribution and Origin of Intraspecific Social Variation in the California Harvester Ant *Pogonomyrmex californicus*.” *Insectes Sociaux*, vol. 63, no. 4, Nov. 2016, pp. 531–41. *Crossref*, doi:10.1007/s00040-016-0497-8.

Palmer, Kellie A., and Benjamin P. Oldroyd. “Evolution of Multiple Mating in the Genus *Apis*.” *Apidologie*, vol. 31, no. 2, Mar. 2000, pp. 235–48. *Crossref*, doi:10.1051/apido:2000119.

Paradis, E. “Analysis of Phylogenetics and Evolution with R (Second Edition).” New York: *Springer*. 2012.

Paradis, E., Claude, J. and K. Strimmer. “APE: analyses of phylogenetics and evolution in R language.” *Bioinformatics*, vol. 20, 2004, pp. 289–290.

Parr, Catherine L., et al. “*GlobalAnts* : A New Database on the Geography of Ant Traits (Hymenoptera: Formicidae).” *Insect Conservation and Diversity*, edited by Raphael Didham and Jerome Orivel, vol. 10, no. 1, Jan. 2017, pp. 5–20. *Crossref*, doi:10.1111/icad.12211.

Passera, L. “Characteristics of tramp species.” In: *Exotic Ants: Biology, Impact and Control of Introduced Species* (Ed. by D. F. Williams), Boulder, Colorado: Westview Press, 1994, pp. 23-43.

Pedersen, Jes S., and Jacobus J. Boomsma. “Positive Association of Queen Number and Queen-Mating Frequency in *Myrmica* Ants: A Challenge to the Genetic-Variability Hypotheses”. *Behav. Ecol. Sociobiol*., vol. 45, 1999, pp. 185-193.

Pew, Jack, et al. “Related: An R Package for Analysing Pairwise Relatedness from Codominant Molecular Markers.” *Molecular Ecology Resources*, vol. 15, no. 3, May 2015, pp. 557–61. *Crossref*, doi:10.1111/1755-0998.12323.

Pohlert, T. “The Pairwise Multiple Comparison of Mean Ranks Package (PMCMR).” R package, 2014, http://CRAN.R-project.org/package=PMCMR.

Pollock, Gregory B., and Steven W. Rissing. “Mating season and colony foundation of the seed-harvester ant, *Veromessor pergandei*.” *Psyche*, vol. 92, pp. 125-134.

Qiu W., Chavarro J., Lazarus R., Rosner B., and J. Ma. “powerSurvEpi: Power and sample size calculation for survival analysis of epidemiological studies.” R package version 0.0, 6., 2012.

Queller, David C., and Keith F. Goodnight. “Estimating Relatedness Using Genetic Markers.” *Evolution*, vol. 43, no. 2, Mar. 1989, p. 258. *Crossref*, doi:10.2307/2409206.

Rambaut, A. “Figtree 1.4.0.” 2012. http://tree.bio.ed.ac.uk/software/figtree/.

Raymond, M., and F. Rousset. “GENEPOP (Version 1.2): Population Genetics Software for Exact Tests and Ecumenicism.” *Journal of Heredity*, vol. 86, no. 3, May 1995, pp. 248–49. *Crossref*, doi:10.1093/oxfordjournals.jhered.a111573.

Rettenmeyer, Carl W., and Julian F. Watkins II. “Polygyny and monogyny in army ants (Hymenoptera: Formicidae).” *Journal of the Kansas Entomological Society*, vol. 51, no. 4, 1978, pp. 581-591.

Richard A. Becker, and Allan R. Wilks. “mapdata: Extra Map Databases.” R package version 2.3.0., 2018, https://CRAN.R-project.org/package=mapdata.

Richard A. Becker, and Allan R. Wilks. “maps: Draw Geographical Maps.” R package version 3.3.0. 2018.

Rissing, Steven W., and Gregory B. Pollock. “Pleometrosis and polygyny in ants.” *Interindividual behavioral variability in social insects*, 1988, pp. 179-222.

Rissing, Steven W., Johnson, Robert A., and Gregory B. Pollock. “Natal nest distribution and pleometrosis in the desert leaf-cutter ant *Acromyrmex versicolor* (Pergande) (Hymenoptera: Formicidae).” *Psyche*, vol. 93, 1986, pp. 177-186.

Rissing, Steven W., et al. “Colony Founding Behavior of Some Desert Ants: Geographic Variation in Metrosis.” *Psyche: A Journal of Entomology*, vol. 103, no. 1–2, 2000, pp. 95–101. *Crossref*, doi:10.1155/2000/20135.

Rissing, Steven W., and Gregory B. Pollock. “Queen Aggression, Pleometrotic Advantage and Brood Raiding in the Ant *Veromessor pergandei* (Hymenoptera: Formicidae).” *Animal Behaviour*, vol. 35, no. 4, Aug. 1987, pp. 975–81. *Crossref*, doi:10.1016/S0003-3472(87)80154-9.

Rosenberg, Michael S., and Corey Devin Anderson. “PASSaGE: Pattern Analysis, Spatial Statistics and Geographic Exegesis. Version 2: PASSaGE.” *Methods in Ecology and Evolution*, vol. 2, no. 3, June 2011, pp. 229–32. *Crossref*, doi:10.1111/j.2041-210X.2010.00081.x.

Ross, Kenneth G. “The breeding system of the fire ant *Solenopsis invicta*: effects on colony genetic structure.” *The American Naturalist*, vol. 141, no. 4, 1993, pp. 554-576.

Ross, Keneth G., and David J. C. Fletcher. “Comparative Study of Genetic and Social Structure in Two Forms of the Fire Ant *Solenopsis invicta* (Hymenoptera: Formicidae).” *Behavioral Ecology and Sociobiology*, vol. 17, no. 4, Oct. 1985, pp. 349–56. *Crossref*, doi:10.1007/BF00293212.

Rousset, FrançOis. “Genepop’007: A Complete Re-Implementation of the Genepop Software for Windows and Linux.” *Molecular Ecology Resources*, vol. 8, no. 1, Jan. 2008, pp. 103–06. *Crossref*, doi:10.1111/j.1471-8286.2007.01931.x.

R Core Team. “R: A language and environment for statistical computer.: R Foundation for Statistical Computing, Vienna, Austria, 2013, ISBN 3-900051-07-0, URL http://www.R-project.org/.

Rubin, B. E. R., et al. “Polygyny in the Nest-Site Limited Acacia-Ant *Crematogaster mimosae*.” *Insectes Sociaux*, vol. 60, no. 2, May 2013, pp. 231–41. *Crossref*, doi:10.1007/s00040-013-0287-5.

Santos, SimôNi, et al. “Population Genetic Structuring of the King Weakfish, *Macrodon ancylodon* (Sciaenidae), in Atlantic Coastal Waters of South America: Deep Genetic Divergence without Morphological Change: GENETIC DIFFERENTIATION OF MACRODON ANCYLODON.” *Molecular Ecology*, vol. 15, no. 14, Nov. 2006, pp. 4361–73. *Crossref*, doi:10.1111/j.1365-294X.2006.03108.x.

Sayyari, Erfan, and Siavash Mirarab. “Fast Coalescent-Based Computation of Local Branch Support from Quartet Frequencies.” *Molecular Biology and Evolution*, vol. 33, no. 7, July 2016, pp. 1654–68. *arXiv.org*, doi:10.1093/molbev/msw079.

Schindelin, Johannes, et al. “Fiji: An Open-Source Platform for Biological-Image Analysis.” *Nature Methods*, vol. 9, no. 7, July 2012, pp. 676–82. *Crossref*, doi:10.1038/nmeth.2019.

Schlick-Steiner, Birgit C., et al. “More than One Species of *Messor* Harvester Ants (Hymenoptera: Formicidae) in Central Europe.” *European Journal of Entomology*, vol. 103, no. 2, Apr. 2006, pp. 469–76. *Crossref*, doi:10.14411/eje.2006.060.

SchlüNs, E. A., et al. “Breeding System, Colony and Population Structure in the Weaver Ant *Oecophylla smaragdina*.” *Molecular Ecology*, vol. 18, no. 1, Jan. 2009, pp. 156–67. *Crossref*, doi:10.1111/j.1365-294X.2008.04020.x.

Schmid-Hempel, Paul, and Ross H. Crozier. “Polyandry versus Polygyny versus Parasites.” *Phil.Trans. R. Soc. Lond. B*, vol. 354, 1999, pp. 507-515.

Schrempf, A., and J. Heinze. “Back to One: Consequences of Derived Monogyny in an Ant with Polygynous Ancestors.” *Journal of Evolutionary Biology*, vol. 20, no. 2, Mar. 2007, pp. 792–99. *Crossref*, doi:10.1111/j.1420-9101.2006.01235.x.

Seifert, Bernhard, and Sandor Csosz. “*Temnothorax crasecundus sp. n.* – a Cryptic Eurocaucasian Ant Species (Hymenoptera, Formicidae) Discovered by Nest Centroid Clustering.” *ZooKeys*, vol. 479, Jan. 2015, pp. 37–64. *Crossref*, doi:10.3897/zookeys.479.8510.

Charif, Delphine, and Jean R. Lobry. “SeqinR 1.0-2: A Contributed Package to the R Project for Statistical Computing Devoted to Biological Sequences Retrieval and Analysis.” Structural Approaches to Sequence Evolution: Molecules, Networks, Populations, edited by Ugo Bastolla et al., *Springer* Berlin Heidelberg, 2007, pp. 207–32, doi:10.1007/978-3-540-35306-5_10.

Shi, N. N., et al. “Keeping Cool: Enhanced Optical Reflection and Radiative Heat Dissipation in Saharan Silver Ants.” *Science*, vol. 349, no. 6245, July 2015, pp. 298–301. *Crossref*, doi:10.1126/science.aab3564.

Slaa, E. J., et al. “Colony Genetic Diversity Affects Task Performance in the Red Ant *Myrmica rubra*.” *Behavioral Ecology and Sociobiology*, vol. 68, no. 6, June 2014, pp. 903–14. *Crossref*, doi:10.1007/s00265-014-1703-1.

Smith, M. A., et al. “DNA Barcoding for Effective Biodiversity Assessment of a Hyperdiverse Arthropod Group: The Ants of Madagascar.” *Philosophical Transactions of the Royal Society B: Biological Sciences*, vol. 360, no. 1462, Oct. 2005, pp. 1825–34. *Crossref*, doi:10.1098/rstb.2005.1714.

Snelling, Roy R. “A revision of the honey ants, genus *Myrmecocystus* (Hymenoptera: Formicidae).” *Natural History Museum of Los Angeles County Science Bulletin*, vol. 24, 1976, pp. 1-166.

Steiner, Florian M., et al. “A Multisource Solution for a Complex Problem in Biodiversity Research: Description of the Cryptic Ant Species *Tetramorium alpestre sp.n.* (Hymenoptera: Formicidae).” *Zoologischer Anzeiger - A Journal of Comparative Zoology*, vol. 249, no. 3–4, Nov. 2010, pp. 223–54. *Crossref*, doi:10.1016/j.jcz.2010.09.003.

Stöver, Ben C., and Kai F. Müller. “TreeGraph 2: Combining and Visualizing Evidence from Different Phylogenetic Analyses.” *BMC Bioinformatics*, vol. 11, no. 1, 2010, p. 7. *Crossref*, doi:10.1186/1471-2105-11-7.

Strassmann, J. “The Rarity of Multiple Mating by Females in the Social Hymenoptera.” *Insectes Sociaux*, vol. 48, no. 1, Mar. 2001, pp. 1–13. *Crossref*, doi:10.1007/PL00001737.

Pritchard, J. K., Stephens, M., and P. Donnelly. “Inference of population structure using multilocus genotype data.” *Genetics*, vol. 155, 2000, pp. 945–959.

Suarez, Andrew V., et al. “Behavioral and Genetic Differentiation Between Native and Introduced Populations of the Argentine Ant” *Biological Invasions*, vol. 1, 1999, pp. 43-53.

Tan, Ge, et al. “Current Methods for Automated Filtering of Multiple Sequence Alignments Frequently Worsen Single-Gene Phylogenetic Inference.” *Systematic Biology*, vol. 64, no. 5, Sept. 2015, pp. 778–91. *Crossref*, doi:10.1093/sysbio/syv033.

Therneau, T. “A Package for Survival Analysis in S. version 2.38”. 2015, https://CRAN.R-project.org/package=survival.

Therneau, T., and P. Grambsch. “Modeling Survival Data: Extending the Cox Model.” Springer, New York, 2000, ISBN 0-387-98784-3.

Trunzer, B., et al. “Cooperative Colony Founding and Experimental Primary Polygyny in the Ponerine Ant *Pachycondyla villosa*.” *Insectes Sociaux*, vol. 45, no. 3, Aug. 1998, pp. 267–76. *Crossref*, doi:10.1007/s000400050087.

Tschinkel, Walter, R. “Brood raiding in the fire ant, *Solenopsis invicta* (Hymenoptera: Formicidae): laboratory and field observations.” *Ann. Entomol. Soc. Am.*, vol. 85, 1992, pp. 638-646.

Vásquez, Gissella M., and Jules Silverman. “Intraspecific Aggression and Colony Fusion in the Argentine Ant.” *Animal Behaviour*, vol. 75, no. 2, Feb. 2008, pp. 583–93. *Crossref*, doi:10.1016/j.anbehav.2007.06.019.

Oksanen, Jari, et al. “vegan: Community Ecology Package.” R package version 2.5-2., 2018, https://CRAN.R-project.org/package=vegan

Via, Sara, and Joan West. “The Genetic Mosaic Suggests a New Role for Hitchhiking in Ecological Speciation.” *Molecular Ecology*, vol. 17, no. 19, Oct. 2008, pp. 4334–45. *Crossref*, doi:10.1111/j.1365-294X.2008.03921.x.

Waloff, N. “The effect of the number of queens of the ant *Lasius flavus* (Fab.) (Hym., Formicidae) on their survival and on the rate of development of the first brood.” *Insectes Sociaux* vol. 4, 1957, pp. 391-408.

Walter R. Tschinkel, and Dennis F. Howard. “Colony Founding by Pleometrosis in the Fire Ant, *Solenopsis invicta*.” *Behavioral Ecology and Sociobiology*, vol. 12, no. 2, 1983, pp. 103–13.

Wang, J. “Sibship Reconstruction From Genetic Data With Typing Errors.” *Genetics*, vol. 166, no. 4, Apr. 2004, pp. 1963–79. *Crossref*, doi:10.1534/genetics.166.4.1963.

Weir, B.S., and C. Clark Cockerham. “Estimating F-statistics for the analysis of population structure.” *Evolution*, vol. 38, no. 6, 1984, pp. 1358-1370.

Wheeler, W.M. “The pleometrosis of *Myrmecocystus*.” *Psyche* vol. 24, 1917, pp. 180–182.

Wickham, H. “ggplot2: Elegant Graphics for Data Analysis.” *Springer-Verlag* New York, 2009.

Whitford, Walter G., et al. “Water Loss in Chihuahuan Desert Ants.” *Physiological Zoology*, vol. 48, no. 4, Oct. 1975, pp. 390–97. *Crossref*, doi:10.1086/physzool.48.4.30155664.

Wilcox, Thomas P., et al. “Mitochondrial DNA Sequencing Reveals Extreme Genetic Differentiation in a Cryptic Species Complex of Neotropical Pseudoscorpions.” *Molecular Phylogenetics and Evolution*, vol. 7, no. 2, Apr. 1997, pp. 208–16. *Crossref*, doi:10.1006/mpev.1996.0388.

Yamamichi, M., and H. Innan. “Estimating the Migration Rate from Genetic Variation Data.” *Heredity*, vol. 108, no. 4, Apr. 2012, pp. 362–63. *Crossref*, doi:10.1038/hdy.2011.83.

Yu, Guangchuang, et al. “GGTREE : An R Package for Visualization and Annotation of Phylogenetic Trees with Their Covariates and Other Associated Data.” *Methods in Ecology and Evolution*, edited by Greg McInerny, vol. 8, no. 1, Jan. 2017, pp. 28–36. *Crossref*, doi:10.1111/2041-210X.12628.

Zhang, Chao, et al. “ASTRAL-III: Polynomial Time Species Tree Reconstruction from Partially Resolved Gene Trees.” *BMC Bioinformatics*, vol. 19, no. S6, May 2018. *Crossref*, doi:10.1186/s12859-018-2129-y.

Zink, Robert M., and George F. Barrowclough. “Mitochondrial DNA under Siege in Avian Phylogeography: NuDNA VS. MtDNA in Phylogeography.” *Molecular Ecology*, vol. 17, no. 9, May 2008, pp. 2107–21. *Crossref*, doi:10.1111/j.1365-294X.2008.03737.x.

APPENDIX A

MULTI-LOCUS MICROSATELLITE GENOTYPES OF *MYRMECOCYSTUS MENDAX* SPECIMENS FROM CHAPTER TWO

Legend:

- Column 1: Population ID (e.g. SIE-A)
- Column 2: Colony ID_individual ID (e.g. Sie6_w1)
- Column 3+4: genotype at locus Mm3
- Column 5+6: genotype at locus Mm4
- Column 7+8: genotype at locus Mm5
- Column 9+10: genotype at locus FE17
- CHI: Chiricahua; SIE-A: Sierra Ancha
- L: lab colonies; FA: female alates; Q: queen; w: worker; larv: larva

**** Sierra Ancha field colonies ****

SIE-A	Sie6_w1	173	199	268	292	213	223	171	193
SIE-A	Sie6_w2	137	163	290	292	219	223	153	155
SIE-A	Sie6_w3	181	199	270	292	191	213	193	209
SIE-A	Sie6_w4	165	199	270	306	207	239	153	193
SIE-A	Sie6_w6	169	199	270	306	213	223	151	193
SIE-A	Sie6_w7	137	167	292	306	191	237	151	153
SIE-A	Sie6_w8	161	163	290	290	219	223	155	159
SIE-A	Sie6_w9	139	173	268	306	223	239	171	193
SIE-A	Sie6_w10	139	143	280	292	185	239	151	153
SIE-A	Sie6_w11	169	199	270	292	213	223	151	151
SIE-A	Sie6_w12	161	181	292	306	213	223	151	159
SIE-A	Sie6_w13	139	163	290	290	219	223	155	159
SIE-A	Sie6_w14	139	161	290	290	179	213	153	153
SIE-A	Sie6_w15	139	161	290	290	179	213	151	193
SIE-A	Sie6_w17	139	169	290	300	197	239	175	193
SIE-A	Sie6_w18	139	169	270	306	213	223	151	151
SIE-A	Sie6_w19	139	161	290	292	179	239	153	153
SIE-A	Sie6_w20	139	181	290	298	185	213	149	193
SIE-A	Sie6_w21	139	181	292	306	213	223	149	151
SIE-A	Sie6_w23	143	143	284	306	185	213	149	151
SIE-A	Sie6_w24	0	0	268	306	213	223	171	193
SIE-A	Sie6_w26	157	163	290	290	219	223	151	153
SIE-A	Sie6_w27	139	167	290	300	197	239	175	191
SIE-A	Sie6_w29	143	199	280	306	185	239	151	153
SIE-A	Sie6_w30	161	181	292	306	223	239	151	153
SIE-A	Sie7_w1	171	185	294	306	213	243	151	183
SIE-A	Sie7_w2	169	175	274	306	197	213	151	201
SIE-A	Sie7_w3	175	175	274	306	185	213	151	201
SIE-A	Sie7_w4	169	175	274	306	197	213	151	201
SIE-A	Sie7_w5	175	175	290	306	197	213	151	151

SIE-A	Sie7_w6	175	175	274	306	185	213	151	201
SIE-A	Sie7_w7	175	175	274	306	197	213	0	0
SIE-A	Sie7_w8	143	199	290	294	179	195	0	0
SIE-A	Sie7_w9	169	175	274	306	197	213	151	151
SIE-A	Sie7_w10	169	175	290	306	197	213	151	201
SIE-A	Sie7_w11	169	175	274	306	185	213	151	151
SIE-A	Sie7_w12	175	175	274	306	197	213	151	201
SIE-A	Sie7_w13	175	175	290	306	185	213	151	201
SIE-A	Sie7_w14	169	175	290	306	185	213	151	151
SIE-A	Sie7_w15	143	199	288	294	179	223	0	0
SIE-A	Sie7_w16	175	175	274	306	185	213	151	201
SIE-A	Sie7_w17	169	175	290	306	197	213	151	201
SIE-A	Sie7_w18	169	175	274	306	185	213	151	151
SIE-A	Sie7_w19	169	175	274	306	197	213	151	201
SIE-A	Sie7_w20	175	175	274	306	185	213	151	201
SIE-A	Sie7_w21	169	175	274	306	185	213	151	151
SIE-A	Sie7_w22	169	175	290	306	185	213	151	201
SIE-A	Sie7_w23	169	175	274	306	197	213	151	151
SIE-A	Sie7_w24	175	175	290	306	197	213	0	0
SIE-A	Sie7_w25	169	175	290	306	197	213	151	201
SIE-A	Sie7_w26	169	175	274	306	197	213	151	151
SIE-A	Sie7_w27	199	199	290	294	179	195	153	159
SIE-A	Sie7_w28	143	199	288	294	179	223	153	193
SIE-A	Sie7_w29	175	175	290	306	197	213	151	151
SIE-A	Sie7_w30	175	175	274	306	197	213	151	201
SIE-A	Sie8_w1	147	181	276	288	225	227	153	207
SIE-A	Sie8_w2	147	197	300	310	215	227	207	209
SIE-A	Sie8_w3	147	209	296	302	217	217	207	207
SIE-A	Sie8_w4	173	181	276	288	219	219	153	153
SIE-A	Sie8_w5	0	0	288	288	195	219	193	207
SIE-A	Sie8_w6	147	169	268	288	195	221	153	207
SIE-A	Sie8_w7	139	181	280	288	179	195	151	207
SIE-A	Sie8_w8	157	167	296	310	179	221	157	207
SIE-A	Sie8_w9	167	177	284	310	205	227	151	191
SIE-A	Sie8_w10	147	193	272	302	185	227	153	207
SIE-A	Sie8_w11	169	169	268	288	195	221	153	207
SIE-A	Sie8_w12	163	181	280	302	227	235	153	157
SIE-A	Sie8_w13	181	193	272	310	185	227	0	0
SIE-A	Sie8_w14	139	143	280	288	179	227	151	151
SIE-A	Sie8_w15	147	175	292	310	195	195	179	207
SIE-A	Sie8_w16	181	209	288	310	221	251	203	207
SIE-A	Sie8_w17	173	181	276	288	221	219	0	0
SIE-A	Sie8_w18	181	191	292	310	195	227	137	151
SIE-A	Sie8_w19	143	161	288	310	195	219	153	193

SIE-A	Sie8_w20	163	181	272	302	205	227	153	157
SIE-A	Sie8_w21	175	181	292	310	195	227	151	179
SIE-A	Sie8_w22	147	167	292	302	191	195	153	207
SIE-A	Sie8_w23	167	177	284	310	205	227	191	191
SIE-A	Sie8_w24	147	193	272	310	185	195	153	207
SIE-A	Sie8_w25	147	157	296	310	175	221	151	157
SIE-A	Sie8_w26	147	163	272	302	205	221	153	157
SIE-A	Sie8_w27	167	167	292	310	191	195	153	153
SIE-A	Sie8_w28	157	167	288	296	175	221	151	157
SIE-A	Sie8_w29	139	147	280	288	179	229	151	151
SIE-A	Sie8_w30	147	173	276	288	221	229	153	207
SIE-A	Sie9_w1	153	163	276	290	191	227	151	205
SIE-A	Sie9_w2	181	199	276	292	219	241	151	151
SIE-A	Sie9_w3	161	169	268	298	227	227	151	151
SIE-A	Sie9_w4	143	153	272	292	227	239	151	151
SIE-A	Sie9_w5	181	197	292	292	185	221	151	205
SIE-A	Sie9_w6	153	185	270	274	207	227	151	151
SIE-A	Sie9_w7	139	143	286	304	179	217	151	205
SIE-A	Sie9_w8	143	169	292	349	213	221	151	209
SIE-A	Sie9_w9	141	181	274	290	221	227	151	205
SIE-A	Sie9_w10	149	165	272	292	0	0	151	151
SIE-A	Sie9_w11	181	195	268	294	213	239	151	153
SIE-A	Sie9_w12	181	197	282	296	179	221	151	153
SIE-A	Sie9_w13	171	181	282	292	205	239	151	151
SIE-A	Sie9_w14	165	199	274	290	213	239	151	205
SIE-A	Sie9_w15	147	169	286	286	221	221	151	165
SIE-A	Sie9_w16	163	195	268	286	191	213	151	159
SIE-A	Sie9_w17	163	197	290	294	191	217	151	177
SIE-A	Sie9_w18	143	153	274	306	221	239	151	179
SIE-A	Sie9_w19	165	185	268	282	227	239	151	153
SIE-A	Sie9_w20	153	181	286	286	227	227	151	209
SIE-A	Sie9_w21	197	199	286	304	191	239	151	171
SIE-A	Sie9_w22	171	181	274	276	191	195	153	179
SIE-A	Sie9_w23	161	165	274	348	221	227	153	207
SIE-A	Sie9_w24	181	203	290	286	205	217	153	209
SIE-A	Sie9_w25	165	193	286	296	195	227	153	153
SIE-A	Sie9_w26	193	195	282	296	195	195	153	153
SIE-A	Sie9_w27	143	199	290	286	191	205	159	209
SIE-A	Sie9_w28	171	181	286	294	195	233	171	190
SIE-A	Sie9_w29	195	199	284	304	191	241	209	209
SIE-A	Sie9_w30	193	199	270	296	185	195	213	213
SIE-A	Sie10_w1	193	199	288	288	185	227	153	159
SIE-A	Sie10_w2	157	163	286	300	185	229	155	155
SIE-A	Sie10_w3	173	199	288	292	213	215	153	185

SIE-A	Sie10_w4	179	199	276	292	179	239	155	177
SIE-A	Sie10_w5	183	199	294	310	197	191	151	153
SIE-A	Sie10_w6	143	191	300	300	185	195	171	189
SIE-A	Sie10_w7	195	201	276	288	201	249	159	179
SIE-A	Sie10_w8	175	201	272	292	195	207	165	213
SIE-A	Sie10_w9	185	205	294	296	229	229	151	183
SIE-A	Sie10_w10	199	201	296	310	197	215	151	159
SIE-A	Sie10_w11	163	195	304	306	191	229	151	213
SIE-A	Sie10_w12	177	195	292	306	191	229	203	213
SIE-A	Sie10_w13	195	197	294	276	215	221	137	171
SIE-A	Sie10_w14	181	197	272	276	193	205	181	191
SIE-A	Sie10_w15	143	183	272	300	191	229	153	153
SIE-A	Sie10_w16	163	179	292	294	195	197	147	147
SIE-A	Sie10_w17	199	205	276	316	179	239	155	171
SIE-A	Sie10_w18	193	197	294	300	205	219	159	171
SIE-A	Sie10_w19	199	205	288	292	205	219	159	173
SIE-A	Sie10_w20	199	201	288	310	213	227	137	153
SIE-A	Sie10_w21	177	199	296	310	191	219	153	171
SIE-A	Sie10_w22	143	191	300	306	185	195	173	193
SIE-A	Sie10_w23	143	173	268	300	185	221	151	173
SIE-A	Sie10_w24	163	191	300	300	185	195	173	193
SIE-A	Sie10_w25	163	191	300	300	195	219	153	189
SIE-A	Sie10_w26	193	193	292	294	195	209	159	195
SIE-A	Sie10_w27	187	203	272	288	195	215	153	159
SIE-A	Sie10_w28	173	201	268	288	221	229	151	153
SIE-A	Sie10_w29	179	205	292	294	195	225	147	171
SIE-A	Sie10_w30	163	191	270	286	183	247	159	175
SIE-A	Sie12_w1	147	181	276	328	191	245	0	0
SIE-A	Sie12_w2	165	193	268	286	213	235	159	187
SIE-A	Sie12_w3	181	195	272	314	213	217	137	161
SIE-A	Sie12_w4	181	193	272	308	195	197	151	211
SIE-A	Sie12_w5	0	0	282	286	211	233	153	185
SIE-A	Sie12_w6	167	175	276	276	191	249	151	201
SIE-A	Sie12_w7	165	179	294	296	187	195	185	189
SIE-A	Sie12_w8	165	165	272	280	213	213	159	175
SIE-A	Sie12_w9	193	195	272	286	195	197	157	211
SIE-A	Sie12_w10	173	187	268	296	195	241	157	161
SIE-A	Sie12_w11	169	181	290	296	201	241	159	187
SIE-A	Sie12_w12	163	163	272	280	213	213	159	175
SIE-A	Sie12_w13	143	169	290	290	195	249	0	0
SIE-A	Sie12_w14	0	0	272	280	185	195	159	159
SIE-A	Sie12_w15	0	0	272	302	195	197	151	211
SIE-A	Sie12_w16	0	0	272	280	213	213	159	161
SIE-A	Sie12_w17	193	195	272	288	197	205	157	211

SIE-A	Sie12_w19	179	193	272	288	185	249	153	153
SIE-A	Sie12_w20	145	153	276	312	191	191	153	159
SIE-A	Sie12_w21	163	169	290	294	213	243	153	161
SIE-A	Sie12_w22	187	195	272	280	205	243	157	161
SIE-A	Sie12_w23	195	195	268	294	195	205	157	161
SIE-A	Sie12_w24	163	171	262	268	185	219	153	159
SIE-A	Sie12_w25	163	171	272	290	0	0	151	159
SIE-A	Sie12_w26	145	201	276	312	191	219	153	159
SIE-A	Sie12_w27	157	179	0	0	205	233	157	157
SIE-A	Sie12_w28	139	169	280	294	185	229	159	179
SIE-A	Sie12_w29	149	199	276	286	197	215	153	159
SIE-A	Sie12_w30	167	169	282	296	201	249	153	183
SIE-A	Sie14_w1	185	195	258	288	197	231	131	193
SIE-A	Sie14_w2	0	0	268	288	217	249	151	151
SIE-A	Sie14_w3	167	183	268	288	197	217	153	193
SIE-A	Sie14_w4	165	195	268	288	197	231	131	131
SIE-A	Sie14_w5	173	197	268	290	197	217	151	153
SIE-A	Sie14_w6	167	193	268	290	205	227	151	153
SIE-A	Sie14_w7	139	139	268	290	197	213	153	159
SIE-A	Sie14_w8	173	185	270	290	203	225	153	179
SIE-A	Sie14_w9	139	143	270	290	197	223	187	189
SIE-A	Sie14_w10	141	149	272	290	209	209	155	159
SIE-A	Sie14_w11	169	185	278	290	205	209	153	157
SIE-A	Sie14_w12	175	181	278	290	197	209	151	191
SIE-A	Sie14_w13	157	175	278	292	217	247	133	133
SIE-A	Sie14_w14	149	185	280	292	205	231	131	193
SIE-A	Sie14_w15	185	195	282	292	191	231	153	153
SIE-A	Sie14_w16	157	175	282	292	247	247	191	205
SIE-A	Sie14_w17	163	195	282	294	209	241	151	151
SIE-A	Sie14_w18	143	181	286	294	185	223	153	153
SIE-A	Sie14_w19	161	179	286	296	197	219	151	187
SIE-A	Sie14_w20	167	185	286	296	209	239	151	151
SIE-A	Sie14_w21	167	193	286	296	197	205	179	187
SIE-A	Sie14_w22	185	199	286	296	191	219	153	193
SIE-A	Sie14_w23	175	195	288	296	245	247	155	179
SIE-A	Sie14_w24	181	201	288	296	197	229	175	203
SIE-A	Sie14_w25	149	185	288	296	219	227	153	153
SIE-A	Sie14_w26	147	149	288	298	229	229	155	157
SIE-A	Sie14_w27	167	195	288	310	197	205	153	159
SIE-A	Sie14_w28	149	185	288	310	209	219	153	155
SIE-A	Sie14_w29	181	193	288	310	229	245	175	203
SIE-A	Sie14_w30	181	201	288	322	229	245	175	187
SIE-A	Sie16_w2	173	195	280	288	185	205	137	137
SIE-A	Sie16_w3	189	195	272	280	185	249	137	137

SIE-A	Sie16_w4	189	195	272	280	185	205	137	137
SIE-A	Sie16_w5	189	189	272	280	185	205	137	205
SIE-A	Sie16_w6	173	195	272	280	185	249	137	137
SIE-A	Sie16_w7	173	173	288	288	223	239	137	205
SIE-A	Sie16_w8	175	179	288	288	179	239	137	137
SIE-A	Sie16_w9	189	195	272	280	185	205	137	205
SIE-A	Sie16_w10	173	195	272	280	185	249	137	137
SIE-A	Sie16_w11	189	195	272	280	185	205	137	137
SIE-A	Sie16_w12	189	195	272	280	185	249	137	137
SIE-A	Sie16_w13	189	195	272	280	185	249	137	205
SIE-A	Sie16_w14	189	195	272	280	185	249	137	137
SIE-A	Sie16_w15	189	195	288	288	185	205	137	205
SIE-A	Sie16_w16	173	195	280	288	185	205	151	151
SIE-A	Sie16_w17	173	173	272	280	185	205	137	137
SIE-A	Sie16_w18	0	0	272	280	185	205	137	205
SIE-A	Sie16_w19	173	179	288	288	223	239	141	151
SIE-A	Sie16_w20	189	195	272	280	185	249	137	137
SIE-A	Sie16_w21	189	195	272	280	185	205	137	137
SIE-A	Sie16_w22	189	195	272	280	185	249	137	205
SIE-A	Sie16_w23	175	179	288	288	179	239	151	225
SIE-A	Sie16_w24	173	195	282	294	185	249	137	137
SIE-A	Sie16_w25	189	195	272	280	185	205	137	137
SIE-A	Sie16_w26	173	195	280	288	185	205	137	205
SIE-A	Sie16_w27	189	195	280	288	185	249	137	137
SIE-A	Sie16_w28	189	195	272	280	185	205	137	137
SIE-A	Sie16_w29	189	195	280	288	185	249	137	205
SIE-A	Sie16_w30	173	179	288	288	223	239	151	225
SIE-A	Sie17_w2	163	181	288	302	177	229	159	209
SIE-A	Sie17_w3	181	181	288	302	229	231	173	209
SIE-A	Sie17_w4	143	199	0	0	207	233	159	187
SIE-A	Sie17_w5	143	199	262	288	217	233	159	185
SIE-A	Sie17_w6	143	199	262	288	0	0	159	189
SIE-A	Sie17_w7	179	179	272	302	229	231	173	209
SIE-A	Sie17_w8	143	149	262	288	207	233	0	0
SIE-A	Sie17_w10	163	179	286	302	229	231	173	209
SIE-A	Sie17_w11	143	199	0	0	207	233	159	185
SIE-A	Sie17_w13	163	181	272	302	177	229	159	209
SIE-A	Sie17_w14	181	181	272	302	177	229	173	209
SIE-A	Sie17_w15	163	181	272	302	177	229	173	209
SIE-A	Sie17_w16	143	199	0	0	207	233	159	187
SIE-A	Sie17_w17	143	149	262	288	217	233	0	0
SIE-A	Sie17_w18	173	179	296	296	179	239	159	205
SIE-A	Sie17_w19	163	181	272	302	177	229	173	209
SIE-A	Sie17_w20	143	149	262	288	207	233	159	185

SIE-A	Sie17_w21	143	149	262	288	207	233	159	185
SIE-A	Sie17_w22	163	181	286	302	229	231	159	209
SIE-A	Sie17_w23	143	199	0	0	217	233	159	179
SIE-A	Sie17_w24	143	149	0	0	207	233	159	185
SIE-A	Sie17_w25	181	181	286	302	177	229	159	209
SIE-A	Sie17_w26	143	199	262	288	0	0	159	185
SIE-A	Sie17_w29	163	181	286	302	177	229	173	209
SIE-A	Sie17_w30	181	181	286	302	177	229	159	209
SIE-A	Sie18_w1	147	181	308	348	205	213	153	190
SIE-A	Sie18_w2	151	157	272	274	179	251	155	207
SIE-A	Sie18_w3	173	181	274	348	205	213	153	190
SIE-A	Sie18_w5	185	195	270	290	227	251	190	190
SIE-A	Sie18_w6	147	181	274	348	205	251	153	157
SIE-A	Sie18_w8	151	157	272	274	179	251	0	0
SIE-A	Sie18_w10	147	167	274	286	177	185	151	211
SIE-A	Sie18_w11	185	195	270	290	195	227	153	190
SIE-A	Sie18_w12	147	185	270	288	191	195	153	190
SIE-A	Sie18_w13	147	173	290	304	213	219	183	190
SIE-A	Sie18_w14	161	173	270	272	195	219	155	183
SIE-A	Sie18_w15	173	181	304	348	205	251	153	190
SIE-A	Sie18_w16	185	195	272	290	195	227	0	0
SIE-A	Sie18_w18	157	181	292	304	197	205	159	167
SIE-A	Sie18_w19	177	195	290	298	219	219	157	183
SIE-A	Sie18_w20	177	195	290	304	213	219	183	190
SIE-A	Sie18_w21	147	167	286	292	177	239	153	211
SIE-A	Sie18_w22	167	175	286	292	177	185	151	211
SIE-A	Sie18_w23	173	181	274	348	205	251	153	159
SIE-A	Sie18_w24	157	157	292	304	197	205	159	167
SIE-A	Sie18_w25	173	173	290	302	217	219	183	190
SIE-A	Sie18_w26	151	185	272	310	179	251	159	207
SIE-A	Sie18_w27	173	195	290	308	213	219	157	183
SIE-A	Sie18_w28	173	167	286	292	177	239	153	211
SIE-A	Sie18_w29	139	185	272	308	205	227	159	161
SIE-A	Sie18_w30	177	195	290	308	217	219	183	190
SIE-A	Sie20_w1	143	165	294	308	191	231	149	157
SIE-A	Sie20_w2	175	199	270	306	195	211	153	175
SIE-A	Sie20_w3	149	167	280	292	241	249	151	151
SIE-A	Sie20_w4	149	169	292	306	177	233	131	171
SIE-A	Sie20_w5	149	193	268	306	211	243	151	171
SIE-A	Sie20_w6	149	183	280	292	205	229	157	159
SIE-A	Sie20_w7	165	173	290	294	191	221	157	179
SIE-A	Sie20_w8	167	167	272	296	179	213	153	171
SIE-A	Sie20_w9	177	199	284	284	233	243	151	157
SIE-A	Sie20_w10	169	185	292	296	191	229	159	179

SIE-A	Sie20_w11	199	199	272	284	195	241	151	151
SIE-A	Sie20_w12	143	191	294	294	191	241	171	187
SIE-A	Sie20_w13	169	173	274	296	195	243	155	165
SIE-A	Sie20_w14	149	193	268	292	191	223	159	181
SIE-A	Sie20_w15	167	193	272	290	195	205	159	159
SIE-A	Sie20_w16	175	183	290	294	0	0	171	179
SIE-A	Sie20_w17	165	199	272	292	195	247	173	191
SIE-A	Sie20_w18	165	179	284	294	197	251	131	159
SIE-A	Sie20_w19	165	173	294	322	211	247	171	171
SIE-A	Sie20_w20	173	193	268	308	191	205	153	209
SIE-A	Sie20_w21	147	199	272	272	211	217	177	191
SIE-A	Sie20_w22	153	189	284	284	217	227	175	213
SIE-A	Sie20_w23	173	177	272	276	195	227	137	181
SIE-A	Sie20_w24	173	177	292	322	0	0	151	179
SIE-A	Sie20_w25	173	181	272	272	217	237	179	191
SIE-A	Sie20_w26	147	199	272	306	185	211	171	179
SIE-A	Sie20_w27	165	199	284	330	223	241	159	181
SIE-A	Sie20_w28	165	169	284	292	0	0	171	179
SIE-A	Sie20_w29	175	181	290	290	185	241	151	171
SIE-A	Sie20_w30	169	169	290	290	195	223	131	151
SIE-A	Sie-L49_larv1	143	186	270	302	189	211		
SIE-A	Sie-L49_larv10		145	186	270	287	189	226	
SIE-A	Sie-L49_larv11		145	187	0	0	189	226	
SIE-A	Sie-L49_larv12		145	186	270	302	189	211	
SIE-A	Sie-L49_larv13		143	186	270	287	189	211	
SIE-A	Sie-L49_larv14		145	186	0	0	189	226	
SIE-A	Sie-L49_larv16		145	186	270	302	189	226	
SIE-A	Sie-L49_larv17		177	194	266	287	215	242	
SIE-A	Sie-L49_larv18		143	187	270	287	189	211	
SIE-A	Sie-L49_larv2	143	186	270	287	189	211		
SIE-A	Sie-L49_larv20		143	186	270	302	189	211	
SIE-A	Sie-L49_larv21		145	186	270	287	189	211	
SIE-A	Sie-L49_larv22		143	186	0	0	189	211	
SIE-A	Sie-L49_larv23		143	186	270	302	189	211	
SIE-A	Sie-L49_larv24		145	186	270	302	189	211	
SIE-A	Sie-L49_larv25		143	186	270	287	189	226	
SIE-A	Sie-L49_larv26		173	177	270	289	211	217	
SIE-A	Sie-L49_larv27		143	186	270	302	189	226	
SIE-A	Sie-L49_larv28		143	186	0	0	189	226	
SIE-A	Sie-L49_larv29		145	186	270	287	189	211	
SIE-A	Sie-L49_larv3	145	186	270	302	189	211		
SIE-A	Sie-L49_larv30		143	186	270	287	189	211	
SIE-A	Sie-L49_larv4	143	186	270	302	189	211		
SIE-A	Sie-L49_larv5	143	186	270	302	189	211		

SIE-A	Sie-L49_larv6	177	179	268	289	211	217		
SIE-A	Sie-L49_larv7	143	186	270	287	189	226		
SIE-A	Sie-L49_larv8	143	186	270	302	189	211		
SIE-A	Sie-L49_larv9	143	186	270	287	189	211		
SIE-A	Sie-L49_Q-RG		183	194	266	274	226	242	
SIE-A	Sie-L49_Q-Y	143	145	287	302	211	226		
SIE-A	Sie-L49_Q-R	173	177	268	270	177	217		
CHI	Chi2_w1	163	165	316	318	197	229	129	153
CHI	Chi2_w2	163	189	326	326	193	199	153	153
CHI	Chi2_w3	165	171	316	318	197	229	129	153
CHI	Chi2_w4	165	171	318	318	197	199	153	153
CHI	Chi2_w5	165	165	316	326	197	229	153	153
CHI	Chi2_w6	163	189	318	318	193	229	129	153
CHI	Chi2_w7	163	189	326	326	193	229	129	153
CHI	Chi2_w8	171	189	326	326	193	229	129	153
CHI	Chi2_w9	165	171	316	326	197	199	129	153
CHI	Chi2_w10	171	189	318	318	193	229	129	153
CHI	Chi2_w11	165	171	316	318	197	199	153	153
CHI	Chi2_w12	163	165	316	326	197	229	153	153
CHI	Chi2_w13	165	171	316	318	197	199	129	153
CHI	Chi2_w14	163	165	316	326	197	229	129	153
CHI	Chi2_w15	163	165	316	326	197	199	153	153
CHI	Chi2_w16	165	171	316	318	197	199	129	153
CHI	Chi2_w17	171	189	318	318	193	199	129	153
CHI	Chi2_w18	163	165	316	326	197	199	153	153
CHI	Chi2_w19	171	189	318	318	193	199	153	153
CHI	Chi2_w20	163	165	316	326	197	199	129	153
CHI	Chi2_w21	163	165	316	318	197	229	153	153
CHI	Chi2_w22	163	165	316	318	197	229	129	153
CHI	Chi2_w23	163	189	326	326	193	229	129	153
CHI	Chi2_w24	165	171	316	318	197	229	129	153
CHI	Chi2_w25	163	189	326	326	193	199	153	153
CHI	Chi2_w26	163	189	318	318	193	199	153	153
CHI	Chi2_w27	163	189	318	318	193	199	153	153
CHI	Chi2_w28	165	171	316	326	197	199	129	153
CHI	Chi2_w29	163	165	316	318	197	229	129	153
CHI	Chi2_w30	165	171	316	318	197	199	153	153
CHI	Chi3_w1	193	197	298	298	193	205	0	0
CHI	Chi3_w2	193	197	290	298	193	205	129	129
CHI	Chi3_w3	193	197	290	298	195	205	0	0
CHI	Chi3_w4	169	197	290	298	195	205	129	129
CHI	Chi3_w5	193	197	290	298	193	205	129	129
CHI	Chi3_w6	169	197	298	298	195	205	0	0
CHI	Chi3_w7	169	197	298	298	193	205	129	129

CHI	Chi3_w8	169	197	298	298	193	205	129	129
CHI	Chi3_w9	193	197	290	298	0	0	129	129
CHI	Chi3_w10	193	197	290	298	195	205	129	129
CHI	Chi3_w12	193	197	290	298	0	0	129	129
CHI	Chi3_w13	193	197	290	298	193	205	129	129
CHI	Chi3_w14	193	197	298	298	195	205	129	129
CHI	Chi3_w15	193	197	290	298	0	0	129	129
CHI	Chi3_w16	193	197	290	298	195	205	129	129
CHI	Chi3_w17	165	169	290	294	189	195	129	129
CHI	Chi3_w18	169	197	298	298	195	205	129	129
CHI	Chi3_w19	169	197	298	298	193	205	0	0
CHI	Chi3_w20	169	197	290	298	195	205	129	129
CHI	Chi3_w21	193	197	290	298	193	205	129	129
CHI	Chi3_w22	169	197	290	298	195	205	129	129
CHI	Chi3_w23	193	197	290	298	195	205	129	129
CHI	Chi3_w24	169	197	290	298	193	205	129	129
CHI	Chi3_w25	169	197	290	298	193	205	129	129
CHI	Chi3_w26	193	197	290	298	195	205	129	129
CHI	Chi3_w27	193	197	290	298	195	205	129	129
CHI	Chi3_w28	169	197	298	298	195	205	129	129
CHI	Chi3_w30	169	197	290	298	193	205	129	129
CHI	Chi4_w1	189	193	324	324	189	219	129	129
CHI	Chi4_w2	193	199	306	306	193	219	129	129
CHI	Chi4_w3	191	199	0	0	193	219	129	129
CHI	Chi4_w5	189	191	306	324	189	201	129	129
CHI	Chi4_w6	193	199	0	0	193	219	129	129
CHI	Chi4_w7	193	199	0	0	193	201	129	129
CHI	Chi4_w9	193	199	306	306	193	201	129	129
CHI	Chi4_w10	189	191	324	324	189	201	129	129
CHI	Chi4_w11	189	191	324	324	189	219	129	129
CHI	Chi4_w12	191	199	306	306	193	219	129	129
CHI	Chi4_w13	189	193	306	324	189	201	129	129
CHI	Chi4_w14	189	191	324	324	189	219	129	129
CHI	Chi4_w15	191	199	0	0	193	201	129	129
CHI	Chi4_w16	191	199	306	306	193	201	129	129
CHI	Chi4_w17	191	199	0	0	193	201	129	129
CHI	Chi4_w18	191	199	306	306	193	219	0	0
CHI	Chi4_w21	193	199	306	306	193	219	129	129
CHI	Chi4_w22	193	199	0	0	193	201	129	129
CHI	Chi4_w23	191	199	0	0	193	219	129	129
CHI	Chi4_w24	191	199	0	0	193	201	129	129
CHI	Chi4_w25	189	191	0	0	189	201	129	129
CHI	Chi4_w26	191	199	0	0	193	219	129	129
CHI	Chi4_w27	193	199	0	0	193	219	129	129

CHI	Chi4_w28	193	199	0	0	193	201	129	129
CHI	Chi4_w29	191	199	306	306	193	201	129	129
CHI	Chi4_w30	193	199	306	306	193	219	129	129
CHI	Chi6_w1	151	191	0	0	207	253	129	129
CHI	Chi6_w2	151	191	310	316	207	253	129	129
CHI	Chi6_w3	177	191	310	312	201	207	129	129
CHI	Chi6_w4	151	191	310	316	0	0	129	129
CHI	Chi6_w5	151	179	288	316	191	253	129	129
CHI	Chi6_w6	177	191	310	312	201	207	129	129
CHI	Chi6_w7	151	191	310	312	207	253	129	129
CHI	Chi6_w8	151	179	288	316	191	253	129	129
CHI	Chi6_w9	151	191	310	312	211	207	129	129
CHI	Chi6_w10	151	179	288	316	191	253	129	129
CHI	Chi6_w11	177	179	288	312	191	191	129	129
CHI	Chi6_w12	177	191	310	312	211	253	129	129
CHI	Chi6_w13	151	151	288	316	0	0	129	129
CHI	Chi6_w14	177	191	310	316	211	253	129	129
CHI	Chi6_w15	151	191	310	316	207	253	129	129
CHI	Chi6_w16	177	179	288	312	191	253	129	129
CHI	Chi6_w17	151	191	310	312	201	207	129	129
CHI	Chi6_w18	177	179	288	316	191	253	129	129
CHI	Chi6_w19	177	191	310	312	207	253	129	129
CHI	Chi6_w20	177	179	288	316	191	201	129	129
CHI	Chi6_w21	177	191	310	316	201	207	129	129
CHI	Chi6_w22	177	191	310	312	201	207	129	129
CHI	Chi6_w23	177	191	310	312	201	207	129	129
CHI	Chi6_w24	151	179	288	312	191	201	129	129
CHI	Chi6_w25	177	191	310	312	201	201	129	129
CHI	Chi6_w26	177	191	310	316	201	207	129	129
CHI	Chi6_w27	151	179	288	312	191	253	129	129
CHI	Chi6_w28	177	191	310	316	201	207	129	129
CHI	Chi6_w29	151	179	288	316	191	201	129	129
CHI	Chi6_w30	151	151	288	312	191	201	129	129
CHI	Chi8_w1	165	169	330	348	191	193	129	153
CHI	Chi8_w2	155	165	330	348	193	195	153	193
CHI	Chi8_w3	155	169	276	316	195	207	129	129
CHI	Chi8_w4	155	155	276	316	191	207	129	193
CHI	Chi8_w5	165	169	348	348	191	193	129	153
CHI	Chi8_w6	155	165	276	276	193	195	0	0
CHI	Chi8_w7	155	165	330	348	191	193	153	193
CHI	Chi8_w9	165	169	276	330	191	193	129	153
CHI	Chi8_w10	155	169	316	348	191	207	129	193
CHI	Chi8_w11	155	169	316	348	191	207	129	193
CHI	Chi8_w12	155	169	316	348	195	207	129	129

CHI	Chi8_w13	155	155	276	316	195	207	129	193
CHI	Chi8_w14	0	0	276	330	193	195	153	193
CHI	Chi8_w15	155	155	316	348	195	207	129	129
CHI	Chi8_w16	155	169	276	316	191	207	0	0
CHI	Chi8_w17	155	155	276	316	191	207	129	193
CHI	Chi8_w18	165	169	276	330	191	193	129	153
CHI	Chi8_w19	0	0	276	276	191	193	0	0
CHI	Chi8_w20	155	165	276	330	191	193	129	153
CHI	Chi8_w21	155	155	316	348	0	0	129	193
CHI	Chi8_w22	155	169	276	316	195	207	129	193
CHI	Chi8_w23	0	0	276	330	193	195	129	153
CHI	Chi8_w24	155	169	316	348	195	207	129	129
CHI	Chi8_w25	165	169	330	348	191	193	153	193
CHI	Chi8_w26	155	169	316	348	195	207	129	193
CHI	Chi8_w27	165	169	276	276	191	193	129	153
CHI	Chi8_w28	0	0	316	348	191	207	129	129
CHI	Chi8_w29	155	155	316	348	191	207	129	193
CHI	Chi8_w30	165	169	330	330	191	193	153	193
CHI	Chi9_w1	163	171	316	316	199	199	129	151
CHI	Chi9_w2	163	171	310	342	195	199	129	151
CHI	Chi9_w3	165	171	308	342	195	199	129	129
CHI	Chi9_w4	165	171	0	0	199	199	129	151
CHI	Chi9_w5	165	171	308	308	0	0	129	129
CHI	Chi9_w6	165	171	308	342	195	199	129	151
CHI	Chi9_w7	165	171	308	308	195	199	129	151
CHI	Chi9_w8	165	171	308	308	195	199	129	151
CHI	Chi9_w9	165	171	316	316	199	199	129	129
CHI	Chi9_w10	165	171	308	308	195	199	129	151
CHI	Chi9_w11	163	171	316	316	199	199	129	151
CHI	Chi9_w12	165	171	316	316	195	199	129	129
CHI	Chi9_w13	163	171	0	0	195	199	129	129
CHI	Chi9_w14	163	171	0	0	199	199	129	129
CHI	Chi9_w15	165	171	316	316	195	199	129	151
CHI	Chi9_w16	163	171	308	308	199	199	129	129
CHI	Chi9_w17	165	171	316	316	199	199	129	151
CHI	Chi9_w18	163	171	308	308	195	199	129	151
CHI	Chi9_w19	165	171	308	342	199	199	129	151
CHI	Chi9_w20	163	171	0	0	199	199	129	129
CHI	Chi9_w21	165	171	316	342	199	199	129	129
CHI	Chi9_w22	163	171	316	316	195	199	129	151
CHI	Chi9_w23	165	171	310	310	199	199	129	129
CHI	Chi9_w24	163	171	0	0	199	199	129	151
CHI	Chi9_w25	163	171	316	342	199	199	129	151
CHI	Chi9_w26	163	171	310	310	199	199	129	151

CHI	Chi9_w27	165	171	308	342	195	199	0	0
CHI	Chi9_w28	163	171	316	342	199	199	129	151
CHI	Chi10_w1	163	183	302	346	195	217	129	129
CHI	Chi10_w2	163	183	310	346	195	195	129	129
CHI	Chi10_w3	163	167	302	346	195	217	129	129
CHI	Chi10_w4	163	183	310	346	195	195	129	129
CHI	Chi10_w5	163	183	302	346	195	195	129	129
CHI	Chi10_w6	163	183	302	346	195	195	129	129
CHI	Chi10_w7	163	183	310	346	195	217	129	129
CHI	Chi10_w8	163	167	302	346	195	217	129	129
CHI	Chi10_w9	163	167	310	346	195	217	129	129
CHI	Chi10_w10	167	183	302	304	195	217	131	131
CHI	Chi10_w11	167	167	304	310	195	195	131	131
CHI	Chi10_w12	163	167	310	346	195	195	129	129
CHI	Chi10_w13	163	167	310	346	195	195	129	129
CHI	Chi10_w14	163	167	302	346	195	217	129	129
CHI	Chi10_w15	163	183	310	346	195	195	129	129
CHI	Chi10_w16	163	183	0	0	195	195	129	129
CHI	Chi10_w17	163	183	302	346	195	195	129	129
CHI	Chi10_w18	163	183	302	346	195	195	129	129
CHI	Chi10_w19	163	183	0	0	195	195	129	129
CHI	Chi10_w20	167	183	0	0	195	215	131	131
CHI	Chi10_w21	163	167	310	346	195	195	129	129
CHI	Chi10_w22	163	167	310	346	195	195	129	129
CHI	Chi10_w23	167	167	302	304	195	195	131	131
CHI	Chi10_w24	163	167	310	346	195	195	129	129
CHI	Chi10_w25	163	183	310	346	195	195	129	129
CHI	Chi10_w26	163	167	302	346	195	195	129	129
CHI	Chi10_w27	167	183	304	310	195	215	131	131
CHI	Chi10_w28	167	167	302	304	195	195	131	131
CHI	Chi10_w29	163	183	302	346	195	215	129	129
CHI	Chi11_w1	191	197	316	326	195	203	129	129
CHI	Chi11_w3	163	191	316	326	193	203	129	129
CHI	Chi11_w4	163	191	316	326	195	203	129	129
CHI	Chi11_w5	191	197	316	326	195	203	0	0
CHI	Chi11_w6	163	191	316	326	193	203	129	129
CHI	Chi11_w7	191	197	326	326	193	203	129	129
CHI	Chi11_w8	191	197	316	326	195	203	129	129
CHI	Chi11_w9	191	197	316	326	193	203	129	129
CHI	Chi11_w10	191	197	316	326	195	203	129	129
CHI	Chi11_w11	163	191	326	326	193	203	129	129
CHI	Chi11_w12	163	191	0	0	193	203	129	129
CHI	Chi11_w13	191	197	0	0	193	203	129	129
CHI	Chi11_w14	163	191	316	326	195	203	0	0

CHI	Chi11_w15	163	191	326	326	193	203	129	129
CHI	Chi11_w17	163	191	316	326	193	203	129	129
CHI	Chi11_w18	191	197	326	326	195	203	129	129
CHI	Chi11_w19	163	191	326	326	193	203	129	129
CHI	Chi11_w20	163	191	326	326	195	203	129	129
CHI	Chi11_w21	191	197	326	326	193	203	129	129
CHI	Chi11_w22	191	197	326	326	193	203	129	129
CHI	Chi11_w23	191	197	326	326	195	203	129	129
CHI	Chi11_w24	191	197	0	0	193	203	129	129
CHI	Chi11_w25	191	197	326	326	193	203	129	129
CHI	Chi11_w26	191	197	326	326	195	203	129	129
CHI	Chi11_w27	191	197	316	326	193	203	129	129
CHI	Chi11_w28	163	191	326	326	193	203	0	0
CHI	Chi11_w29	191	197	326	326	193	203	129	129
CHI	Chi11_w30	0	0	326	326	195	203	129	129
CHI	Chi12_w1	161	165	308	328	195	203	129	153
CHI	Chi12_w2	161	165	308	328	195	203	129	153
CHI	Chi12_w3	165	203	308	328	195	203	129	153
CHI	Chi12_w4	161	165	308	324	195	203	129	153
CHI	Chi12_w5	165	203	308	328	193	195	129	129
CHI	Chi12_w6	165	203	308	324	195	203	129	129
CHI	Chi12_w7	161	165	308	328	195	203	129	153
CHI	Chi12_w8	161	165	308	328	195	203	129	153
CHI	Chi12_w10	165	203	308	328	195	203	129	153
CHI	Chi12_w11	165	203	308	324	193	195	129	129
CHI	Chi12_w12	165	203	308	324	193	195	129	129
CHI	Chi12_w13	173	203	328	348	203	219	129	129
CHI	Chi12_w14	161	165	308	324	193	195	129	129
CHI	Chi12_w15	161	165	308	328	193	195	129	153
CHI	Chi12_w16	165	203	308	328	195	203	129	153
CHI	Chi12_w17	0	0	308	328	193	195	129	153
CHI	Chi12_w18	161	173	324	348	193	219	129	153
CHI	Chi12_w19	161	165	308	324	195	203	129	129
CHI	Chi12_w20	165	203	308	328	195	203	129	129
CHI	Chi12_w21	161	173	324	348	193	219	129	129
CHI	Chi12_w22	165	203	308	324	193	195	129	129
CHI	Chi12_w23	161	165	308	328	193	195	129	153
CHI	Chi12_w24	161	173	328	348	193	219	129	129
CHI	Chi12_w26	161	165	308	328	193	195	129	129
CHI	Chi12_w27	173	203	324	348	193	219	129	153
CHI	Chi12_w28	165	203	308	328	195	195	129	153
CHI	Chi12_w29	161	165	308	324	195	203	129	129
CHI	Chi12_w30	173	203	324	348	193	219	129	153
CHI	Chi17_w1	157	183	310	328	193	193	129	153

CHI	Chi17_w2	0	0	310	328	193	203	129	153
CHI	Chi17_w3	153	183	314	328	193	203	129	153
CHI	Chi17_w4	157	183	314	328	193	193	129	153
CHI	Chi17_w5	153	163	310	310	193	203	131	153
CHI	Chi17_w6	157	183	310	328	193	193	129	153
CHI	Chi17_w7	153	183	310	328	193	193	129	153
CHI	Chi17_w8	153	163	314	314	193	193	131	153
CHI	Chi17_w9	157	183	310	328	193	203	129	153
CHI	Chi17_w10	157	183	310	328	193	193	129	153
CHI	Chi17_w11	153	183	310	328	193	203	129	153
CHI	Chi17_w12	157	163	310	310	193	193	131	153
CHI	Chi17_w13	153	163	314	314	193	203	131	153
CHI	Chi17_w14	157	183	314	328	193	193	129	153
CHI	Chi17_w15	153	163	310	310	193	193	131	153
CHI	Chi17_w16	153	163	310	310	193	203	131	153
CHI	Chi17_w17	157	183	314	328	193	193	129	153
CHI	Chi17_w18	153	163	314	314	193	203	131	153
CHI	Chi17_w19	157	183	310	328	193	193	129	153
CHI	Chi17_w21	157	183	310	328	193	193	129	153
CHI	Chi17_w23	157	183	310	328	193	193	129	153
CHI	Chi17_w24	157	163	314	314	193	203	131	153
CHI	Chi17_w25	153	163	310	370	193	193	131	153
CHI	Chi17_w26	153	183	314	328	193	203	129	153
CHI	Chi17_w27	153	163	314	370	193	203	131	153
CHI	Chi17_w28	157	183	310	328	193	193	129	153
CHI	Chi17_w29	153	163	310	370	193	203	131	153
CHI	Chi17_w30	153	183	314	328	193	203	129	153
CHI	Chi20_w1	133	165	310	348	197	237	129	153
CHI	Chi20_w2	133	165	324	348	197	197	129	153
CHI	Chi20_w3	133	165	310	348	197	237	129	153
CHI	Chi20_w4	161	165	324	348	197	197	129	153
CHI	Chi20_w5	133	165	324	348	197	237	129	153
CHI	Chi20_w6	133	165	310	348	197	237	129	153
CHI	Chi20_w7	133	165	324	348	197	237	129	153
CHI	Chi20_w8	161	165	324	348	197	237	129	153
CHI	Chi20_w9	161	165	324	348	197	197	129	153
CHI	Chi20_w10	161	165	310	348	197	237	129	153
CHI	Chi20_w11	161	165	324	348	197	197	0	0
CHI	Chi20_w12	161	165	310	348	197	237	129	153
CHI	Chi20_w13	133	165	310	348	197	197	129	153
CHI	Chi20_w14	161	165	0	0	197	237	129	153
CHI	Chi20_w15	133	165	0	0	197	237	129	153
CHI	Chi20_w16	161	165	324	348	197	197	0	0
CHI	Chi20_w17	161	165	310	348	197	197	129	153

CHI	Chi20_w18	133	165	310	348	197	237	129	153
CHI	Chi20_w19	165	165	324	348	197	197	129	153
CHI	Chi20_w20	161	165	324	348	197	197	129	153
CHI	Chi20_w21	161	165	324	348	197	197	129	153
CHI	Chi20_w22	161	165	0	0	197	237	129	153
CHI	Chi20_w23	161	165	0	0	197	197	129	153
CHI	Chi20_w24	133	165	0	0	197	197	129	153
CHI	Chi20_w25	161	165	324	348	197	197	0	0

**** data end **** 163

APPENDIX B

ANALYSIS CONDITIONS AND TECHNICAL RESULTS FOR MATESOFT AND COLONY

Run conditions: MATESOFT can reconstruct genotypes of putative matrilines and patrilines from offspring genotypes to estimate observed paternity (i.e. number of males siring offspring of a queen, K_{obs}) and effective paternity (pedigree effective mate number, $m_{e,p}$, in MATESOFT) in monogynous colonies, but not in polygynous colonies. These two quantities, defined according to Jaffe (2014) inform us on queen mating behavior. MATESOFT is relatively more conservative as it tries to minimize the number of male mates when inferring queen genotypes. Queen genotype deduction F analyses were set to use the broad deduction algorithm to account for the possibility of polyandry. Male genotype deduction FQ analyses and mating frequency FQM (1-2 matings) analyses were estimated using the F analysis outputs.

COLONY on the other hand can reconstruct matrilines and patrilines simultaneously and is not constrained by gyny. The sibship prior was set to "No" and "Dioecious" and "Haplodiploid" conditions were selected. The number of runs was set at 5 to increase the probability of obtaining the most accurate maximum-likelihood configurations. Female polygamy was allowed based on the observed polyandry from the MATESOFT analysis, while male mating strategy was assumed to be monogamy. Sibship scaling, an option preventing erroneous splitting of large full sibship (hundreds of siblings), was set to "No" because full sibship size is likely to be small in our 30-worker samples especially when the source colonies are polygynous and/or queens are polyandrous. COLONY was allowed to update allele frequencies. The rates of allelic dropout and other types of genotyping error were set at 0.5% for all markers. All other

parameters were assigned their default values (analysis method: full likelihood, run length: medium, seed number: 1234)

Technical results pertaining to Chapter Two: The probability of failing to distinguish offspring of two patrilines with identical multi-locus haplotypes (i.e. non-detection error) was calculated as in Gadau et al. (2003) and is 0.036 and 0.001 for the CHI and SIE-A populations, respectively. The probability of failing to sample offspring from all matrilines and their mates (i.e. non-sampling errors) given the sample size of 30 workers is likely very high for SIE-A colonies due to the presence of both polygyny and polyandry. Nearly 18.2% of 309 successfully genotyped CHI workers failed to amplify one of the four loci. In the initial analysis, MATESOFT detected polygyny in 3 of the 11 colonies sampled. One worker genotype from one colony and two genotypes from each of the other two colonies, representing 3.4 - 7.1% of the total number of workers in the colonies, were determined to be the causes of the polygyny warnings. Excluding these workers and rerunning the analysis showed that all colonies are consistent with monogyny. Subsequent queen mating frequency estimates for the CHI colonies were made without these genotypes. Intraspecific raiding and worker drifting are possible sources of sampling errors, in addition to genotyping errors and novel germline mutations. Excluding the anomalous genotypes provides some measures of correction without compromising the sample size.

Similarly, most of the 314 SIE-A workers genotyped successfully amplified all four loci, with 10.2% m data at a single locus. In stark contrast to the CHI colonies, both MATESOFT and COLONY consistently classified all 11 SIE-A colonies as polygynous.

While each CHI matriline inferred by COLONY uniquely associated with a single colony, 60.3% of the SIE-A inferred matrilines were detected in multiple colonies. In fact, each of the 11 colonies has at least one matriline (average = 7.82 ± 1.81 matrilines) which appears in other colonies (average = 4.91 ± 0.77 colonies). Brood raiding cannot entirely explain the occurrence of matrilines with identical genotype in different colonies because some of these colonies are kilometers apart, beyond the range at which raiding can conceivably occur. Alternatively, the number of colonies contributed to the pool of reproductives may be relatively small in the SIE-A population, leading to individuals sharing recent ancestry inhabiting different colonies. It is also possible that our microsatellite markers are insufficiently sensitive to distinguish all matrilines.

References:

Gadau, J., et al. "Determinants of Intracolonial Relatedness in *Pogonomyrmex rugosus* (Hymenoptera; Formicidae): Mating Frequency and Brood Raids." *Molecular Ecology*, vol. 12, no. 7, July 2003, pp. 1931–38. *Crossref*, doi:10.1046/j.1365-294X.2003.01853.x.

Jaffé, Rodolfo. "AN UPDATED GUIDE TO STUDY POLYANDRY IN SOCIAL INSECTS." *Sociobiology*, vol. 61, no. 1, Apr. 2014. *Crossref*, doi:10.13102/sociobiology.v61i1.1-8.

APPENDIX C

MULTI-LOCUS MICROSATELLITE GENOTYPES OF *MYRMECOCYSTUS MENDAX* SPECIMENS FROM CHAPTER THREE

Legend:

- Column 1: Population ID (e.g. SIE-A)
- Column 2: Colony ID_individual ID (e.g. Sie6_w1)
- Column 3+4: genotype at locus Mm3
- Column 5+6: genotype at locus Mm4
- Column 7+8: genotype at locus Mm5
- Column 9+10: genotype at locus FE17
- Population ID: see Table 3.1
- L: lab colonies; FA: female alates; Q: queen; w: worker; larv: larva
- m: missing data

**** Chiricahua field colonies ****

CHI	Chi10_w12	161	165	303	343	193	193	125	125
CHI	Chi10_w21	161	165	303	343	193	193	125	125
CHI	Chi10_w22	161	165	303	343	193	193	125	125
CHI	Chi10_w24	161	165	303	343	193	193	125	125
CHI	Chi10_w25	161	181	303	343	193	193	125	125
CHI	Chi10_w27	165	181	293	303	193	215	125	127
CHI	Chi10_w3	161	165	289	343	191	215	125	125
CHI	Chi10_w5	161	181	289	343	193	193	125	125
CHI	Chi10_w6	161	181	289	343	193	193	125	125
CHI	Chi10_w7	161	181	303	343	191	215	125	125
CHI	Chi11_w15	191	201	323	325	191	201	125	125
CHI	Chi11_w18	189	197	311	323	193	201	125	125
CHI	Chi11_w19	163	189	323	325	191	201	125	125
CHI	Chi11_w20	163	189	323	325	193	201	125	125
CHI	Chi11_w22	189	197	323	325	191	201	125	125
CHI	Chi11_w25	189	197	323	325	191	201	125	125
CHI	Chi11_w27	189	197	311	323	191	201	125	125
CHI	Chi11_w6	163	189	311	323	191	201	125	125
CHI	Chi11_w7	189	197	323	325	191	201	125	125
CHI	Chi11_w9	189	197	311	323	191	201	125	125
CHI	Chi12_w1	159	163	299	331	193	201	125	151
CHI	Chi12_w12	163	201	299	319	191	193	125	125
CHI	Chi12_w15	159	163	299	331	191	193	125	151
CHI	Chi12_w2	159	163	299	331	193	201	125	151
CHI	Chi12_w20	163	201	299	331	193	201	125	125
CHI	Chi12_w26	159	163	299	331	191	193	125	125

CHI	Chi12_w27	171	201	319	347	191	217	125	151
CHI	Chi12_w28	163	201	299	331	193	193	125	151
CHI	Chi12_w5	163	201	299	331	191	193	125	125
CHI	Chi12_w8	159	163	299	331	193	201	125	151
CHI	Chi17_w1	155	181	303	327	191	191	125	151
CHI	Chi17_w10	155	181	303	327	191	191	125	151
CHI	Chi17_w11	151	181	303	327	191	201	125	151
CHI	Chi17_w12	155	161	303	375	191	191	127	151
CHI	Chi17_w16	151	161	303	375	191	201	127	151
CHI	Chi17_w18	151	161	307	307	191	201	127	151
CHI	Chi17_w21	155	181	303	327	191	191	125	151
CHI	Chi17_w23	155	181	303	327	191	191	125	151
CHI	Chi17_w28	155	181	307	307	191	191	125	151
CHI	Chi17_w6	155	181	303	327	191	191	125	151
CHI	Chi2_w1	161	163	311	313	195	227	125	151
CHI	Chi2_w14	161	163	311	323	195	227	125	151
CHI	Chi2_w15	161	163	311	323	195	197	151	151
CHI	Chi2_w20	161	163	311	323	195	197	125	151
CHI	Chi2_w21	161	163	311	313	195	227	151	151
CHI	Chi2_w23	161	187	323	323	191	227	125	151
CHI	Chi2_w24	163	169	311	313	195	227	125	151
CHI	Chi2_w27	161	187	313	313	191	197	151	151
CHI	Chi2_w29	161	163	311	313	195	227	125	151
CHI	Chi2_w30	163	169	311	313	195	197	151	151
CHI	Chi20_w1	131	163	301	347	195	237	125	151
CHI	Chi20_w12	159	163	301	347	195	237	125	151
CHI	Chi20_w13	131	163	301	347	195	195	125	151
CHI	Chi20_w17	159	163	301	347	195	195	125	151
CHI	Chi20_w19	163	163	321	347	195	195	125	151
CHI	Chi20_w2	131	163	321	347	195	237	125	151
CHI	Chi20_w5	131	163	321	347	195	237	125	151
CHI	Chi20_w6	131	163	301	347	195	237	125	151
CHI	Chi20_w7	131	163	321	347	195	237	125	151
CHI	Chi20_w8	159	163	321	347	195	237	125	151
CHI	Chi3_w13	191	197	303	313	191	203	125	125
CHI	Chi3_w17	165	167	303	323	187	193	125	125
CHI	Chi3_w22	167	197	303	313	193	203	125	125
CHI	Chi3_w23	191	197	303	313	193	203	125	125
CHI	Chi3_w25	167	197	303	313	191	203	125	125
CHI	Chi3_w26	191	197	303	313	193	203	125	125
CHI	Chi3_w27	191	197	303	313	193	203	125	125

CHI	Chi3_w30	167	197	303	313	191	203	125	125
CHI	Chi3_w7	167	197	313	313	191	203	125	125
CHI	Chi3_w8	167	197	313	313	191	203	125	125
CHI	Chi4_w1	187	191	327	327	187	217	125	125
CHI	Chi4_w10	187	189	327	327	187	199	125	125
CHI	Chi4_w12	189	197	307	307	191	217	125	125
CHI	Chi4_w13	187	191	307	327	187	199	125	125
CHI	Chi4_w14	187	189	327	327	187	217	125	125
CHI	Chi4_w2	191	197	307	307	191	217	125	125
CHI	Chi4_w21	191	197	307	307	191	217	125	125
CHI	Chi4_w29	189	197	307	307	191	199	125	125
CHI	Chi4_w30	191	197	307	307	191	217	125	125
CHI	Chi4_w5	187	189	307	327	187	199	125	125
CHI	Chi6_w15	149	189	303	311	205	253	125	125
CHI	Chi6_w17	149	189	303	307	199	205	125	125
CHI	Chi6_w2	149	189	303	311	205	253	125	125
CHI	Chi6_w20	175	177	277	311	189	199	125	125
CHI	Chi6_w22	175	189	303	307	199	205	125	125
CHI	Chi6_w23	175	189	303	307	199	205	125	125
CHI	Chi6_w24	149	177	277	307	189	199	125	125
CHI	Chi6_w26	175	189	303	311	199	205	125	125
CHI	Chi6_w7	149	189	303	307	205	253	125	125
CHI	Chi6_w8	149	177	277	311	189	253	125	125
CHI	Chi8_w1	163	167	331	333	189	191	125	151
CHI	Chi8_w10	153	167	305	333	189	205	125	191
CHI	Chi8_w13	153	153	243	305	193	205	125	191
CHI	Chi8_w15	153	153	305	333	193	205	125	125
CHI	Chi8_w17	153	153	243	305	189	205	125	191
CHI	Chi8_w20	153	163	243	331	189	191	125	151
CHI	Chi8_w25	163	167	331	333	189	191	151	191
CHI	Chi8_w26	153	167	305	333	193	205	125	191
CHI	Chi8_w27	163	167	243	243	189	191	125	151
CHI	Chi8_w7	153	163	331	333	189	191	151	191
CHI	Chi9_w12	163	169	311	339	193	197	125	125
CHI	Chi9_w19	163	169	299	339	197	199	125	149
CHI	Chi9_w2	161	169	301	339	193	197	125	149
CHI	Chi9_w21	163	169	311	339	197	199	125	125
CHI	Chi9_w23	163	169	301	339	197	199	125	125
CHI	Chi9_w26	161	169	301	339	197	199	125	149
CHI	Chi9_w6	163	169	299	339	193	197	125	149

CHI	Chi9_w7	163	169	299	339	193	197	125	149
CHI	Chi9_w8	163	169	299	339	193	197	125	149
CHI	Chi9_w9	163	169	311	339	197	199	125	125

**** Dragoons field colonies ****

DRA	Coc01_w1	163	165	333	339	195	207	125	149
DRA	Coc01_w10	163	177	333	339	195	207	125	151
DRA	Coc01_w2	163	177	333	339	195	207	125	149
DRA	Coc01_w3	163	177	333	339	195	207	125	149
DRA	Coc01_w4	163	165	333	339	207	221	125	149
DRA	Coc01_w5	163	177	333	339	207	221	125	151
DRA	Coc01_w6	163	177	277	339	207	221	125	151
DRA	Coc01_w7	163	177	277	339	195	207	125	149
DRA	Coc01_w8	163	165	277	339	207	221	125	151
DRA	Coc01_w9	163	165	277	339	195	207	125	149
DRA	Coc02_w1	179	187	299	341	193	207	125	125
DRA	Coc02_w10	163	179	299	341	193	201	125	125
DRA	Coc02_w2	179	187	299	341	193	201	125	125
DRA	Coc02_w3	179	187	341	357	193	207	125	125
DRA	Coc02_w4	163	179	341	357	193	207	125	125
DRA	Coc02_w5	179	187	341	357	193	207	125	125
DRA	Coc02_w6	179	187	341	357	193	201	125	125
DRA	Coc02_w7	179	187	299	341	193	201	125	125
DRA	Coc02_w8	163	179	341	357	193	201	125	125
DRA	Coc02_w9	163	179	341	357	193	207	125	125
DRA	Coc03_w1	141	159	293	301	195	203	125	125
DRA	Coc03_w10	141	167	301	307	195	203	125	125
DRA	Coc03_w2	141	159	293	301	203	223	125	125
DRA	Coc03_w3	141	159	293	301	195	203	125	125
DRA	Coc03_w4	141	159	293	301	203	223	125	125
DRA	Coc03_w5	141	159	293	301	203	223	125	125
DRA	Coc03_w6	141	167	293	301	195	203	125	125
DRA	Coc03_w7	141	167	293	301	203	223	125	125
DRA	Coc03_w8	141	167	293	301	203	223	125	125
DRA	Coc03_w9	141	167	293	301	203	223	125	125
DRA	Coc04_w1	189	193	339	345	191	201	125	125
DRA	Coc04_w10	189	193	327	345	201	203	125	125
DRA	Coc04_w2	167	193	327	345	201	203	125	125
DRA	Coc04_w3	189	193	327	345	201	203	125	125
DRA	Coc04_w4	189	193	339	345	201	203	125	125

DRA	Coc04_w5	167	193	339	345	201	203	125	125
DRA	Coc04_w6	189	193	327	345	201	203	125	125
DRA	Coc04_w7	189	193	327	345	191	201	125	125
DRA	Coc04_w8	167	193	339	345	191	201	125	125
DRA	Coc04_w9	189	193	327	345	191	201	125	125
DRA	Coc05_w1	163	165	275	315	191	223	125	125
DRA	Coc05_w10	163	187	299	315	191	207	125	125
DRA	Coc05_w2	163	187	275	315	191	207	125	125
DRA	Coc05_w3	163	165	299	315	191	223	125	125
DRA	Coc05_w4	163	165	299	315	191	223	125	125
DRA	Coc05_w5	163	165	275	315	191	223	125	125
DRA	Coc05_w6	163	165	275	315	191	207	125	125
DRA	Coc05_w7	163	187	299	315	191	223	125	125
DRA	Coc05_w8	163	187	299	315	191	223	125	125
DRA	Coc05_w9	163	187	299	315	191	207	125	125
DRA	Coc07_w1	167	173	301	337	193	223	125	149
DRA	Coc07_w10	167	173	301	337	205	223	125	149
DRA	Coc07_w2	167	193	301	331	205	219	125	125
DRA	Coc07_w3	167	173	301	337	205	223	125	149
DRA	Coc07_w4	167	167	291	331	205	219	125	125
DRA	Coc07_w5	167	193	301	331	205	219	125	125
DRA	Coc07_w6	167	173	291	337	193	223	125	149
DRA	Coc07_w7	167	173	301	337	193	223	125	149
DRA	Coc07_w8	167	167	291	331	205	219	125	125
DRA	Coc07_w9	167	173	301	337	205	223	125	149
DRA	Coc08_w1.1	161	163	295	295	195	197	125	125
DRA	Coc08_w10	163	189	269	295	195	229	125	125
DRA	Coc08_w2	163	187	299	299	191	207	125	125
DRA	Coc08_w3	163	163	269	295	195	229	125	149
DRA	Coc08_w4	161	163	269	295	195	197	125	149
DRA	Coc08_w5	163	189	295	379	195	197	125	125
DRA	Coc08_w6	161	163	295	379	195	197	125	125
DRA	Coc08_w7	161	163	295	379	195	197	125	149
DRA	Coc08_w8	161	163	295	295	195	229	125	149
DRA	Coc08_w9	163	189	295	295	195	229	125	125
DRA	Coc10_w1	153	167	279	311	193	203	125	131
DRA	Coc10_w10	153	167	279	311	193	203	125	131
DRA	Coc10_w2	153	167	279	295	193	203	125	131
DRA	Coc10_w3	153	167	279	295	193	203	125	131
DRA	Coc10_w4	159	167	279	295	193	203	125	131

DRA	Coc10_w5	153	167	279	295	193	203	125	131
DRA	Coc10_w6	159	167	279	311	193	203	125	131
DRA	Coc10_w7	159	167	279	311	193	203	125	131
DRA	Coc10_w8	153	167	279	295	197	203	125	131
DRA	Coc10_w9	153	167	279	279	197	203	125	131

**** Mt. Graham field colonies ****

GRA	Sky01_w1	157	169	287	315	191	209	127	127
GRA	Sky01_w10	157	169	287	315	191	209	127	127
GRA	Sky01_w2	155	157	287	289	189	191	127	127
GRA	Sky01_w3	155	157	287	289	189	191	125	127
GRA	Sky01_w4	157	169	289	315	205	209	125	149
GRA	Sky01_w5	155	157	287	315	189	191	125	127
GRA	Sky01_w6	155	157	287	315	191	209	125	127
GRA	Sky01_w7	157	169	287	289	189	191	125	127
GRA	Sky01_w8	157	169	287	315	189	191	125	127
GRA	Sky01_w9	155	157	287	315	189	191	127	127
GRA	Sky02_w1	155	177	299	321	189	189	125	171
GRA	Sky02_w10	155	173	299	325	199	235	125	171
GRA	Sky02_w2	155	177	299	325	191	235	125	127
GRA	Sky02_w3	155	173	299	325	199	235	125	171
GRA	Sky02_w4	155	173	299	321	191	235	125	127
GRA	Sky02_w5	155	177	299	325	191	235	125	127
GRA	Sky02_w6	155	177	299	321	189	199	125	127
GRA	Sky02_w7	155	173	299	321	191	235	125	171
GRA	Sky02_w8	155	173	299	325	191	235	125	127
GRA	Sky02_w9	155	173	299	321	199	235	125	171
GRA	Sky03_w1	165	167	293	299	189	205	125	179
GRA	Sky03_w10	165	167	293	299	189	205	125	125
GRA	Sky03_w2	165	175	287	299	189	197	149	179
GRA	Sky03_w3	165	167	299	299	189	205	125	125
GRA	Sky03_w4	165	167	293	293	197	205	125	179
GRA	Sky03_w5	165	167	299	299	189	205	125	125
GRA	Sky03_w6	167	175	293	299	197	205	125	125
GRA	Sky03_w7	165	165	287	293	191	197	149	179
GRA	Sky03_w8	167	175	299	299	197	205	125	179
GRA	Sky03_w9	167	175	293	299	189	205	125	125
GRA	Sky04_w1	169	195	297	349	189	189	125	151
GRA	Sky04_w10	169	195	297	297	189	199	125	149
GRA	Sky04_w2	159	169	297	297	189	199	125	151

GRA	Sky04_w3	159	169	297	349	189	199	125	151
GRA	Sky04_w4	169	195	297	297	189	189	125	149
GRA	Sky04_w5	169	195	297	349	189	199	125	151
GRA	Sky04_w6	159	169	297	349	189	189	125	149
GRA	Sky04_w7	169	195	297	349	189	189	125	151
GRA	Sky04_w8	159	169	297	297	189	199	125	149
GRA	Sky04_w9	169	195	297	297	189	189	125	149
GRA	Sky05_w1	163	183	291	335	195	213	125	171
GRA	Sky05_w10	163	183	281	291	195	213	125	171
GRA	Sky05_w2	153	183	281	291	195	213	125	171
GRA	Sky05_w3	163	183	281	291	195	213	125	171
GRA	Sky05_w4	153	183	281	291	193	213	125	171
GRA	Sky05_w5	153	183	281	291	195	213	125	171
GRA	Sky05_w6	163	183	281	291	193	213	125	171
GRA	Sky05_w7	153	183	291	335	193	213	125	171
GRA	Sky05_w8	153	183	291	335	195	213	125	171
GRA	Sky05_w9	153	183	291	335	193	213	125	171
GRA	Sky06_w1	147	149	301	301	191	191	125	127
GRA	Sky06_w10	147	149	301	301	191	201	125	127
GRA	Sky06_w2	149	175	301	301	191	191	125	127
GRA	Sky06_w3	147	149	301	301	191	201	125	127
GRA	Sky06_w4	149	175	301	301	191	191	125	125
GRA	Sky06_w5	149	175	301	301	191	191	125	125
GRA	Sky06_w6	149	175	301	301	191	201	125	127
GRA	Sky06_w7	149	175	301	301	191	191	125	125
GRA	Sky06_w8	147	149	301	301	191	201	125	125
GRA	Sky06_w9	147	151	301	301	191	195	125	125
GRA	Sky08_w1	149	169	281	299	189	193	125	183
GRA	Sky08_w10	149	169	281	317	189	193	125	183
GRA	Sky08_w2	149	175	281	299	189	193	125	125
GRA	Sky08_w3	149	175	281	299	189	193	125	125
GRA	Sky08_w4	149	169	281	317	193	201	125	183
GRA	Sky08_w5	149	169	281	299	189	193	125	183
GRA	Sky08_w6	149	175	281	317	193	201	125	183
GRA	Sky08_w7	149	169	281	317	189	201	125	125
GRA	Sky08_w8	149	175	281	299	193	201	125	183
GRA	Sky08_w9	149	175	281	299	193	201	125	125
GRA	Sky09_w1	165	177	323	357	203	211	125	185
GRA	Sky09_w10	165	177	323	357	203	203	125	125
GRA	Sky09_w2	177	187	323	357	203	211	125	185

GRA	Sky09_w3	165	177	323	357	203	211	125	125
GRA	Sky09_w4	165	177	301	357	197	211	125	125
GRA	Sky09_w5	165	177	323	357	197	211	125	185
GRA	Sky09_w6	165	177	301	357	197	197	125	125
GRA	Sky09_w7	165	177	323	357	197	211	125	125
GRA	Sky09_w8	165	177	301	357	197	211	125	185
GRA	Sky09_w9	165	177	323	357	197	211	125	125
GRA	Sky10_w1	157	173	293	317	193	205	125	161
GRA	Sky10_w10	157	177	303	331	191	197	125	125
GRA	Sky10_w2	155	177	303	331	191	193	125	125
GRA	Sky10_w3	155	173	303	317	193	205	125	161
GRA	Sky10_w4	157	173	293	317	197	205	125	125
GRA	Sky10_w5	157	177	293	331	191	193	125	161
GRA	Sky10_w6	157	177	293	331	191	197	125	125
GRA	Sky10_w7	155	177	303	331	191	193	125	125
GRA	Sky10_w8	157	177	303	331	191	197	125	125
GRA	Sky10_w9	157	177	293	331	191	193	125	161
GRA	Sky13_w1	159	165	289	299	195	201	125	129
GRA	Sky13_w10	165	181	289	299	195	201	125	129
GRA	Sky13_w2	159	173	317	323	203	223	125	125
GRA	Sky13_w3	159	165	289	299	195	223	125	129
GRA	Sky13_w4	159	165	299	323	195	201	125	129
GRA	Sky13_w5	165	181	299	323	195	201	125	129
GRA	Sky13_w6	165	181	299	323	195	201	125	129
GRA	Sky13_w7	173	181	289	317	201	203	125	125
GRA	Sky13_w8	159	165	299	323	195	201	125	129
GRA	Sky13_w9	173	181	317	323	201	203	125	125

**** Huachucas field colonies ****

HUAC	Bro01_w1	161	163	311	317	195	195	125	125
HUAC	Bro01_w10	161	163	311	323	195	195	125	125
HUAC	Bro01_w2	163	181	311	323	191	195	125	125
HUAC	Bro01_w3	161	163	311	323	195	195	125	125
HUAC	Bro01_w4	161	163	311	317	191	195	125	125
HUAC	Bro01_w5	161	163	311	317	195	195	125	125
HUAC	Bro01_w6	161	163	311	323	191	195	125	125
HUAC	Bro01_w7	163	181	311	323	195	195	125	125
HUAC	Bro01_w8	161	163	311	323	191	195	125	125
HUAC	Bro01_w9	161	163	311	317	191	195	125	125
HUAC	Bro04_w1	163	175	273	353	191	217	125	139

HUAC Bro04_w10	163	175	317	353	191	215	125	139
HUAC Bro04_w2	163	163	317	317	201	215	125	125
HUAC Bro04_w3	167	175	273	353	191	217	125	139
HUAC Bro04_w4	163	163	273	317	201	215	125	125
HUAC Bro04_w5	163	167	273	317	201	215	125	125
HUAC Bro04_w6	167	175	273	353	191	215	125	139
HUAC Bro04_w7	167	175	273	353	191	215	125	139
HUAC Bro04_w8	167	175	317	353	191	217	125	139
HUAC Bro04_w9	163	163	317	317	201	217	125	125
HUAC Bro05_w1	161	167	327	351	189	205	125	129
HUAC Bro05_w10	161	169	327	351	189	205	125	129
HUAC Bro05_w2	161	169	327	351	189	205	125	129
HUAC Bro05_w3	161	169	327	341	189	205	125	125
HUAC Bro05_w4	161	169	327	351	189	205	125	129
HUAC Bro05_w5	161	169	327	341	189	189	125	129
HUAC Bro05_w6	161	169	327	351	189	205	125	129
HUAC Bro05_w7	161	169	327	351	189	189	125	129
HUAC Bro05_w8	161	169	327	341	189	189	125	125
HUAC Bro05_w9	161	169	327	351	189	189	125	125
HUAC Bro06_w1	161	161	273	293	195	205	125	125
HUAC Bro06_w10	161	173	273	293	195	199	125	125
HUAC Bro06_w2	141	161	273	287	195	205	125	125
HUAC Bro06_w3	141	173	273	287	195	199	125	125
HUAC Bro06_w4	141	173	273	287	195	205	125	125
HUAC Bro06_w5	141	161	273	287	195	205	125	125
HUAC Bro06_w6	161	161	293	295	195	205	125	125
HUAC Bro06_w7	141	173	287	295	195	199	125	125
HUAC Bro06_w8	161	161	273	293	195	205	125	125
HUAC Bro06_w9	141	161	287	295	195	205	125	125
HUAC Bro07_w1	149	161	305	315	193	197	125	125
HUAC Bro07_w10	157	159	305	323	203	205	125	125
HUAC Bro07_w2	149	159	305	323	193	205	125	125
HUAC Bro07_w3	149	159	323	331	203	205	125	125
HUAC Bro07_w4	157	159	323	331	203	205	125	125
HUAC Bro07_w5	157	159	323	331	203	205	125	125
HUAC Bro07_w6	149	159	305	323	193	205	125	125
HUAC Bro07_w7	149	161	315	331	193	197	125	125
HUAC Bro07_w8	157	159	323	331	203	205	125	125
HUAC Bro07_w9	149	159	323	331	193	205	125	125
HUAC Car01_w1	163	173	293	321	197	233	125	125

HUAC Car01_w10	163	173	293	321	193	197	125	125
HUAC Car01_w2	163	173	293	321	193	197	125	125
HUAC Car01_w3	163	173	293	321	197	233	125	125
HUAC Car01_w4	149	165	311	323	189	199	125	125
HUAC Car01_w5	141	163	293	321	193	197	125	125
HUAC Car01_w6	163	173	293	321	193	197	125	125
HUAC Car01_w7	163	173	293	321	193	197	125	125
HUAC Car01_w8	141	163	293	321	197	233	125	125
HUAC Car01_w9	141	163	293	321	193	197	125	125
HUAC Car02_w1	179	195	285	343	197	233	125	125
HUAC Car02_w10	177	177	285	385	193	197	125	125
HUAC Car02_w2	177	177	285	385	193	197	125	125
HUAC Car02_w3	177	195	285	385	193	233	125	125
HUAC Car02_w4	177	195	285	385	189	199	125	125
HUAC Car02_w5	177	195	333	385	193	197	125	125
HUAC Car02_w6	177	195	333	385	193	197	125	125
HUAC Car02_w7	179	195	333	343	193	197	125	125
HUAC Car02_w8	177	177	285	343	197	233	125	125
HUAC Car02_w9	179	195	333	343	193	197	125	125
HUAC Car03_w1	149	161	309	323	203	215	125	125
HUAC Car03_w10	141	179	311	321	197	205	125	125
HUAC Car03_w2	149	161	309	323	203	205	125	125
HUAC Car03_w3	141	161	309	321	203	205	125	125
HUAC Car03_w4	141	179	311	323	197	205	125	125
HUAC Car03_w5	149	179	311	321	197	205	125	125
HUAC Car03_w6	149	161	309	323	203	215	125	125
HUAC Car03_w7	149	179	311	323	197	215	125	125
HUAC Car03_w8	149	161	309	323	203	205	125	125
HUAC Car03_w9	141	179	311	321	197	215	125	125
HUAC Mil01_w1	163	165	289	291	193	231	149	181
HUAC Mil01_w16	163	167	319	345	189	205	125	125
HUAC Mil01_w17	163	167	299	345	191	205	125	125
HUAC Mil01_w18	163	185	319	345	191	205	125	125
HUAC Mil01_w19	163	185	299	345	189	205	125	125
HUAC Mil01_w2	165	195	299	345	173	231	149	149
HUAC Mil01_w20	163	185	299	345	191	205	125	125
HUAC Mil01_w3	149	173	319	345	173	191	149	149
HUAC Mil01_w4	165	195	319	345	203	231	149	151
HUAC Mil01_w5	165	175	273	289	203	223	149	153
HUAC Ram01_w1	135	155	311	341	193	227	125	125

HUAC	Ram01_w10	149	155	311	341	189	193	125	173
HUAC	Ram01_w2	135	155	311	341	189	193	125	125
HUAC	Ram01_w3	135	155	309	311	193	227	125	125
HUAC	Ram01_w4	149	155	309	311	189	193	125	173
HUAC	Ram01_w5	135	155	311	341	193	227	125	173
HUAC	Ram01_w6	149	155	311	341	193	227	125	173
HUAC	Ram01_w7	149	155	309	311	193	227	125	125
HUAC	Ram01_w8	135	155	311	341	189	193	125	173
HUAC	Ram01_w9	135	155	309	311	189	193	125	125
LEM	Mol01_w1	145	157	281	299	189	189	125	153
LEM	Mol01_w10	151	173	273	317	189	195	151	153
LEM	Mol01_w2	147	157	275	297	189	217	149	189
LEM	Mol01_w3	147	157	281	299	189	189	125	153
LEM	Mol01_w4	151	173	273	317	189	195	151	153
LEM	Mol01_w5	145	165	299	299	189	219	127	153
LEM	Mol01_w6	151	173	281	317	189	195	151	153
LEM	Mol01_w7	173	179	273	317	189	195	151	153
LEM	Mol01_w8	173	179	273	317	189	195	151	153
LEM	Mol01_w9	147	165	285	299	189	219	127	153
LEM	Mol02_w1	161	185	295	309	189	195	151	211
LEM	Mol02_w10	145	179	287	301	195	215	149	187
LEM	Mol02_w12	145	179	287	301	189	215	149	187
LEM	Mol02_w14	149	179	301	303	195	215	149	187
LEM	Mol02_w17	145	179	301	303	195	215	149	187
LEM	Mol02_w18	149	179	287	301	195	215	149	187
LEM	Mol02_w2	161	185	295	309	195	231	151	211
LEM	Mol02_w20	143	143	281	309	189	215	185	211
LEM	Mol02_w3	143	143	281	291	189	215	149	185
LEM	Mol02_w8	143	147	285	287	213	229	151	151
LEM	Mol03_w1	147	203	273	291	189	215	149	197
LEM	Mol03_w10	147	203	273	291	189	215	149	149
LEM	Mol03_w2	143	153	273	287	189	189	203	205
LEM	Mol03_w3	143	153	273	287	189	189	203	205
LEM	Mol03_w4	147	153	273	291	189	215	149	149
LEM	Mol03_w5	143	153	273	287	189	189	m	m
LEM	Mol03_w6	143	203	273	287	189	189	203	205
LEM	Mol03_w7	143	153	273	287	189	189	197	203
LEM	Mol03_w8	143	153	273	287	189	189	203	205
LEM	Mol03_w9	143	203	273	287	189	189	203	205
LEM	Mol04_w1	155	165	281	285	195	195	151	153

LEM	Mol04_w10	155	165	281	287	195	231	151	151
LEM	Mol04_w2	151	165	281	287	195	231	151	153
LEM	Mol04_w3	151	165	281	287	195	195	151	151
LEM	Mol04_w4	151	167	287	333	189	195	151	151
LEM	Mol04_w5	155	165	281	285	195	231	151	153
LEM	Mol04_w6	151	165	281	287	195	231	151	153
LEM	Mol04_w7	155	165	281	285	195	195	151	153
LEM	Mol04_w8	155	165	281	287	195	231	151	151
LEM	Mol04_w9	155	165	281	285	195	231	151	153
LEM	Mol05_w1	147	165	271	295	221	245	197	203
LEM	Mol05_w10	149	173	267	301	195	229	149	149
LEM	Mol05_w2	147	147	271	273	189	195	149	149
LEM	Mol05_w3	147	147	271	273	189	195	149	149
LEM	Mol05_w4	147	165	271	291	189	221	197	203
LEM	Mol05_w5	147	165	271	295	189	221	149	203
LEM	Mol05_w6	147	165	271	295	189	221	197	203
LEM	Mol05_w7	147	165	271	291	221	245	197	203
LEM	Mol05_w8	147	165	271	295	221	245	197	203
LEM	Mol05_w9	147	165	271	291	221	245	197	203
LEM	Mol06_w1	143	185	281	309	189	215	185	211
LEM	Mol06_w10	149	153	291	303	189	189	149	187
LEM	Mol06_w2	161	179	279	295	189	203	149	151
LEM	Mol06_w3	145	153	291	303	189	189	149	153
LEM	Mol06_w4	149	153	287	291	189	195	149	187
LEM	Mol06_w5	143	147	285	287	213	229	151	151
LEM	Mol06_w6	147	155	285	297	229	229	151	151
LEM	Mol06_w7	147	155	285	287	213	229	151	151
LEM	Mol06_w8	149	153	287	291	189	195	149	153
LEM	Mol06_w9	145	153	287	291	189	195	149	153
LEM	Mol08_w1	145	157	273	287	209	217	149	153
LEM	Mol08_w10	145	157	273	291	209	217	149	195
LEM	Mol08_w2	147	157	273	287	209	217	149	153
LEM	Mol08_w3	145	157	273	291	189	217	149	153
LEM	Mol08_w4	147	157	273	287	189	217	149	153
LEM	Mol08_w5	147	157	273	291	189	217	149	153
LEM	Mol08_w6	147	157	273	287	189	217	149	195
LEM	Mol08_w7	145	157	273	287	209	217	149	195
LEM	Mol08_w8	145	157	273	291	189	217	149	153
LEM	Mol08_w9	145	157	273	291	189	217	149	153
LEM	Mol10_w1	155	165	291	301	193	237	203	207

LEM	Mol10_w10	155	165	291	301	189	193	203	207
LEM	Mol10_w2	149	165	287	291	189	193	149	203
LEM	Mol10_w3	149	165	291	301	189	193	149	203
LEM	Mol10_w4	149	165	291	301	189	193	203	207
LEM	Mol10_w5	155	165	291	301	193	237	149	203
LEM	Mol10_w6	155	165	291	301	193	237	203	207
LEM	Mol10_w7	145	155	287	293	191	215	151	151
LEM	Mol10_w8	149	165	291	301	189	193	203	207
LEM	Mol10_w9	155	165	291	301	193	237	203	207
LEM	Mol11_w1	127	147	245	311	193	195	153	203
LEM	Mol11_w10	153	161	287	311	229	229	153	153
LEM	Mol11_w2	147	161	245	305	195	229	171	203
LEM	Mol11_w3	147	161	245	305	195	229	153	203
LEM	Mol11_w4	127	153	287	305	193	229	153	153
LEM	Mol11_w5	127	147	245	311	195	229	171	203
LEM	Mol11_w6	153	161	287	311	229	229	171	171
LEM	Mol11_w7	153	161	287	311	193	229	153	153
LEM	Mol11_w8	127	147	245	305	195	229	171	203
LEM	Mol11_w9	147	161	245	305	193	195	171	203
LEM	Syc03_w1	151	153	291	301	195	195	149	197
LEM	Syc03_w10	153	157	291	291	195	195	149	149
LEM	Syc03_w2	151	153	291	301	195	195	149	197
LEM	Syc03_w3	153	157	291	291	195	195	149	197
LEM	Syc03_w4	151	153	291	301	195	195	149	149
LEM	Syc03_w5	151	153	291	301	195	195	149	149
LEM	Syc03_w6	153	157	291	301	195	195	149	197
LEM	Syc03_w7	151	153	291	291	195	195	149	197
LEM	Syc03_w8	151	157	291	301	195	195	149	197
LEM	Syc03_w9	153	157	291	301	195	195	149	149

**** Mt. Ord field colonies ****

ORD	Ord01_w1	177	203	265	351	187	191	181	181
ORD	Ord01_w10	177	177	265	311	187	205	149	181
ORD	Ord01_w2	159	203	265	351	187	191	181	181
ORD	Ord01_w3	159	203	265	351	187	191	181	181
ORD	Ord01_w4	159	203	265	351	187	187	215	215
ORD	Ord01_w5	159	203	265	351	187	187	215	215
ORD	Ord01_w6	177	203	265	351	187	187	181	181
ORD	Ord01_w7	177	203	265	351	187	191	181	181
ORD	Ord01_w8	159	179	265	311	187	205	149	181

ORD	Ord02_w1	135	173	287	313	183	189	149	149
ORD	Ord02_w10	135	173	253	313	189	189	149	149
ORD	Ord02_w2	135	173	287	313	183	189	149	149
ORD	Ord02_w3	135	173	253	313	183	189	149	149
ORD	Ord02_w4	135	173	253	313	189	189	149	149
ORD	Ord02_w5	155	169	333	375	175	189	149	151
ORD	Ord02_w6	173	173	253	313	183	189	149	149
ORD	Ord02_w7	135	173	253	313	189	189	149	149
ORD	Ord02_w8	135	173	253	313	183	189	149	149
ORD	Ord03_w1	135	165	285	309	179	183	151	153
ORD	Ord03_w10	157	165	285	309	179	183	151	153
ORD	Ord03_w2	157	195	273	283	187	195	149	151
ORD	Ord03_w3	157	195	273	283	187	195	149	151
ORD	Ord03_w4	135	195	283	285	187	195	149	151
ORD	Ord03_w5	157	195	283	285	179	187	149	151
ORD	Ord03_w6	135	195	273	283	179	187	149	151
ORD	Ord03_w7	157	195	283	285	179	187	149	151
ORD	Ord03_w8	157	165	273	309	179	183	151	153
ORD	Ord03_w9	157	195	283	285	187	195	149	151
ORD	Ord04_w1	177	177	281	309	195	195	149	151
ORD	Ord04_w10	177	205	291	309	195	195	149	151
ORD	Ord04_w2	177	177	291	309	195	215	149	151
ORD	Ord04_w3	177	205	291	309	195	195	151	151
ORD	Ord04_w4	177	205	291	309	195	195	149	151
ORD	Ord04_w5	177	205	281	309	195	215	151	151
ORD	Ord04_w6	159	205	281	307	181	215	151	151
ORD	Ord04_w7	177	177	281	309	195	215	149	151
ORD	Ord04_w8	159	205	281	307	181	215	151	151
ORD	Ord04_w9	177	177	281	309	195	195	149	151
ORD	Ord05_w1	167	179	253	287	183	215	153	153
ORD	Ord05_w10	167	179	253	287	183	215	153	157
ORD	Ord05_w2	147	179	253	309	183	183	133	153
ORD	Ord05_w3	147	179	287	309	183	183	133	153
ORD	Ord05_w4	145	169	263	291	191	205	137	151
ORD	Ord05_w5	167	173	253	287	183	215	153	153
ORD	Ord05_w6	167	179	287	287	183	215	153	153
ORD	Ord05_w7	147	173	287	309	183	183	133	153
ORD	Ord05_w8	147	173	253	309	183	183	133	157
ORD	Ord05_w9	147	179	253	309	183	183	133	157
ORD	Ord06_w1	173	173	287	329	179	189	149	149

ORD	Ord06_w10	173	185	287	329	187	193	149	151
ORD	Ord06_w2	173	173	277	329	179	187	149	149
ORD	Ord06_w3	173	185	277	329	179	187	149	151
ORD	Ord06_w4	173	185	287	329	179	187	149	149
ORD	Ord06_w5	173	179	277	293	187	187	149	151
ORD	Ord06_w6	179	185	277	293	187	187	151	151
ORD	Ord06_w7	185	173	287	329	179	187	149	149
ORD	Ord06_w8	173	185	287	329	179	189	149	151
ORD	Ord06_w9	173	185	287	329	179	187	149	149
ORD	Ord07_w1	163	177	277	373	183	185	151	151
ORD	Ord07_w10	163	177	277	373	183	185	149	151
ORD	Ord07_w2	163	177	277	373	185	195	149	151
ORD	Ord07_w3	163	177	295	373	185	195	151	151
ORD	Ord07_w4	163	177	277	373	183	185	151	151
ORD	Ord07_w5	167	181	263	277	183	187	149	149
ORD	Ord07_w6	177	181	295	373	183	185	151	151
ORD	Ord07_w7	163	177	295	373	183	185	151	151
ORD	Ord07_w8	177	181	277	373	183	185	151	151
ORD	Ord07_w9	167	181	263	277	185	195	149	149
ORD	Ord08_w1	173	189	269	271	187	193	149	151
ORD	Ord08_w10	173	189	269	271	187	193	139	151
ORD	Ord08_w2	173	189	269	271	187	193	139	151
ORD	Ord08_w3	173	173	269	271	187	193	149	151
ORD	Ord08_w4	173	189	269	299	187	193	149	151
ORD	Ord08_w5	173	189	269	271	193	219	149	151
ORD	Ord08_w6	173	173	269	299	193	219	149	151
ORD	Ord08_w7	173	173	269	271	187	193	139	151
ORD	Ord08_w8	173	189	269	271	187	193	149	151
ORD	Ord08_w9	173	173	269	299	187	193	139	151

**** Patagonia field colonies ****

PAT	Pat01_w1	157	171	265	311	191	199	125	125
PAT	Pat01_w10	157	171	265	311	191	233	125	125
PAT	Pat01_w2	157	171	265	283	191	233	125	125
PAT	Pat01_w3	157	171	261	311	233	235	125	125
PAT	Pat01_w4	141	157	265	283	191	199	125	125
PAT	Pat01_w5	157	171	265	283	191	199	125	159
PAT	Pat01_w6	157	171	261	283	199	235	125	159
PAT	Pat01_w7	141	157	261	311	233	235	125	159
PAT	Pat01_w8	157	171	265	311	191	199	125	159
PAT	Pat01_w9	157	171	261	311	199	235	125	125

PAT	Pat06_w1	167	179	265	327	191	191	125	127
PAT	Pat06_w10	167	179	263	265	191	191	125	127
PAT	Pat06_w2	167	179	263	265	191	191	125	125
PAT	Pat06_w3	163	179	263	265	191	191	125	125
PAT	Pat06_w4	163	179	263	265	191	191	125	127
PAT	Pat06_w5	167	179	263	265	191	191	125	125
PAT	Pat06_w6	163	179	265	327	191	191	125	125
PAT	Pat06_w7	163	179	265	327	191	191	125	127
PAT	Pat06_w8	163	179	263	265	191	191	125	127
PAT	Pat06_w9	163	179	265	327	191	191	125	125
PAT	Pat07_w1	163	201	265	291	193	199	125	125
PAT	Pat07_w2	163	201	265	291	193	199	125	125
PAT	Pat07_w3	163	195	265	291	199	225	125	125
PAT	Pat07_w4	169	201	287	287	189	225	125	127
PAT	Pat07_w5	163	195	265	287	199	225	125	125
PAT	Pat07_w6	169	201	287	287	189	193	125	125
PAT	Pat07_w7	163	201	265	291	193	199	125	127
PAT	Pat07_w8	163	201	265	291	199	225	125	127
PAT	Pat07_w9	163	195	265	291	193	199	125	125
PAT	Pat08_w1	149	149	265	285	239	249	125	125
PAT	Pat08_w10	149	149	265	285	233	249	125	125
PAT	Pat08_w2	145	145	265	285	191	239	127	127
PAT	Pat08_w3	149	177	265	285	233	249	125	125
PAT	Pat08_w4	149	177	265	277	239	249	125	127
PAT	Pat08_w5	149	149	265	277	233	249	125	127
PAT	Pat08_w6	149	177	265	277	233	249	125	125
PAT	Pat08_w7	149	177	265	277	233	249	125	127
PAT	Pat08_w8	145	177	265	285	191	239	125	127
PAT	Pat08_w9	149	149	265	285	233	249	125	125
PAT	Pat09_w1	143	167	305	311	193	195	125	127
PAT	Pat09_w10	143	167	275	311	191	195	125	127
PAT	Pat09_w2	143	167	305	311	193	195	127	127
PAT	Pat09_w3	153	175	269	275	191	195	125	125
PAT	Pat09_w4	151	153	275	277	193	203	125	127
PAT	Pat09_w5	143	167	305	311	193	195	125	127
PAT	Pat09_w6	151	153	275	277	191	203	125	125
PAT	Pat09_w7	143	151	275	277	193	203	125	125
PAT	Pat09_w8	143	151	275	277	193	203	125	127
PAT	Pat09_w9	153	167	305	311	191	195	127	127

PAT	Pat11_w1	145	149	281	391	189	255	125	127
PAT	Pat11_w10	145	173	265	281	193	255	125	127
PAT	Pat11_w2	145	149	281	391	189	189	125	127
PAT	Pat11_w3	149	195	281	391	189	189	125	127
PAT	Pat11_w4	149	195	391	391	189	189	125	127
PAT	Pat11_w5	173	195	265	281	193	255	125	127
PAT	Pat11_w6	173	195	265	391	193	193	125	127
PAT	Pat11_w7	173	195	265	391	193	255	125	127
PAT	Pat11_w8	149	195	281	391	189	255	125	127
PAT	Pat11_w9	145	173	265	281	193	193	125	127
PAT	Pat12_w1	147	165	265	265	193	193	125	127
PAT	Pat12_w10	159	165	265	265	193	251	125	125
PAT	Pat12_w2	147	171	265	265	189	193	125	127
PAT	Pat12_w3	159	171	265	265	189	193	125	127
PAT	Pat12_w4	147	171	265	265	189	193	127	127
PAT	Pat12_w5	159	165	265	265	189	193	125	125
PAT	Pat12_w6	147	171	265	265	189	193	127	127
PAT	Pat12_w7	147	165	265	265	193	251	125	127
PAT	Pat12_w8	159	165	265	265	189	193	125	125
PAT	Pat12_w9	147	171	265	265	193	251	125	127
PAT	Pat13_w1	149	177	273	315	191	237	125	127
PAT	Pat13_w10	149	169	283	315	191	263	125	127
PAT	Pat13_w2	167	169	283	315	191	263	127	127
PAT	Pat13_w3	149	177	273	315	191	237	127	127
PAT	Pat13_w4	167	177	273	315	237	263	125	127
PAT	Pat13_w5	149	177	273	273	191	237	127	127
PAT	Pat13_w6	167	177	273	273	237	263	125	127
PAT	Pat13_w7	167	169	283	315	191	191	125	127
PAT	Pat13_w8	149	169	283	315	191	263	125	127
PAT	Pat13_w9	167	177	273	315	191	237	127	127

**** Pinal Peak field colonies ****

PIN	Pin03_w1	175	183	289	289	187	229	149	165
PIN	Pin03_w10	175	183	289	289	187	229	149	165
PIN	Pin03_w2	147	183	289	289	173	229	149	165
PIN	Pin03_w3	147	183	289	289	187	229	149	165
PIN	Pin03_w4	169	175	281	289	173	193	149	153
PIN	Pin03_w5	147	183	289	289	187	229	149	165
PIN	Pin03_w6	175	183	289	289	187	229	149	165
PIN	Pin03_w7	147	175	281	289	173	193	149	153
PIN	Pin03_w8	147	183	289	289	187	193	149	165

PIN	Pin03_w9	147	183	289	289	187	229	149	165
PIN	Pin04_w1	133	153	287	291	195	207	151	153
PIN	Pin04_w10	133	163	285	287	195	207	151	165
PIN	Pin04_w2	133	153	287	291	207	219	151	153
PIN	Pin04_w3	153	165	287	291	195	207	151	153
PIN	Pin04_w4	133	163	285	287	207	219	151	165
PIN	Pin04_w5	163	165	m	m	207	219	151	165
PIN	Pin04_w6	133	153	287	291	207	219	151	153
PIN	Pin04_w7	163	165	287	287	207	219	151	165
PIN	Pin04_w8	133	153	287	291	195	207	151	153
PIN	Pin04_w9	153	165	287	291	195	207	151	153
PIN	Pin06_w1	149	149	293	293	195	213	149	149
PIN	Pin06_w10	149	149	293	293	195	213	149	151
PIN	Pin06_w2	149	149	293	293	195	213	149	153
PIN	Pin06_w3	149	161	261	281	189	205	149	153
PIN	Pin06_w4	145	149	293	293	195	213	149	153
PIN	Pin06_w5	149	149	281	293	195	205	149	151
PIN	Pin06_w6	145	149	293	293	195	205	149	151
PIN	Pin06_w7	149	149	293	293	195	205	149	151
PIN	Pin06_w8	145	149	293	293	195	213	149	151
PIN	Pin06_w9	145	161	261	281	189	205	153	153
PIN	Pin07_w1	145	203	289	293	195	231	151	151
PIN	Pin07_w10	147	147	269	291	193	209	151	151
PIN	Pin07_w2	147	147	291	291	193	209	151	151
PIN	Pin07_w3	147	161	269	291	195	209	151	151
PIN	Pin07_w4	147	195	269	291	193	209	149	149
PIN	Pin07_w5	145	203	269	293	195	199	151	151
PIN	Pin07_w6	147	147	269	291	195	209	149	149
PIN	Pin07_w7	145	203	269	293	193	231	149	149
PIN	Pin07_w9	147	195	291	291	195	209	151	151
PIN	Pin08_w1	143	143	287	321	205	245	149	149
PIN	Pin08_w10	143	173	287	321	205	245	149	193
PIN	Pin08_w2	143	173	287	321	197	245	189	193
PIN	Pin08_w3	143	143	267	321	197	245	189	193
PIN	Pin08_w4	143	173	267	321	197	245	149	149
PIN	Pin08_w5	143	173	287	321	205	245	189	193
PIN	Pin08_w6	143	173	287	321	197	245	189	193
PIN	Pin08_w7	143	143	287	321	205	245	149	193
PIN	Pin08_w8	143	143	267	321	205	245	189	193
PIN	Pin08_w9	143	173	267	321	197	245	149	193

PIN	Pin09_w1	147	161	291	303	231	245	149	151
PIN	Pin09_w10	161	171	275	291	235	245	149	149
PIN	Pin09_w2	161	171	275	291	231	245	149	149
PIN	Pin09_w3	161	171	291	303	231	245	149	149
PIN	Pin09_w4	147	161	275	291	235	245	149	149
PIN	Pin09_w5	161	171	275	291	235	245	149	149
PIN	Pin09_w6	161	171	275	291	231	245	149	149
PIN	Pin09_w7	147	161	275	291	235	245	149	151
PIN	Pin09_w8	147	161	275	291	231	245	149	149
PIN	Pin09_w9	147	189	275	287	203	231	151	151
PIN	Pin11_w1	143	161	291	291	189	197	137	165
PIN	Pin11_w10	141	161	289	295	189	223	157	165
PIN	Pin11_w2	141	161	289	295	189	223	157	165
PIN	Pin11_w3	141	163	291	295	193	223	157	165
PIN	Pin11_w4	141	163	291	295	193	223	157	165
PIN	Pin11_w5	141	163	291	295	185	191	157	165
PIN	Pin11_w6	143	163	291	291	193	197	137	165
PIN	Pin11_w7	141	163	289	295	193	223	157	165
PIN	Pin11_w8	141	161	291	295	189	223	157	165
PIN	Pin11_w9	141	161	291	295	189	223	153	157
PIN	Pin12_w1	143	147	291	291	173	209	149	171
PIN	Pin12_w10	143	209	291	291	173	209	149	171
PIN	Pin12_w2	147	209	281	291	203	235	149	155
PIN	Pin12_w3	143	147	291	291	173	203	149	171
PIN	Pin12_w4	147	147	281	291	209	235	149	155
PIN	Pin12_w5	143	209	291	291	173	209	149	171
PIN	Pin12_w6	143	147	291	291	173	203	149	171
PIN	Pin12_w7	147	209	281	291	209	235	149	155
PIN	Pin12_w8	147	147	281	291	209	235	149	155
PIN	Pin12_w9	143	147	291	291	173	209	149	171
PIN	Pin13_w1	165	173	273	289	195	213	125	151
PIN	Pin13_w10	165	169	273	273	209	213	125	151
PIN	Pin13_w2	173	183	289	289	189	195	149	151
PIN	Pin13_w3	171	183	289	289	189	209	149	151
PIN	Pin13_w4	171	183	289	289	189	195	151	151
PIN	Pin13_w5	165	171	273	273	195	213	125	149
PIN	Pin13_w6	171	183	289	289	189	195	151	151
PIN	Pin13_w7	171	183	289	289	189	209	149	151
PIN	Pin13_w8	163	165	273	273	195	213	125	151
PIN	Pin13_w9	165	169	273	273	209	213	125	151

PIN	Pin14_w1	149	177	289	291	195	257	125	149
PIN	Pin14_w10	149	177	277	289	193	195	125	149
PIN	Pin14_w2	149	177	289	291	195	257	125	157
PIN	Pin14_w3	149	159	277	277	193	243	153	157
PIN	Pin14_w4	149	159	277	291	193	243	153	157
PIN	Pin14_w5	149	159	277	277	241	257	149	153
PIN	Pin14_w6	149	159	277	291	193	243	149	153
PIN	Pin14_w7	149	177	289	291	193	195	125	149
PIN	Pin14_w8	149	177	289	291	193	195	125	149
PIN	Pin14_w9	149	177	289	291	195	257	125	157

**** Santa Ritas field colonies ****

SAN	Hop03_w1	145	199	263	291	191	255	125	125
SAN	Hop03_w10	163	177	m	m	193	197	125	125
SAN	Hop03_w2	145	163	291	291	197	255	125	125
SAN	Hop03_w3	145	163	263	291	197	255	125	125
SAN	Hop03_w4	145	163	291	291	191	255	125	125
SAN	Hop03_w5	145	163	263	291	197	255	125	125
SAN	Hop03_w6	177	199	263	263	193	197	125	125
SAN	Hop03_w7	145	199	263	291	197	255	125	125
SAN	Hop03_w8	145	199	263	291	197	255	125	125
SAN	Hop03_w9	145	163	263	291	197	255	125	125
SAN	Hop04_w1	131	147	265	293	189	213	127	127
SAN	Hop04_w10	131	147	265	293	189	213	127	127
SAN	Hop04_w2	131	147	265	293	195	213	127	127
SAN	Hop04_w3	147	183	265	291	189	213	127	127
SAN	Hop04_w4	131	147	265	291	189	213	127	127
SAN	Hop04_w5	147	183	265	293	189	213	127	127
SAN	Hop04_w6	147	183	265	293	195	213	127	127
SAN	Hop04_w7	131	147	265	291	189	213	127	127
SAN	Hop04_w8	131	147	265	293	189	213	127	127
SAN	Hop04_w9	147	183	265	293	189	213	127	127
SAN	Hop05_w1	143	203	265	291	195	255	125	151
SAN	Hop05_w10	143	145	265	291	195	211	125	151
SAN	Hop05_w2	143	203	265	291	195	211	125	151
SAN	Hop05_w3	143	145	265	291	195	211	125	151
SAN	Hop05_w4	143	203	265	291	195	255	125	151
SAN	Hop05_w5	143	145	265	291	195	211	125	125
SAN	Hop05_w6	143	203	265	291	195	211	125	151
SAN	Hop05_w7	143	203	265	291	195	211	125	151

SAN	Hop05_w8	141	145	265	315	211	213	125	127
SAN	Hop05_w9	141	203	265	315	213	255	125	127
SAN	Hop06_w1	131	135	309	335	189	189	169	171
SAN	Hop06_w10	131	135	309	335	189	189	169	171
SAN	Hop06_w2	131	131	309	335	189	189	169	171
SAN	Hop06_w3	131	135	309	333	189	189	171	175
SAN	Hop06_w4	131	135	309	333	189	189	169	171
SAN	Hop06_w5	129	135	307	335	187	189	169	169
SAN	Hop06_w6	131	135	309	335	189	189	169	171
SAN	Hop06_w7	131	131	309	333	189	189	171	175
SAN	Hop06_w8	131	135	309	333	189	189	171	175
SAN	Hop06_w9	131	135	309	333	189	189	169	171
SAN	Hop07_w1	135	147	313	337	189	189	163	169
SAN	Hop07_w10	135	147	313	337	189	189	169	171
SAN	Hop07_w2	129	135	315	337	189	189	163	169
SAN	Hop07_w3	135	147	315	337	189	189	169	171
SAN	Hop07_w4	129	135	315	337	189	189	169	171
SAN	Hop07_w5	129	135	315	337	189	189	169	171
SAN	Hop07_w6	129	135	313	337	189	189	169	171
SAN	Hop07_w7	135	147	315	337	189	189	163	169
SAN	Hop07_w8	129	135	315	337	189	189	163	169
SAN	Hop07_w9	129	135	313	337	189	189	163	169
SAN	Hop08_w1	129	145	265	321	189	243	125	171
SAN	Hop08_w10	129	145	265	321	189	243	125	169
SAN	Hop08_w2	129	145	265	321	189	238	125	171
SAN	Hop08_w3	129	145	265	321	189	238	125	171
SAN	Hop08_w4	129	145	265	321	189	238	125	171
SAN	Hop08_w5	129	145	265	321	189	238	125	171
SAN	Hop08_w6	129	145	265	321	189	238	125	169
SAN	Hop08_w7	129	145	265	321	189	238	125	169
SAN	Hop08_w8	129	145	265	321	189	238	125	169
SAN	Hop08_w9	129	145	265	321	189	238	125	171
SAN	Hop09_w1	133	137	307	329	187	189	169	173
SAN	Hop09_w10	133	137	307	329	187	189	169	173
SAN	Hop09_w2	133	147	307	327	187	189	161	169
SAN	Hop09_w3	133	137	307	329	189	191	161	169
SAN	Hop09_w4	133	137	307	329	189	191	169	173
SAN	Hop09_w5	133	147	307	323	189	191	161	169
SAN	Hop09_w6	133	147	307	323	187	189	169	173
SAN	Hop09_w7	133	137	307	329	189	191	169	173

SAN	Hop09_w8	133	137	307	323	187	189	169	173
SAN	Hop09_w9	133	137	307	323	189	191	169	173
SAN	Hop11_w1	129	161	279	311	189	211	127	163
SAN	Hop11_w10	129	171	279	311	189	193	127	163
SAN	Hop11_w2	127	171	293	345	189	211	127	171
SAN	Hop11_w3	129	161	293	311	189	211	127	163
SAN	Hop11_w4	127	161	279	345	189	193	127	171
SAN	Hop11_w5	127	171	293	345	189	211	127	171
SAN	Hop11_w6	127	171	279	345	189	211	127	171
SAN	Hop11_w7	127	161	293	345	189	211	127	171
SAN	Hop11_w8	129	171	279	311	189	193	127	163
SAN	Hop11_w9	129	171	293	311	189	211	127	163
SAN	Mon01_w1	145	159	281	361	219	229	125	125
SAN	Mon01_w10	145	159	281	361	219	229	125	125
SAN	Mon01_w2	145	159	281	291	189	219	125	125
SAN	Mon01_w3	145	159	281	291	189	219	125	125
SAN	Mon01_w4	141	159	281	361	219	229	125	125
SAN	Mon01_w5	145	159	281	361	219	229	125	125
SAN	Mon01_w6	145	159	281	291	189	219	125	125
SAN	Mon01_w7	141	159	281	361	219	229	125	125
SAN	Mon01_w8	141	159	281	361	189	219	125	125
SAN	Mon01_w9	145	159	281	291	219	229	125	125
**** Sedona field colonies ****									
SED	Sch01_w1	179	195	289	295	175	195	137	137
SED	Sch01_w10	173	177	267	299	173	175	151	197
SED	Sch01_w11	173	177	267	267	173	175	151	151
SED	Sch01_w12	171	177	m	m	173	175	151	151
SED	Sch01_w13	173	177	267	267	173	175	151	151
SED	Sch01_w14	171	171	m	m	195	213	127	151
SED	Sch01_w15	171	171	m	m	195	213	151	151
SED	Sch01_w16	171	171	m	m	185	213	151	151
SED	Sch01_w17	171	171	m	m	195	213	151	151
SED	Sch01_w18	173	177	m	m	173	175	151	151
SED	Sch01_w19	173	177	267	267	173	175	151	151
SED	Sch01_w2	171	177	295	299	173	175	151	197
SED	Sch01_w20	171	177	267	267	173	175	151	151
SED	Sch01_w3	171	195	283	291	195	213	151	151
SED	Sch01_w4	171	177	295	299	173	175	151	197
SED	Sch01_w5	171	195	283	291	195	213	151	151
SED	Sch01_w6	173	177	267	299	173	175	151	193
SED	Sch01_w7	171	177	295	299	173	175	151	193

SED	Sch01_w8	171	177	295	299	173	175	151	197
SED	Sch01_w9	171	177	267	299	173	175	151	193
SED	Sch02_w11	147	185	255	259	191	195	177	177
SED	Sch02_w12	169	173	289	293	195	199	139	177
SED	Sch02_w14	167	173	289	293	195	199	139	177
SED	Sch02_w16	167	173	289	293	195	199	177	177
SED	Sch02_w19	147	165	255	259	183	191	177	189
SED	Sch02_w2	167	173	289	295	195	199	177	221
SED	Sch02_w5	169	173	289	295	195	199	177	221
SED	Sch02_w7	167	173	289	295	195	199	177	221
SED	Sch02_w8	147	185	255	257	191	195	177	189
SED	Sch02_w9	169	173	289	295	195	199	139	177
SED	Sch03_w1	171	187	261	295	177	185	151	189
SED	Sch03_w10	171	187	261	293	185	191	151	189
SED	Sch03_w2	171	171	261	295	185	191	151	189
SED	Sch03_w3	171	171	261	293	177	185	151	189
SED	Sch03_w4	171	187	261	293	177	185	151	189
SED	Sch03_w5	171	171	261	295	185	191	151	189
SED	Sch03_w6	171	171	261	293	185	191	151	189
SED	Sch03_w7	171	171	261	293	177	185	151	189
SED	Sch03_w8	183	187	281	293	191	191	137	151
SED	Sch03_w9	171	187	261	295	185	191	151	189
SED	Sch07_w1	175	187	277	289	171	175	137	151
SED	Sch07_w10	173	175	279	289	199	199	151	229
SED	Sch07_w2	173	175	265	289	199	199	151	229
SED	Sch07_w3	147	177	265	289	185	195	151	151
SED	Sch07_w4	175	187	277	289	175	177	137	151
SED	Sch07_w5	175	187	277	301	171	175	137	151
SED	Sch07_w6	147	167	265	289	185	195	151	151
SED	Sch07_w7	167	199	289	293	185	189	151	179
SED	Sch07_w8	175	187	277	289	175	177	137	151
SED	Sch07_w9	175	187	277	301	171	175	137	151
SED	Sch08_w1	173	173	293	295	183	197	137	151
SED	Sch08_w10	173	173	281	293	183	197	137	151
SED	Sch08_w2	175	191	263	295	183	199	151	157
SED	Sch08_w3	173	173	293	295	183	197	137	151
SED	Sch08_w4	173	173	281	293	177	197	137	151
SED	Sch08_w5	173	191	281	293	183	197	137	151
SED	Sch08_w6	173	191	281	293	183	197	137	151
SED	Sch08_w7	173	173	293	295	183	197	137	151

SED	Sch08_w8	173	191	293	295	183	197	137	151
SED	Sch08_w9	173	191	281	293	177	197	137	151
SED	Sch09_w1	167	181	279	289	173	175	151	183
SED	Sch09_w10	167	181	279	289	175	199	151	183
SED	Sch09_w2	167	175	279	289	175	199	151	183
SED	Sch09_w3	167	175	279	289	175	199	183	195
SED	Sch09_w4	167	175	279	289	175	199	151	183
SED	Sch09_w5	175	175	279	289	191	199	151	185
SED	Sch09_w6	167	175	279	289	173	175	151	183
SED	Sch09_w7	181	181	279	289	191	199	183	195
SED	Sch09_w8	167	181	279	289	173	175	183	195
SED	Sch09_w9	167	181	279	289	175	199	183	195
SED	Sch11_w1	171	173	261	283	185	189	127	127
SED	Sch11_w10	173	173	283	293	185	189	127	127
SED	Sch11_w2	171	173	283	293	189	199	127	127
SED	Sch11_w3	171	173	261	283	189	199	127	127
SED	Sch11_w4	171	191	281	293	171	199	127	225
SED	Sch11_w5	171	173	283	293	189	199	127	127
SED	Sch11_w6	173	173	283	293	185	189	127	127
SED	Sch11_w7	191	191	261	281	171	185	137	137
SED	Sch11_w8	171	173	261	283	189	199	127	127
SED	Sch11_w9	173	173	283	293	189	199	127	127
SED	Sch29_w1	171	181	279	289	177	185	149	229
SED	Sch29_w10	171	185	279	289	177	185	149	229
SED	Sch29_w2	171	185	279	289	177	185	149	229
SED	Sch29_w3	171	185	279	295	177	185	149	229
SED	Sch29_w4	171	185	279	289	177	185	149	229
SED	Sch29_w5	171	189	279	295	175	177	149	229
SED	Sch29_w6	171	189	279	289	175	177	149	229
SED	Sch29_w7	171	181	279	289	177	185	137	149
SED	Sch29_w8	153	169	255	295	185	199	151	151
SED	Sch29_w9	171	189	279	289	177	185	149	229
SED	Sed01_w1	153	169	281	281	175	181	127	231
SED	Sed01_w10	173	193	279	279	189	199	151	163
SED	Sed01_w2	153	169	281	301	171	181	127	231
SED	Sed01_w3	153	169	281	301	175	181	137	231
SED	Sed01_w4	183	187	279	281	171	181	137	151
SED	Sed01_w5	193	193	279	279	189	199	151	163
SED	Sed01_w6	193	193	279	279	189	199	151	163
SED	Sed01_w7	183	187	279	281	175	181	137	151

SED	Sed01_w8	193	193	279	279	189	199	151	163
SED	Sed01_w9	153	183	281	281	171	181	137	231
SED	Sed02_w1	163	169	281	289	195	199	151	221
SED	Sed02_w10	173	195	277	281	195	199	151	185
SED	Sed02_w2	169	195	277	281	173	195	151	185
SED	Sed02_w3	163	173	281	281	173	195	137	221
SED	Sed02_w4	169	195	277	281	195	199	151	185
SED	Sed02_w5	163	173	281	301	171	173	137	151
SED	Sed02_w6	173	195	277	281	195	199	137	185
SED	Sed02_w7	163	173	281	281	195	199	151	221
SED	Sed02_w8	169	195	277	289	195	199	151	185
SED	Sed02_w9	163	169	281	289	195	199	151	221
SHO	Mor01_w1	141	161	291	351	203	203	125	133
SHO	Mor01_w10	141	161	291	351	199	203	125	133
SHO	Mor01_w2	141	161	283	351	203	203	125	125
SHO	Mor01_w3	155	161	283	351	199	203	125	133
SHO	Mor01_w4	141	161	291	351	203	203	125	125
SHO	Mor01_w5	141	161	291	351	199	203	125	125
SHO	Mor01_w6	141	161	291	351	199	203	125	133
SHO	Mor01_w7	155	161	291	351	203	203	125	125
SHO	Mor01_w8	141	161	283	351	199	203	125	125
SHO	Mor01_w9	141	161	283	351	199	203	125	133
SHO	Mor02_w1.1	161	165	283	351	187	209	125	125
SHO	Mor02_w10	161	165	283	351	187	209	125	133
SHO	Mor02_w2	161	165	283	351	187	203	125	133
SHO	Mor02_w3	161	165	283	351	187	209	125	133
SHO	Mor02_w4	161	165	285	351	187	209	125	125
SHO	Mor02_w5	161	165	285	351	187	203	125	133
SHO	Mor02_w6	161	165	283	351	187	209	125	125
SHO	Mor02_w7	161	165	285	351	187	203	125	125
SHO	Mor02_w8	161	165	283	351	187	203	125	125
SHO	Mor02_w9	161	165	285	351	187	203	125	125
SHO	Mor04_w1	161	179	273	285	203	209	125	125
SHO	Mor04_w10	161	179	273	285	203	209	125	125
SHO	Mor04_w2	161	179	273	285	203	209	125	133
SHO	Mor04_w3	161	179	273	285	203	209	125	133
SHO	Mor04_w4	161	179	273	283	203	209	125	125
SHO	Mor04_w5	161	179	273	283	203	203	125	133
SHO	Mor04_w6	161	179	273	283	203	209	125	133
SHO	Mor04_w7	161	179	273	285	203	203	125	125

SHO	Mor04_w8	161	179	273	285	203	203	125	133
SHO	Mor04_w9	161	175	291	351	203	207	125	125
SHO	Mor05_w1	157	165	273	283	201	203	125	125
SHO	Mor05_w10	157	165	273	283	201	203	125	125
SHO	Mor05_w2	157	165	275	275	201	203	125	125
SHO	Mor05_w3	157	165	275	275	201	205	125	125
SHO	Mor05_w4	157	165	275	275	201	205	125	125
SHO	Mor05_w5	157	165	275	275	201	203	125	125
SHO	Mor05_w6	157	165	275	275	201	205	125	125
SHO	Mor05_w7	157	165	275	275	201	205	125	125
SHO	Mor05_w8	157	165	275	275	201	205	125	125
SHO	Mor05_w9	157	165	275	275	201	201	125	125
SHO	Mor06_w1	155	175	287	289	187	189	125	149
SHO	Mor06_w10	175	189	287	289	187	207	125	149
SHO	Mor06_w2	175	189	289	289	187	189	125	149
SHO	Mor06_w3	155	175	287	289	187	189	125	149
SHO	Mor06_w4	175	189	287	289	187	207	125	125
SHO	Mor06_w5	175	189	287	289	187	189	125	149
SHO	Mor06_w6	155	175	289	351	187	207	125	125
SHO	Mor06_w7	155	175	289	351	187	189	125	149
SHO	Mor06_w8	175	189	289	351	187	189	125	149
SHO	Mor06_w9	175	189	289	351	187	207	125	149
SHO	Mor07_w1.1	157	157	273	311	193	199	125	149
SHO	Mor07_w10	157	161	311	349	179	199	125	149
SHO	Mor07_w2	157	157	273	311	179	199	125	149
SHO	Mor07_w3	157	157	273	311	179	199	125	149
SHO	Mor07_w4	157	157	273	311	179	199	125	149
SHO	Mor07_w5	157	157	273	311	179	199	125	149
SHO	Mor07_w6	157	161	311	349	179	199	125	149
SHO	Mor07_w7	157	157	273	311	193	199	125	149
SHO	Mor07_w8	157	161	311	349	179	199	125	149
SHO	Mor07_w9	157	157	311	349	179	199	125	149
SHO	Mor08_w1	161	161	303	351	203	203	125	125
SHO	Mor08_w10	161	161	287	351	197	203	125	125
SHO	Mor08_w2	161	183	287	351	203	203	125	125
SHO	Mor08_w3	161	161	287	351	203	203	125	125
SHO	Mor08_w4	161	183	303	351	197	203	125	125
SHO	Mor08_w5	161	183	303	351	203	203	125	125
SHO	Mor08_w6	161	183	287	351	203	203	125	125
SHO	Mor08_w7	161	183	303	351	203	205	125	125

SHO	Mor08_w8	161	183	303	351	203	203	125	125
SHO	Mor08_w9	161	183	303	351	197	203	125	125

**** Sierra Anchas field colonies ****

SIE-A	Sie10_w11	161	193	301	303	189	231	149	209
SIE-A	Sie10_w12	175	193	291	303	189	231	201	209
SIE-A	Sie10_w13	193	195	293	305	213	221	133	175
SIE-A	Sie10_w14	179	195	271	275	191	203	179	189
SIE-A	Sie10_w17	197	203	275	313	177	235	157	175
SIE-A	Sie10_w18	193	195	293	299	203	219	157	169
SIE-A	Sie10_w2	155	161	285	297	183	231	151	153
SIE-A	Sie10_w21	175	197	295	305	189	219	151	175
SIE-A	Sie10_w25	161	189	297	297	193	219	151	187
SIE-A	Sie10_w27	185	201	271	289	193	213	151	157
SIE-A	Sie12_w1	145	179	275	329	189	245	159	197
SIE-A	Sie12_w10	171	185	267	293	193	241	155	159
SIE-A	Sie12_w19	175	191	271	289	183	249	151	179
SIE-A	Sie12_w2	161	191	267	285	211	239	157	185
SIE-A	Sie12_w24	161	169	261	267	183	219	151	157
SIE-A	Sie12_w26	139	199	275	305	189	219	151	157
SIE-A	Sie12_w4	179	191	271	305	193	195	149	209
SIE-A	Sie12_w5	155	171	279	285	209	231	151	189
SIE-A	Sie12_w7	161	177	291	293	185	193	185	189
SIE-A	Sie12_w8	161	161	271	279	211	211	157	173
SIE-A	Sie14_w1	181	193	283	287	193	231	127	127
SIE-A	Sie14_w11	167	183	267	269	203	211	151	155
SIE-A	Sie14_w12	173	179	281	297	193	211	149	189
SIE-A	Sie14_w22	183	197	279	289	189	219	151	191
SIE-A	Sie14_w26	145	147	267	325	229	229	151	153
SIE-A	Sie14_w28	147	183	305	305	211	219	149	151
SIE-A	Sie14_w29	179	191	267	293	229	247	173	197
SIE-A	Sie14_w3	165	181	257	269	193	215	151	191
SIE-A	Sie14_w8	171	183	275	291	189	223	151	177
SIE-A	Sie14_w9	137	141	287	291	193	221	187	189
SIE-A	Sie16_w12	187	193	271	281	183	249	149	149
SIE-A	Sie16_w13	187	193	271	281	183	249	149	185
SIE-A	Sie16_w15	187	193	291	291	183	203	149	185
SIE-A	Sie16_w19	171	177	291	291	219	235	151	157
SIE-A	Sie16_w20	187	193	271	281	183	249	149	149
SIE-A	Sie16_w22	187	193	271	281	183	249	149	185

SIE-A	Sie16_w24	171	193	281	293	183	249	149	149
SIE-A	Sie16_w5	187	193	271	281	183	203	149	185
SIE-A	Sie16_w6	171	193	271	281	183	249	149	149
SIE-A	Sie16_w9	187	193	271	281	183	203	149	185
SIE-A	Sie18_w10	141	165	273	285	175	183	149	209
SIE-A	Sie18_w11	183	193	269	293	193	227	151	187
SIE-A	Sie18_w2	145	155	271	273	177	249	153	205
SIE-A	Sie18_w21	141	165	285	291	175	235	151	209
SIE-A	Sie18_w25	171	171	289	301	217	219	181	187
SIE-A	Sie18_w27	171	193	289	305	211	219	155	181
SIE-A	Sie18_w3	171	179	273	349	203	211	151	187
SIE-A	Sie18_w30	171	193	289	305	217	219	181	187
SIE-A	Sie18_w5	183	193	269	293	229	249	185	187
SIE-A	Sie18_w6	141	181	273	349	203	249	151	155
SIE-A	Sie20_w1	141	161	291	309	189	231	155	155
SIE-A	Sie20_w10	165	167	289	299	189	225	157	177
SIE-A	Sie20_w17	161	197	271	289	193	247	177	193
SIE-A	Sie20_w2	173	197	269	305	193	211	151	173
SIE-A	Sie20_w22	147	187	285	285	213	229	173	209
SIE-A	Sie20_w4	147	165	293	307	175	229	127	171
SIE-A	Sie20_w6	147	181	279	293	203	227	157	157
SIE-A	Sie20_w7	161	171	287	291	189	241	155	177
SIE-A	Sie20_w8	163	165	271	299	177	211	151	171
SIE-A	Sie20_w9	175	197	285	285	229	243	149	155
SIE-A	Sie6-10_w1	171	197	267	293	213	221	169	189
SIE-A	Sie6-10_w11	169	197	269	293	213	229	149	151
SIE-A	Sie6-10_w13	137	161	289	291	219	231	153	157
SIE-A	Sie6-10_w17	137	169	289	297	193	239	171	189
SIE-A	Sie6-10_w21	137	179	293	305	213	229	149	151
SIE-A	Sie6-10_w23	141	141	279	305	183	213	149	151
SIE-A	Sie6-10_w29	141	197	279	305	183	239	149	151
SIE-A	Sie6-10_w4	163	197	269	305	205	239	151	189
SIE-A	Sie6-10_w7	137	165	293	305	231	235	149	151
SIE-A	Sie6-10_w9	137	171	267	305	221	239	169	189
SIE-A	Sie7_w1	183	183	291	305	211	243	149	149
SIE-A	Sie7_w12	173	173	273	305	195	211	149	197
SIE-A	Sie7_w14	167	173	289	305	183	211	149	149
SIE-A	Sie7_w16	173	173	273	305	183	211	149	197
SIE-A	Sie7_w17	167	173	289	305	195	211	149	197
SIE-A	Sie7_w22	167	173	289	305	183	211	149	197

SIE-A	Sie7_w25	167	173	289	305	195	211	149	197
SIE-A	Sie7_w28	141	193	287	291	177	235	151	193
SIE-A	Sie7_w30	173	173	273	305	195	211	149	197
SIE-A	Sie7_w6	173	173	273	305	183	211	149	197
SIE-A	Sie8_w1	141	181	275	287	221	225	151	205
SIE-A	Sie8_w10	141	191	271	303	183	225	151	205
SIE-A	Sie8_w12	161	179	279	303	225	231	151	157
SIE-A	Sie8_w19	141	159	287	305	193	219	151	191
SIE-A	Sie8_w20	161	179	271	303	203	225	151	157
SIE-A	Sie8_w23	165	175	279	305	203	225	149	189
SIE-A	Sie8_w24	141	191	271	305	183	193	151	205
SIE-A	Sie8_w25	141	155	293	305	173	217	149	157
SIE-A	Sie8_w30	141	171	275	287	219	225	151	205
SIE-A	Sie8_w9	165	175	279	305	203	225	149	189
SIE-A	Sie9_w1	147	161	275	287	189	225	149	205
SIE-A	Sie9_w17	159	193	287	293	193	213	191	209
SIE-A	Sie9_w18	141	147	273	303	219	225	151	207
SIE-A	Sie9_w19	163	181	267	279	225	225	149	195
SIE-A	Sie9_w2	177	195	275	291	219	247	149	149
SIE-A	Sie9_w21	193	195	291	305	193	235	149	157
SIE-A	Sie9_w26	191	191	279	295	191	193	149	207
SIE-A	Sie9_w27	141	197	287	291	189	203	169	179
SIE-A	Sie9_w30	191	197	269	293	183	193	151	151
SIE-A	Sie9_w7	137	141	291	307	177	213	127	149

**** Sierra Buenos Aires field colonies ****

SIE-B	Bue01_w1	137	189	267	315	187	203	125	175
SIE-B	Bue01_w10	137	159	267	315	187	203	125	175
SIE-B	Bue01_w2	137	159	315	321	187	219	125	175
SIE-B	Bue01_w3	137	189	315	321	187	219	125	175
SIE-B	Bue01_w4	137	189	315	321	187	219	125	175
SIE-B	Bue01_w5	137	159	267	315	187	203	125	175
SIE-B	Bue01_w6	137	159	315	321	187	219	129	175
SIE-B	Bue01_w7	137	159	267	315	187	219	129	175
SIE-B	Bue01_w8	137	159	267	315	187	203	129	175
SIE-B	Bue01_w9	137	159	267	315	187	219	129	175
SIE-B	Bue02_w1.1	153	189	267	321	193	201	125	127
SIE-B	Bue02_w10	153	189	303	321	201	201	125	181
SIE-B	Bue02_w2	153	189	303	321	201	201	125	181
SIE-B	Bue02_w3	153	189	303	321	193	201	125	181

SIE-B	Bue02_w4	153	189	303	321	201	201	125	127
SIE-B	Bue02_w5	153	189	303	321	201	201	125	181
SIE-B	Bue02_w6	153	181	267	309	191	193	125	127
SIE-B	Bue02_w7	153	189	303	321	201	201	125	181
SIE-B	Bue02_w8	153	189	303	321	201	201	125	127
SIE-B	Bue02_w9	153	189	303	321	201	201	125	127
SIE-B	Bue03_w1.1	153	163	275	305	197	205	125	183
SIE-B	Bue03_w10	153	163	275	275	197	205	125	183
SIE-B	Bue03_w2	153	163	275	305	197	219	125	183
SIE-B	Bue03_w3	131	153	275	275	197	219	125	183
SIE-B	Bue03_w4	137	171	283	337	193	197	125	129
SIE-B	Bue03_w5	153	163	275	275	197	219	125	183
SIE-B	Bue03_w6	131	153	275	305	197	219	125	177
SIE-B	Bue03_w7	153	163	275	305	197	205	125	183
SIE-B	Bue03_w8	153	163	275	275	197	205	125	183
SIE-B	Bue03_w9	131	153	275	305	197	205	125	183
SIE-B	Bue04_w1.1	135	143	319	327	187	193	169	187
SIE-B	Bue04_w10	135	143	319	347	187	187	171	187
SIE-B	Bue04_w2	131	135	319	327	187	187	171	187
SIE-B	Bue04_w3	131	135	319	327	187	187	171	187
SIE-B	Bue04_w4	135	143	319	347	187	187	169	187
SIE-B	Bue04_w5	135	143	319	347	187	193	169	187
SIE-B	Bue04_w6	135	143	319	347	187	187	169	187
SIE-B	Bue04_w7	135	143	319	347	187	187	169	187
SIE-B	Bue04_w8	135	143	319	347	187	193	171	187
SIE-B	Bue04_w9	131	135	319	327	187	193	171	187
SIE-B	Bue05_w1	133	141	327	335	191	207	131	151
SIE-B	Bue05_w10	133	141	m	m	191	207	131	151
SIE-B	Bue05_w2	133	141	m	m	191	207	131	151
SIE-B	Bue05_w3	123	133	m	m	191	207	131	151
SIE-B	Bue05_w4	123	133	327	335	191	207	131	151
SIE-B	Bue05_w5	133	141	327	335	187	207	131	151
SIE-B	Bue05_w6	123	133	327	335	187	207	131	151
SIE-B	Bue05_w7	133	141	327	335	187	207	131	151
SIE-B	Bue05_w8	133	141	m	m	187	207	131	151
SIE-B	Bue05_w9	123	133	m	m	191	207	131	151
SIE-B	Bue06_w1	127	137	297	327	187	191	175	175
SIE-B	Bue06_w10	127	137	297	327	187	191	175	197
SIE-B	Bue06_w2	127	137	297	327	187	191	175	175
SIE-B	Bue06_w3	127	137	297	327	187	191	175	175

SIE-B	Bue06_w4	127	137	297	351	187	187	175	175
SIE-B	Bue06_w5	127	137	297	327	187	187	175	175
SIE-B	Bue06_w6	127	137	297	327	187	187	175	197
SIE-B	Bue06_w7	127	137	297	327	187	191	175	175
SIE-B	Bue06_w8	127	137	297	327	187	191	175	197
SIE-B	Bue06_w9	127	137	297	327	187	187	175	175
SIE-B	Bue07_w1	135	157	275	321	189	213	125	163
SIE-B	Bue07_w10	135	157	275	321	189	195	125	163
SIE-B	Bue07_w2	135	157	271	321	189	195	125	163
SIE-B	Bue07_w3	135	135	275	321	189	195	125	163
SIE-B	Bue07_w4	119	135	271	315	187	213	125	187
SIE-B	Bue07_w5	135	135	275	321	189	195	125	163
SIE-B	Bue07_w6	135	157	271	321	189	189	125	163
SIE-B	Bue07_w7	119	157	271	315	187	213	125	187
SIE-B	Bue07_w8	135	157	275	321	189	213	125	163
SIE-B	Bue07_w9	119	135	271	315	187	195	125	187
SIE-B	Bue09_w1	135	143	319	327	187	187	173	175
SIE-B	Bue09_w10	135	143	319	355	187	187	173	177
SIE-B	Bue09_w2	135	143	319	327	187	187	173	175
SIE-B	Bue09_w3	135	143	319	327	187	187	173	175
SIE-B	Bue09_w4	135	143	319	327	187	187	175	189
SIE-B	Bue09_w5	119	143	319	327	187	187	173	175
SIE-B	Bue09_w6	119	143	319	327	187	187	175	189
SIE-B	Bue09_w7	119	143	319	355	187	187	175	189
SIE-B	Bue09_w8	119	143	319	355	187	187	175	189
SIE-B	Bue09_w9	119	143	319	327	187	187	175	189
SIE-B	Bue10_w1	133	143	319	323	191	195	151	169
SIE-B	Bue10_w10	133	139	319	329	191	195	151	169
SIE-B	Bue10_w2	133	139	319	323	191	195	151	169
SIE-B	Bue10_w3	133	139	319	329	191	195	169	171
SIE-B	Bue10_w4	133	139	319	323	175	195	151	169
SIE-B	Bue10_w5	133	143	319	329	191	195	169	171
SIE-B	Bue10_w6	133	139	319	323	175	195	151	169
SIE-B	Bue10_w7	133	139	319	329	175	195	169	171
SIE-B	Bue10_w8	133	139	319	323	175	195	151	169
SIE-B	Bue10_w9	133	139	319	323	191	195	151	169
SIE-B	Bue11_w1	123	151	251	327	189	207	125	209
SIE-B	Bue11_w10	151	173	251	327	189	199	125	129
SIE-B	Bue11_w2	123	151	251	327	189	207	125	209
SIE-B	Bue11_w3	123	151	251	327	189	207	125	209

SIE-B	Bue11_w4	151	173	251	361	189	199	125	129
SIE-B	Bue11_w5	123	151	251	327	189	207	125	209
SIE-B	Bue11_w6	151	173	251	327	189	199	125	129
SIE-B	Bue11_w7	123	151	251	327	189	199	125	209
SIE-B	Bue11_w8	151	173	251	361	189	207	125	129
SIE-B	Bue11_w9	123	151	251	361	189	207	125	209

**** Superstitions field colonies ****

SUP	Pcr01_w1	153	157	271	297	189	233	149	183
SUP	Pcr01_w10	153	157	271	297	189	193	149	183
SUP	Pcr01_w2	141	153	271	301	189	233	149	183
SUP	Pcr01_w3	141	153	271	301	189	233	177	183
SUP	Pcr01_w4	143	157	271	301	189	233	177	183
SUP	Pcr01_w5	141	153	271	301	189	233	149	183
SUP	Pcr01_w6	153	157	271	301	189	193	177	183
SUP	Pcr01_w7	141	153	271	301	189	193	149	183
SUP	Pcr01_w8	153	157	271	297	189	233	177	183
SUP	Pcr01_w9	153	157	271	301	189	233	177	183
SUP	Pcr02_w1	171	173	281	287	191	231	149	149
SUP	Pcr02_w10	143	171	281	295	191	233	149	149
SUP	Pcr02_w2	171	173	281	287	191	233	149	149
SUP	Pcr02_w3	171	173	281	295	233	237	149	149
SUP	Pcr02_w4	143	171	281	295	191	233	149	149
SUP	Pcr02_w5	143	171	281	287	233	237	149	149
SUP	Pcr02_w6	171	173	281	295	191	233	149	149
SUP	Pcr02_w7	143	171	281	287	233	237	149	149
SUP	Pcr02_w8	143	171	281	287	191	233	149	149
SUP	Pcr02_w9	143	171	281	287	233	237	149	149
SUP	Pcr03_w1	167	179	281	287	191	213	149	175
SUP	Pcr03_w10	175	179	273	277	191	263	149	179
SUP	Pcr03_w2	137	175	271	287	209	263	137	179
SUP	Pcr03_w3	167	179	277	281	191	213	149	179
SUP	Pcr03_w4	137	167	271	277	209	213	137	179
SUP	Pcr03_w5	137	167	271	287	209	263	137	179
SUP	Pcr03_w6	175	179	277	281	191	213	149	175
SUP	Pcr03_w7	167	179	281	287	191	213	149	179
SUP	Pcr03_w8	175	179	281	287	191	213	149	179
SUP	Pcr03_w9	167	179	277	281	191	263	149	175
SUP	Pcr04_w1	143	163	285	329	191	211	149	149
SUP	Pcr04_w10	163	171	307	329	191	251	149	149

SUP	Pcr04_w2	143	163	285	329	191	211	149	151
SUP	Pcr04_w3	163	171	307	329	191	211	149	151
SUP	Pcr04_w4	163	171	307	329	191	251	149	149
SUP	Pcr04_w5	143	163	285	329	191	251	149	149
SUP	Pcr04_w6	143	163	285	329	191	211	149	151
SUP	Pcr04_w7	143	163	285	329	191	211	149	151
SUP	Pcr04_w8	163	171	307	329	191	211	149	151
SUP	Pcr04_w9	143	163	307	329	191	251	149	149
SUP	Pcr05_w1	143	153	249	287	225	267	149	209
SUP	Pcr05_w10	143	153	249	287	225	267	149	181
SUP	Pcr05_w2	153	189	249	287	225	267	149	181
SUP	Pcr05_w3	153	189	249	287	225	267	149	209
SUP	Pcr05_w4	143	153	249	287	225	293	149	209
SUP	Pcr05_w5	143	153	249	287	225	293	149	209
SUP	Pcr05_w6	143	153	249	287	225	267	149	209
SUP	Pcr05_w7	143	153	281	287	225	267	149	181
SUP	Pcr05_w8	153	189	281	287	225	267	149	181
SUP	Pcr05_w9	143	153	249	287	225	293	149	209
SUP	Pcr06_w1	155	161	291	295	191	207	149	171
SUP	Pcr06_w10	155	161	281	295	191	207	149	171
SUP	Pcr06_w2	155	187	291	295	191	207	149	171
SUP	Pcr06_w3	155	161	291	295	191	195	149	171
SUP	Pcr06_w4	155	187	291	295	191	195	149	171
SUP	Pcr06_w5	155	161	291	295	191	195	149	171
SUP	Pcr06_w6	155	161	291	295	191	207	149	171
SUP	Pcr06_w7	155	187	291	295	191	207	149	171
SUP	Pcr06_w8	155	161	281	295	191	207	149	171
SUP	Pcr06_w9	155	187	291	295	191	207	149	171
SUP	Pcr07_w1	167	177	281	283	209	245	149	149
SUP	Pcr07_w10	159	167	283	283	193	231	137	149
SUP	Pcr07_w2	167	177	281	283	209	245	149	149
SUP	Pcr07_w3	167	177	281	287	231	245	149	149
SUP	Pcr07_w4	167	177	281	287	231	245	149	149
SUP	Pcr07_w5	167	177	281	283	231	245	149	149
SUP	Pcr07_w6	159	167	283	283	193	231	137	149
SUP	Pcr07_w7	159	167	287	287	193	209	137	149
SUP	Pcr07_w8	167	177	281	287	209	245	149	149
SUP	Pcr07_w9	167	177	281	287	209	245	149	149
SUP	Pcr09_w1	135	153	271	271	173	211	151	189
SUP	Pcr09_w10	135	153	271	271	173	253	151	189

SUP	Pcr09_w2	153	155	271	271	173	211	151	189
SUP	Pcr09_w3	135	153	271	293	173	211	189	189
SUP	Pcr09_w4	153	155	271	271	173	253	151	189
SUP	Pcr09_w5	145	155	293	367	195	211	149	189
SUP	Pcr09_w6	145	145	293	367	195	211	149	189
SUP	Pcr09_w7	135	145	367	367	195	211	149	189
SUP	Pcr09_w8	135	145	367	367	195	211	149	151
SUP	Pcr09_w9	135	145	293	367	195	211	149	151
SUP	Pcr10_w1	167	177	281	283	231	245	149	149
SUP	Pcr10_w10	159	167	287	287	193	231	137	149
SUP	Pcr10_w2	159	167	283	283	193	231	137	149
SUP	Pcr10_w3	167	177	281	283	209	245	149	149
SUP	Pcr10_w4	159	167	287	287	193	209	137	149
SUP	Pcr10_w5	167	177	281	287	209	245	149	149
SUP	Pcr10_w6	159	167	287	287	193	209	137	149
SUP	Pcr10_w7	167	177	281	283	231	245	149	149
SUP	Pcr10_w8	167	177	281	283	231	245	149	149
SUP	Pcr10_w9	167	177	281	287	231	245	149	149
SUP	Pcr13_w1	141	165	275	311	211	221	149	149
SUP	Pcr13_w10	165	173	275	289	211	221	149	149
SUP	Pcr13_w2	141	165	275	289	189	221	149	149
SUP	Pcr13_w3	165	173	275	289	211	221	149	149
SUP	Pcr13_w4	141	169	289	291	211	249	149	149
SUP	Pcr13_w5	165	173	275	289	189	221	149	149
SUP	Pcr13_w6	141	169	291	311	211	249	149	149
SUP	Pcr13_w7	165	173	275	289	211	221	149	149
SUP	Pcr13_w8	165	173	275	311	211	221	149	149
SUP	Pcr13_w9	141	169	289	291	211	249	149	149

**** Whetstones field colonies ****

WHE	Dry01_w1	157	159	291	329	219	241	125	125
WHE	Dry01_w10	157	159	291	291	219	241	125	125
WHE	Dry01_w2	157	159	291	329	219	241	125	125
WHE	Dry01_w3	157	159	291	329	219	241	125	125
WHE	Dry01_w4	157	159	291	291	201	241	125	125
WHE	Dry01_w5	159	161	291	291	219	241	125	125
WHE	Dry01_w6	159	161	291	291	201	241	125	125
WHE	Dry01_w7	159	161	291	291	201	241	125	125
WHE	Dry01_w8	159	161	291	291	219	241	125	125
WHE	Dry01_w9	157	159	291	291	219	241	125	125

WHE	Dry02_w1	167	189	341	347	191	239	131	131
WHE	Dry02_w10	167	209	321	347	191	239	125	125
WHE	Dry02_w2	167	189	321	347	191	239	125	125
WHE	Dry02_w3	167	209	341	347	217	239	125	131
WHE	Dry02_w4	167	189	321	347	217	239	125	131
WHE	Dry02_w5	167	209	341	347	217	239	125	131
WHE	Dry02_w6	167	189	321	347	217	239	125	131
WHE	Dry02_w7	167	189	321	347	191	239	125	125
WHE	Dry02_w8	167	189	321	347	217	239	125	125
WHE	Dry02_w9	167	209	341	347	191	239	125	125
WHE	Dry03_w1	153	181	295	295	189	195	125	125
WHE	Dry03_w10	153	181	303	303	189	239	125	125
WHE	Dry03_w2	153	173	295	317	219	239	125	125
WHE	Dry03_w3	157	173	303	317	219	239	125	125
WHE	Dry03_w4	153	173	295	317	219	239	125	125
WHE	Dry03_w5	157	173	295	317	195	219	125	125
WHE	Dry03_w6	153	181	303	303	189	195	125	125
WHE	Dry03_w7	157	173	303	317	219	239	125	125
WHE	Dry03_w8	157	181	303	303	189	195	125	125
WHE	Dry03_w9	153	181	303	303	189	195	125	125
WHE	Dry04_w1	161	191	297	325	189	213	125	127
WHE	Dry04_w10	175	177	289	325	189	227	125	125
WHE	Dry04_w2	161	177	289	325	189	189	125	127
WHE	Dry04_w3	161	191	297	351	213	227	125	125
WHE	Dry04_w4	175	191	297	351	213	227	125	127
WHE	Dry04_w5	175	177	289	289	189	189	125	125
WHE	Dry04_w6	161	191	297	351	189	213	125	125
WHE	Dry04_w7	161	191	297	325	213	227	125	127
WHE	Dry04_w8	175	177	289	351	189	227	125	125
WHE	Dry04_w9	175	177	289	325	189	227	125	125
WHE	Dry05_w1	157	207	271	319	223	241	125	125
WHE	Dry05_w10	157	157	317	317	221	239	125	127
WHE	Dry05_w2	151	157	317	357	221	239	125	127
WHE	Dry05_w3	157	207	271	319	223	241	125	125
WHE	Dry05_w4	157	157	317	317	221	239	125	127
WHE	Dry05_w5	157	157	317	357	221	239	125	127
WHE	Dry05_w6	151	157	317	357	221	239	125	127
WHE	Dry05_w7	157	179	271	319	223	241	125	125
WHE	Dry05_w8	157	179	319	337	223	241	125	125
WHE	Dry05_w9	157	207	319	337	189	241	125	125

WHE	Fre02_w1	141	161	273	273	191	211	125	125
WHE	Fre02_w10	141	141	273	273	191	211	125	125
WHE	Fre02_w2	141	141	273	273	191	197	125	125
WHE	Fre02_w3	141	141	279	279	191	211	125	125
WHE	Fre02_w4	141	141	273	273	191	197	125	125
WHE	Fre02_w5	141	141	273	273	191	197	125	125
WHE	Fre02_w6	141	161	279	279	191	211	125	125
WHE	Fre02_w7	141	141	279	279	191	211	125	125
WHE	Fre02_w8	141	141	273	273	191	211	125	125
WHE	Fre02_w9	141	161	271	279	191	211	125	125
WHE	Fre05_w1	183	183	333	339	191	201	125	125
WHE	Fre05_w10	177	183	279	333	191	193	125	125
WHE	Fre05_w2	177	183	333	339	191	193	125	125
WHE	Fre05_w3	175	183	279	279	193	201	125	125
WHE	Fre05_w4	175	183	279	279	193	201	125	125
WHE	Fre05_w5	175	183	339	339	201	201	125	125
WHE	Fre05_w6	177	183	279	333	191	193	125	125
WHE	Fre05_w7	183	183	279	333	191	193	125	125
WHE	Fre05_w8	183	183	333	339	191	201	125	125
WHE	Fre05_w9	175	183	339	339	193	201	125	125
WHE	Gui01_w1	161	193	275	295	195	209	125	125
WHE	Gui01_w10	155	155	275	313	209	221	125	125
WHE	Gui01_w2	161	193	295	339	195	209	125	125
WHE	Gui01_w3	161	193	275	295	195	209	125	125
WHE	Gui01_w4	155	193	295	339	189	195	125	125
WHE	Gui01_w5	155	155	275	313	209	221	125	125
WHE	Gui01_w6	155	193	295	339	195	209	125	125
WHE	Gui01_w7	155	155	313	339	189	221	125	125
WHE	Gui01_w8	161	193	275	295	189	195	125	125
WHE	Gui01_w9	155	193	295	339	195	209	125	125